

The Impact of Climate Change on Amur Tiger Habitat in Russia:
Applying the FAREAST Model at the Regional Scale

Nancy Jean Sherman
Charlottesville, Virginia

A.B., Princeton University, 1976
M.A., University of Virginia, 2005

A Dissertation presented to the Graduate Faculty
of the University of Virginia in Candidacy for the Degree of
Doctor of Philosophy

Environmental Sciences Department

University of Virginia
August, 2013

© by Nancy Jean Sherman
Charlottesville, Virginia, USA
All Rights Reserved
August 2013

ABSTRACT

Characterizing forest structure and composition at the landscape scale can assist in understanding the impact of global phenomena such as climate change on complex ecosystems. In this study, remote sensing data and output from a computer forest succession gap model are compared with field results in a vast and biologically diverse area in Far Eastern Russia. Projected climate change is applied within the model to determine the effect on the trophic network of the endangered Amur, or Siberian, tiger.

The forest succession gap model FAREAST has been validated at 31 sites in Far Eastern Russia, where simulated results matched forest inventory data at 23 sites in terms of the four dominant tree genera by biomass. FAREAST produces old growth forests using inputs of temperature, precipitation, site quality and species characteristics.

To calibrate and explore the model's capabilities, output at 1,000 randomly selected points was compared with land covers developed from a synthesis of the Moderate Resolution Imaging Spectrometer (MODIS) land cover product, the Global Land Cover 2000 (GLC 2000) map, and a Russian forest map. Comparing remotely sensed with modeled land covers suggested that disturbance occurred at 461 of the 608 points (76%) where forest types differed.

FAREAST estimates of canopy height (based on the tallest tree) and biomass were compared with the ratio of canopy height to biomass derived from the Geoscience Laser Altimeter System (GLAS) on ICESAT. The LiDAR-derived ratio was continuous with the FAREAST results ($y = 6.3178e^{0.1004x}$, $R^2 = 0.9468$). This reaffirms the confidence with which both approaches can be used to estimate forest biomass from canopy height.

FAREAST results were compared with field data at eleven sites in three strictly protected reserves. Simulated total basal area approximated observed at seven of eight sites with primary old growth forests, and the model was able to correctly identify forest type at all old growth sites. FAREAST results most closely approximated observed at the southernmost sites, close to Changbai Mountain in northeastern China, where the model was developed and verified. The presence or absence of large Korean pine trees at field sites accounted for much of the difference between modeled and observed results at other sites with old growth forests.

Model parameters were adjusted for climate change to represent the approximate average temperature increase for the research area in 2070 – 2099 compared with 1961 - 1990 under two Intergovernmental Panel on Climate Change (2007) scenarios, B1 (+3.5 °C) and A1F1 (+6.0 °C). Testing was conducted to determine the temperature increase that would cause the disappearance of Korean pine, a critical food species for Amur tiger prey. Climate change of 1.5 – 1.8 °C at the southernmost field sites in Ussurisky Reserve would cause Korean pine to decline, and warming of 2.4 – 2.8 °C would cause it to disappear. Climate change up to 3.9 °C would allow Korean pine to expand range in Sikhote-Alin Biosphere Reserve in Central Sikhote-Alin, but the species

would disappear with climate warming of 4.2 °C. At the northernmost sites, warming of 2.1 – 2.5 °C caused Korean pine to decline and 2.5 – 3.2 °C warming resulted in its disappearance. At 1,000 random points representing sites across Amur tiger range, warming of 3.5 °C caused dark conifer forests to convert to mixed deciduous broadleaf/Korean pine/conifer within 60 years of the new temperature regime (160 years from present) and southern mixed forests to change to deciduous broadleaf. With 6 °C warming, mixed and dark conifer forests convert to deciduous broadleaf, and forests disappear at about 10% of sites. These results are consistent with simulations for the field sites. Atmospheric temperature is expected to warm more quickly in East Asia than globally, and global average temperature increases projected for the end of this century (~1.8 °C for B1; ~4.0 °C for A1F1) would cause these levels of warming to occur in the study area.

ACKNOWLEDGEMENTS

This research was made possible by ROSES-2006 Grant 06-IDS06-93, funded under NASA Research Announcement (NRA) NNH06ZDA001N Research Opportunities in Space and Earth Science (ROSES-2006). This work would not have been possible without the expertise and support of Dale Miquelle, Russia Program Director, Wildlife Conservation Society, the scientific staff of Sikhote-Alin Biosphere Reserve, especially A.A. Astafiev, Director, and Lena Pimenova, Deputy Director and Chief Scientist, as well as botanists and field workers from Bolshekhkhtsirskiy and Ussurisky Reserves. H. H. Shugart, W. W. Corcoran Professor of Environmental Sciences and Director, Center for Regional Environmental Studies, also provided generous and essential guidance and support. The computer programming expertise of K. Holcombe of the University of Virginia's Alliance for Computational Science and Engineering was essential and is much appreciated, as is the expertise and infinite patience of ArcGIS gurus Chris Gist and Kelly Johnston in the UVA Scholars' Lab. Thanks also to my PhD Committee: Paolo D'Odorico, Deborah Lawrence, Mark Kopeny, and John Seidensticker, for their expertise, time and energy in reviewing and providing guidance on my proposal and various drafts; to Will Tomanek, EVSC Computer Systems Engineer, for saving my computer and my sanity on multiple occasions; to the Shugart lab; and to my family for their unflagging support and patience.

TABLE OF CONTENTS

	Abstract.....	ii
	Acknowledgements.....	v
	Table of Contents.....	vi
	List of Tables.....	xi
1.0	Introduction.....	1
1.1	References.....	5
2.0	Comparing Remote Sensing and Computer Modeling to Analyze a Biologically Diverse and Topographically Complex Landscape in the Russian Far East.....	7
	Abstract.....	7
2.1	Introduction.....	8
2.2	Background.....	10
	2.2.1 Disturbance and succession.....	14
	2.2.2 Climate.....	15
	2.2.3 FAREAST Model.....	16
	2.2.4 GLAS LiDAR.....	17
2.3	Materials and Methods.....	20
	2.3.1 FAREAST model parameterization.....	22
	2.3.2 Comparison of GLAS results with simulated metrics.....	26
	2.3.3 Assessing fire probability at potentially disturbed sites.....	27
2.4	Results.....	28
	2.4.1 Canopy height – biomass relationship.....	30

2.4.2	Fire probability at sites where disturbance may have occurred.....	31
2.5	Discussion.....	33
2.5.1	Forest succession and disturbance.....	35
2.5.2	Wildfires and other disturbances.....	40
2.5.3	LiDAR vs. Modeling – Biomass to canopy height relationship.....	41
2.6	Conclusion.....	44
2.7	References.....	45
3.0	Comparison of Results from a Forest Succession Gap Model with Field Observations...	58
	Abstract.....	58
3.1	Introduction.....	59
3.2	Background.....	60
3.2.1	FAREAST model - Overview.....	63
3.2.2	Climate.....	65
3.2.3	Field research.....	67
3.3	Materials and Methods.....	69
3.3.1	Forest categories.....	72
3.3.2	FAREAST Model.....	73
3.3.2.1	MORTALITY sub-model.....	76
3.3.2.2	REGENERATION sub-model.....	77
3.3.2.3	ENVIRON sub-model.....	77
3.3.3	Data analysis.....	79
3.4	Results.....	80
3.4.1	Field site vs. FAREAST results.....	86

3.4.1.1	Altitude adjustment.....	87
3.4.1.2	Results by site.....	90
3.4.1.2.1	Burn site – Maysa in SABZ.....	100
3.5	Discussion.....	101
3.5.1	Southernmost sites – closest match between simulated and observed..	103
3.5.2	Sikhote-Alin Biosphere <i>Zapovednik</i> (Reserve).....	108
3.5.2.1	Mid-elevation forests – Kabaniy 1 and 2.....	108
3.5.2.2	High elevation forests – Kabaniy 3 and 4.....	111
3.5.2.3	Maysa – Fire disturbance site.....	114
3.5.2.4	Coastal oak forests – Blagodatnoye.....	116
3.5.3	Northernmost sites (Polovinka 1 and 2).....	122
3.5.4	Summary of modeled vs. site results.....	124
3.5.5	Possible causes of differences in modeled vs. observed.....	126
3.5.6	Future studies.....	126
3.6	Conclusion.....	127
3.7	References.....	128
3.8	Appendix – English translation of Latin species names.....	137
4.0	Using Remote Sensing and Modeling to Predict the Effect of Climate Change on Amur Tiger Habitat in the Russian Far East.....	138
	Abstract.....	138

4.1	Introduction.....	140
4.2	Background.....	146
4.2.1	Amur tigers.....	148
4.2.2	Tiger nutritive requirements.....	149
4.2.3	Resource Selection Function Analysis (RSF).....	151
4.2.4	Diet of ungulate prey.....	156
4.2.5	Forest vegetation in Amur tiger range.....	157
4.2.6	Climate in Amur tiger range.....	159
4.2.7	FAREAST model – overview.....	161
4.3	Materials and Methods.....	161
4.3.1	Field research.....	162
4.3.2	FAREAST model.....	162
4.3.2.1	Temperature inputs and scenarios used.....	165
4.3.2.2	FAREAST simulation.....	166
4.3.2.3	Random points.....	168
4.3.2.4	Adjusting FAREAST for climate change.....	169
4.4	Results.....	170
4.4.1	Ussurisky <i>Zapovednik</i> (Reserve).....	171
4.4.2	Kabaniy sites in Sikhote-Alin Biosphere <i>Zapovednik</i> (Reserve).....	176
4.4.3	Wildfire site in SABZ – Maysa.....	183
4.4.4	Oak forests in SABZ.....	185
4.4.5	Polovinka sites in Bolshekhokhtsirskiy <i>Zapovednik</i> (Reserve).....	190
4.4.6	Results at 1,000 random points.....	195

4.5	Discussion.....	199
4.5.1	Southernmost sites - Ussurisky Reserve.....	200
4.5.2	Coastal climate - Sikhote-Alin Biosphere Reserve.....	205
4.5.3	Northernmost sites - Bolshekhkhtsirskiy Reserve.....	213
4.5.4	Mongolian oak.....	215
4.5.5	Analysis at 1,000 random points.....	216
4.5.6	Impact of forest vegetation changes on tiger prey.....	217
4.5.7	Potential range shift and wildlife corridors.....	222
4.5.8	Other climate considerations.....	228
4.5.9	Effects of fire and other disturbances.....	230
4.5.10	Political, social and economic considerations.....	235
4.5.11	Possible future studies.....	236
4.6	Conclusion.....	237
4.7	References.....	239
4.8	Appendix – English translation of Latin species names.....	261
5.0	Conclusion.....	262

LIST OF TABLES

Table 2.1	Comparison of simulated and remote-sensing-based forest types.....	28
Table 2.2	Results of comparing remotely-sensed forest types with modeled at sites in protected areas.....	29
Table 2.3	Matches of forest cover by aspect (out of total number of random points with the specified aspect.....)	30
Table 2.4	Assessment of fire risk potential at sites where simulated vs. observed forest covers suggest disturbance.....	32
Table 3.1	Field sites.....	70
Table 3.2	Summary of simulated vs. observed at year of best match.....	124
Table 4.1	Summary of relationships between forest type and prey presence, based on track encounter rate.....	158
Table 4.2	Predicted precipitation increases (%) by season for East Asia.....	169
Table 4.3	Summary of site results.....	197

CHAPTER 1. INTRODUCTION

Computer modeling and remote sensing are useful tools to study vast and inaccessible landscapes, providing access to rugged and impassible terrain that would be physically difficult and cost-prohibitive to measure directly. Challenges of consistency and continuous coverage give modeling and remote sensing an edge over ground-based measurements in some cases. Models also are useful for studying hypothetical situations, such as the effects of climate warming on forests. Trends and patterns may become visible across the extended temporal scale that modeling can provide. Modeling and remote sensing also permit studies using large data sets, such as analysis of the relationship between tree diameter and tree height based on thousands of individual trees.

In the first part of this research, output from the forest succession gap model FAREAST was compared with land covers developed at the University of Maryland from a synthesis of remotely sensed data and Russian vegetation maps at 1,000 random points across tiger range (Chapter 2). In FAREAST, temperature and precipitation estimates, as well as soil characteristics, were assigned to each point according to the nearest or most appropriate weather station and soil type. Later, temperature was adjusted using the FAREAST model to simulate climate change scenarios (Chapter 4). The study builds on a comparison of modeled and remotely sensed land covers in strictly protected reserves (*zapovedniks*) in southeastern Russian Far East (Sherman *et al.*, 2012).

Like modeling, remote sensing offers a hypothesis of reality. Ratios of canopy height to biomass produced by the model were compared with canopy height: biomass relationships developed from Light Detection and Ranging (LiDAR) data from the Geoscience Laser Altimeter System (GLAS)

instrument on NASA's Ice, Cloud, and Land Elevation Satellite (ICESAT) to reinforce the confidence with which these tools can be used. Accurate measurement of biomass is a pressing scientific need in order to create better carbon metrics, which will increase the precision and accuracy of climate modeling and help the effort to develop options to address climate change.

These studies were based in the southeastern Russian Far East, the last remaining range of the Amur, or Siberian, tiger. All tiger subspecies are endangered, and only 3,200 are estimated in the wild, down from about 100,000 across Asia around 1900 (Wikramanayake *et al.*, 2011). The Amur tiger's range is the farthest north and supports the lowest density of all the tiger subspecies, existing in an unusually biologically diverse region on the eastern coast of Russia. Amur tiger range in Russia extends south-to-north from about 42 – 50 °N latitude and east-to-west from the Sea of Japan to the Amur River and, further south, to the border of Jilin and Heilongjiang Provinces in northeastern China (Miquelle *et al.*, 1999; Hebblewhite *et al.*, 2012).

The Russian Far East represents an excellent location to study the effects of climate change because much of the landscape is forested, pristine, and undeveloped, and plant and animal biodiversity is unusually rich. The area represents a mix of forest zones: the northern boreal forest zone, dominated by larch, and, further south, spruce, gradually gives way at latitudes 46 – 50° N to mixed hardwood-conifer forests of the temperate zone (Krestov, 2003). The large and well-studied populations of felids and ungulates, and developing knowledge bank regarding vegetation, facilitate analysis of the impact of climate change at multiple levels.

In this region, tigers are part of a complex trophic web. Tigers have large caloric needs and studies demonstrate that, while they eat many things -- deer, wild boar, small mammals, fish,

amphibians, and seaweed, for example -- their key prey are red deer (*cervus elaphus*) and wild boar (*sus scrofa*)(Miquelle *et al.*, 2010a&b). The presence of these and other ungulate prey is associated with forests containing Korean pine (*Pinus koraiensis*) and Mongolian oak (*Quercus mongolica*), seeds of which provide important energy and nutrition, especially during cold and snowy winters (Miquelle *et al.*, 2010a). While protection from poaching is an immediate and high-priority need, preservation of forests and, in particular, tree species on which tiger prey depend is both a current and long-term need, in light of logging and climate change pressures.

In preparation for the climate change analysis, data from field research at eleven sites in tiger range were compared with model output (Chapter 3) in order to examine model results with respect to small-scale field observations in the temperate forests of the Russian Far East. Field measurements were taken at Ussurisky Reserve near Vladivostok in southern Primorskiy Krai, in Sikhote-Alin Biosphere Reserve in Central Sikhote-Alin, and at Bolshekhokhtsirskiy Reserve near Khabarovsk in Khabarovsk Krai.

Chapter 4 examines the likely impact of climate change predicted in fossil-fuel emission scenarios developed by the Intergovernmental Panel on Climate Change (IPCC, 2007) on forest structure and forest species composition in Amur tiger habitat, and possible results for the Amur tiger. Two scenarios were utilized: 1. B1, in which the world population peaks mid-century and then starts to decline, national economies are increasingly service- and information-based, and resource-efficient and “clean” technologies are adopted, and 2. A1F1, based on rapid global economic growth, fossil-fuel intensive energy sources, increasing technological efficiency, and the same world population pattern as the B1 scenario.

Most conservation and research resources are focused on current threats. Fewer are looking at the impact of climate change across time. Climate change effects will ripple through ecosystems, affecting flora as well as fauna. Warmer and drier conditions have already been associated with the disappearance and presumed extinction of amphibians, insects and plants (Parmesan, 2006, 2007). Changes are occurring in the timing of flowering and fruiting, which can reduce or eliminate critical resources for species that are dependent on pollen, seeds and fruits from these species (Parmesan, 2006, 2007; McKinney *et al.*, 2012). The loss of a keystone or umbrella species, or temporal changes in reproductive patterns, can set in motion a chain of excess or depleted populations and critical nutrient deficiencies that can affect range choices, migrating species, and long-term patterns of evolution.

1.1 REFERENCES

Hebblewhite MF, Zimmerman F, Li Z *et al.* (2012) Is there a future for Amur tigers in a restored tiger conservation landscape in Northeast China? *Animal Conservation*, 1469-1795.

IPCC (2007) *Climate Change 2007. Impacts, Adaptation and Vulnerability. Contribution of Working Group II to the Fourth Assessment Report of the Intergovernmental Panel on Climate Change* (eds Parry M, Canziani O, Palutikof J, van der Linden P, Hanson C), pp. 479, 484. Cambridge University Press, Cambridge, UK.

Krestov PV (2003) Forest Vegetation of Easternmost Russia (Russian Far East). In: *Forest Vegetation of Northeast Asia* (eds Kolbek T, Strutek M, Box EO) Kluwer, New York.

McKinney AM, CaraDonna PJ, Inouye, DW *et al.* (2012) Asynchronous changes in phenology of migrating Broad-tailed Hummingbirds and their early-season nectar resources. *Ecology*, **93**, 1987 – 1993.

Miquelle DG, Merrill TW, Dunishenko YM *et al.* (1999) A habitat protection plan for the Amur tiger: developing political and ecological criteria for a viable land-use plan. In: *Riding the Tiger* (eds Seidensticker J, Christie S, Jackson P), pp. 273-295. Cambridge University Press, Cambridge.

Miquelle DG, Goodrich JM, Kerley L *et al.* (2010a) Science-based Conservation of Amur Tigers in the Russian Far East and Northeast China. In: *Tigers of the World 2nd Edition* (eds Tilson R, Nyhus P), pp. 403 – 423. Elsevier Inc., London.

Miquelle DG, Goodrich JM, Smirnov EN *et al.* (2010b) Amur tiger: a case study of living on the edge. In: *Biology and Conservation of Wild Felids* (eds MacDonald DW, Loveridge AJ), pp. 325-339. Oxford Press, Oxford.

Parmesan C (2006) Ecological and Evolutionary Responses to Recent Climate Change. *Annual Review of Ecology, Evolution, and Systematics*, **37**, 637-639.

Parmesan C (2007) Influence of species, latitude and methodologies on estimates of phenological response to global warming. *Global Change Biology*, **13**, 1860 – 1872.

Sherman NJ, Loboda TV, Sun G, Shugart HH (2012) Remote Sensing and Modeling for Assessment of Complex Amur (Siberian) Tiger and Amur (Far Eastern) Leopard Habitats in the Russian Far East. In: *Remote Sensing of Protected Lands* (ed Wang YQ), pp. 379 – 407. CRC Press, New York.

Wikramanayake E, Dinerstein E, Seidensticker J *et al.* (2011) A landscape-based conservation strategy to double the wild tiger population. *Conservation Letters*, 1-9.

CHAPTER 2. COMPARING REMOTE SENSING AND COMPUTER MODELING TO ANALYZE A BIOLOGICALLY DIVERSE AND TOPOGRAPHICALLY COMPLEX LANDSCAPE IN THE RUSSIAN FAR EAST

ABSTRACT

Remote sensing and computer-based succession modeling allow characterization of forest structure and composition in vast and inaccessible areas. Comparing remotely sensed results with output from a validated model also permits assessment of the consistency of these techniques and increases the confidence with which they can be used. Comparing the two outputs also may offer a new method to identify areas of disturbance in a complex and biologically diverse landscape.

In this study, forest vegetation covers and the ecological metrics of basal area, biomass, and canopy height, all derived from remote sensing, were compared with output from the boreal forest gap model FAREAST (Yan and Shugart 2005). FAREAST results matched remote-sensing-based land covers at 392 of 1000 points (39%). Comparing remotely sensed with modeled land covers suggested that disturbance occurred at 461 of the 608 points (76%) where forest types differed. The mathematical relationship between canopy height and biomass for the two approaches was affirmed.

Although seemingly consistent forest types cover the study landscape, the mosaic nature of forests dictates that ground-truthing may be needed in addition to comparison of remotely sensed and modeled results to determine the status of sites that appear to have experienced disturbance.

2.1 INTRODUCTION

Remote sensing and computer-based succession modeling allow characterization of forest structure and composition in vast and inaccessible areas (Lauenroth *et al.*, 1993; Shugart, 1998; Dubaya & Drake, 2000; Drake *et al.*, 2002; Hudak *et al.*, 2002; Lefsky *et al.*, 2002, 2005, 2007; Patenaude *et al.*, 2005; Boudreau *et al.*, 2008; Shugart *et al.*, 2010). Comparing remotely sensed results with output from a validated model permits assessment of the consistency of these techniques and increases the confidence with which they can be used. Comparing the two outputs may also offer a new method to identify areas of disturbance in a complex and biologically diverse landscape.

In this study, forest vegetation covers and ecological metrics derived from remote sensing, such as biomass and canopy closure, were compared with output from the boreal forest gap model FAREAST. Identifying areas where disturbance has occurred is valuable in order to estimate forest stocks of valuable tree species and carbon quantity, to analyze landscapes utilized by wildlife, to understand fire and logging impacts, and potentially to identify areas for commercial activities, such as agriculture and logging (Cushman and Wallin, 2000; Kerr and Ostrovsky, 2003; Hyde *et al.*, 2006; Loboda *et al.*, 2012). Causes of forest disturbance in the Russian Far East include wildfires, logging, community development, and agriculture, transportation corridors, such as highways, roads, and railways, storms and snowfall, and natural tree

senescence (Ishikawa *et al.*, 1999; Cushman and Wallin, 2000; Newell, 2004; Nakamura and Krestov, 2005; Loboda *et al.*, 2012).

In the first part of the project, forest land cover types derived from remote sensing were compared with modeled results at 1,000 points selected at random across the region. The model simulates an old-growth forest, whereas remotely sensed data reflects current conditions. Remote-sensing-based land covers also were compared with field results at eleven field locations. My hypothesis is that comparing the two outputs, and considering typical stages of forest succession, will assist in identifying areas where disturbance may have occurred.

In the second part of the project, satellite-borne Light Detection and Ranging (LiDAR) was used to explore forest structure in this area. The relationship between canopy height and biomass derived from LiDAR data was compared with the tree height-to-biomass ratio estimated by the FAREAST model. Highly consistent forest height to biomass relationships would reinforce the usefulness of these tools to calculate biomass from canopy height.

This research expands on previous studies that compared remotely sensed data with modeled results in strictly protected forest reserves (*zapovedniks*) (Sherman *et al.*, 2012) by refining analytical techniques and including all of Amur tiger range rather than just protected areas.

2.2 BACKGROUND

The area of study extends from 42.51°N to 51.35°N latitude and from 130.48°E to 140.63°E longitude along the coast of the Sea of Japan in the Russian Far East (RFE). Most of this territory is in the Russian provinces, or *krais*, of Primorskiy (or Primorye), and southern Khabarovski. It is bordered by the Sea of Japan to the east, the People's Republic of China to the west, and the Democratic People's Republic of Korea (DPRK – North Korea) to the southwest (Figure 2.1). An extensive network of streams and rivers, including the northeastward flowing Amur River, which marks the Russia-China border, drain the area (Rosenberg *et al.*, 1998; Newell, 2004).



Fig. 2.1 Primorskiy and Khabarovski Krai, with Amur tiger range. Source: Wildlife Conservation Society

The Sikhote-Alin Mountains extend about 1200 miles along the length of the region and create a rugged, topographically varied landscape (Rosenberg *et al.*, 1998; Ishikawa *et al.*, 1999). The mountain range was formed by volcanic activity and earth surface folding during the late Cretaceous period (144 - 66 mybp) (Krestov, 2003; Hickman *et al.*, 2003). Mountain height is generally about 500 - 800 meters above sea level (m asl) (Miquelle *et al.*, 2010c), and usually doesn't exceed 1200 m asl. The highest peak is Mt. Tardoki-Yani (2077 m) (Rosenberg *et al.*, 1998). Foothills extend to the eastern Russian coast along the Sea of Japan, creating steep gradients and deep ravines (Qian *et al.*, 2003a).

The study area is one of the world's most biologically diverse, with about 2,000 plant species and many rare and endemic plants and animals (Qian *et al.*, 2003a; Newell, 2004; Krestov *et al.*, 2006). It is the only remaining natural habitat of the Amur, or Siberian, tiger (*Panthera tigris altaica*) (Miquelle *et al.*, 1999; Dinerstein *et al.*, 2007; Miquelle *et al.*, 2010a&b) and the Far Eastern or Amur leopard (*Panthera pardus orientalis*) (Uphyrkina *et al.*, 2002; Jackson and Newell, 2008; Hebblewhite *et al.*, 2011). Many other unique and rare plant and animal species exist in this region, such as the Asian black bear (*Ursus thibetanus*), Blakiston's fish owl (*Ketupa blackistoni*), and Mandarin duck (*Aix galericulata*) (Newell, 2004). The middle part of the study area, Central Sikhote-Alin, which includes the Sikhote-Alin Biosphere Reserve, has been designated as an UNESCO World Heritage Site because of rich plant diversity, many endemic and endangered species, and unusual plant and animal assemblages (UNESCO, 2013). The WWF has designated southeastern Russian Far East as a vulnerable Global 2000 Broadleaf and Mixed Forest Ecoregion (Olsen and Dinerstein, 2002)

About 70% of Primorye is forested (Miquelle *et al.*, 2010c), although legal and illegal logging is reducing forest cover rapidly (Rosenberg *et al.*, 1998; Krestov *et al.*, 2003; Newell, 2004). The major types of forest in this region are mixed broadleaf/pine/conifer, deciduous broadleaf, Mongolian oak/Black or Dahurian birch, and dark conifer (consisting mainly of fir and spruce) (Nakamura and Krestov, 2005). The study region includes cities and towns, agricultural and industrial areas, small villages and large logging operations. Commercial activities, except for logging and mining, are mostly concentrated in the south and west (Newell, 2004). For the comparison of remote sensing to modeled output, only sites in forested areas were selected.

The juxtaposition of the Asian continental climate with the ocean monsoonal climate south and east of the Sikhote-Alin Mountains leads to conditions that promote species richness, as does the region's geographic location at the intersection of boreal forests, Siberian taiga and temperate Manchurian forests (<http://whc.unesco/en/list/766>; Qian *et al.*, 2003b; Nakamura and Krestov, 2005).

Deciduous broadleaf forests of Mongolian oak (*Quercus mongolica*), Birch species (*Betula dahurica*, *B. mandshurica*), Amur linden (*Tilia amurensis*), Maple species (*Acer spp*), Ash (*Fraxinus mandshurica*) and other species occur at lower elevations (Krestov *et al.*, 2006). Predominantly Mongolian oak forests may grow on disturbed sites that previously supported Korean pine and mixed conifer/pine/broadleaf forests (Krestov *et al.*, 2006) (Figure 2.2).

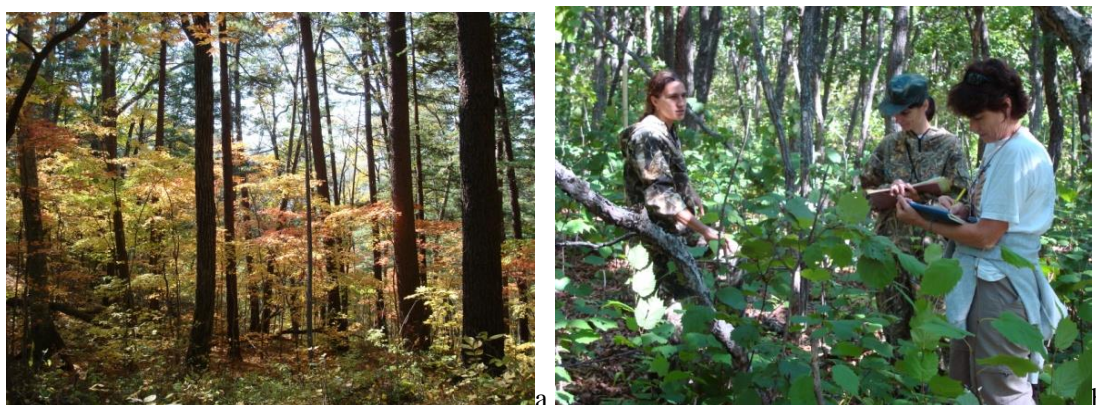


Fig. 2.2 a. Mixed deciduous broadleaf/Korean pine/conifer forest in Ussurisky Reserve, southern Primorskiy Krai, Russia. b. Secondary coastal oak forests in Sikhote-Alin Biosphere Reserve, central Primorskiy Krai. Photos: N. J. Sherman

In lower latitudes, Yezo spruce (*Picea ajanensis*) grows at altitudes up to 1500 – 2000 m (Krestov, 2003), and mixed deciduous broadleaf/Korean pine stands occur up to 1100 – 1200 m (Qian *et al.*, 2003a; Krestov, 2003; Nakamura and Krestov, 2005). In coastal areas in Central Sikhote-Alin, broadleaf/pine forests are found up to 400-500 m (Qian *et al.*, 2003a), Yezo spruce and Manchurian fir mix in with deciduous broadleaf/Korean pine at about 600 – 800 m asl, and Korean pine co-occurs with spruce and fir up to about 900 m. Above about 1200 m in the south and 400 m in the north, forests consist of fir and spruce alone (Nakamura and Krestov, 2005). The dark conifer forests extend northward to latitude 55° – 57 °N, where they give way to larch (*Larix dahurica*) deciduous conifer forests (Nakamura and Krestov, 2005) .

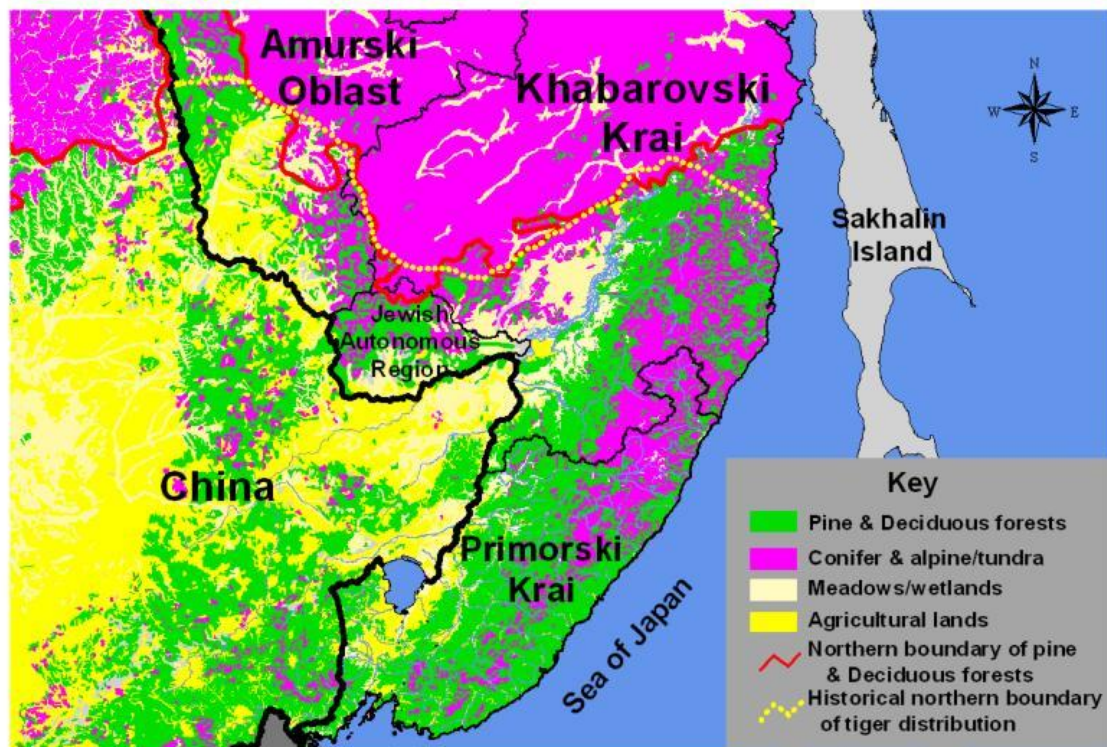


Fig. 2.3 Land covers of southeastern Russian Far East. Source: Wildlife Conservation Society, Russia program. Distribution of mixed pine/broadleaf and deciduous forests based on vegetation map (Sochavi, V. H., Soviet Academy of Sciences, 1968) and Landsat 5 imagery (V. V. Ermoshin, A. A. Murzin, V. V. Aramilev (Institute of Geography, Far Eastern Branch of the Russian Academy of Sciences) (Miquelle *et al.*, 2010b) Tiger distribution reconstructed from Heptner & Sludskii (1992).

2.2.1 Disturbance and succession

In addition to climate and topography, disturbance shapes Primorye forests. Logging and wildfire account for the greatest proportion of disturbance, followed by intense storms, wind, heavy snowfall and pest outbreaks (Rosenberg *et al.*, 1998; Cushman and Wallin, 2000; Loboda *et al.*,

2012). These forces influence forest composition by creating gaps in the forest canopy that allow light to penetrate to the forest floor. Light availability can determine forest structure by facilitating or inhibiting tree growth (Watt, 1947; Shugart, 1984; Shugart, 1998; Shugart *et al.*, 2010).

2.2.2 *Climate*

Climate is an important determinant of forest composition and structure, especially in mesic forests, and is a critical model parameter (Lauenroth *et al.*, 1993; Krestov, 2003; Shugart, 1998; Cheng and Yan, 2009; Zhang *et al.*, 2009). Primorye is bisected by the Sikhote-Alin Mountains into two climate regimes: a humid submarine ocean monsoonal climate to the east of the mountains, and a continental climate, with colder winters and hotter summers, on the western side of the mountains (Krestov, 2003; Qian *et al.*, 2003a; Miquelle *et al.*, 2010c).

In the southernmost part of this area, near Vladivostok (43° N, 132° E), average annual temperature is about 1.4 °C, with an average of 21.0 °C in the warmest month and –13.5 °C in the coldest month (Nakamura and Krestov 2005). Annual precipitation (1966 – 1971) is about 800 mm.

In the central coastal area near SABZ (46° N, 137° E), annual temperature is 2.3 °C, with a peak in August at about 17 - 20 °C. Average temperature in January is -14 to -10.0 °C (Ishikawa *et al.*, 1999; Qian *et al.*, 2003b; Nakamura and Krestov, 2005; Miquelle *et al.*, 2010c). In continental areas west of the Sikhote-Alin Mountains, summer temperatures are about 5° C warmer and

winter temperatures are about 10 °C cooler than near the coast (Nakamura and Krestov, 2005; Qian *et al.*, 2003a).

Annual precipitation in the central coastal area is about 800 - 900 mm. More than 75% of rainfall occurs in April through November (Miquelle *et al.*, 2010c). Annual precipitation is about 300 mm lower inland than in coastal areas (600 mm vs. 800 – 900 mm, respectively) (Qian *et al.*, 2003a), and peak precipitation in coastal areas occurs in August (Ishikawa *et al.*, 1999; Qian *et al.*, 2003a).

In the north at Khabarovsk (49° N, 135° E), average annual temperature is 1.4° C, the warmest month averages 21.1 C, and the coldest month averages about -22.3. Annual precipitation (1966 - 1971) in the north at Khabarovsk is 569 mm (Nakamura and Krestov, 2005).

2.2.3 *FAREAST Model*

FAREAST simulates a mostly undisturbed forest, except for natural tree mortality and the creation of gaps in the canopy. The model was developed and verified along altitudinal gradients in the montane forests of Changbai Mountain in Jilin Province in northeastern China. It is derived from the NEWCOP model, which was developed to test the sensitivity of Changbai Mountain forests to climate change (Yan & Shugart, 2005; Yan & Zhao, 1996). The model was validated at 31 sites in Far Eastern Russia, where simulated results matched forest inventory data at 23 sites in terms of the four dominant tree genera by biomass. Of the eight sites that didn't match, simulated results were close to observed at three sites. At another four of the eight sites, sparse larch (*larix*)

forests occurred, with atypical hydrological conditions, i.e. permafrost with impeded soil drainage (Yan and Shugart, 2005).

2.2.4 GLAS LiDAR

In the second part of the study, I compared canopy height derived from the Geoscience Laser Altimeter System (GLAS) instrument on NASA's Ice, Cloud, and Land Elevation Satellite (ICESAT) with simulated results from FAREAST. The purpose was to verify a consistent quantitative relationship between canopy height and aboveground biomass. Tree dimensions such as height and volume are factors in tree growth, competition, photosynthesis, and, ultimately, forest structure, and therefore can be related to biomass, carbon production and carbon sequestration (Shugart, 1984; Lauenroth *et al.*, 1998; Shugart, 1998; Shugart *et al.*, 2010). Consistency between modeled and remote sensing results would affirm the mathematical relationship used to derive biomass from canopy height for both the remotely sensed and modeled approaches (Lefsky, 2002; Lim *et al.*, 2003; Shugart *et al.*, 2010; Van Leeuwen *et al.*, 2010; Sherman *et al.*, 2012)

GLAS is a Light Detection and Ranging (LiDAR) instrument that was designed to measure minute (to 15 cm accuracy (Shugart *et al.*, 2010)) changes in the elevation of ice sheets in order to better understand the impact of climate change on ice and ice melt (Zwally *et al.*, 2002; Schutz *et al.*, 2005).

GLAS also was able to measure the height and vertical structure of clouds and aerosols, surface topography, and forest canopy height (Zwally *et al.*, 2002). It operated in the 1064 nm wavelength, which is considered optimal for measuring forest biomass and structure (Shugart *et al.*, 2010). The orbit altitude was 600 km, with a 94 degree inclination and a 183-day repeat period (Zwally *et al.*, 2002). ICESAT was launched in January 2003 (Lefsky *et al.*, 2002), decommissioned in 2008 (Lefsky *et al.*, 2002), and re-entered the atmosphere in 2010 (Nelson, 2010).

LiDAR is an active remote sensing system that deploys and recaptures photons to assess surface characteristics. The round-trip time of a laser pulse is measured from emission until the reflected energy is detected. Multiplying this travel time by the speed of light gives the round trip distance to the target. Half of this produces distance to the target, such as ground or tree top. The difference between measurements at the top of the canopy and those at ground level represents the canopy height (Sun *et al.*, 2008; Sherman *et al.*, 2012). The level-1 products GLA01 (waveform) and level-2 product GLA14 (land/canopy elevation) were used in this study. Gaussian peaks, which represent points of reflectance of the laser pulse and therefore the general shape of the canopy, were fitted to the waveform. The difference between the beginning of the waveform signal and the lowest and last Gaussian peak, which is considered to represent the ground, is the maximum canopy height. Up to six Gaussian peaks can fit to a waveform. Characteristics of the canopy structure can be determined with appropriate software (Figure 2.4) (Dubayah and Drake, 2000; Hudak *et al.*, 2002; Lefsky, 2002; Lefsky *et al.*, 2007; Sun *et al.*, 2008; Shugart *et al.*, 2010; Sherman *et al.*, 2012).

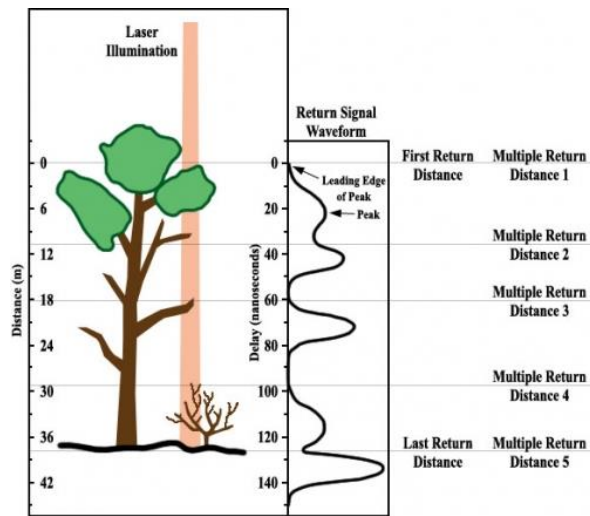


Fig. 2.4 Analysis of a GLAS waveform. The distance from the beginning of the signal to the first peak (ground peak) is the top of the canopy (Source: www.intechopen.com).

LiDAR provides the advantage of being able to measure forest structure, whereas passive sensors, such as Landsat Thematic Mapper (TM) and Landsat Enhanced Thematic Mapper Plus (ETM+) see only top surfaces (Hyde *et al.*, 2006). This allows measurement of forest characteristics with spatial and temporal consistency in remote areas and across large landscapes, an advantage over field-based estimates (Boudreau *et al.*, 2008). Basal area, aboveground biomass and carbon can be estimated from LiDAR-derived vertical canopy height and profile data using allometric equations (Dubayah and Drake, 2000; Drake *et al.*, 2002; Lefsky *et al.*, 2002; Lim *et al.*, 2003; Lefsky *et al.*, 2005; Hyde *et al.*, 2006; Sun *et al.* 2008; Shugart *et al.*, 2010; Sherman *et al.*, 2012).

Measurements of forest structure can assist in the study and management of wildlife (North *et al.*, 1999; Hyde *et al.*, 2006). For example, LiDAR has demonstrated the ability to distinguish between primary and secondary forests based on canopy structure (Hudak *et al.*, 2002; Drake *et al.*, 2002), which means that LiDAR can be a tool to identify old growth forests (Sherman *et al.*, 2012). Old growth forests are suitable for certain wildlife species such as the spotted owl (*Strix occidentalis*) and the Cerulean warbler (*Setophaga cerulea*) (North *et al.*, 1999; Birdlife International, 2012).

2.3 MATERIALS AND METHODS

Simulated results were compared with observed forest types at 1,000 points selected at random by computer across the southeastern Russian Far East (Figure 2.5). At each point, forest types outputted by the FAREAST model were compared with forest cover types derived using remote sensing. Elevation, aspect and observed forest cover were developed for each point by T. V. Loboda, Dept. of Geography, University of Maryland (Sherman *et al.*, 2012).

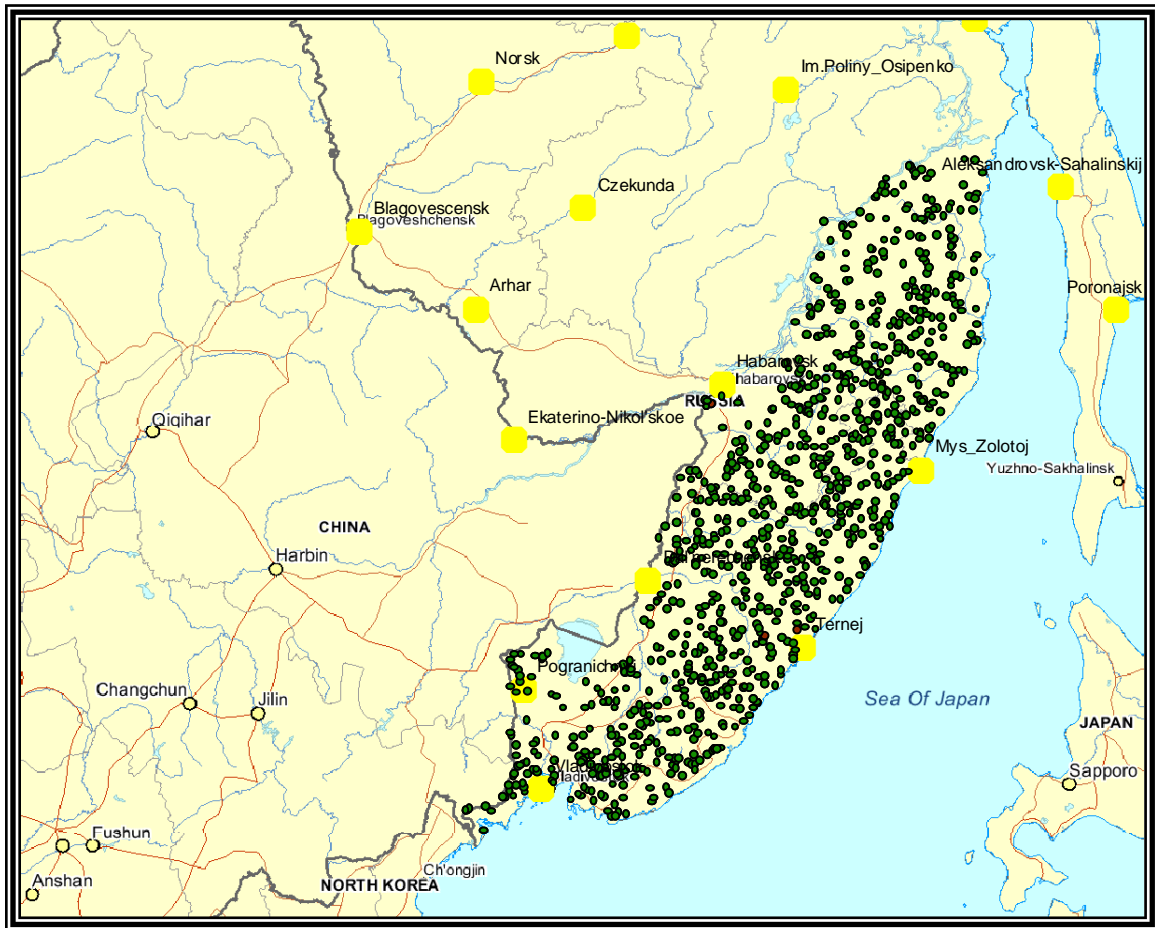


Fig. 2.5 The FAREAST model was calibrated for temperature and precipitation data from local weather stations (yellow dots) at 1,000 points (green dots) across the southeastern RFE and processed on the UVA computer cluster system. Results were compared with remote sensing (MODIS) based estimates of basal area and forest cover (Sherman *et al.*, 2012).

For the remote sensing – based consensus approach, forest cover categorization was based on forest canopy composition. Forest covers at each of the points were derived from a fusion of three sets of coarse-resolution data: 1. the Moderate Resolution Imaging Spectrometer (MODIS)

land cover product (MOD12Q1 collection4) (Friedl *et al.*, 2002); 2. Global Land Cover 2000 (GLC2000) map (Bartalev *et al.*, 2003); and 3. map of Russian forests (Bartalev *et al.*, 2004). Areas of agreement in forested landscapes were identified, and the data sets were combined to minimize differences associated with individual products and maps with respect to spatial resolution, mapping algorithm errors, and map legends. From these data sets, six forest types were developed: 1. Dark coniferous; 2. Larch; 3. Pine; 4. Mixed broadleaf/pine/conifer; 5. Deciduous broadleaf; 6. Siberian dwarf pine. Forest type was assigned based on data indication of at least 60% of the canopy being consistent with the assigned type (Loboda, 2009a; Sherman *et al.*, 2012).

An ESRI ArcGIS map of vegetation in the southeastern RFE also was used to compare forest types (Figure 2.3). The map was developed from Landsat 5 imagery (V. V. Ermoshin, A. A. Murzin, V. V. Aramilev (Institute of Geography, Far Eastern Branch of the Russian Academy of Sciences) and a forest vegetation map (Sochavi, V. H., Soviet Academy of Sciences, 1968) (Miquelle *et al.*, 2010). The ArcGIS image was made available by the Wildlife Conservation Society Russia program and adapted for use in Sherman *et al.*, 2012.

2.3.1 *FAREAST model parameterization*

The FAREAST model simulates the growth, death and regeneration of individual trees on a 0.05 hectare (500 m²) plot, which represents the gap created in the forest canopy when a large tree

falls. At each site, FAREAST processes 200 plots and averages the results for biomass, basal area, stem count and other characteristics.

FAREAST model input includes species characteristics for 44 tree species found in the southeastern RFE. Characteristics include maximum height, maximum diameter at breast height (1.3 m)(dbh), growing degree days required, drought, shade and low nutrient tolerance, and other characteristics (See Yan and Shugart, 2005, for more species parameters). Only tree species found in the southeastern Russian Far East were used for the model's species input parameter because of the statistical weight associated with species presence and proximate seed deposition. Having a local seed source at a site greatly increases the likelihood of persistence of that species in that location as compared with species that might tolerate local soil and climate conditions, but are not found in the region (Horn, 1974; Horn *et al.*, 1975; Horn, 2002).

FAREAST incorporates four sub-models: GROWTH, REGENERATION, MORTALITY and ENVIRON. GROWTH, REGENERATION, AND MORTALITY are based on species-specific vegetation characteristics that are applied to each simulated tree, such as maximum age and size, tolerance of shade, drought and temperature extremes, and rate of growth. ENVIRON calculates daily temperature and precipitation, from which it estimates soil moisture and soil nutrients (carbon and nitrogen).

The GROWTH sub-model is based on the optimal diameter increment formula and actual diameter increment formula of Botkin *et al.* (1972) and Leemans & Prentice (1989). The

relationship between tree height and diameter is based on formulas used in the FORSKA model (Leemans & Prentice, 1989), and is:

$$H = 1.3 + (Hm - 1.3) \cdot \left(1 - \exp\left(\frac{sDBH}{Hm - 1.3}\right)\right) \quad (1)$$

The rate of tree growth depends on light availability, climate, soil conditions and competition with other species. Tree growth is calculated on an annual time-step as a function of changes in diameter at breast height (dbh) and clear branch bole height (CH).

Climate information from the U.S. National Oceanic and Atmospheric Administration (NOAA) National Climatic Data Center (NCDC) was applied to each random point and each GLAS point. These data include temperature, precipitation, and standard deviation for both temperature and precipitation based on daily fluctuation around monthly averages. Temperature and precipitation data were applied from the World Meteorological Organization (WMO) weather station most likely to have reliable data and similar weather, based on proximity and topography. Data from weather stations at Vladivostok, Terney and Khabarovsk were considered more continuous and reliable, being associated with centers of scientific research, than data from Dalnerecensk and Pogranichy, which also were in the area, so the former were used when topography and proximity didn't suggest a clear choice.

The altitude adjustment feature of the model was not used for this study because the humid coastal conditions of Central Sikhote-Alin are not consistent with the adiabatic lapse rate used in

the model. Altitude-adjusted model output in the Sikhote-Alin coastal area tended to reflect vegetation that normally would occur at a higher elevation. The model makes a slight adjustment for latitude based on the angle of the sun.

Model processing was performed using the University of Virginia (UVA) computer cluster, a Linux-based large memory system managed by the UVA Alliance for Computational Science and Engineering. The FAREAST model processed data simulating 300 years of succession, representing the old growth forests in the area. Forest covers were defined using the International Global Biosphere Program (IGBP) classification system and were assigned when a forest type comprised more than 60% of basal area. A combination of fir, spruce and pine species was considered Dark Conifer. Broadleaf forests consisted of deciduous species including Mongolian oak (*Quercus mongolica*), Amur linden (*Tilia amurensis*), Chinese or Korean birch (*Betula costata*), Japanese White or Paper birch (*Betula Platyphylla*) and maple species (*Acer spp*). If neither dark conifer nor broadleaf species made up more than 60% of basal area, the forest type was considered to be Mixed broadleaf deciduous/Korean pine/conifer. Sites with basal area greater than 60% larch, pine, and Siberian dwarf pine did not occur in the simulation, so these species were assigned to Dark Conifer or Mixed forest categories, as appropriate. For more details about the FAREAST model, see Yan and Shugart 2005.

2.3.2 Comparison of GLAS results with simulated metrics

Biomass and canopy height estimated from GLAS data at 988 points along the ICESat track in the study area (Figure 2.6) were compared with simulated biomass (tC/ha) and canopy height based on the average height of the tallest tree at each site. In FAREAST, biomass was calculated as a function of diameter at breast height (dbh, 1.3 m), clear bole height (base of the canopy) diameter, and tree growth rate. Simulated wood biomass was halved to get carbon biomass in tons per hectare.

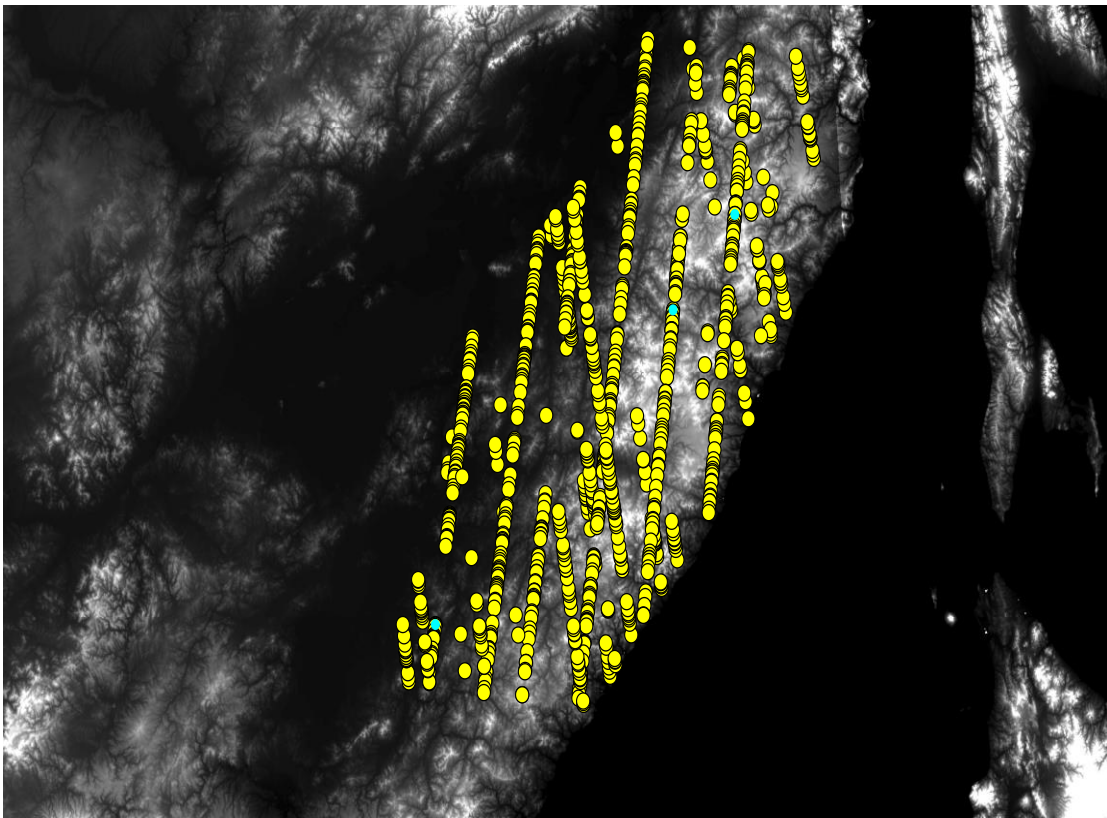


Fig. 2.6 The FAREAST model was run at 988 points on the UVA computer cluster system and results were compared with LiDAR based estimates of biomass and canopy height.

The GLAS footprint is about 65 m in diameter, which is about 2.5 times greater than the diameter and 6.6 times the area of the FAREAST plot size (0.05 ha). Neural networks (Kimes *et al.*, 1998, Kimes *et al.*, 2006) were used to identify the most accurate relationship between GLAS data and measured forest biomass. The neural network approach identifies the linear or non-linear function that has the highest R^2 and lowest root mean square error. The function, in this case non-linear, became the model for predicting biomass based on canopy height at the 988 GLAS footprint points. For more details on neural networks and how GLAS data was processed, see Sun *et al.* (2008) and Sherman *et al.* (2012).

2.3.3 *Assessing fire probability at potentially disturbed sites*

Sites where disturbance might have occurred based on the difference between remotely sensed and modeled results at the 1,000 random points were compared with the probability of fire occurrence using fire probability surfaces developed by Loboda (2009a&b) to test the likelihood that fire might have caused the disturbance.

Fire occurrence probability is based on MODIS data from 2001 – 2005 and validated against 2006 fire occurrence in the RFE (Sherman *et al.*, 2012). Disturbance is considered possible where observed results indicate a forest at an earlier stage of succession than modeled results. For the protocol used to develop the fire occurrence probability surfaces, see Loboda (2009b).

2.4 RESULTS

Results from the forest succession model FAREAST (Yan and Shugart, 2005) were compared with observed forest covers for comparison with observed at the 1,000 random points. The forest cover type derived from remotely sensed and consensus data matched forest type predicted by the FAREAST model at 392 out of 1000 points (39%) (Table 2.1). Broadleaf forests accounted for the greatest proportion (43%) of matching cases, followed by dark coniferous forests (39%), and then mixed broadleaf/pine/conifer (18%).

Table 2.1 Comparison of simulated and remote-sensing-based forest types

<u>Forest cover type</u>	<u>No. of sites</u>	<u>Matches</u>	<u>Match % (out of 392)</u>
Overall	1000	392	39%
Dark coniferous		152	39%
Broadleaf		169	43%
Mixed brdlf/pine/con		71	18%
Larch	0	0	0

The match rate for the study area is slightly lower than the match rate found within protected areas (43%) (Table 2.2)(Sherman *et al.*, 2012), as might be expected, since protected areas are

more likely to contain the primary, old growth forests that the FAREAST model simulates. Of the 146 points/sites where remote sensing and modeled results show dark conifer forests, containing mostly Yezo spruce and Manchurian fir, 80 (55%) were at sites where elevation was above 800 meters, the elevation at which dark conifer forest could be expected in most parts of the study area (Krestov, 2003; Qian *et al.*, 2003a; Nakamura and Krestov, 2005). Of these, 23 (29%) had a northeastern, northern, or northwestern aspect, which would have cooler and moister soils than south-facing slopes, conditions that would favor dark conifer forests (Van Cleve and Vierick, 1981).

Table 2.2 Results of comparing remotely-sensed forest types with modeled at sites in protected areas.

	# of sites	# of FAREAST plots (200/site)	Match %
1000 Random points	1,000	200,000	39
Bolshekhkhtsirskiy Reserve	3	600	67
Lazovsky Reserve	4	800	50
Sikhote-Alin Reserve	15	3000	40
Ussurisky Reserve	1	200	0

Aspect did not affect the likelihood of a match between remotely sensed and simulated forest types. Points where forest cover type matched were split almost evenly by aspect (Table 2.2).

Different species and biomass amounts occurred on north-facing slopes compared with south, southeast, and southwest facing slopes, which might be attributed to greater exposure to sunlight, or insolation, which can cause increased evapotranspiration and drier soils (Van Cleve and Vierick, 1981; Shugart, 1998). These variations did not change the overall forest types, such as dark conifer, mixed pine/conifer/broadleaf, or deciduous broadleaf.

Table 2.3 Matches of forest cover by aspect (out of total number of random points with the specified aspect)

<u>Aspect</u>	<u>Total sites/points with aspect</u>	<u># of matches</u>	<u>% (out of 392)</u>
North-NE-NW	252	97	38
South-SE-SW	217	85	39
East	282	118	42
West	247	93	38

2.4.1 Canopy height – biomass relationship

The relationship of canopy height to biomass derived from GLAS data shows continuity with the tallest tree to biomass relationship developed from FAREAST output (Figure 2.7). Comparison of the canopy height: biomass relationship for GLAS LiDAR with the FAREAST-derived relationship can be explained by an exponential trendline of $y = 6.317^{e^{0.1004x}}$, $R^2 = 0.9468$.

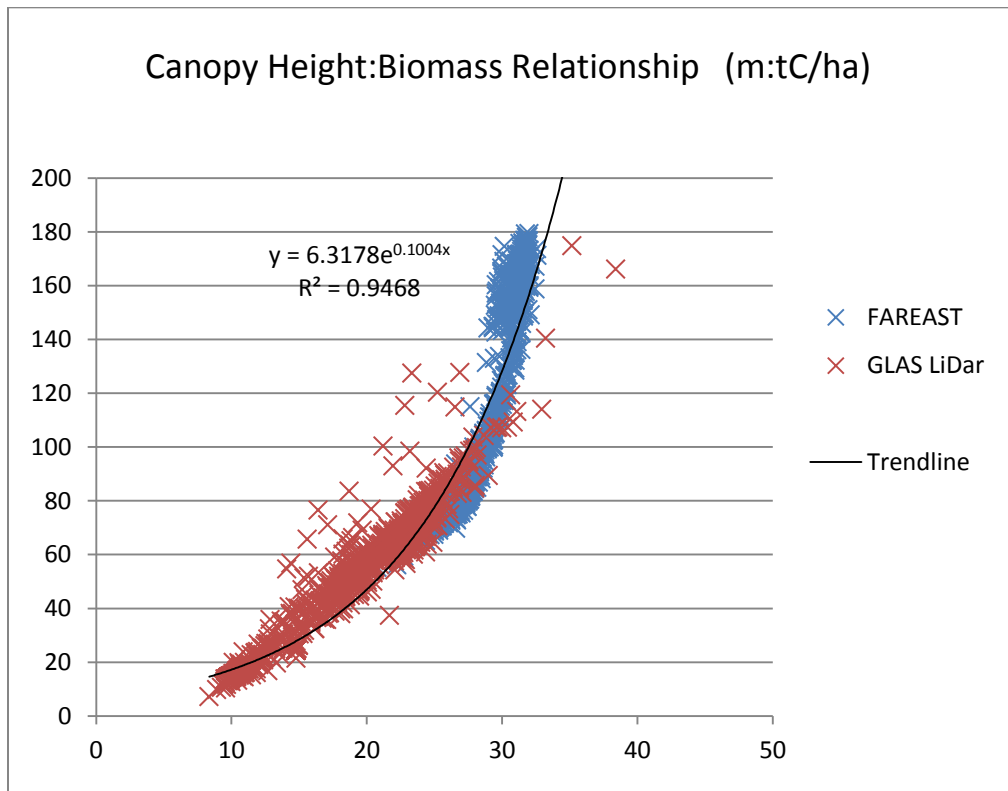


Figure 2.7 Relationship of canopy height to biomass derived from GLAS data to the simulated tallest tree: biomass relationship.

2.4.2 Fire probability at sites where disturbance may have occurred

The probability of fire occurrence at sites where disturbance is suggested by the comparison of modeling to remote sensing results comparison is slightly higher than the probability of fire for all sites. Fire occurrence also is slightly more likely at possibly disturbed sites than at sites where comparing modeled to remotely sensed results shows no sign of disturbance. Of the 461 points

where site disturbance is suggested based on comparison of the type of forest and likely stage of forest succession, the annual fire probability is greater than 1 in 1000 (.001) at 351 (76%) points. Fire probability is greater than 1 in 100 (.01) at 137 (35%) of these points. Average fire probability for all 461 points is 11.5 in 1000 (0.0115), and the average fire probability for sites where simulation and remote-sensing suggest the same forest type and less likelihood of disturbance is 9.51 in 1000 (.0095). Average fire probability for all 1,000 points is 10.24 out of 1,000 (0.01). Out of all the points, the highest probability is 197 (0.197).

Table 2.4 Assessment of fire risk potential at sites where simulated vs. observed forest covers suggest disturbance.

<i>Fire Risk at Potential Disturbance Sites (461 sites)</i>	
Fire risk	% of sites
>1 in 1000 (.001)	76%
>1 in 100 (.01)	35%
Highest possible risk: 0.197	

When areas with relatively high fire probability were found by both modeled and remotely sensing-based approaches to be broadleaf forests, it wasn't possible to tell if disturbance might have occurred.

The points with the greatest fire risk probability were located south of latitude 44.9° N, in the southern section of the study area (Figure 2.8), where temperatures are higher and more agricultural and commercial activity occurs.

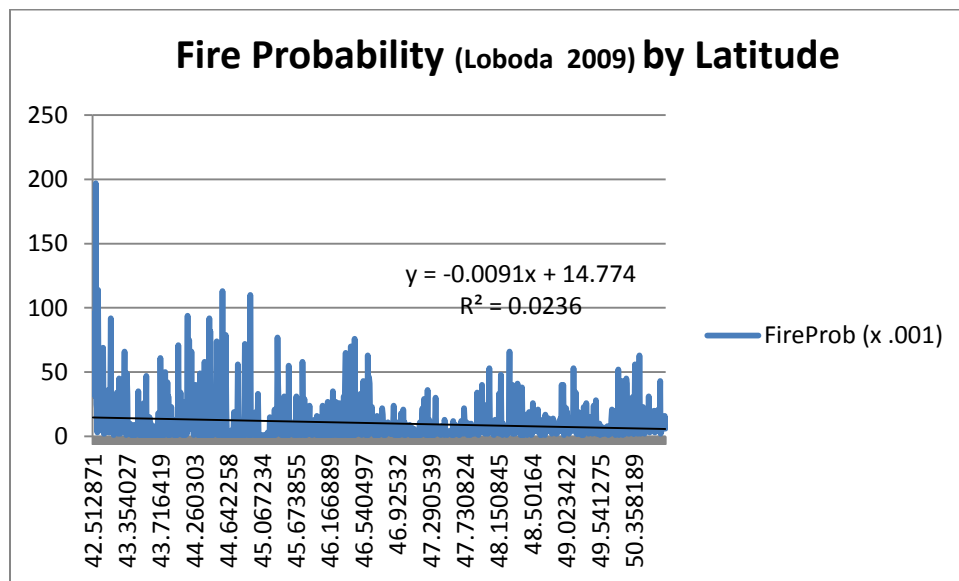


Figure 2.8 Fire probability increases as latitude declines.

2.5 DISCUSSION

This research compares simulated results with forested land covers developed from remote sensing and vegetation mapping to determine the consistency of the two approaches and to test a potentially efficient and spatially consistent way of discerning areas of disturbance. Comparing modeled with remotely sensed results potentially can highlight areas of disturbance because the model shows undisturbed forest, whereas remote sensing data represents “observed” forest,

showing the extant forest at the time data were collected. Identifying likely disturbed areas has many potential uses, including characterization of available future forest resources, calculating carbon stocks, and identification of areas that potentially will transform to a different ecosystem under predicted climate change scenarios (Loboda *et al.*, 2012).

The main types of disturbance in the study area are timber harvesting, fire (Loboda *et al.*, 2012), snow, and wind damage (Rosenberg *et al.*, 1998; Ishikawa *et al.*, 1999). Forests in the study area may re-grow slowly after disturbance (Krestov, 2003; Loboda *et al.*, 2012). For example, logged or fire-damaged areas, including dark conifer forests, may remain as grassland or shrub-dominated for 10 – 30 years after disturbance (Loboda, 2009; Nakamura & Krestov, 2005; Sherman *et al.*, 2012). In a deciduous broadleaf/Korean pine forest, the post-fire succession process can take centuries, and the original forest may never recur if a stable, “self-regenerating” ecosystem dominated by Mongolian oak or larch (*L. dahurica*) becomes established (Nakamura & Krestov, 2005).

In the first part of the study, composite forest covers derived from three sources -- MODIS land cover product (MOD12Q1 collection4) (Friedl *et al.*, 2002), the Global Land Cover 2000 (GLC2000) map (Bartalev *et al.*, 2003) and a map of Russian forests (Bartalev *et al.*, 2004) -- were compared with forest types outputted by FAREAST. These remote-sensing-based covers reflect current conditions, where burning, logging or development for agricultural, commercial, or community purposes may have occurred. FAREAST simulates a largely undisturbed forest, except for the creation of gaps in the canopy by tree mortality.

2.5.1 Forest succession and disturbance

Possible disturbance is indicated where observed results show an earlier stage of succession than modeled results (Figure 2.9). After a tree-stand destroying disturbance, such as clear cut logging or a severe fire, primary succession begins with pioneer (Chapin *et al.*, 2002) species, such as aspen and birch that are shade-intolerant and reproduce rapidly (Grime, 1979; Shugart, 1998). At lower and mid-level elevations (up to 800 – 900 m) in the Central Sikhote-Alin, early successional broadleaf forests give way to mixed broadleaf/Korean pine/conifer, with Korean pine as a dominant or co-dominant species (Nakamura and Krestov, 2005; Qian *et al.*, 2003a; Krestov, 2003). At higher elevations, such as 1500 – 2000 m at lower latitudes and at lower altitudes further north, Yezo spruce and Hinggan or Black fir (*Abies nephrolepis*) form the canopy of dark conifer forests in undisturbed areas (Zyryanova *et al.*, 2005; Nakamura and Krestov, 2005).

At 461 out of the 608 sites (76%), where simulated and remote-sensing-based forest types differed, simulated output represented a later stage of succession than the remote sensing approach, suggesting that disturbance may have occurred. For example, at 211 points, FAREAST indicated later successional mixed pine/conifer/broadleaf, while remote sensing shows deciduous broadleaf.

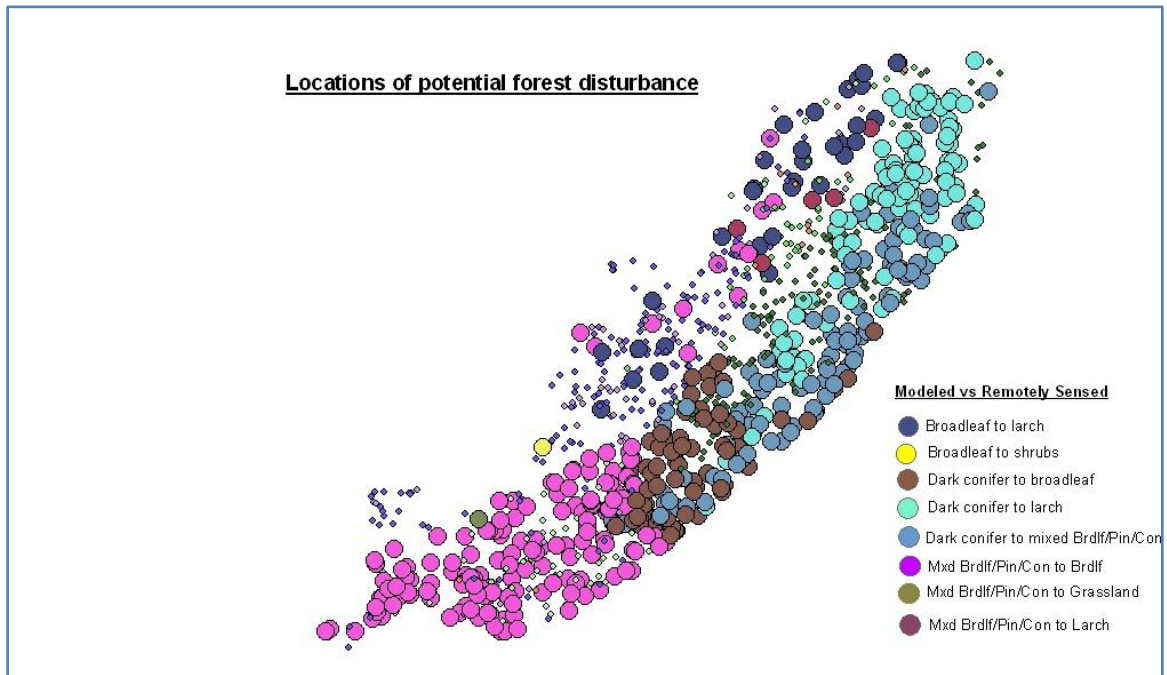


Figure 2.9 Locations of potential forest disturbance, based on comparison of remote sensing results (observed) with simulated (mature old growth).

Of 184 points or sites with elevation above 800 m asl, at 80 points (43%), both modeling and remote sensing approaches indicated dark conifer forests, as would be expected (Nakamura and Krestov 2005). Of 47 points above 800 m with a NW-N-NE aspect, with moister and cooler soils, 23 (49%) were identified as dark conifer using both approaches. At 282 points, modeling indicates a dark conifer forest, while the remote-sensing-based approach shows larch, mixed pine/conifer/broadleaf, or deciduous broadleaf, which suggests that disturbance has occurred.

Along the coast of the Sea of Japan in Central Sikhote-Alin, FAREAST indicates dark conifer or mixed forests that include Korean pine (Figure 2.9). In contrast, consistent with the literature, remote sensing data show coastal oak forests, a prevalent ecosystem in this area (Krestov, 2003;

Zyryanova *et al.*, 2005). Broadleaf forests have replaced mixed Korean pine/deciduous broadleaf in Central Sikhote-Alin after extensive timber harvesting since the 1920s, as well as fires near populated areas (Katsuta *et al.*, 1998; Krestov, 2003; Zyryanova *et al.*, 2005). Mongolian oak is a Role 1 species, which requires sunlight for regeneration and produces a gap when it dies (Shugart, 1984). In coastal oak forests, Mongolian oak forms a dense canopy that blocks sunlight from the forest floor and creates only a small opening in the canopy when it dies because the trees are stunted due to harsh conditions (Figures 2.2b, 2.10). However, the species is considered to be “self-regenerating” because it produces many seeds (acorns) and sprouts readily (Katsuta *et al.*, 1998; Zyryanova *et al.*, 2005; Kobayashi *et al.*, 2007), so growth can take place as soon as small gaps occur.



Fig. 2.10 Coastal oak forests have replaced Korean pine forests that were cleared or burned by early settlers.

Dense or sparse larch (*Larix spp*) was identified as a forest type at 143 points in the remote sensing approach (Figure 2.9), but did not dominate any forest categories in the FAREAST

results. This is consistent with Krestov (2003), who observed that larch does not play a large role in primary forests. Secondary larch forests can be found on level, moist soil near rivers (Krestov, 2003). Remote sensing also indicates larch forests close to areas of disturbance near Bolshekhokhtsirskiy Reserve, based on ArcGIS vegetation maps developed by A. A. Murzin and colleagues from remote sensing imagery (Figure 2.11).

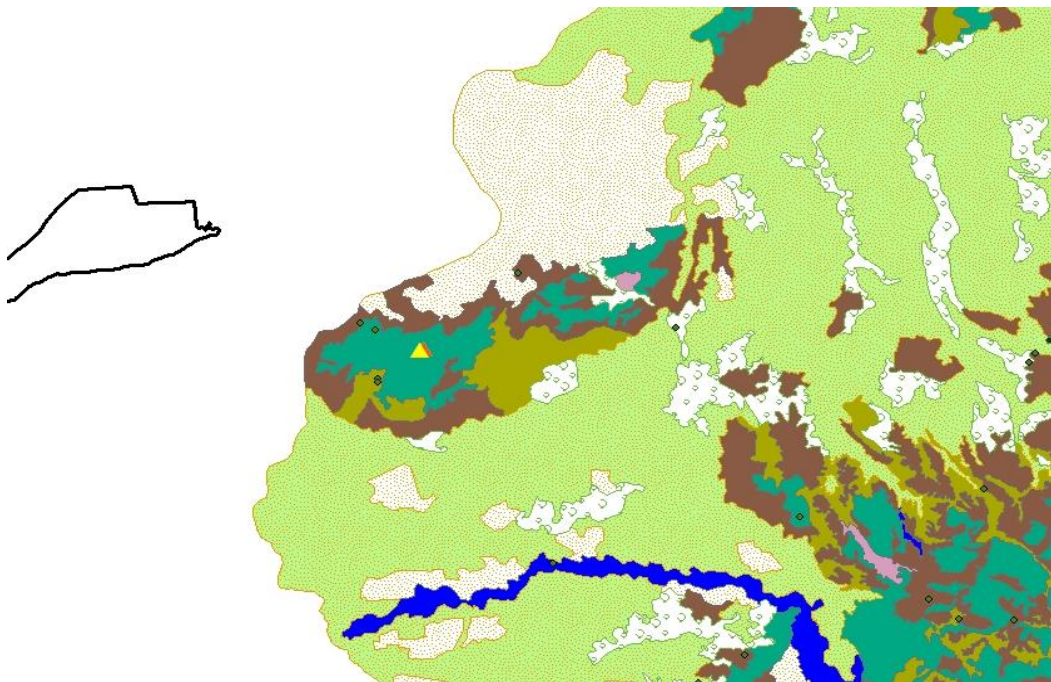


Figure 2.11 Larch (light green) and dark conifer (dark green) forests indicate disturbed area near Bolshekhokhtsirskiy Reserve. Triangles represent field sites, and green diamonds are random points. ArcGIS layer source: Wildlife Conservation Society, Russia program. Distribution of mixed pine/broadleaf and deciduous forests based on vegetation map (Sochavi, V. H., Soviet Academy of Sciences, 1968) and Landsat 5 imagery (V. V. Ermoshin, A. A. Murzin, V. V. Aramilev (Institute of Geography, Far Eastern Branch of the Russian Academy of Sciences)

At the remainder of the locations where FAREAST and remote sensing-derived results differed, FAREAST suggested forests at an earlier stage of succession than observed. For example, at Point 72 at 51.06° N, 138.57° E, with an elevation of 470 m, FAREAST output showed a broadleaf forest, while remote sensing results suggested dark conifer. This counter-intuitive result might be a function of random variation, remote sensing data interpretation, or local conditions.

In sum, comparing remote sensing based land covers with model output indicates 461 out of 1000 (46%) locations (Figure 2.8) where disturbance may have occurred. These are sites where: 1. Modeling suggests a dark conifer forest and remote sensing indicates a larch, broadleaf, or mixed forest; 2. Modeling suggests a mixed forest, but remote sensing indicates a larch or broadleaf forest; or 3. Modeling suggests a broadleaf forest and remote sensing indicates a larch forest. The comparison accurately identified a known disturbance area near the coast, where Mongolian oak forests have replaced Korean pine and mixed pine/deciduous broadleaf forests that were burned or logged by early settlers.

Although seemingly consistent forest types cover the study landscape, the mosaic nature of forests dictates that an additional mechanism may be needed to determine the status of sites that appear to have experienced disturbance. The modeling-remote sensing comparison may be able to quickly signal clusters of likely disturbance or pinpoint anomalies for further exploration, but ground-truthing would help to ascertain local forest status.

2.5.2 *Wild fires and other disturbances*

Wildfires are important in shaping the structure and composition of forests in southeastern Russian Far East (Nakamura and Krestov, 2005; Loboda and Csiszar, 2007; Loboda, 2009; Loboda *et al.*, 2012). Because forest fires are not recorded in unprotected areas, and resources to control fires are insufficient in protected areas, tools to detect wildfire sites and assess fire impacts, such as modeling or remote sensing, are especially useful (Korovin, 2012; Loboda *et al.*, 2012).

The number of fires is increasing in mixed pine/conifer/broadleaf forests in southeastern Russian Far East (Rosenberg *et al.*, 1998; Kobayashi *et al.*, 2007). Fires occur most frequently in spring and fall, when agricultural fields are burned to return nutrients to the soil, and occur most often near areas of human activity (Loboda and Csiszar, 2007; Loboda, 2009; Korovin, 2012; Sherman *et al.*, 2012). In the summer, the number of anthropogenic fires decreases, but wildfires possibly caused by lightening can lead to very large conflagrations, especially during drought years such as 2003 (Loboda and Csiszar, 2007; Sherman *et al.*, 2012). Before human settlement, disturbances that led to growth release of Korean pine and shade intolerant species such as birch, especially Chinese birch, probably most frequently were wind, followed by fire and snow (Ishikawa *et al.*, 1999).

While spring ground fires can stimulate germination in some species, such as White or Paper birch (*Betula platyphylla*), ground fires can kill conifer seedlings, which leads to a gradual change in forest type (Krestov 2003). Young Korean pine seedlings are very sensitive and not able to

withstand fires, although Korean pine can grow on fire-disturbed sites if a seed source exists (Li and Zhu, 1991; Krestov, 2003). After a severe wildfire, dark conifer forests may appear as non-forested or sparsely forested areas in remote sensing images (Loboda *et al.*, 2012).

Mongolian oak can become established and persist in an area where fires occur of moderate intensity and duration, because the species can grow in xeric soils, the buds are protected, and acorn seeds are abundant and productive (Katsuta *et al.*, 1998; Krestov *et al.*, 2006; Kobayashi *et al.*, 2007).

Comparing potentially disturbed sites with fire probability is one of several possible tools for determining site history and the cause of disturbance. Fire probability was slightly higher at sites where comparing remotely sensed with modeled results suggested forest disturbance (11.5 in 1000 for potentially disturbed vs. 9.51 in 1000 for undisturbed). Field observation would be needed to ascertain whether fire disturbance actually occurred at a site.

2.5.3 LiDAR vs. Modeling – Biomass-to-canopy height relationship

Both remote sensing and modeling are useful tools for analyzing large landscapes in inaccessible areas. Comparing the two approaches in terms of the relationships of forest characteristics reinforces the consistency of the two approaches and affirms confidence in their utility.

FAREAST simulates a mature forested landscape, whereas GLAS LiDAR represents current landscape conditions. The comparison of the canopy height: biomass relationship derived from LiDAR data with the FAREAST-based ratio shows continuity between the two approaches ($y =$

$6.317^{e0.1004x}$, $R^2 = 0.9468$). For both approaches, the canopy/tallest tree to biomass relationships were developed independently based on observed data.

The topography of the research area in the RFE is very complex and varied. With LiDAR, an accurate ground measurement is essential because canopy height is determined relative to the ground (Hyde *et al.* 2005; Sun *et al.* 2008). Our research used the Shuttle Radar Topography Mission (SRTM) digital elevation model (DEM) to correct for ground surfaces (Sherman *et al.*, 2012; Sun *et al.*, 2008). Before digital elevation model (DEM) data were available, uneven and steep slopes led to inaccuracies in LiDAR measurements (Hyde *et al.*, 2005).

FAREAST generally predicted higher canopy height than that derived from GLAS data (Figure 2.7). GLAS data analysis produced canopy height with a mean of 18.3 m (median 19.2 m) and biomass with mean 48.98 tC/ha (median 53.9 tC/ha.) FAREAST output showed the mean height of the tallest tree (averaged over 988 points and 200 plots/point) to be 28.3 m (median 28.3 m) and mean biomass of 110.3 tC/ha (median 93.7 tC/ha). This difference may be partially explained by the higher canopy height of an old growth forest simulated by FAREAST compared with the existing landscape represented by GLAS data. It might also be associated with the presence of an emergent tree in the simulated results, although the effect of anomalous trees should be mitigated because results at one site, or point, represents the average over 200 plots, or computer processing runs.

These findings also are consistent with earlier studies that found using LiDAR can lead to an underestimation of canopy height. The tallest tree on a plot, especially the peak of a conifer, may be missed or not return enough energy to appear in a waveform (Lefsky *et al.*, 2002; Hyde *et al.*, 2005; Boudreau *et al.*, 2008; Gonzalez *et al.*, 2010; Van Leeuwen *et al.*, 2010). The sparse density of GLAS images, i.e., 170 m between data samples in GLAS/ICESAT, adds to the challenge of identifying tree tops (Gonzalez *et al.*, 2010). Since biomass is keyed to canopy height in the LiDAR approach, biomass is proportionally lower when compared with simulated results.

Combining sensors such as LiDAR, combined with Landsat ETM+, has produced more accurate measurements for maximum canopy height, mean canopy height and biomass than LiDAR, Quickbird, synthetic aperture radar (SAR)/interferometric synthetic aperture radar (InSAR), or Landsat ETM+ alone (Hyde *et al.* 2006). Utilizing LiDAR and radio detecting and imaging (radar) such as InSAR may prove to be the most effective approach for characterizing forest structure and metrics (Shugart *et al.*, 2010). Radar is an active sensor that uses microwave energy to detect woody components such as tree stems and branches. Combining LiDAR with radar permits three-dimensional characterization of trees and forests by using allometric equations derived from InSAR polarimetric backscatter and nadir and near-nadir LiDAR data to create a 3-D, multi-angle-based reconstruction of forest components and biomass at a 25 – 100 m scale. LiDAR-InSAR synthesis is an emerging area of study (Shugart *et al.*, 2010).

Because LiDAR results in this analysis systematically are lower than simulated results, it is difficult to identify disturbed areas by comparing output from the two methodologies. However, consistency between the modeled and remote sensing results affirms the mathematical relationship used to derive biomass from canopy height for these approaches and increases the confidence with which they can be used.

2.6 CONCLUSION

Remote sensing instruments like MODIS, LANDSAT and GLAS allow spatially consistent characterization of forest structure and composition across inaccessible and large-scale landscapes, and thus are important tools for studying the history, current status and potential future evolution of these ecosystems. Comparison of forest covers derived from FAREAST with remote-sensing-based approaches showed that assessing differences between simulated mature forests and current forest covers can contribute to understanding of the characteristics of a landscape and help to identify areas where disturbances such as wildfires or logging have occurred. Ground truthing or comparison with small-scale vegetation maps would increase the confidence with which this technique can be used.

LiDAR is an important tool that contributes to landscape analysis by allowing characterization of forest dimensions. Comparison of canopy height and biomass, both derived from GLAS, with the height of the tallest tree, a proxy for canopy height, and biomass, simulated by the FAREAST model, reinforced the validity of the relationship between canopy height and biomass used in

each approach and the usefulness of these tools in assessing forest structure. GLAS canopy height and biomass were slightly lower than modeled, which may be a result of the old growth, primary forest simulated by FAREAST compared with extant conditions, the use of an emergent tree as a proxy in FAREAST for canopy height, or possibly a result of the underestimation of canopy height by GLAS as a result of missing tree apexes. Both approaches can assist in measuring forest structure, estimating productivity and carbon sequestration, and analyzing and predicting landscapes utilized by wildlife.

2.7 REFERENCES

Abshire JB, Sun X, Riris H *et al.* (2005) Geoscience Laser Altimeter System (GLAS) on the ICESat Mission: On-orbit measurement performance. *Geophysical Research Letters*, **32**, LS1S02.

Bartalev SA, Belward A, Ershov D *et al.* (2003) A New SPOT4-VEGETATION derived land cover map of Northern Eurasia. *International Journal of Remote Sensing*, **24**, 1977-1982.

Botkin DB, Janak JF, Wallis FR (1972) Some ecological consequences of a computer model of forest growth. *Journal Ecology*, **60**, 849-873.

Boudreau J, Nelson R, Margolis H *et al.* (2008) Regional aboveground forest biomass using airborne and spaceborne LiDAR in Quebec. *Remote Sensing of the Environment*, **112**, 3876 – 3890.

Chapin FS III, Matson PA, Mooney HA (2002) *Principles of Terrestrial Ecosystem Ecology*. p. 290. Springer, New York.

Cheng X, Yan X (2009) Effects of climate change on typical forests in northeastern China. *Forestry of China*, **4**, 409-415.

Cushman SA, Wallin DO (2000) Rates and patterns of landscape change in the Central Sikhotealin Mountains, Russian Far East. *Landscape Ecology*, **15**, 643-659.

Dinerstein E, Loucks C, Heydlauff A (2006) *Setting Priorities for the Conservation and Recovery of Wild Tigers: 2005-2015. A User's Guide*. WWF, WCS, Smithsonian, and NFWF-STF, Washington, DC – New York.

Dinerstein E, Loucks C, Wikramanayake E *et al.* (2007) The Fate of Wild Tigers. *Bioscience*, **57**, 508-514.

Drake JB, Dubayah RO, Clark DB *et al.* (2002) Estimation of tropical forest structural characteristics using large-footprint lidar. *Remote Sensing of the Environment*, **79**, 305-319.

Dubayah RO, Drake JB (2000) LiDAR Remote Sensing for Forestry. *Journal of Forestry*, **98**, 44-46.

Friedl, M, McIver D, Hodges J *et al.* (2002) Global Land Cover Mapping from MODIS: Algorithms and Early Results. *Remote Sensing of Environment*, **83**, 287-302.

Giglio L, Descloitres J, Justice C *et al.* (2003) An Enhanced Contextual Fire Detection Algorithm for MODIS. *Remote Sensing of Environment*, **87**, 273-282.

Gonzalez P, Asner GP, Battles JJ *et al.* (2010) Forest carbon densities and uncertainties from QuickBird, and field measurements in California. *Remote Sensing of the Environment*, **114**, 1561-1575.

Grime JP (1979) *Plant Strategies and Vegetation Processes*. Wiley, Chichester, England.

Harding DJ, Carabajal CC (2005) ICESat waveform measurements of within-footprint topographic relief and vegetation vertical structure. *Geophysical Research Letters*, **32**, L21S10.

Hebblewhite M, Miquelle DG, Murzin A *et al.* (2011) Predicting potential habitat and population size for reintroduction of the Far Eastern leopards in the Russian Far East. *Biological Conservation*, **144**, 2403-2413.

Heptner VG, Sludskii AA (1992) *Mammals of the Soviet Union Vol. II, Part 2*. Smithsonian Institution Libraries and National Science Foundation, Washington, D.C.

Hickman Jr. CP, Roberts LS, Larson A (2003) *Animal Diversity Third Edition*. McGraw-Hill, New York.

Holmgeon J, Nilsson M, Olsson H (2003) Simulating the effects of LiDAR scanning angle for estimation of mean tree height and canopy closure. *Canadian Journal of Remote Sensing*, **29**, 623-632.

Horn HS (1974) The Ecology of Secondary Succession. *Annual Review of Ecology and Systematics*, **5**, 25 – 37.

Horn HS (2002) Some Causes of Variety in Patterns of Secondary Succession. In: *Forest Succession Concepts and Application* (eds West, DC, Shugart HH, Botkin DB) New York: Springer-Verlag, New York.

Horn HS, Cody ML, Diamond JM (1975) Markovian properties of forest succession. In: *Ecology and Evolution in Communities* (eds Cody M, Diamond J.) Harvard University Press, Cambridge.

Hudak AT, Lefsky MA, Cohen WB, Berterretche M (2002) Integration of lidar and Landsat ETM+ data for estimating and mapping forest canopy height. *Remote Sensing of the Environment*, **82**, 397-416.

Hyde P, Dubayah R, Peterson B *et al.* (2005) Mapping forest structure for wildlife habitat analysis using waveform lidar; validation of montane ecosystems. *Remote Sensing of the Environment*, **96**, 427-437.

Hyde P, Dubayah R, Walker W *et al.* (2006) Mapping forest structure for wildlife habitat analysis using multi-sensor (LiDAR, SAR/InSAR, ETM+, Quickbird) synergy. *Remote Sensing of Environment*, **102**, 63-73.

Ishikawa Y, Krestov PV, Namikawa K (1999) Disturbance history and tree establishment in old-growth *Pinus koraiensis*-hardwood forests in the Russian Far East. *Journal of Vegetation Science*, **10**, 439-448.

Justice CO, Vermote EF, Townshend JRG (1998) The Moderate Resolution Imaging Spectroradiometer (MODIS): Land Remote Sensing for Global Change Research. *IEEE Transactions on Geoscience and Remote Sensing*, **36**, 1228-1249.

Justice CO, Townshend JRG, Vermote EF *et al.* (2002) An overview of MODIS Land data processing and product status. *Remote Sensing of Environment*, **83**, 3-15.

Katsuta M, Morij T, Yokoyama T (1998) Seed of woody plants in Japan. Japan Forest Tree Breeding Association, Tokyo, Japan (in Japanese).

Kerr JT, Ostrovsky M (2003) From space to species: ecological applications for remote sensing. *Trends in Ecology and Evolution*, 18, 299-305.

Kimes D, Nelson R, Manry M *et al.* (1998) Attributes of neural networks for extracting continuous vegetation variables from optical and radar measurements. *International Journal of Remote Sensing*, **19**, 2639-2663.

Kimes D, Ranson KJ, Sun G *et al.* (2006) Predicting LiDAR-measured forest vertical structure from multi-angle spectral data. *Remote Sensing of the Environment*, **100**, 503-511.

Kobayashi M, Nemilostiv YP, Zyryanova OA *et al.* (2007) Regeneration after forest fires in mixed conifer broad-leaved forests of the Amur region in Far Eastern Russia: the relationship between species specific traits against fire and recent fire regimes. *Eurasian Journal of Forestry Research*, **10-1**, 51-58.

Koike T (1991) Photosynthetic characteristics of deciduous broad-leaved tree species. *Technical Report*, FFPRI, Hokkaido, **23**, 1-8.

Krestov PV (2003) Forest Vegetation of Easternmost Russia (Russian Far East). In: *Forest Vegetation of Northeast Asia* (eds Kolbek T, Strutek M, Box EO), pp. 93-180. Kluwer, New York.

Krestov PV, Song J-S, Nakamura Y, Verkholat VP (2006) A phytosociological survey of the deciduous temperate forests of mainland Northeast Asia. *Phytocoenologica*, **36**, 77-150.

Lauenroth WK, Urban DL, Coffin DP *et al.* (1993) Modeling vegetation structure-ecosystem process interactions across sites and ecosystems. *Ecological Modelling*, **67**, 49-80.

Leemans R, Prentice IC (1989) *FORSKA, a general forest succession model*. Institute of Ecological Botany, Uppsala, Sweden.

Lefsky MA, Cohen WB, Parker GG *et al.* (2002) Lidar Remote Sensing for Ecosystem Studies. *BioScience*, **52**, 19-30.

Lefsky MA, Harding DJ, Keller M *et al.* (2005) Estimates of forest canopy height and aboveground biomass using ICESat. *Geophysical Research Letters*, **32** (22), L22S02.

Lefsky MA, Keller M, Pang Y *et al.* (2007) Revised method for forest canopy height estimation from Geoscience Laser Altimeter System waveforms. *Journal of Applied Remote Sensing*, 1:013537.

Li J, Zhu N (1991) Structure and process of Korean pine population in the natural forests. *Forest Ecology and Management*, **43**, 125-135.

Lim K, Treitz P, Wulder M, St. Onge B. (2003) LiDAR remote sensing of forest structure.

Progress in Physical Geography, **27**, 633-649.

Loboda TV (2009a) Modeling fire danger in data-poor regions: a case study from the Russian Far East. *International Journal of Wildland Fire*, **18**, 19-35.

Loboda TV (2009b) Russian Far East fire probability surfaces: spatially explicit statistical analysis of MODIS fire information. University of Maryland Geography Department.

Loboda TV, Csiszar IA (2007) Assessing the risk of ignition in the Russian Far East within a modeling framework. *Ecological Applications*, **17**, 791-805.

Loboda TV, Zhang Z, O'Neal KJ *et al.* (2012) Reconstructing disturbance history using satellite-based assessment of the distribution of land cover in the Russian Far East. *Remote Sensing of the Environment*, **118**, 241-248.

Miquelle DG, Goodrich JM, Kerley LL *et al.* (2010a) Science-Based Conservation of Amur Tigers in the Russian Far East and Northeast China. In: *Tigers of the World* (eds Tilson R, Nyhus PJ), pp. 403-423. Elsevier Inc., London.

Miquelle DG, Goodrich JM, Smirnov EN *et al.* (2010b) Amur tiger: a case study of living on the edge. In: *Biology and Conservation of Wild Felids* (eds Macdonald DW, Loveridge AJ), pp. 325-339. Oxford University Press, New York.

Miquelle DG, Smirnov EN, Merrill TW *et al.* (1999) Hierarchical spatial analysis of Amur tiger relationships to habitat and prey. In: *Riding the Tiger* (eds Seidensticker J, Christie S, Jackson P), pp. 71-99. Cambridge University Press, Cambridge.

Nakamura Y, Krestov P (2005) Coniferous forests of the temperate zone of Asia. In: *Ecosystems of the World 6: Coniferous Forests* (ed Andersson F) Elsevier, New York.

Nelson, Ross (2010) Model effects on GLAS-based regional estimates of forest biomass and carbon. *International Journal of Remote Sensing*, **31**, 1359-1372.

Newell, J (2004) *The Russian Far East: A Reference Guide for Conservation and Development*, Daniel & Daniel, McKinleyville, CA.

North MP, Franklin, JF, Carey AB *et al.* (1999) Forest stand structure of the northern spotted owl's foraging habitat. *Forest Science*, **45**, 520-527.

North PRJ, Rosette JAB, Suarez JC *et al.* (2010) A Monte Carlo radiative transfer model of satellite waveform LiDAR. *International Journal of Remote Sensing*, **31**, 1343-1358.

Olsen DM, Dinerstein E (2002) *The Global 200: Priority Ecoregions for Global Conservation*. Annals of the Missouri Botanical Garden, **89**, 199-224.

Patenaude G, Milne R, Dawson TP (2005) Synthesis of remote sensing approaches for forest carbon sequestration: Reporting to the Kyoto protocol. *Environmental Science & Policy*, **8**, 161-178.

Qian H, Krestov P, Fu P-Y (2003a) Phytogeography of Northeast Asia. In: *Forest Vegetation of Northeast Asia* (eds Kolbek J, Srutek M, Box EO), pp. 51 – 91. Kluwer, Norwell, MA.

Qian H, Song J-S, Krestov P *et al.* (2003b) Large-scale phytogeographical patterns in East Asia in relation to latitudinal and climatic gradients. *Journal of Biogeography*, **30**, 129-141.

Rosenberg VA, Bocharnikov VN, Krasnopeeov SM (1998) Biological Diversity in the Sikhote-Alin Forests and Measures of its Conservation. *Integrated Tools Proceedings*. Aug. 16-20, 1998. Boise, Idaho.

Schutz BE, Zwally HJ, Shuman CA *et al.* (2005) Overview of the ICESat mission. *Geophysical Research Letters*, **32**, L21S01.

Sherman NJ, Loboda TV, Sun G, Shugart HH (2012) Remote Sensing and Modeling for Assessment of Complex Amur (Siberian) Tiger and Amur (Far Eastern) Leopard Habitats in the Russian Far East. In: *Remote Sensing of Protected Lands* (ed Wang YQ), pp. 379 – 407. CRC Press, New York.

Shugart HH (1984) (reprint 2003) *A Theory of Forest Dynamics: The Ecological Implications of Forest Succession Models*. The Blackburn Press, Caldwell, NJ.

Shugart HH (1998) *Terrestrial Ecosystems in Changing Environments*. Cambridge University Press, NY.

Shugart HH, Saatchi S, Hall FG (2010) Importance of structure and its measurement in quantifying function of forest ecosystems. *Journal of Geophysical Research*, **115**, G00E13.

Sun G, Ranson KJ, Kimes DS *et al.* (2008) Forest vertical structure from GLAS: an evaluation using LLVIS and SRTM data. *Remote Sensing of the Environment*, **112**, 107-117.

Uphyrkina O, Miquelle DG, Quigley H *et al.* (2002) Conservation Genetics of the Far Eastern Leopard (*Panthera pardus orientalis*). *Journal of Heredity*, **93**, 303-311.

Van Cleve K, Vierick LA (1981) Forest succession in relation to nutrient cycling in the boreal forest of Alaska. In: *Forest Succession: Concepts and Application* (eds West DC, Shugart HH, Botkin DB), pp. 207-208. Springer-Verlag, New York.

Van Leeuwen M, Coopes NC, Wulder MA (2010) Canopy surface reconstruction from a LiDAR point cloud using Hough transformation. *Remote Sensing Letters*, **1**, 125-132.

Vina A, Bearer S, Zhang H *et al.* (2008) Evaluating MODIS data for mapping wildlife habitat distribution. *Remote Sensing of the Environment*, **112**, 2160-2169.

Watt AS (1947) Pattern and process in the plant community. *Journal of Ecology*, **35**, 1-22.

Yan X, Shugart HH (2005) FAREAST: a forest gap model to simulate dynamics and patterns of eastern Eurasian forests. *Journal of Biogeography*, **32**, 1641-1658.

Yan X, Zhao S (1996) Simulating the response of Changbai Mountain forests to potential climate change. *Journal of Environmental Science*, **8**, 354-366.

Zhang N, Shugart HH, Yan X (2009) Simulating the effects of climate changes on Eastern Eurasian forests. *Climatic Change*, **95**, 341-361.

Zwally HJ, Schutz B, Abdalati W *et al.* (2002) ICESat's laser measurements of polar ice, atmosphere, ocean and land. *Journal of Geodynamics*, **34**, 405-445.

Zyryanova OA, Yaborov VT, Abaimov AP *et al.* (2005) Problems in the Maintenance and Sustainable Use of Forest Resources in Priamurye in the Russian Far East. *Eurasian Journal of Forest Research*, **8**, 53-64.

Zwally HJ, Schutz B, Abdalati W, *et al.* (2002) ICESat's laser measurements of polar ice, atmosphere, ocean and land. *Journal of Geodynamics*, **34**, 405-445.

Websites

Bartalev S, Ershov D, Isaev A *et al.* (2004) *Russia's Forests*. TerraNorte Information System.
RAS Space Research Institute <terranorte.iki.ru> 08/05/2005.

Birdlife International <<http://www.birdlife.org/datazone/species/>> 03/24/2013.

Jackson, P. and Newell, K. (2008) *Panthera Pardus ssp. Orientalis*. IUCN 2010. *IUCN Red List of Threatened Species*. Version 2010.4 <www.iucnredlist.org> 02/03/ 2011.

Korovin, G. Land Resources of Russia - Forest fires. IIASA.
<http://www.iiasa.ac.at/Research/FOR/reuuia_cd/forestry_des.htm> 06/08/12.

Miquelle D, Darman Y, Seryodkin I (2010c) *Panthera tigris spp. Altaica*. IUCN 2010. IUCN Red List of Threatened Species. Version 2010.4 <www.iucnredlist.org> 02/09 /2011.

United Nations Educational, Scientific and Cultural Organization (UNESCO) World Heritage Convention. World Heritage List <<http://whc.unesco.org/en/list/766>> 09/24/12.

CHAPTER 3. COMPARISON OF RESULTS FROM A FOREST GAP SUCCESSION MODEL WITH FIELD OBSERVATIONS

ABSTRACT

Computer-based modeling can be a useful tool for understanding the structure and composition of forests at remote and inaccessible locations. The computer model FAREAST simulates forest succession at a canopy gap scale, representing the break in the forest canopy that occurs when a large tree falls, which allows sunlight to reach the forest floor and stimulate re-generation.

The FAREAST model has been validated against forest inventory data in northeastern China and across Russia (Yan and Shugart, 2005; Shuman and Shugart, 2009). This study compares FAREAST output with field observations at eleven locations in three strictly protected wildlife reserves (*zapovedniks*) in the southeastern Russian Far East in order to calibrate the model for temperate forests at a plot-level scale close to that of the model (500 m²). The exceptional biodiversity of Primorye forests makes study at a detailed scale useful for understanding forest composition, but presents more challenges than plantations or other less diverse ecosystems.

FAREAST was able to correctly identify the forest type at all sites with primary old growth forests. Model output for total basal area approximated observed at seven of eleven field sites and at seven of eight sites with primary forests. The simulated deciduous/conifer ratio matched observed at five of the eight old growth sites. For multiple species at all sites, Kolmogorov-Smirnov testing suggested that modeled and observed basal area represents the same distribution.

Although underlying natural processes may be similar, differences in climate, seed bank, forest age, access to light and soil resources, as well as random variation, make it possible for species composition at the gap level to vary significantly within a seemingly homogeneous landscape-scale forest. Simulated results best match field observations at field sites closest to the location from which data were used to verify the model.

3.1 INTRODUCTION

Assessing forest composition and structure at a detailed scale across large and inaccessible landscapes is important, but can be difficult. Small-scale analysis of forest composition can uncover temporal and spatial variations that may not be apparent at coarser scales (Shugart, 1998; Shugart *et al.*, 2010). Understanding forest composition at a detailed scale is especially useful in the context of understanding the contribution of discrete ecosystems to large-scale carbon, water and energy cycles (Shugart *et al.*, 2010). Variations in forest composition at a small scale can skew large-scale biomass and carbon sequestration estimates, on which public policy and carbon credit compensation are based.

Disturbance, such as logging, fires, or damage from snow and wind, shapes forest composition by creating gaps in the forest canopy that allow light to penetrate to the forest floor (Watt, 1947; Shugart, 1984; Prentice & Leemans, 1990). This study represents the first time the individual tree-based boreal forest gap model FAREAST (Yan and Shugart, 2005) has been measured against non-government inventory field data in the Russian Far East (RFE). The purpose of the research was to assess the validated model's performance at a detailed scale in a region with

large, dense old growth forests and unusual assemblages of tree species in preparation for using the model to assess the potential impact of climate change in this area.

The study compares forest composition and structure simulated by the model with canopy gap scale field observations from southeastern Russian Far East along gradients of latitude, climate, and altitude. Basal area predicted by the FAREAST model is compared with field observations made at eleven forest study locations across a latitudinal gradient of 4.6 degrees (4.6×10^4 km).

The FAREAST model was developed in northeastern China and has correctly simulated observed forest type, based on forest inventory data, at 23 of 31 locations across the Russian Far East (Yan and Shugart, 2005). Simulated biomass for multiple species correlated with forest inventory data ($R^2 = 0.75$, $p < 0.05$) in 85 comparisons across Russia (Shuman and Shugart, 2009). FAREAST incorporates local climate data (temperature and precipitation), biological characteristics of 43 tree species, physiological processes, and interspecies competition to simulate changes in forest structure and composition across an analyst-designated time span (Yan and Shugart, 2005).

3.2 BACKGROUND

The field research sites were located in the provinces (*krais*) of Primorski (or Primorye) and southern Khabarovsk and include the last remaining habitat of the endangered Amur, or Siberian tiger (*Panthera tigris altaica*) (Miquelle *et al.*, 1999; Miquelle *et al.*, 2010a&b), as well as the critically endangered Amur leopard (*Panthera pardus orientalis*) (Jackson and Nowell, 2008) and other rare and endemic species (Newell, 2004; Nakamura and Krestov, 2005; Krestov *et al.*, 2006). The field sites ranged from southern Primorski Krai near the port city of Vladivostok

(43.65° N, 132.35° E) to southern Khabarovsk Krai near the commercial and political center of Khabarovsk (48.24° N, 134.9° E) (Figure 3.1).

The two southernmost study sites were located in one of the world's most biologically diverse temperate forest zones (Newell, 2004; Krestov *et al.*, 2006). Seven of the field sites were in forests of Central Sikhote-Alin, which have been designated as an IUCN Natural Heritage site because of the unusual and biologically diverse mix of temperate and boreal species of plants and animals recorded (UNESCO 2013). For example, mixed broadleaf/Korean pine in the southern and Sikhote-Alin forests are estimated to contain 445 - 645 species of vascular plants (Nakamura and Krestov, 2005; Krestov *et al.*, 2006).

This extraordinary biological diversity is attributed to geology, climate history, and latitudinal location (Qian *et al.*, 2003; Krestov, 2003; Nakamura and Krestov, 2005; Krestov *et al.*, 2006). During the early Tertiary Period (65 mya), a warm climate across the northern hemisphere allowed tropical species to flourish. As climate cooled in the late Tertiary Period, which ended about 1.8 mya, only cold-tolerant plants survived, leading to a mix in this area of temperate,



Fig. 3.1 Study locations (triangles) and federal and provincial reserves in southeastern Russian Far East (ArcMap layer from WWF – Russia)

boreal, and a few hardy tropical species (Qian *et al.*, 2003; Nakamura and Krestov, 2005). Lack of glaciation during the Pleistocene epoch (2.6 m – 11,600 years ago), and possibly earlier, allowed uninterrupted evolution of the rich mixture of species (Nakamura and Krestov, 2005). Connection with the rest of Asia, Africa and, via the Bering land bridge, the Americas, also contributed to plant diversity (Qian *et al.*, 2003). Furthermore, varied topography in the study area creates a multitude of microclimates that support atypical and endemic species.

The Sikhote-Alin Mountains extend about 1200 km along the length of the region. Average height is about 800 – 1200 m asl (Kostak *et al.*, 2003; Miquelle *et al.*, 2010b) with the highest peak at Mt. Tardoki-Yani, 2077 m (Kostak *et al.*, 2003; Qian *et al.*, 2003) and foothills along the coast of the Sea of Japan (Figure 3.2).



Figure 3.2 a. Study area in the southeastern Russian Far East. Source: Wildlife Conservation Society, Russia Program. b. Russian coast in Central Sikhote-Alin (Photo: N. Sherman)

3.2.1 *FAREAST model - Overview*

The concepts underlying gap models can be traced back to A.S. Watt (1947), who introduced the idea of forests as a dynamic mosaic, whereby observable patterns of forest composition and structure originate in underlying naturally-occurring cyclical processes. Watt coined the term “gap phase,” which refers to the ecosystem stage that occurs when a large tree dies, which marks the end of a period of increasing plant material and habitat quality associated with tree maturation. The newly-formed canopy gap allows sunlight to reach the forest floor, which triggers regeneration when seedlings become established and/or start to grow (Watt, 1947; Prentice & Leemans, 1990; Shugart, 1998; Shugart *et al.*, 2010).

Forest gap models simulate succession processes in these small areas, or “patches,” newly exposed to sunlight. Individual-based models like FAREAST look at individual trees of all species on a plot. FAREAST simulates changes in forest structure and composition in terms of species, biomass, basal area, stem count and other metrics over time in response to parameters such as local climate, altitude, aspect and species characteristics, such as tolerance of shade and drought (Shuman and Shugart, 2009; Yan and Shugart, 2005; Zhang *et al.*, 2009).

FAREAST was developed and verified based on forest data from the elevational gradient of Changbai Mountain in northeastern China. It was validated at 31 sites in Far Eastern Russia, where simulated results matched forest inventory data at 23 sites in terms of the four dominant tree genera by biomass. Of the eight sites that didn’t match, simulated results were close to observed at three sites. At another four of the eight sites, sparse larch (*larix*) forests occurred, with atypical hydrological conditions, i.e. permafrost with impeded soil drainage (Yan and Shugart, 2005).

A comparison of biomass produced by FAREAST with Russian forest inventory data at sites across Russia showed a strong correlation with multiple species at various stages of succession. Average R^2 (coefficient of determination) for 85 comparisons was 0.75 ($p < 0.05$) (Shuman and Shugart, 2009).

The model calculates the establishment, growth and death of each individual tree in a simulated plot size of $1/20^{\text{th}}$ (0.05) hectare ($5 \times 10^{-6} \text{ km}^2$). Individual tree growth depends on climate, soil characteristics, competition for light and nutrients, and species-specific dimensions and

requirements. At each “site,” the model re-creates the forest succession process 200 times, representing 200 plots, for an analyst-selected number of years, with random variation in temperature and precipitation, based on historical climate patterns. Plot-level results are then averaged for biomass (tons carbon per hectare (tC/ha)), basal area, leaf area index (LAI), stem count, and other output, for each site in order to estimate forest composition and structure in the gap after the specified period of succession. Just as climate is an important factor in shaping forests, temperature and precipitation are among the most important factors in determining forest structure and composition in FAREAST (Qian *et al.*, 2003; Zhang *et al.*, 2009; Nakamura *et al.*, 2009).

3.2.2 *Climate*

Most of the study area has a temperate, ocean monsoonal climate which, together with the diverse topography, supports a mix of deciduous broadleaf, mixed Korean pine/deciduous broadleaf, and spruce/fir/Korean pine (dark conifer) forests (Nakamura and Krestov, 2005).

The Sikhote-Alin Mountains bisect the study area into two climate regimes: a humid Pacific monsoonal climate to the east and a continental climate, with colder winters and hotter summers, west of the mountains (Krestov, 2003). Summer monsoonal rains can cause flooding, especially in coastal areas (Newell, 2004; Gromyko, 2006). Nine of the eleven field sites were located south or east of the Sikhote-Alin Mountains in the Ussuri area (Qian *et al.*, 2003), which has a submaritime climate, meaning that humidity is higher, summers are cooler and winters are warmer than inland continental areas.

Eight field sites were in the Sikhote-Alin Biosphere *Zapovednik* (SABZ) or strictly protected reserve, in Central Sikhote-Alin, the latitudinally central section of the montane complex. Highest temperatures in this area occur in August, with a mean of 17.4 °C, and coldest temperatures are in January (mean of -14.0 °C to -10.0 °C) (Qian *et al.*, 2003, Miquelle *et al.*, 2010b).

Annual rainfall in Terney is 813 mm (Ishikawa *et al.*, 1999; Qian *et al.*, 2003). Average annual precipitation for the entire Central Sikhote-Alin area is 650-800 mm. More than 75% of rainfall occurs in April through November (Miquelle *et al.*, 2010b), with peak precipitation in August (Ishikawa *et al.*, 1999). Between 105 and 120 days per year are frost-free (Miquelle *et al.*, 2010b). Average snow depth in February is 13.7 ± 3.5 cm and 22.6 ± 2.9 cm inland (Primorye Weather Bureau in Miquelle *et al.*, 2010b). Heavy snowfalls can occur in March (Miquelle *et al.*, 2010b).

The climate at the two southernmost field sites, located in Ussurisky Reserve, was drier and warmer in summer than the Sikhote-Alin Reserve, which is about 370 km to the northeast. Mean annual minimum temperature in Vladivostok (43.1 °N, 131.9 °E), close to the sites, is 1.2 °C, and mean annual maximum is 8.3 °C (Yan and Shugart, 2005). At Suputinka, near the Ussurisky Reserve, mean annual temperature is 2.6 °C. August mean temperature is 20.3 °C and January mean is -19.5 °C. Annual rainfall is 719 – 779.6 mm (Qian *et al.*, 2003; Yan and Shugart, 2005).

A continental climate prevails at the two northernmost sites in the Bolshekhkhehtsirskiy Reserve (Polovinka 1 & 2), with colder winters, warmer summers and lower humidity than the other field locations. The reserve is about 29 km S-SW of the major urban area of Khabarovsk (48.5° N, 135.2° E) (Google Earth). Mean annual minimum temperature in Khabarovsk is -2.5 °C and mean

annual maximum is 6.7 °C (Yan and Shugart, 2005). Average annual precipitation is 665 mm (Yan and Shugart, 2005).

3.2.3 *Field Research*

Field data was collected at twelve study locations located in three strictly protected scientific reserves, or *zapovedniks*. Only researchers and park staff are allowed access to the reserves. As a result, the biological diversity and richness of these areas have persisted, and the forests have matured with minimal anthropogenic disturbance. Botanists at each of the reserves estimated the primary forests to be about 300 years old.

Sikhote-Alin Biosphere *Zapovednik* (SABZ), founded in 1935, is 401,428 ha (4,014 km²), much of which is primary forest. Of the eight field sites in this reserve, four represented typical uncut old growth forests. The sites were situated on the eastern slope of the Sikhote-Alin Mountain system (although site aspects varied), where elevation drops quickly from dark conifer (spruce/fir/Korean pine) forests at ~900 m and above (Nakamura and Krestov, 2005) to mixed deciduous broadleaf forests and coastal oak forests along the coast of the Sea of Japan (Figure 3.3).



Fig. 3.3 Forests in the Sikhote-Alin Biosphere Reserve a. Mixed broadleaf deciduous/Korean pine/conifer b. Dark conifer (primarily Yezo spruce and Black fir)

Of the remaining four sites, two were in coastal oak-birch forests that had replaced original mixed deciduous broadleaf/Korean pine forests, one was a mid-successional deciduous broadleaf/Korean pine forest that was regenerating after a severe wildfire, and one was a primary mixed deciduous broadleaf/Korean pine/conifer forest with an unusual combination of species.

The two southernmost sites (Ussurisky 1 and 2) (Figure 3.4) were located in primary forests in the Ussurisky *Zapovednik* near Vladivostok. The reserve is located on the western spurs of the southern end of the Sikhote-Alin Mountains and contains some of the only remaining old growth forests in southern Primorye (Krestov, 2003). About 825 species of vascular plants, including numerous endemic and endangered species, have been measured in the reserve. Founded in 1932, the 404 km² *zapovednik* is managed by the Biology and Soil Institute of the Far Eastern Branch of the Russian Academy of Sciences (Wild Russia, 2013)



Fig. 3.4 Old growth forests in Ussurisky Reserve a. Painted maple (*Acer mono*) in the canopy understory). b. All trees on a circular plot with dbh > 8cm were measured.

The two northernmost field study sites (Polovinka 1 and 2) were in old growth forests in Bolshekhokhtsirskiy *Zapovednik*, slightly southwest of the city of Khabarovsk in Khabarovsk Krai. The 454 km² reserve is located on highland area near the intersection of the Amur River and its tributary, the Ussuri River. It was founded in 1963 and contains mixed and dark conifer forests, with elevations up to 800 m asl (Russian Nature Press 2013).

3.3 MATERIALS AND METHODS

Field sites (Table 3.1) were selected to represent variations in latitude, aspect and elevation. At eleven of the twelve sites, ten 30-meter diameter circular transects were established at random. At one site (Blagodatnoye 3), logistical and field personnel constraints permitted measurements at only one circular transect, so results were not used for data analysis. At each site, forest composition was typical of primary vegetation at the selected elevation and latitude. Elevation

was measured using a Barigo altimeter, and latitude and longitude were measured with a hand-held GPS device.

Table 3.1 Field sites

Reserve – site	Elev. (10 plots)	Aspect	Latitude	Longitude
<i>Ussurisky Res.</i>				
Ussurisky 1	230 – 270 m	S	43.654	132.35
Ussurisky 2	290 – 325 m	S-SE	43.654	132.379
<i>Sikhote-Alin Res.</i>				
Kabaniy 1	500 – 600 m	S-SW	45.111	135.865
Kabaniy 2	585 – 620 m	N	45.114	135.87
Kabaniy 3	920 – 940 m	S-SW-W	45.139	135.884
Kabaniy 4	750 – 780 m	NW	45.152	135.9
Maysa (Post-fire)	200 m	Level	45.23	136.511
Blagodatnoye 1	52 – 110 m	S-SE	44.96	136.563
Blagodatnoye 2	210 – 240 m	SW-W	44.972	136.526
<i>Bolshekhokhtsirskiy Res.</i>				
Polovinka 1	300 – 315 m	NW	48.24	134.906
Polovinka 2	290 – 325 m	SE-E	48.24	134.9

Transects were marked off with four 30-m lengths of measuring tape, which divided each transect into eight sections (Figure 3.5). The 30-m diameter scale was chosen to simulate the approximate size of a large tree crown, to represent the gap in the forest canopy when a large tree falls. A 30-m diameter circle represents 0.07 ha, or 1.4 times the plot size simulated in FAREAST (0.05 ha).

For each circle, the diameter at breast height (dbh) (1.37 m) of every tree equal to or larger than eight centimeters was measured and recorded. Basal area by species for each site was calculated from dbh measurements. Sapling number and species also were recorded for each circle. Saplings were defined as woody species with dbh smaller than eight centimeters. A sample of tree heights and dbh were measured at each site to calculate biomass, but, ultimately, the biomass metric was not used because of the large variability in results associated with using various relevant allometric equations and the inability to measure diameter at clear bole height (CH), a metric used in FAREAST biomass equations.



Figure 3.5 a. Intersection of measuring tapes for delineating transect boundaries. b. Measuring and recording tree diameter.

At six of the twelve sites, transects were selected in pairs on opposite aspects at similar elevations in order to assess differences in vegetation associated with solar insolation relative to model

output. The pairs were:

Kabaniy 1 (S-SW; 500 – 600 m) – Kabaniy 2 (N; 585 – 620 m)

Kabaniy 3 (S-SW-W; 920 – 940 m) – Kabaniy 4 (NW; 750 – 780 m)

Polovinka 1 (NW; 300 - 315 m) – Polovinka 2 (SE-E; 290 – 335 m)

At the remaining field research locations, sites had varying conditions, but were not necessarily on facing aspects. Sites also were selected at significantly different latitudes to compare observed data with modeled output along latitudinal gradients (Table 3.1).

At Kabaniy in SABZ, sites were chosen at different elevations to examine the ability of the model to simulate forest composition changes associated with altitude. Because of the rugged terrain and difficulty of access, the sites in one pair (Kabaniy 3 and 4) were at slightly different altitudes (920 - 940 m vs. 750 – 780 m, respectively).

3.3.1 *Forest categories*

Forest categories were defined based on International Global Biosphere Programme land cover categories (Davis, 2000). The categories are Deciduous broadleaf, Mixed deciduous broadleaf/Korean pine/conifer, and Dark conifer. Deciduous broadleaf was assigned when basal area of 65% or more consisted of deciduous broadleaf species, such as oak, linden, and maple. The dark conifer category includes sites where basal area of 65% or more consisted of primarily spruce and fir, and may include some Korean pine. When less than 65% of basal area at a site was comprised of deciduous broadleaf, fir/spruce or Korean pine, the mixed deciduous broadleaf/Korean pine/conifer label was applied.

3.3.2 FAREAST Model

FAREAST incorporates four sub-models: GROWTH, REGENERATION, MORTALITY and ENVIRON. GROWTH, REGENERATION, AND MORTALITY are based on species-specific vegetation characteristics applied to each individual tree, such as maximum age, rate of growth, and shade, drought and temperature tolerance. ENVIRON represents environmental conditions and applies to all the other sub-models (Yan and Shugart, 2005; Zhang *et al.*, 2009)

The geometric tree form simulated in FAREAST consists of a conic bole for the tree trunk and a cubic cone (pyramid) to represent leaf area. For the purpose of measuring biomass, root volume is considered to be half the branch amount (Yan and Shugart, 2005). Simulated wood biomass in kilograms/hectare is calculated by multiplying wood volume by bulk density times one-half. Multiplying again by 0.5 gives biomass in terms of carbon (tC/ha).

Leaf and fine root biomass are calculated as a function of tree diameter at clear branch bole height. Leaves and fine roots have equal biomass, C:N ratio, and annual renewal ratio. Basal area is calculated as a function of dbh.

Calculation of tree growth in the GROWTH sub-model is based on annual increments in diameter and the height where branches begin, or clear branch bole height. The rate of tree growth depends on light availability, climate, soil conditions and competition with other species. The formula for tree growth is based on the optimal diameter increment formula of Botkin *et al.* (1972) and the

actual diameter increase formula from the Forska model (Leemans and Prentice, 1989; Yan and Shugart, 2005).

$$\left. \frac{dDBH}{dt} \right|_{opt} = gDBH \frac{1 - \frac{DBH \cdot H}{Dm \cdot Hm}}{2H + D \frac{\partial H}{\partial DBH}} \quad \text{Equation 3.1}$$

$$\frac{dDBH}{dt} = \left. \frac{dDBH}{dt} \right|_{opt} \cdot f_L(H) f_T f_N f_D \quad \text{Equation 3.2}$$

Dm (cm) is maximum dbh, Hm (m) is maximum tree height by species, and g is a species-specific scalar parameter for tree growth (Yan and Shugart, 2005). The functions $L(H)$, T , N , and D refer to light transmission through the canopy, atmospheric temperature, soil nutrients, and drought, respectively.

Tree height is calculated as a function of dbh and maximum height for the species.

$$H = 1.3 + (Hm - 1.3) \cdot \left(1 - \exp \left(\frac{sDBH}{Hm - 1.3} \right) \right) \quad \text{Equation 3.3}$$

1. $sDBH$ should be $-sDBH$

Similarly to tree growth, the driving mechanisms for increases in leaf area in FAREAST are climate, soil, light and competition among trees for resources. An important difference between FAREAST and earlier models such as Forska and NEWCOP is that FAREAST calculates photosynthetic activity associated with light filtering through the tree canopy, which permits

competition for light to be incorporated in the simulation (Yan and Shugart, 2005). Light availability is important in determining forest structure, especially in stands with mesic soil, such as that found at the field sites, by facilitating or inhibiting tree growth (Lauenroth *et al.*, 1993). The amount of light available to a tree is calculated in terms of light transmission through the canopy using the Lambert–Beer Law (Monsi and Saeki, 1953):

$$I(Z) = I(0) e^{-kLAI(Z)}$$

$I(Z)$ represents available light at the height Z and k is the light extinction co-efficient.

In the model, deciduous trees are allowed to shade subordinate evergreen species for 80% of the growing season, representing the period when leaves are expanded. The temperature tolerance of a species is based on the observed maximum and minimum temperatures of the species range (Botkin *et al.*, 1972; Yan and Shugart, 2005).

$$f_T(DEGD) = \frac{4(DEGD_{\max} - DEGD)(DEGD - DEGD_{\min})}{(DEGD_{\max} - DEGD_{\min})^2} \quad \text{Equation 3.4}$$

Water availability is calculated using the Hargreaves evaporation equation (Hargreaves and Allen, 2003; Yan and Shugart, 2005), which uses maximum and minimum temperatures to estimate drought conditions. The impact of drought on a particular species depends on the number of drought days and the species' tolerance of drought (D_0), and is calculated using the equation:

$$f_D(DROUT) = \begin{cases} \sqrt{(D_0 - DROUT)/D_0} & DROUT < D_0 \\ 0 & DROUT \geq D_0 \end{cases} \quad \text{Equation 3.5}$$

FAREAST adjusts soil moisture as a function of precipitation, taking into consideration canopy interceptions, evapotranspiration, and slope. Runoff increases with greater degrees of slope. Field capacity (cm), the amount of water in soil after excess water has drained off following saturation, is calculated from available water capacity and is based on Stolbovi and McCallum (2002).

FAREAST calculates tree nutrient requirements on an annual time-step based on DBH increment, the ratio of DBH to the wood carbon: nitrogen ratio, diameter at clear branch bole height (DCH), incremental DCH growth, the annual leaf and fine root renewal ratio (RATIO) and the leaf C:N ratio.

3.3.2.1 MORTALITY sub-model

The MORTALITY sub-model incorporates individual tree death, as well as a tree's contribution to the next generation, such as litter from leaves, fine roots, and fallen branches. Leaf and litter fall form part of the Ao, or top, layer of soil. Branch litter-fall occurs as the tree grows.

The probability of tree death (pn) is a function of a species-dependent category parameter and the maximum age of the tree (Equation 3.6). Slower growing trees have a higher risk of mortality, with only 1 in 100 (1%) expected to survive for 10 years (Shugart, 1984; Yan and Shugart, 2005).

Trees are divided into three groups and assigned a probability of 1%, 0.1% or 0.01% of reaching maximum age.

$$p_n = 1 - \exp\left(\frac{-death}{AGE_{max}}\right),$$

Equation 3.6

3.3.2.2 *REGENERATION sub-model*

FAREAST calculates regeneration based on the size of a species' seed bank relative to other species and random variation. The size of each species' seed bank, which is updated annually, is determined by the production of seeds from trees within the plot, seeds of invasive species outside the plot, seed mortality, and transformation from seed to sprout.

3.3.2.2 *ENVIRON sub-model*

ENVIRON calculates soil moisture, soil nutrients and climate conditions based on climate inputs. Climate inputs include monthly average maximum and minimum temperatures, and standard deviations from these averages, from which the sub-model develops daily temperatures using a random sequence. Average monthly precipitation and its standard deviation are used to calculate daily precipitation amounts. Soil carbon and nitrogen are calculated on an annual basis based on a carbon and nitrogen cycle model (Post and Pastor, 1996). Temperature tolerance is based on growing degree days required on a species basis.

FAREAST provides for the transfer of seeds from exterior sources into the gap, but does not simulate propagation from roots or vegetative effects outside of the gap, such as the transfer of seeds by wind or water. For more information regarding FAREAST, see Yan and Shugart (2005).

Temperature and precipitation data from the World Meteorological Organization (WMO) National Climate Data Center (NCDC) data set were used. Data from the weather station most likely to have similar weather, based on proximity and topography, were assigned to each field site. The closest weather station for Sikhote-Alin Biosphere Reserve sites was Terney at 45.0° N, for Bolshekhkhtsirskiy sites, Khabarovsk at 48.5° N, and for Ussurisky sites, Vladivostok at 43.1° N, 131.9° E.

Randomness in the model is introduced in “seeding” and in calculating fluctuation in temperature and precipitation. Randomness in seeding, which is associated with the seed bank and occurs in the Regeneration sub-model, can be turned on and off.

The FAREAST model is capable of being adjusted for the elevation difference between the location where weather readings were made and the altitude of the simulated site. Sensitivity tests were conducted to determine whether this function improved accuracy.

For the purposes of the basal area analysis, only species found at the field sites were inputted into the model because of the statistical weight associated with species presence and seed rain.

Having a seed source at a site greatly increases the likelihood of persistence of that species in that location (Horn, 1974; Horn *et al.*, 1975; Horn, 2002) as compared with species that might tolerate local soil and climate conditions, but are not found in the area.

Deciduous species that occurred at the field sites in very small quantities, but were not in FAREAST species data set, were considered “Other deciduous” and not broken out separately. All conifer species found at the field sites were included in FAREAST input. A very small amount of Manchurian or Northeast ash (*Fraxinus mandshurica*) was found at four sites, but was excluded because of its tendency to grow in unrealistically large quantities in the simulation.

Soil inputs to the FAREAST model include permanent wilting point, field capacity, soil depth, and soil minerals (carbon and nitrogen). Soil parameters were based on Stolbovi and McCallum (2002). Mixed hardwood-Korean pine forests throughout the Sikhote-Alin area usually grow on brown forest soils (Ishikawa *et al.*, 1999). Sensitivity testing was conducted to test the impact of soil characteristics on forest composition and individual tree species. Sensitivity testing showed that soil type did not change the forest type or dominant species.

The model was run on a MAC OS X MacBook Pro, Version 10.5.8, with a 2.53 GHz Intel Core 2 Duo Processor and memory of 4 GB, 1067 MHZ DDR3.

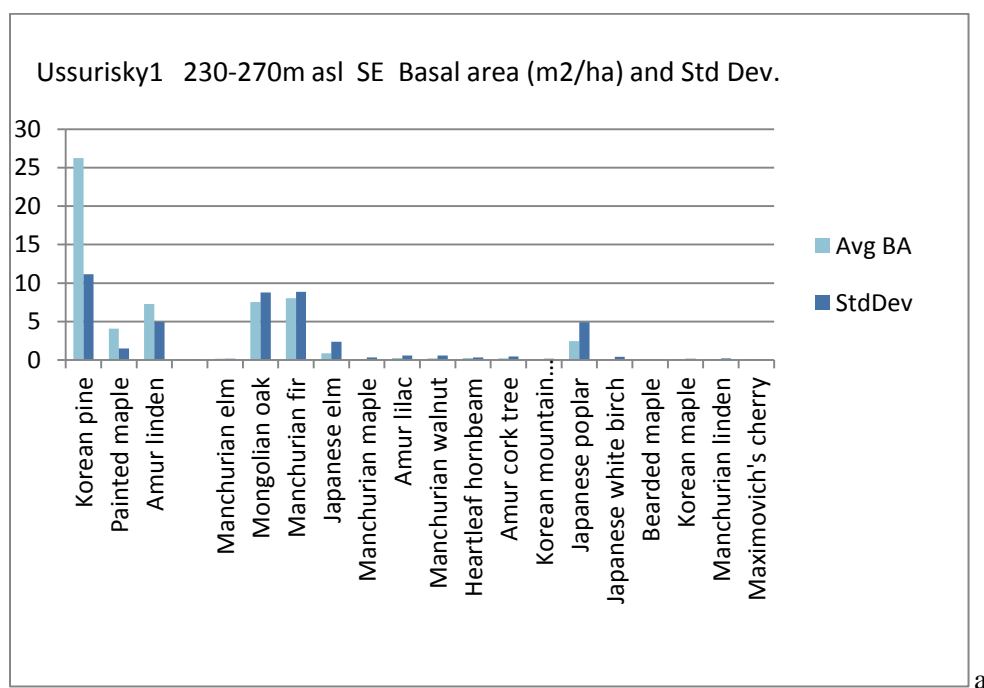
3.3.3 Data analysis

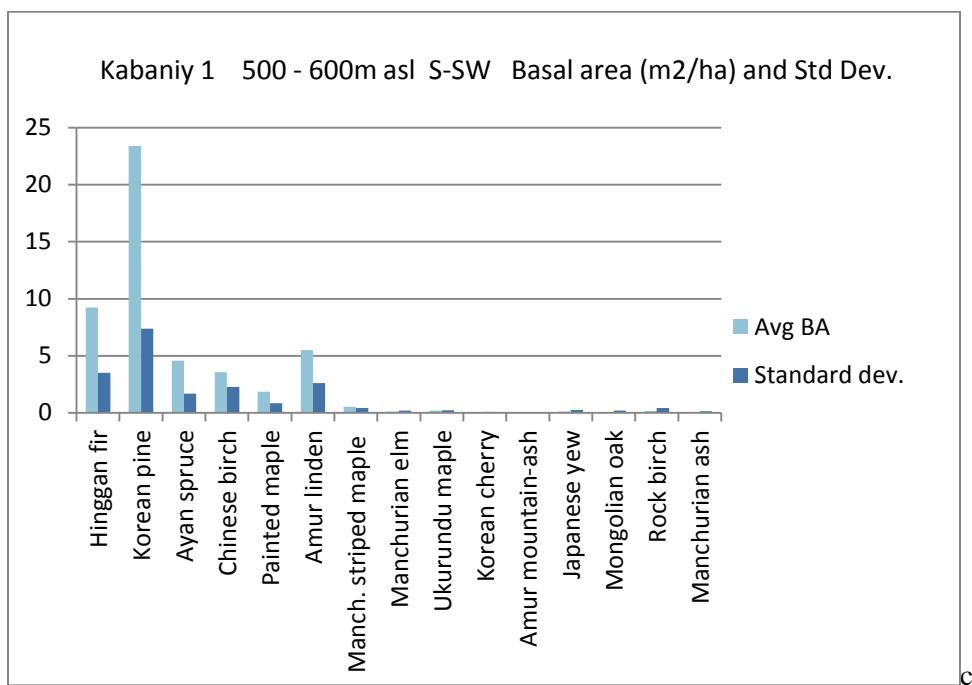
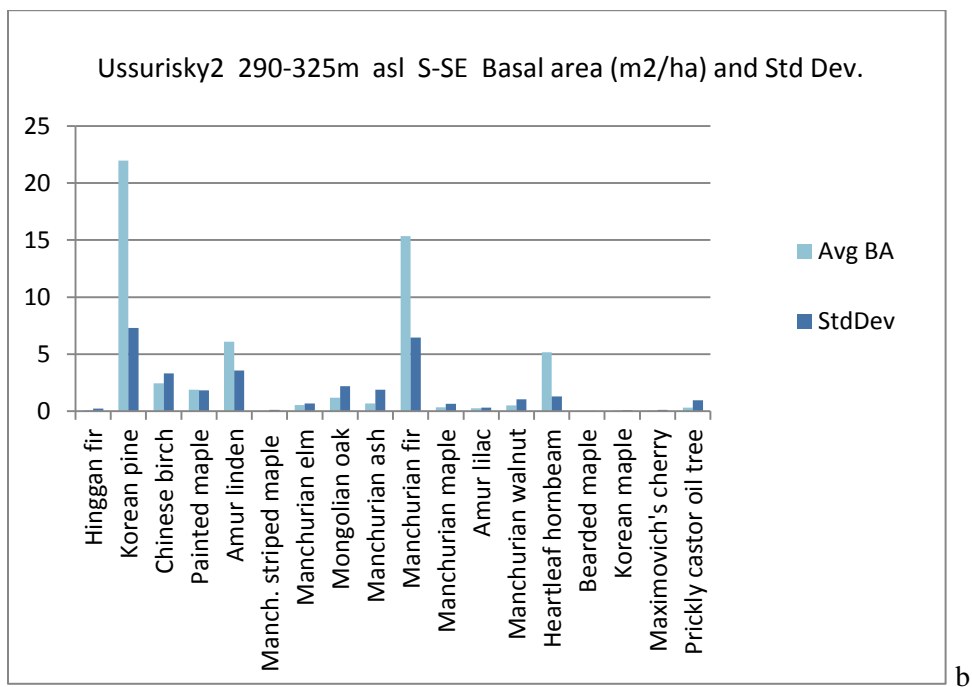
FAREAST results were compared with field data on a species basis using the Kolmogorov-Smirnov (K-S) test (Lilliefors, 1967). The K-S test is a non-parametric test that calculates the distance between two sets of data by calculating the distance between two cumulative distribution functions, each developed from a step function based on the actual empirical data. It is a useful

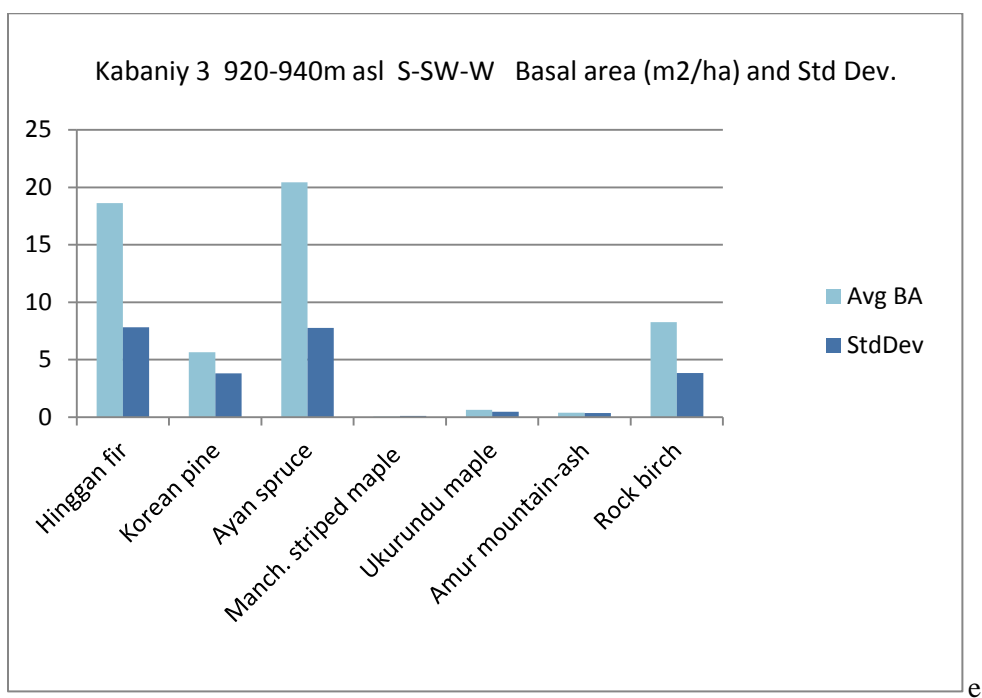
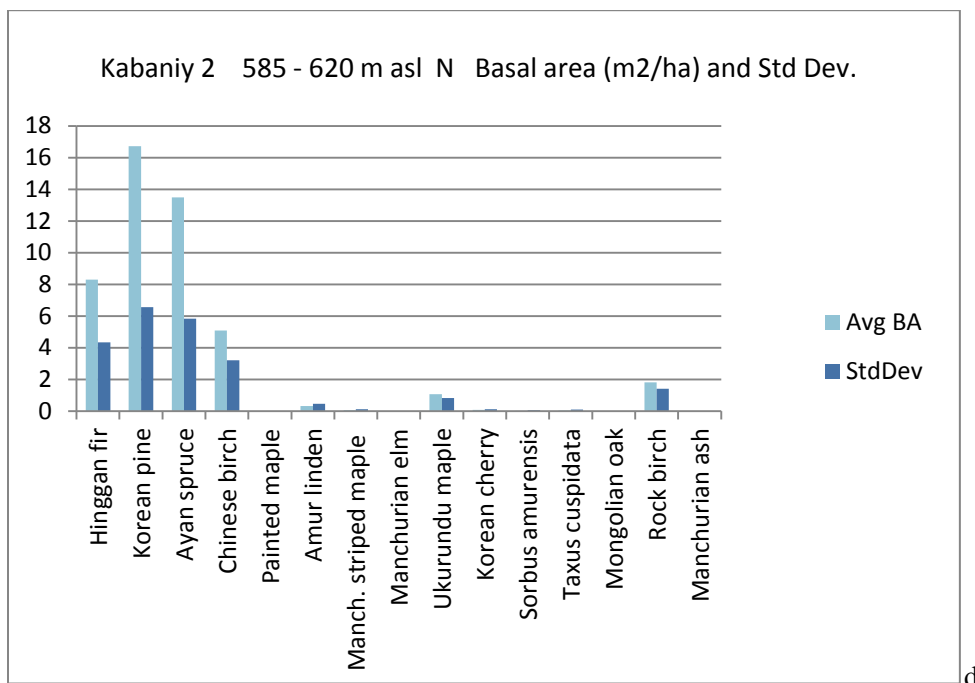
test for small data sets when the mean and variance are unknown. The test was performed from comma-separated data using a Python interface with the statistical software R.

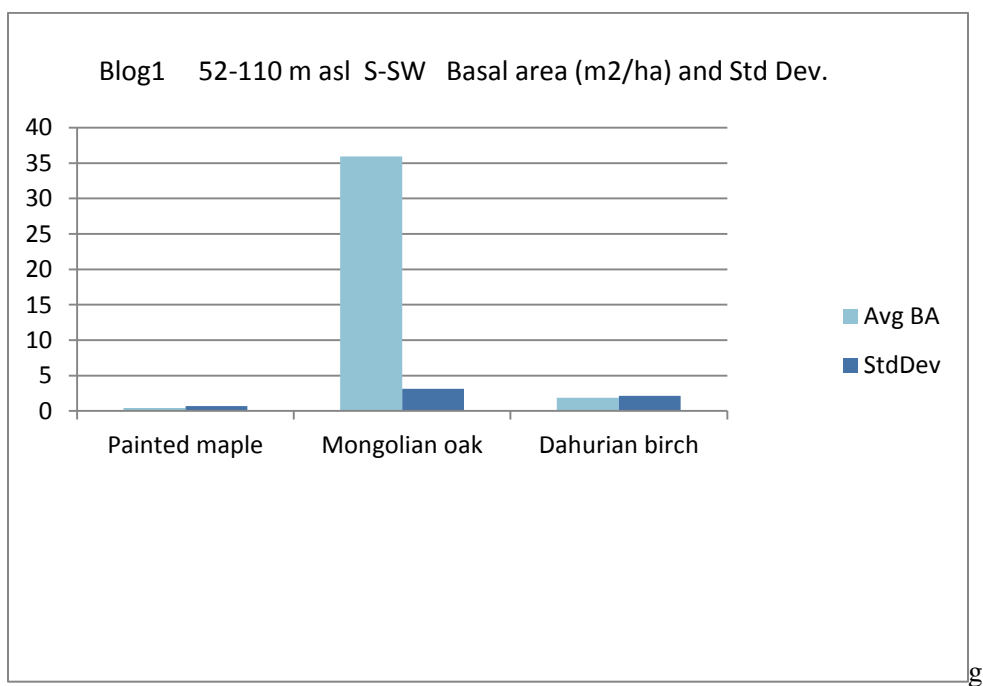
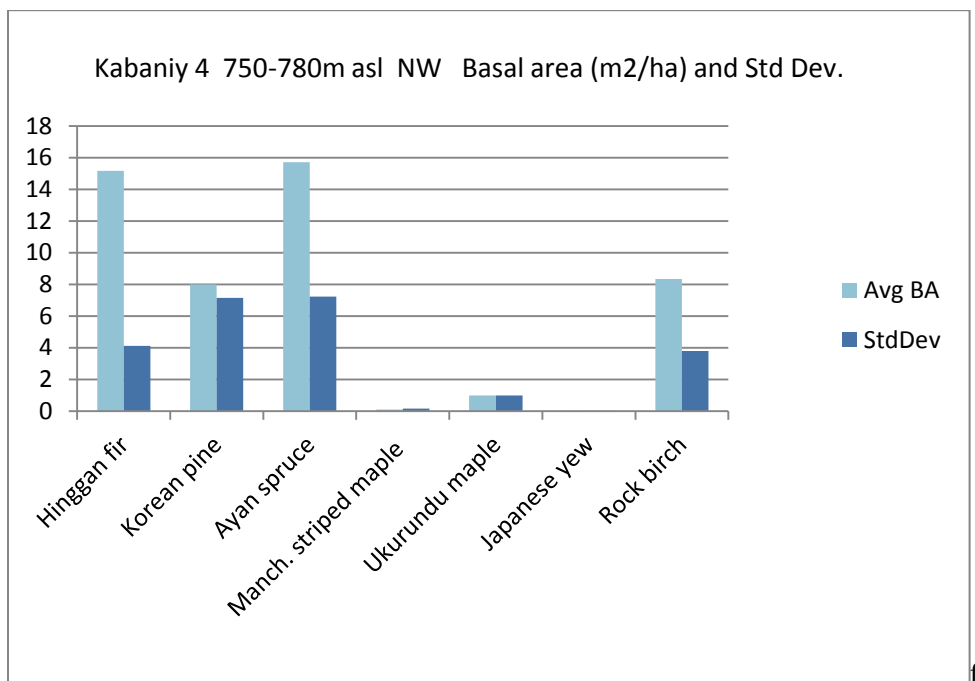
3.4 RESULTS

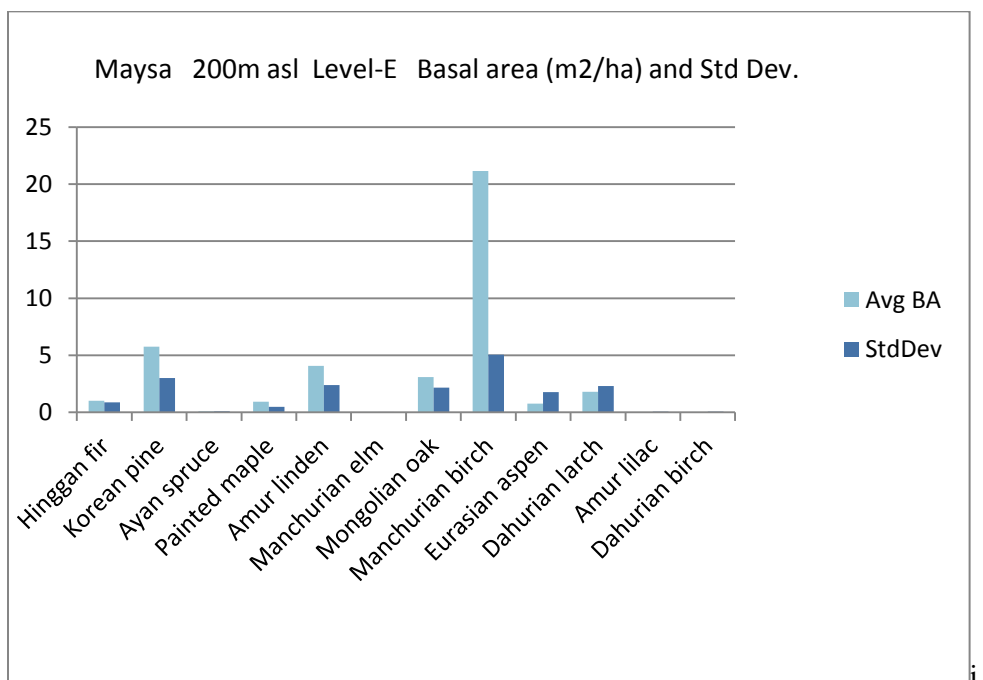
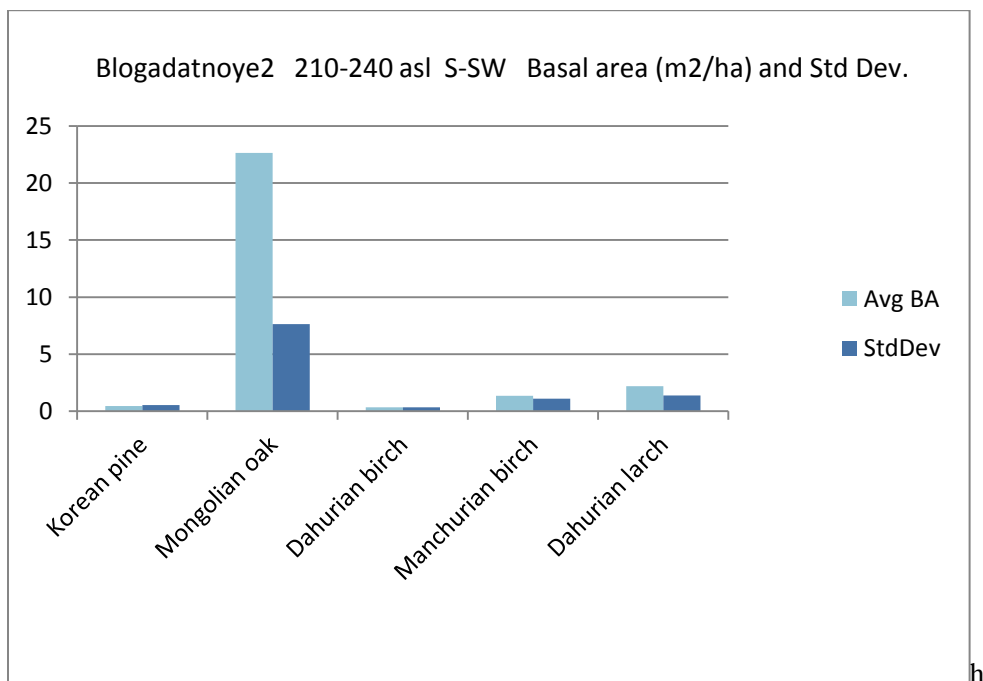
Average measured basal area and standard deviation from the mean by species for the ten plots at each site are shown in Figure 3.6, a-k. Variance in FAREAST is associated with randomness in seeding as well as random variation associated with climate input. Temperature and precipitation vary randomly on a daily basis within the standard deviation from monthly averages.











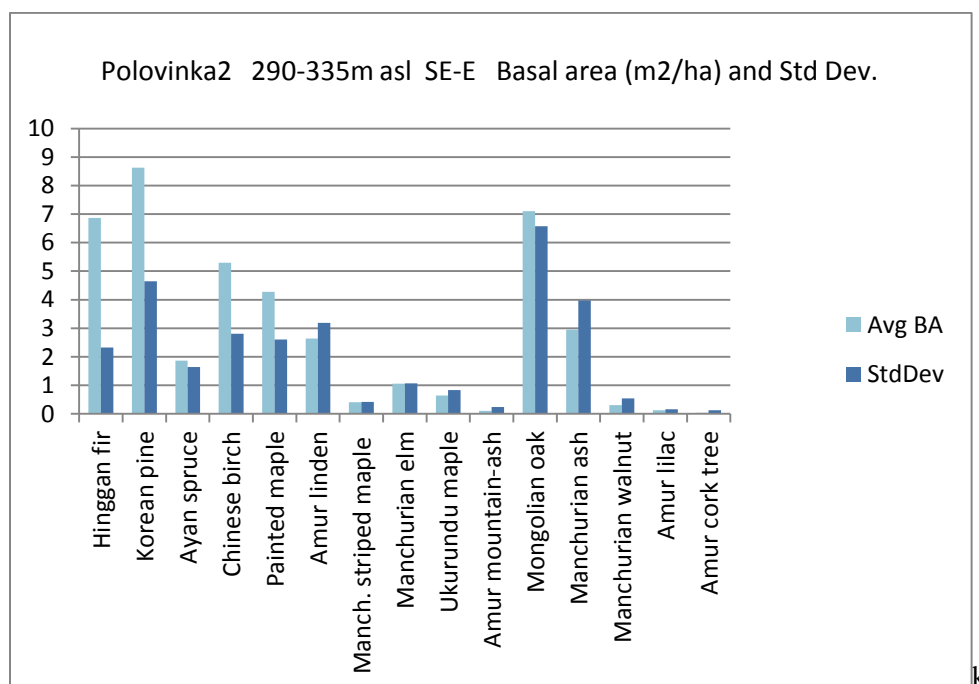
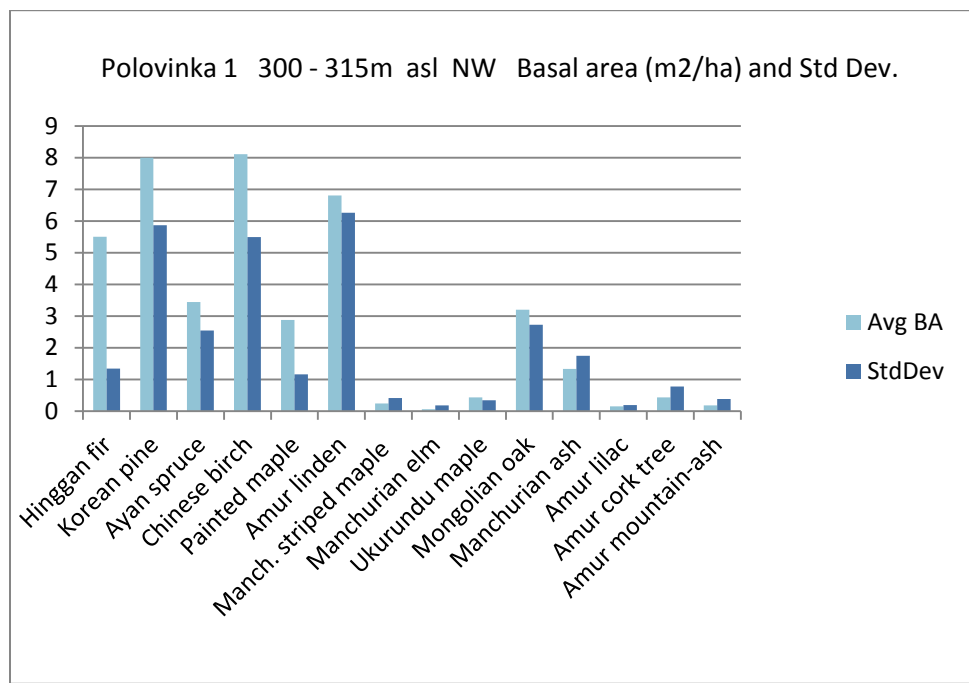


Figure 3.6 a – k Measured basal area (m²/ha) and standard deviation for species at 11 field sites.

3.4.1 Field site vs. FAREAST results

Simulated total basal area closely approximated observed at the seven sites with undisturbed forests (Figure 3.7). At two sites where simulated total basal area was larger than observed (Polovinka 1 and 2), the difference is associated with less observed Korean pine at the site than expected.

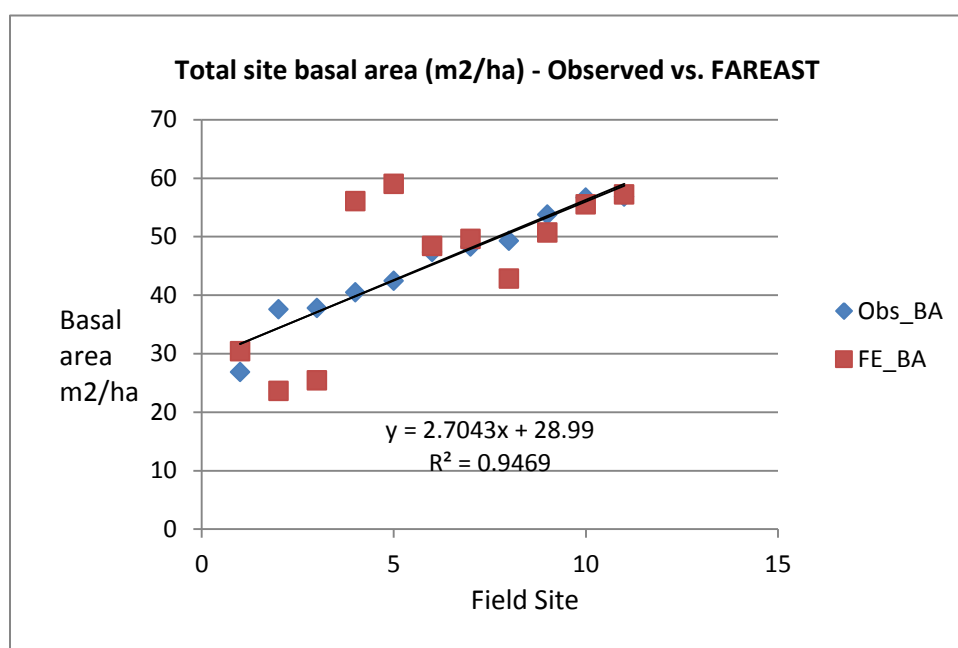


Figure 3.7 FAREAST output for total basal area was closest to observed at field sites with undisturbed forests.

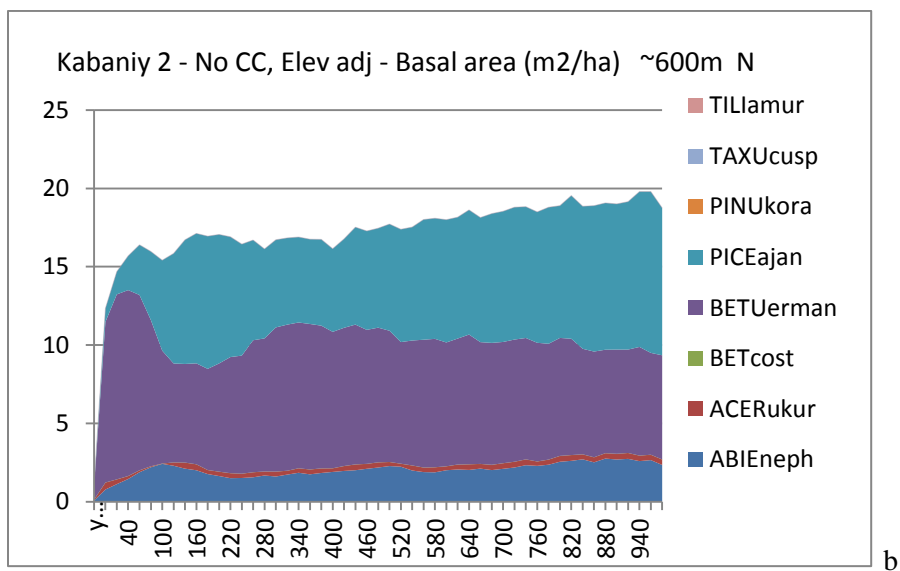
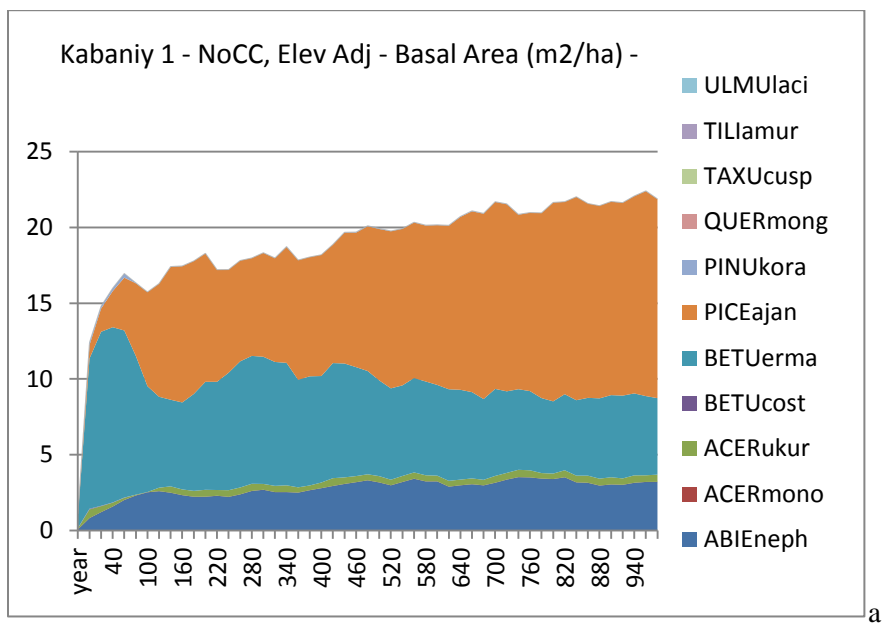
Basal area by species simulated by FAREAST approximated field results at six of the eight sites with old growth forests when the elevation adjustment function was not used. FAREAST results matched observed more closely when the model's altitude adjustment feature was used at the

southernmost and northernmost sites (Ussurisky 1 & 2; Polovinka 1 & 2). Total simulated basal area dropped dramatically with elevation adjustment at the Central Sikhote-Alin sites, where the humid ocean monsoonal climate affected the adiabatic rate (Figure 3.8 a-d).

At all eight primary forest sites, the forest type was correctly identified. For six of the old growth sites, this was mixed deciduous broadleaf/Korean pine/conifer. For Kabaniy 3 and 4, the forest type was dark conifer. The simulated deciduous/conifer ratio matched observed at five sites, all of which were old growth sites.

3.4.1.1 Altitude adjustment

For all the sites on the eastern slope of the Sikhote-Alin Mountain range, the FAREAST model becomes unsettled when elevation is adjusted. Instead of showing an early expansion of basal area, followed by a marked decline then leveling off, total basal area fluctuated, with a slight increasing trend in overall basal area (Figure 3.8).



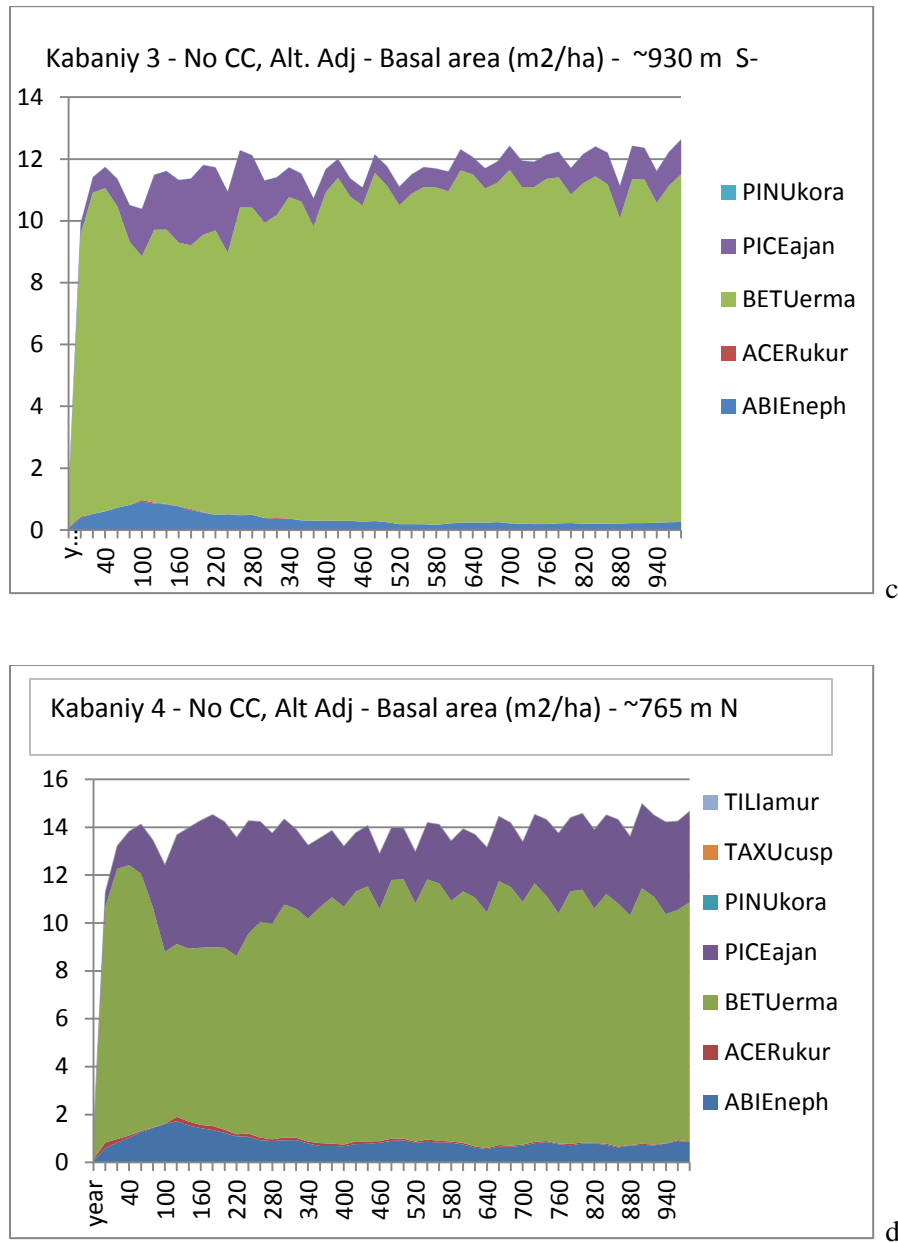


Fig. 3.8 a-d. Altitude-adjusted model results at coastal Sikhote-Alin sites.

At Kabaniy 1, for example, (Figure 3.8a) when adjusted for altitude, FAREAST produced a forest that might be expected at a higher elevation, with Yezo spruce (*Picea ajanensis*) and Erman's

birch (*Betula ermani*) dominating, rather than the dominant observed species, Korean pine, which did not even appear in the output.

This is likely a result of a difference in lapse rates. The eight field sites in the Sikhote-Alin Biosphere Reserve in Central Sikhote-Alin are in a coastal location and experience a moderate and humid climate, which affects the rate of cooling of an ascending parcel of air. The southern sites near the city of Ussurisk and northern sites near Khabarovsk experience a drier and more continental climate, and the model's elevation adjustment feature produces results that are closer to observed.

3.4.1.2 Results by site

Ussurisky 1 and 2 had almost the same aspect (S-SE), gradient ($\sim 20^\circ$), climate and latitude. Observed forest composition at Ussurisky 1 was similar to Ussurisky 2 in terms of species type and basal area. FAREAST correctly identified the two dominant species, Korean pine and Amur linden (*Tilia amurensis*) at the sites and, with adjustment for altitude, correctly identified Manchurian fir as the species with the third largest basal area. At Ussurisky 1, FAREAST results closely approximated field observations (Figure 3.9) at years 260 (altitude-adjusted) and 280 (non-altitude adjusted), where K-S tests showed that the null hypothesis that FAREAST and field-based basal area results are from the same distribution could not be rejected for five of nine species at the site, including Mongolian oak and Manchurian fir ($p > 0.05$). Adjustment for altitude produced an even better match, in which simulated and observed basal area likely were from the same distribution ($p > 0.05$) at year 260 for Korean pine (30.1 vs. 26.3 m²/ha, respectively), Manchurian fir (*Abies holophylla*) (7.0 vs. 8.0 m²/ha), Painted maple (*Acer mono*) (5.7 vs. 4.1

m²/ha), and Amur linden (11.4 vs. 7.3 m²/ha), Manchurian walnut (*Juglans mandshurica*) and Japanese poplar (*Populus maximovihi*). At Ussurisky 2, simulated results most closely matched observed at years 260 and 280 (Figure 3.10), where five of the ten species at the site, including Mongolian oak, appeared to come from the same distribution. With altitude adjustment, simulated was closest to observed at year 280, with 60% of species, including Korean pine and Mongolian oak, representing the same distribution. Simulated Manchurian fir most closely matched observed at year 220 (10.9 vs. 15.3 m²/ha). After year 240, simulated Manchurian fir dropped sharply. Amur linden, Mongolian oak, Chinese birch, and maple species showed greater basal area in the simulation than appeared at the site. Black fir occurred in very small quantities in the simulation as well as at the site, and simulated basal area for Chinese birch, Yezo spruce, Mongolian oak and Manchurian elm (*Ulmus manchurica*) were greater than observed. Model results were similar to observed basal area for maple species and Amur linden.

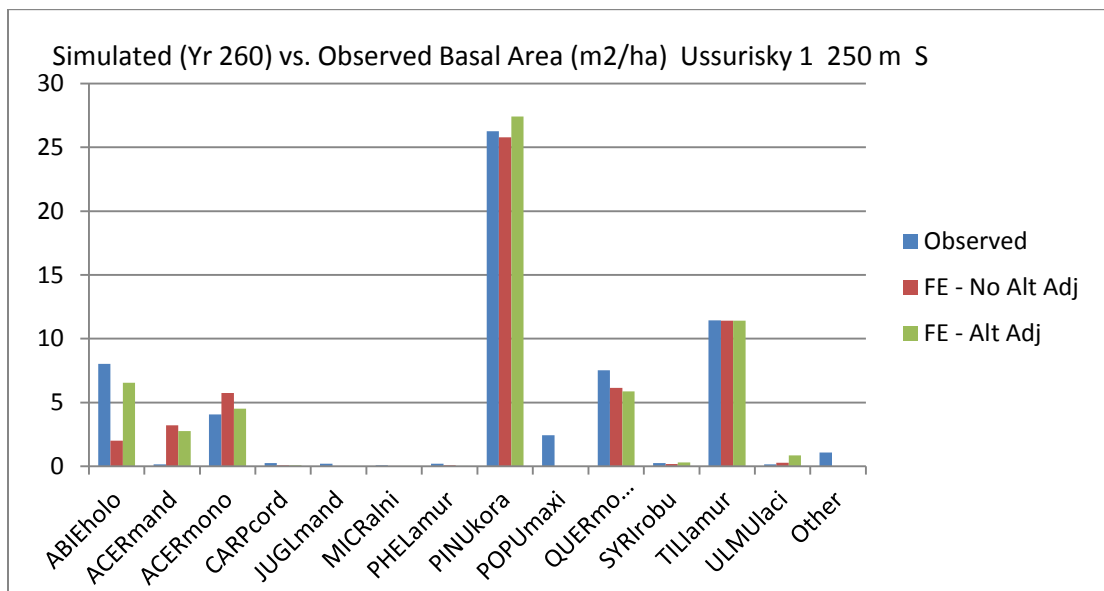


Fig. 3.9 Simulated vs. observed results for the field site Ussurisky 1 with and without adjustment for altitude.

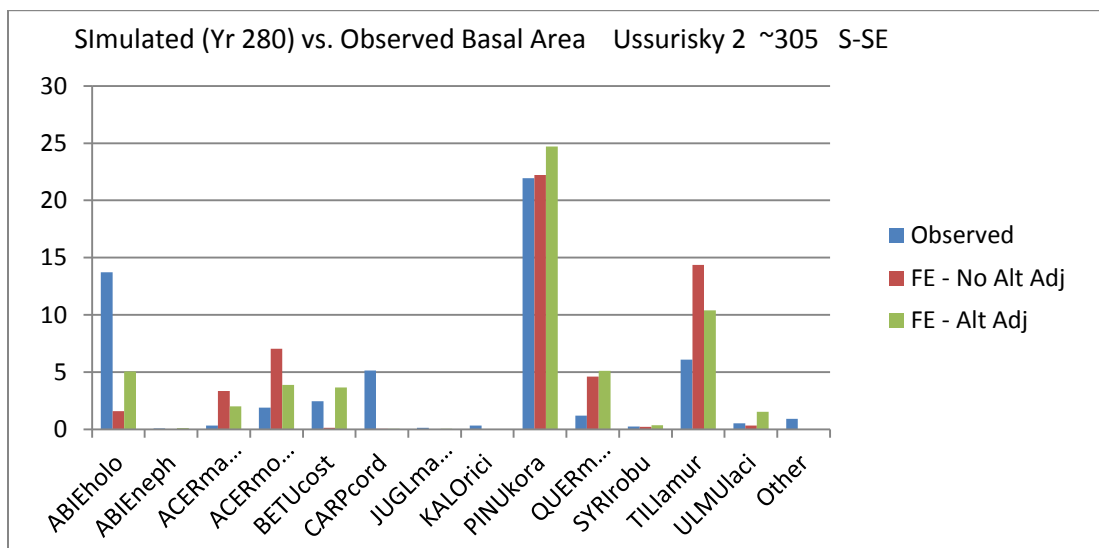


Fig. 3.10 Simulated vs. observed results for the field site Ussurisky 2 with and without adjustment for altitude.

At mid-elevation sites Kabaniy 1 (550 m asl, S-SW aspect) and Kabaniy 2 (600 m asl, N aspect) in Sikhote-Alin Biosphere Reserve in Central Sikhote-Alin, FAREAST without adjustment for altitude correctly identified Korean pine as the dominant species. Kolmogorov-Smirnov (K-S) non-parametric statistical tests (Lilliefors, 1967) for year 340 showed that the null hypothesis that field data and FAREAST results are from the same distribution could not be discarded ($p > 0.05$) for Amur linden, Ukurundu maple (*Acer ukurunduense*), and Japanese yew (*Taxus cuspidata*) (Figure 3.11 and 3.12).

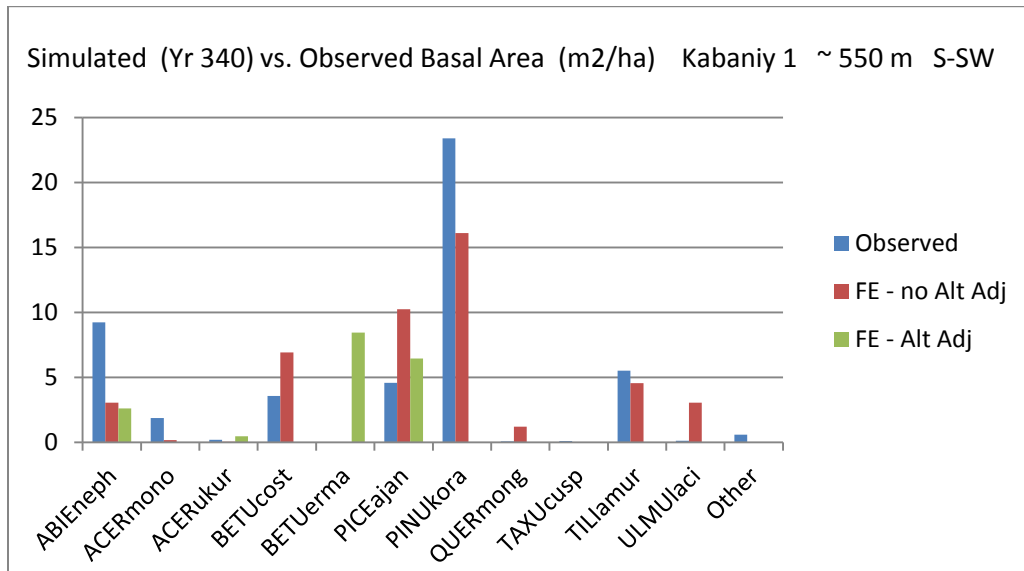


Figure 3.11 FAREAST correctly identified Korean pine as the dominant species at the mid-elevation site Kabaniy 1.

At Kabaniy 1, model output matched the forest type of mixed deciduous broadleaf/Korean pine/conifer. Total simulated basal area (42.8 m²/ha) was 87% of observed (49.3 m²/ha). In the simulation, Mongolian oak basal area peaked at 5.64 m²/ha at around year 200 and declined to less than 2 m²/ha by year 320 (Figure 3.23a), consistent with trajectories associated with competitive processes (Shugart, 1998; Lauenroth *et al.*, 1993; Smith and Urban, 1988). After year 320, oak basal area is less than 2 m²/ha, and drops to less than 1 m²/ha by year 400. As in the simulation, very little Mongolian oak was observed at the site (0.07 m²/ha). Model results suggested less Black fir and more Yezo spruce than observed (Figure 3.11).

At Kabaniy 2, at 600 m asl, with a northern aspect, total observed basal area approximated simulated basal area without elevation adjustment (47.4 m²/ha vs. 48.4 m²/ha, respectively) (Figure 3.12) at year 340 of the simulation. The forest was correctly identified as mixed deciduous broadleaf/Korean pine/conifer. FAREAST accurately showed Korean pine to be the dominant species, followed by Yezo spruce. Simulated Korean pine was close to observed (18.4 m²/ha vs. 16.7 m²/ha respectively). Black fir and Yezo spruce grew in larger quantities than indicated by modeling, whereas Chinese birch and Amur linden appeared in smaller quantities than modeling suggested (Figure 3.12). K-S testing showed Black fir and Japanese yew to be from the same distribution at the 95% confidence level. Mongolian oak was not found on the north-facing slope at Kabaniy 2 or at higher elevations.

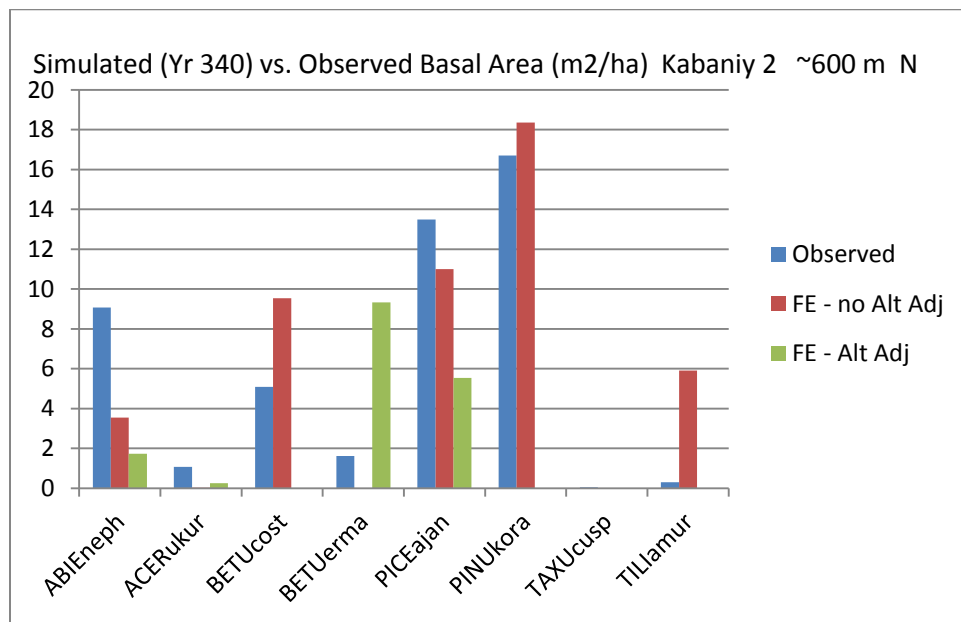


Figure 3.12 Kabaniy 2 – simulated vs. observed basal area by species

At Kabaniy 3 (920 – 940 m, S-SW-W aspect), total simulated basal area without adjustment for altitude was slightly less than observed (50.72 m²/ha vs. 53.77 m²/ha, respectively). Black fir was measured in much larger quantities than simulated, whereas Korean pine was much less represented. Observed Yezo spruce was close to modeled (20.4 m²/ha vs. 18.2 m²/ha, respectively). Manchurian striped maple (*Acer tegmentosum*) and Amur mountain-ash (*Sorbus amurensis*), species that do not appear in FAREAST, were found at the site in small quantities (0.03 m²/ha and .356 m²/ha, respectively).

The K-S test showed that FAREAST results for Kabaniy 3 and 4 for year 340 represented the same distribution as field site results on a species basis for Yezo spruce, Ukurundu maple (Kabaniy 3 only), and Japanese yew (Kabaniy 4 only) ($p > 0.05$). At Kabaniy 3 (930 m, S-SW aspect) (Figure 3.13), without elevation adjustment, total simulated basal area (50.7 m²/ha) at year 340 was close to observed (53.8 m²/ha). Simulated basal area (BA) for Yezo spruce (18.2 m²/ha) also was close to observed (20.4 m²/ha), but simulated Korean pine BA was much larger than observed (26.8 m²/ha vs. 5.6 m²/ha) and simulated Black fir BA was much smaller than observed (5.5 m²/ha vs. 18.6 m²/ha).

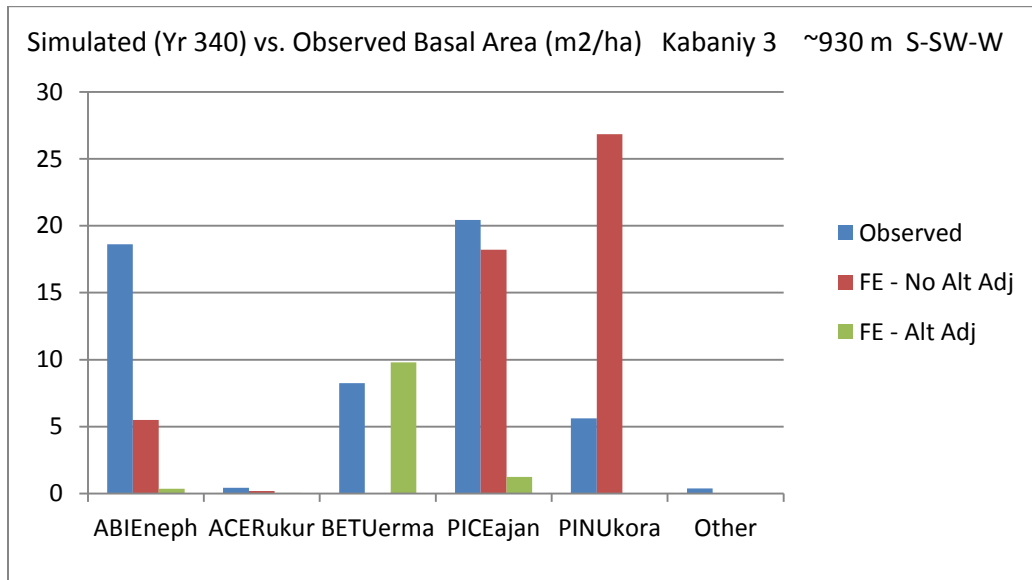


Figure 3.13 Simulated basal area without altitude adjustment at Kabaniy 3.

At Kabaniy 4 (~765 m asl, NW aspect) (Figure 3.14), simulated total basal area with no adjustment for altitude was 49.63 m²/ha, very close to 48.31 m²/ha average total basal area measured at the field site. Similar to Kabaniy 3, the model identified Korean pine as the dominant species, whereas Yezo spruce had the greatest basal area at the site. Amur linden also was produced in the simulation, but had minimal presence at the site. Black fir and Alpine birch (*Betula ermanii*) measured at the site appeared in larger quantities than simulated. When the model was adjusted for elevation, observed Alpine birch was close to simulated, but other species showed little correlation. Manchurian striped maple, a species not in FAREAST, was found in small quantities in the field (0.09 m²/ha). At both Kabaniy 3 and Kabaniy 4, simulated as well as observed maple species basal area was very low (< 1.0 m²/ha).

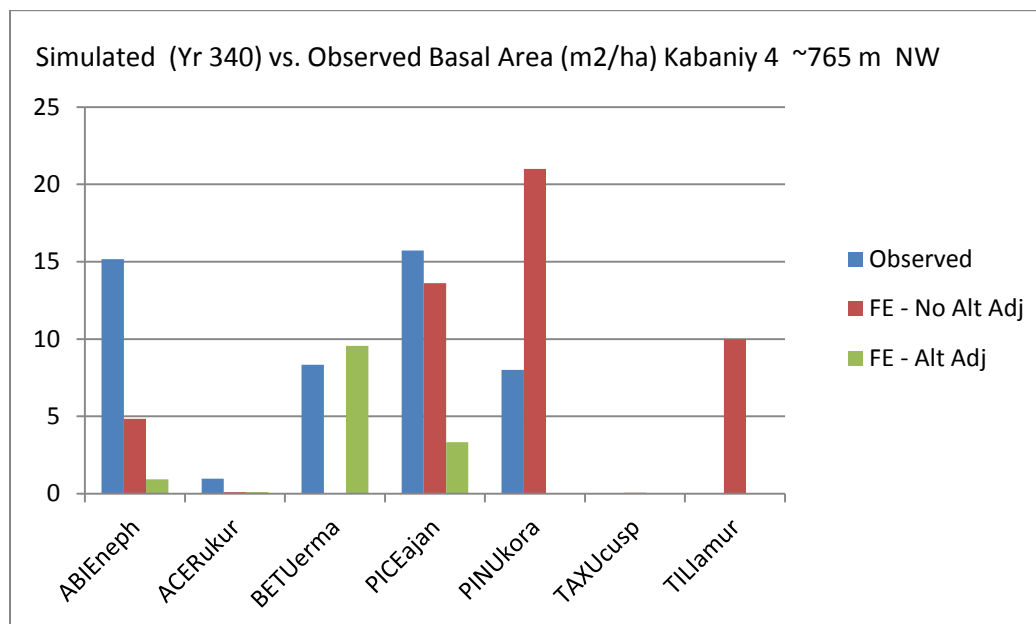


Figure 3.14 Kabaniy 4 – simulated vs. observed basal area by species

Coastal sites in Sikhote-Alin Biosphere Reserve, Blagodatnoye 1 and 2, represented disturbed forests and are addressed in the Discussion section.

At Polovinka 1 (310 m, NW aspect), total simulated basal area without altitude adjustment is 57.9 m²/ha compared with observed basal area of 40.5 m²/ha. K-S test results indicated that FAREAST results and field data likely were from the same distribution at the 95% confidence level for Mongolian oak and Laciniata elm (*Ulmus laciniata*) for years 280 and 300. Species-level simulated basal area most closely matches observed for deciduous species and with adjustment for altitude at year 280 (Figure 3.15). Black fir appeared at the site (5.5 m²/ha), but was reflected only minimally in simulated results. Observed Chinese birch and Yezo spruce were greater than simulated, while observed basal area for maple, Korean pine and Amur linden was much less than modeled. This gap diminished when adjustment was made for site elevation.

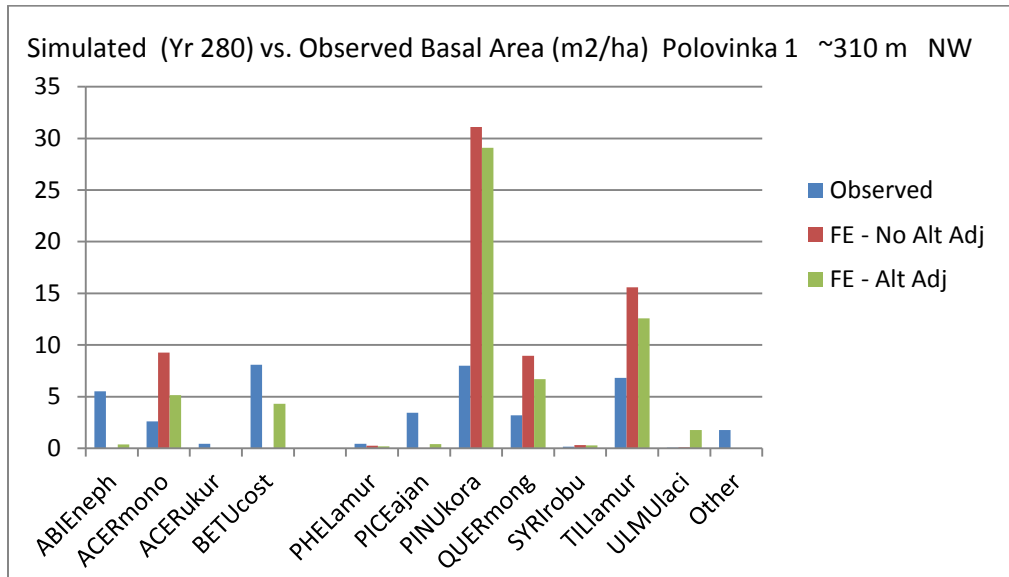


Fig. 3.15 Polovinka 1 – simulated vs. observed basal area by species at year 280.



Fig. 3.16 Mixed broadleaf deciduous/Korean pine/conifer forests at Polovinka 1.

At Polovinka 2, although the simulation correctly shows Korean pine to be the dominant species, the simulated quantity of Korean pine is much larger than observed (26.8 vs. 8.6 m²/ha) (Figure 3.17). K-S test results suggested FAREAST results and observed basal area by species represent

the same distributions at the 95% confidence level for two species, including Mongolian oak, out of nine, at years 280 and 300. Adjusting the model for elevation improves the correlation, with four of nine species likely from the same distribution at years 280 and 300. Simulated Black fir was considerably smaller than observed (0.0 vs. 6.9 m²/ha). Observed basal area was close to simulated for Painted maple, Chinese birch, Yezo spruce, Mongolian oak, Manchurian elm and other deciduous species. Species observed in small quantities at the site that are not included in the FAREAST model were Manchurian striped maple (0.41 m²/ha), Manchurian ash (*Fraxinus mandshurica*) (2.9 m²/ha), and Amur mountain ash (*Sorbus amurensis*) (0.09 m²/ha).

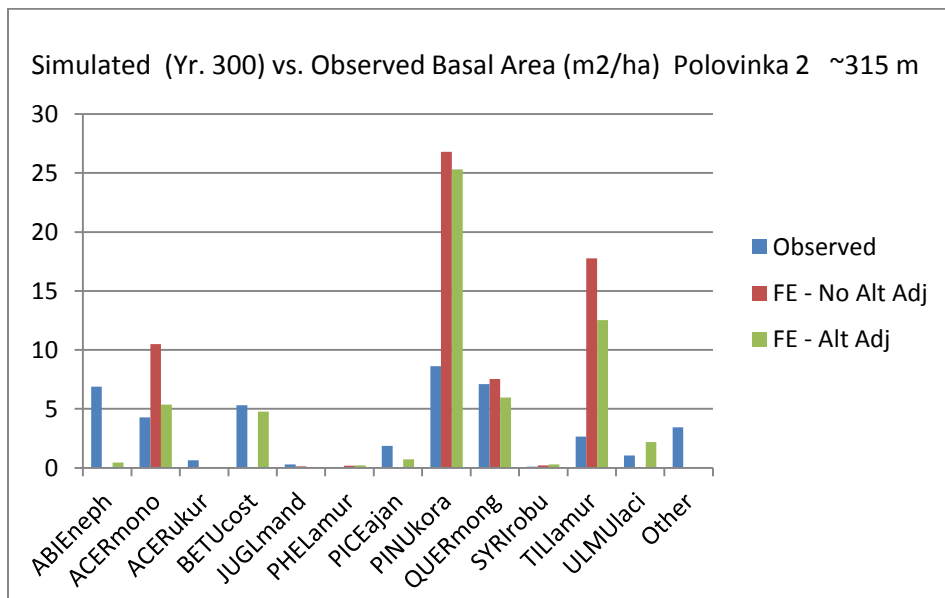


Fig. 3.17 Polovinka 2 (SE – E aspect) Simulated vs. observed basal area by species



Fig.3.18 Research site at Polovinka 2

Section 3.4.1.2.1 Burn site – Maysa in SABZ

At the site of a severe wildfire in Sikhote-Alin Biosphere Reserve about 80 years before the field campaign, FAREAST results at year 80, without elevation adjustment, matched simulated basal

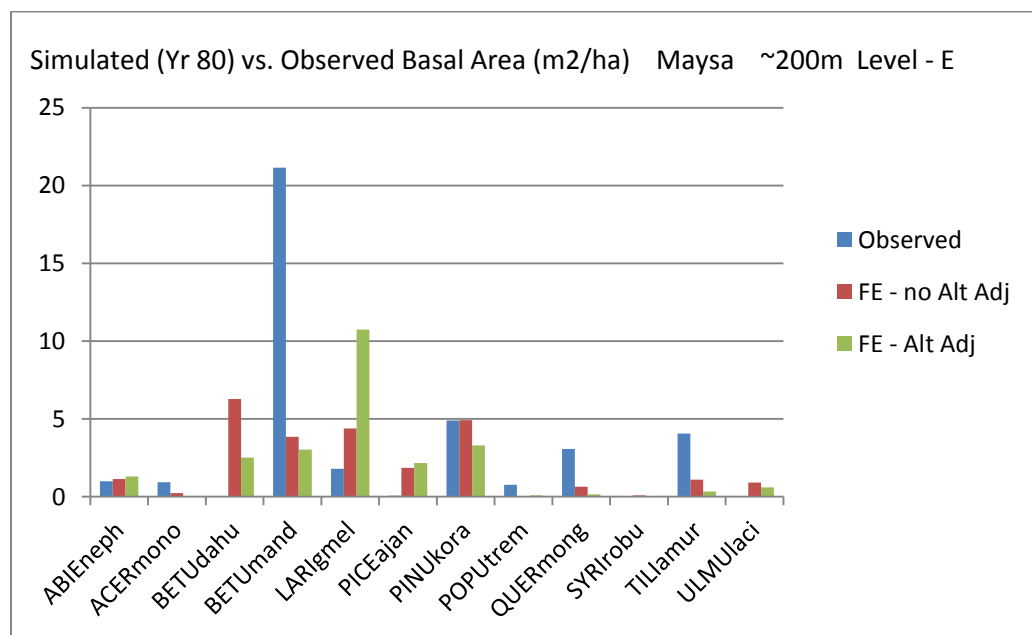


Figure 3.19 Maysa (wildfire site) – basal area by species at year 80.

area for ten of the twelve species at the site (Figure 3.19) and the K-S test showed that FAREAST output and site measurements reflect the same distribution ($p > 0.05$) for six of twelve species (50%), including Mongolian oak.

3.5 DISCUSSION

The purpose of this research was to assess the validated model's performance at a detailed scale in preparation for using the model to assess the impact of projected climate change in this area, the habitat of the wild Amur tiger. This chapter explores the causes of any discrepancies in order to gain insights that might be useful in future applications of the model.

Trees at field sites with uncut primary forests were estimated by scientific staff to be about 300 - 350 years old. Although these forests are considered to be "old growth," which might suggest equilibrium status, forest succession theory and the FAREAST model indicate that, for many forests, the years 240 – 400 of succession represent a period of considerable change in terms of biomass quantity and species composition (Shugart, 1984; Shugart, 1998). The proportion of different species changes rapidly as total biomass peaks and canopy species begin to thin out (Shugart, 1984; Shugart, 1998; Shugart *et al.*, 2010). Some original "pioneer" (Whitmore, 1975; Gomez-Pompa, 1981) species reach their maximum biomass and life span or die as a result of losing the competition for light and soil resources. These trees are replaced by other species, some of which became established in light-limited conditions under the canopy (Shugart, 1998; Kobayashi *et al.*, 2007) and respond quickly when a gap occurs. Simulated results for a particular species may closely match observed field results at one point, but vary greatly twenty years later.

Similarly, field basal area of a species may be higher than expected from modeling when local conditions cause a lag in shrinkage of basal area that the simulation indicates.

In addition, because of the mosaic nature of forest landscapes, component gap-sized units of a large, seemingly homogeneous forest may differ from the forest as a whole and from validated model results because of anomalies at the transect scale caused by variations in disturbance history (Shugart, 1998; Shugart *et al.*, 2010). For example, small-scale logging in the past may have removed canopy trees, causing these species to occur in smaller amounts than expected and allowing greater quantities of shade-intolerant species, such as birch and Mongolian oak, to grow. The site also may contain unusually large diameter trees or species such as Korean pine or Amur linden, which reproduces vegetatively (Koop, 1987) and can dominate a site (Shugart *et al.*, 2010). Regeneration strategies such as root-level sprouting, wind vs. animal borne seeds, different species' seed bank size, and outcomes of competition for light, nutrients, and moisture, can cause marked differences among stands or transects (Shugart, 1998). Even in pristine areas of primary forests, the disturbance history may be unknown and predicting exactly how trees will grow back after disturbance is difficult (Shugart, 1984). Discrepancies between field observations and model output also are due in part to random variations associated with interactions, such as weather patterns and competition for light and nutrients. These stochastic factors are reflected in the field observation data and built into the model.

The degree to which FAREAST model output matched field data varied according to climate, latitude, elevation, and site history. Simulated total basal area approximated observed at seven of the eleven sites, and seven of eight primary forest sites. The model was able to correctly identify the forest type at nine of eleven field sites and at all sites with primary forests. Six of these were

mixed broadleaf deciduous/Korean pine/conifer. Mixed forests were defined when broadleaf deciduous, conifer, Korean pine, and/or larch trees appeared at a site, but comprised less than 65% of total basal area. FAREAST correctly identified the forest type for two sites with dark conifer (Kabaniy 3 and 4). The simulated dominant species, usually Korean pine, was consistent with observed at seven of eleven locations and seven of eight sites with old growth forests.

Black fir generally occurred in greater quantities than the simulation indicated. The Black fir/Yezo spruce forest type is found throughout the Sikhote-Alin area (Krestov, 2003; Nakamura and Krestov, 2005), but appeared less frequently in simulations. The discrepancy may be in part because Black fir tends to occur in clusters because it grows in shaded conditions under the canopy and matures when a gap occurs (Nakamura and Krestov, 2005), so fir basal area at a transect may be disproportionately large.

3.5.1 *Southernmost sites - closest match between simulated and observed*

FAREAST results most closely matched observed at the southernmost study sites, which were located in Ussurisky Reserve (*zapovednik*) in southern Primorski Krai, near the southern end of the Sikhote-Alin Mountain system. These sites were closest to Changbai Mountain, forest data from which were used to develop and verify the FAREAST model. Similarity of latitude, climate and forest type may have contributed to the correspondence of results. This area is characterized by low hills with gentle to moderately steep slopes, large meadows as well as forests, and a temperate but cool subarctic climate (Krestov *et al.*, 2006). The old-growth forests studied are among the few primary forests left in far southeastern RFE, most having been cleared by settlers before 1900 (Krestov 2003). These species-rich mixed deciduous broadleaf/Korean pine/conifer

woodlands, identified as “Southern” or “Southern dry forests ” by Krestov (2003) because of dry soil conditions in spring, are associated with the particular climate and contain the rare Manchurian or Holo fir (*Abies holophylla*), Korean pine, Hornbeam (*Carpinus cordata*), Mongolian oak, Ash (*Fraxinus spp*), Linden (*Tilia spp*), Maple (*Acer spp*), Chinese or Yellow birch (*Betula costata*), and smaller quantities of other species (Krestov, 2003; Yan and Shugart, 2005; Nakamura and Krestov, 2005).

Of all the field sites, simulated results in terms of basal area by species most closely matched observed at Ussurisky 1, a mixed deciduous broadleaf/Korean pine/conifer forest on a south facing slope, elevation 230 – 270 m asl. The dominant species, both observed and modeled, was Korean pine, followed by Amur linden, Mongolian oak and Holo fir (*Abies hollophylla*). The conifer: deciduous ratio was 1.24 (34.3:27.8 m²/ha) for modeled and 1.02 (27.8:27.6 m²/ha) for observed.

Mixed forests that contain Korean pine and Mongolian oak are important for wildlife and, in particular, the ungulate prey of Amur tigers (Heptner and Sludskii, 1992; Heptner *et al.*, 1992; Miquelle *et al.*, 2010a). Seeds and nuts from these species support a large trophic web, particularly during long winters when other food sources may not be available (Liu And Zhu, 1991; Heptner et al., 1992; Zyryanova, 2005; Nakamura and Krestov, 2005).

Simulated Mongolian oak basal area at Ussurisky 1 is about 10 m²/ha from years 80 through 180, but starts to decline after year 140, then drops off steeply and nearly disappears (Figure 3.21). At the site, oak basal area was 7.5 m²/ha, which is consistent with years 240 - 260 of the simulation. The model suggests that Mongolian oak at the site is in the process of declining and will not regenerate.

FAREAST results most closely match observed for Korean pine at Ussurisky 1 at around year 280 (22.2 m²/ha simulated vs. 21.9 m²/ha observed), a time when simulated Korean



Fig. 3.20 Mixed forests at Ussurisky 1

Pine basal area is declining. After a minimum of 13.6 m²/ha in year 340, simulated Korean pine basal area rebuilds and maintains about 19 – 23 m²/ha indefinitely. This is consistent with Ishikawa *et al.* (1999), who asserted that Korean pine can persist indefinitely in a forest with favorable climate conditions and naturally occurring gaps, which allow the species to regenerate. Species observed in small quantities at Ussurisky 1 that aren't in FAREAST input data consisted of two maple species (*Acer pseudozibold*, *A. tegmentosum*) (0.18 m²/ha), Manchurian linden (*Tilia manchurica*) (0.04 m²/ha), and Japanese elm (*Ulmus japonica*) (0.9 m²/ha).

Ussurisky 2 was located at 305 m asl on a south – southeast facing slope, but a ridge to the east blocked morning sunlight. At Ussurisky 2, Korean pine dominated both observed and simulated basal area, followed by Amur linden. Simulated Korean pine was very close to observed at year

300 without elevation adjustment ($21.9 \text{ m}^2/\text{ha}$ field vs. $22.7 \text{ m}^2/\text{ha}$) and at year 280 with elevation adjustment ($21.9 \text{ m}^2/\text{ha}$ field vs. $22.2 \text{ m}^2/\text{ha}$ simulated).

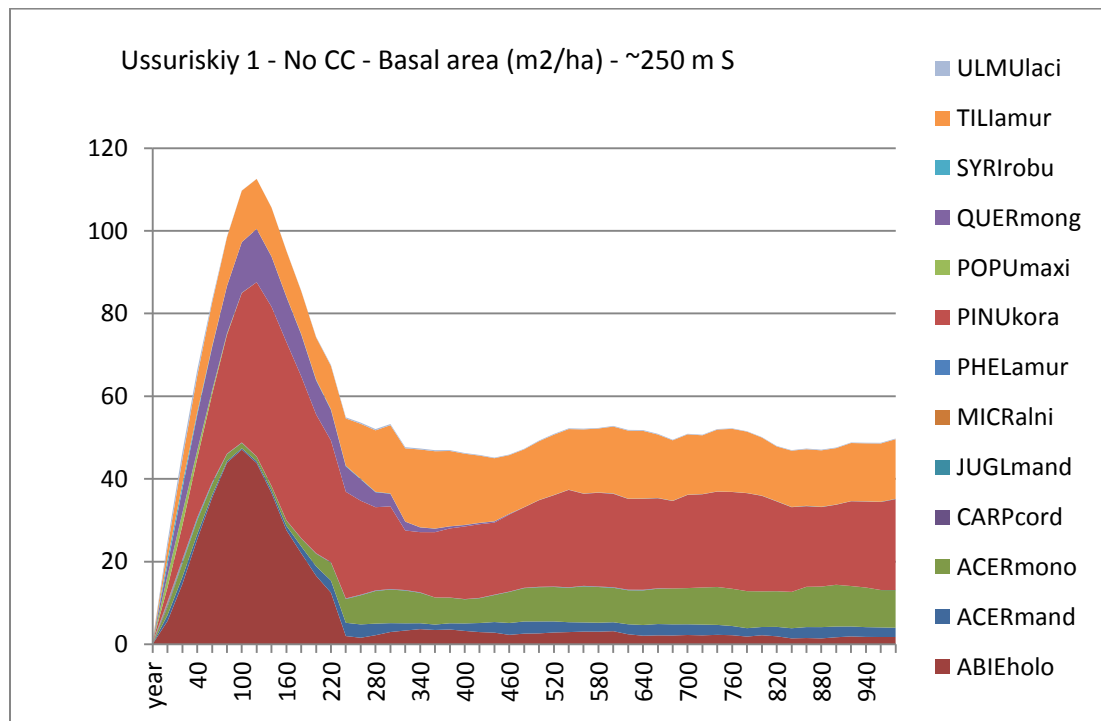


Fig. 3.21 Over time, the forest at Ussurisky 1 will be dominated by Korean pine, Amur linden and Painted maple.

Modeling makes it possible to estimate the age of the forest. For example, simulated basal area of Holo fir drops precipitously at Ussurisky 1, from $12.5 \text{ m}^2/\text{ha}$ to $2.0 \text{ m}^2/\text{ha}$, after about 240 years, as the initial generation of trees dies and is not replaced (Figure 3.22). Observed basal area of $8.0 \text{ m}^2/\text{ha}$ suggests the forests at the first site were no older than 240 years at the time of data collection. Observed Holo fir at the Ussurisky 2 field site ($15.33 \text{ m}^2/\text{ha}$) does not seem to be declining yet, which would suggest that the forest is younger than 240 years. Alternatively, since the exact age of the observed forests is unknown, Holo fir might simply senesce more slowly at

this site, possibly because of morning shade produced by the ridge to the east of the site. Forest age of about 240 years before 2007 (establishment in 1767) in this area is consistent with research on disturbance history and tree establishment of Korean pine in Ussurisky reserve (Ishikawa *et al.*, 1999) that identified 1690 to 1780 as one of only two peak periods of establishment, the second period being 1840 – 1900. A period of Holo fir establishment occurred from 1790 to 1840 (160 – 210 years before field research), with data records starting in 1770 (Ishikawa *et al.*, 1999).

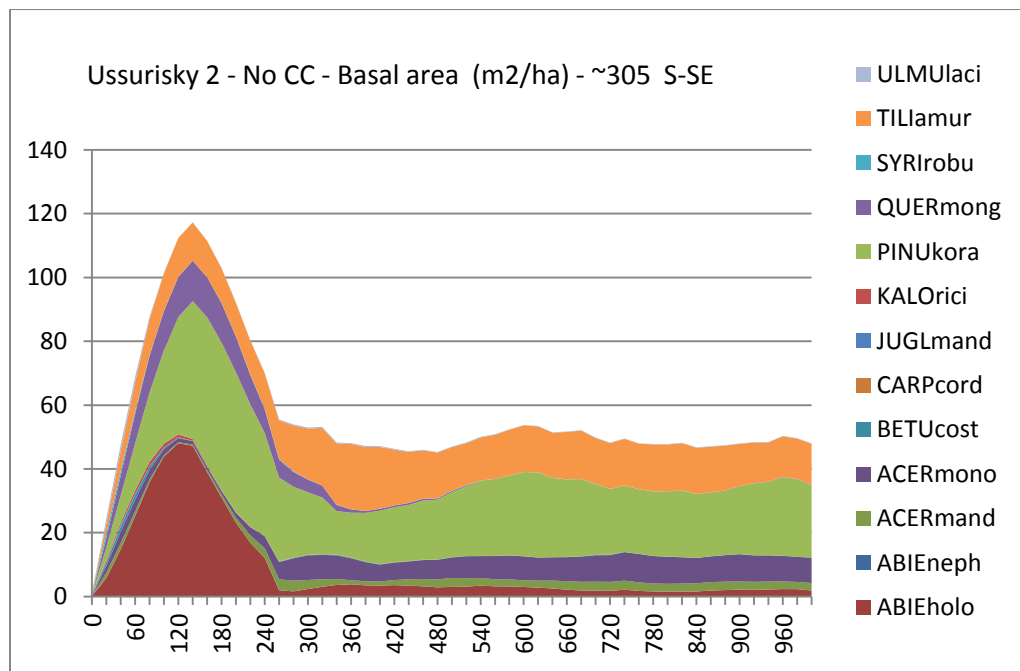


Figure 3.22 Comparing observed Holo fir (*Abies Holophylla*) basal area with simulated is a mechanism to estimate the age of the forest, since the species almost disappears after about 240 years.

3.5.2 *Sikhote-Alin Biosphere Zapovednik (Reserve)*

Seven sites in the Sikhote-Alin Biosphere *Zapovednik/ Reserve* (SABZ) in Central Primorye provided an opportunity to look at the model's results from the perspective of paired opposing aspects, variations in elevation, regeneration of coastal forests after disturbance, and an early successional post-wildfire forest.

3.5.2.1 *Mid-elevation forests - Kabaniy 1 and 2*

The sites Kabaniy 1 and Kabaniy 2 represented typical temperate mixed deciduous broadleaf/Korean pine/conifer forests (Kolesnikov, 1956; Yan and Shugart, 2005; Krestov, 2003; Nakamura and Krestov, 2005) and were located on opposing aspects. FAREAST correctly identified Korean pine as the dominant species at these sites, which had conditions considered the most favorable for this species, i.e., slopes from sea level to 800-900 m asl (Krestov, 2003). Forests were estimated by reserve staff to be approximately 300 – 350 years old. FAREAST results reinforced this estimate, as observed forest composition was closest to year 300 (Kabaniy 1) and 340 (Kabaniy 2) of the simulation (Figures 3.11 and 3.12).

The difference between simulated and observed results at Kabaniy 2 may be in part a result of the northern aspect, a model parameter, which would create cooler atmospheric temperatures and cooler as well as moister soils. Soils on which Korean pine is found are typically mesic, well-drained and rich in nutrients (Zyryanova *et al.*, 2005), although Korean pines grow well both on moist and fertile soil on a north-facing 6 – 15° slope and on a drier and less fertile south-facing 16 – 25° slope (Li and Zhu, 1991). FAREAST, which was adjusted to reflect the species mix,

showed slightly less Korean pine on the southern slope ($15 \text{ m}^2/\text{ha}$) compared with the northern slope ($18 \text{ m}^2/\text{ha}$), which might be associated with the lack of Mongolian oak at Kabaniy 2, which would compete for sunlight and soil nutrients. FAREAST results appear more consistent with observed for Korean pine with a northern aspect, which receives less solar radiation. The model performs similarly regardless of aspect for other conifer species. The model was developed and verified on a northern slope (Yan and Shugart, 2005), which might contribute to this affinity.

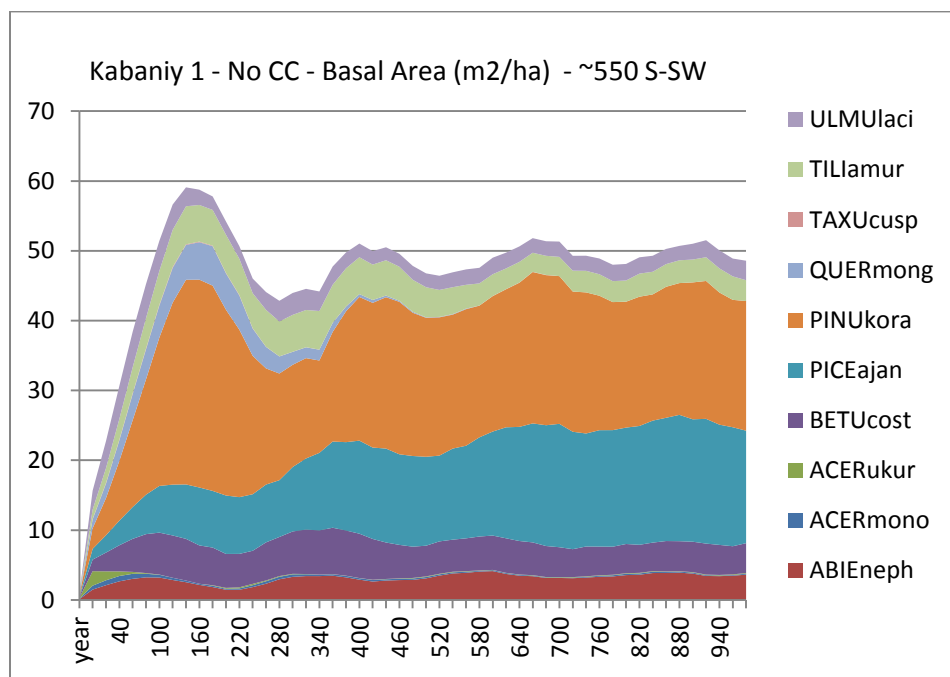


Figure 3.23 At Kabaniy 1, FAREAST correctly identified the forest type as mixed deciduous broadleaf/Korean pine/conifer.

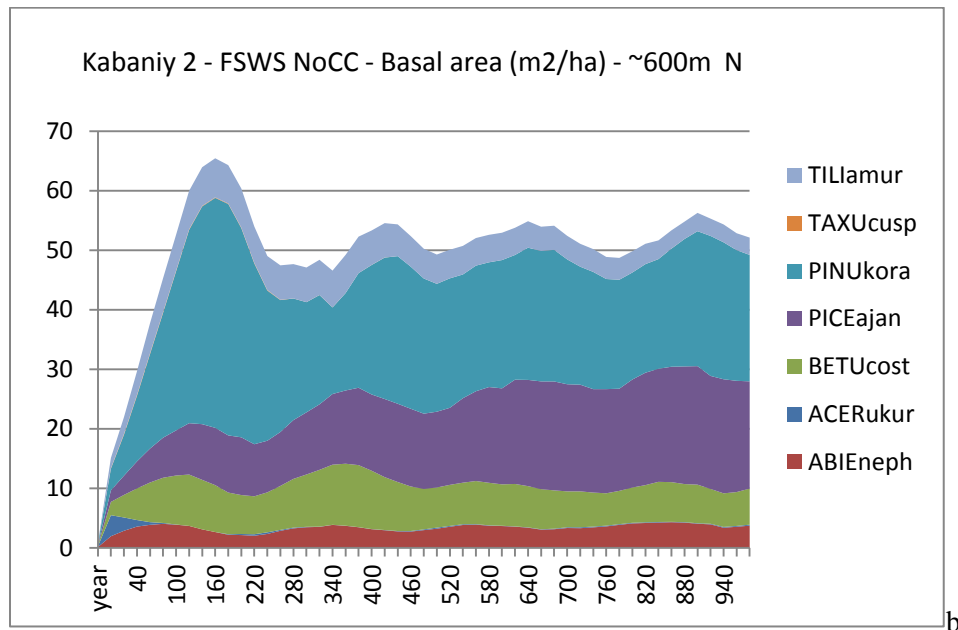


Figure 3.24 FAREAST suggests that Korean pine at Kabaniy 2, like Kabaniy 1, will persist indefinitely at current basal area levels.

Previous studies in Central Sikhote-Alin forests and tree plantations have concluded that Korean pines need a canopy gap to reach full maturity. Ishikawa *et al.* (1999) found that Korean pine saplings in this area tended to grow in clump sizes of 18 m² and 144 m². A circle of 144 m² would have a diameter of 13.5 m and would represent the approximate size of the canopy of a large Korean pine or hardwood tree, which suggests that saplings became established when large canopy trees fell. An 18 m² clump might results from light filtering through branches or a small opening in the canopy. Climate in this area creates many opportunities for gap formation. Heavy snowfall causes limb breakage and fallen trees. Typhoons from the Pacific Ocean occasionally make landfall, causing wind damage and flooding. Towering Korean pine, Yezo spruce and Black fir are vulnerable to lightning strikes (Ishikawa *et al.*, 1999).

Mature Korean Pine trees “nurture” the next generation (Prentice and Leemans, 1990; Li and Zhu, 1991; Zyryanova *et al.*, 2005; Nakamura and Krestov, 2005). As the biomass of the mother Korean pine tree increases, the rate of increase in biomass of seedlings and saplings typically decreases (Li and Zhu, 1991). Two hundred years separates mature Korean pine generations, allowing mature trees to dominate the forest canopy and have access to sunlight, moisture and nutrients (Li and Zhu, 1991). This characteristic allows some Korean pine trees to get very tall and large, which can skew plot-level results. For example, Korean pine trees of 87.5 cm and 69.8 cm dbh were recorded on one circular transect at Kabaniy 2. In this case, average Korean pine basal area for the ten plots was 16.7 m²/ha, std. dev. 6.8, which was consistent with modeled results of 18.3 m²/ha, but a pattern of large trees in a stand could distort observed results.

3.5.2.2 High elevation forests - Kabaniy 3 and 4

Kabaniy 3 and 4 represented typical dark conifer forests, dominated by Black fir and Yezo spruce, with some Korean pine. The Black fir/Yezo spruce mix is a major forest type in the cool sub-maritime coastal area, existing at altitudes above 900 m in Central Sikhote-Alin and as low as sea level further north (Krestov *et al.*, 2003). At lower latitudes, dark conifer forests may occur at altitudes of 1500 – 2000 meters. Spruce can reproduce and grow in shaded conditions (Krestov, 2003; Nakamura and Krestov, 2005).

At both sites, the simulation with no adjustment for altitude produced total basal area close to observed, but showed Korean pine as the dominant species, which would be typical at a lower

elevation. When adjusted for elevation, forest composition reflected a species mix appropriate for an elevation higher than the site.

Black fir may appear in larger quantities than simulated at Kabaniy 3 and 4 because of the life cycle stage of the spruce forest. Yezo spruce can live 500 years, but individuals may die much sooner (Nakamura and Krestov, 2005). At 200 – 240 years, mature spruce trees start to die off, creating canopy gaps. Black fir saplings that have regenerated under the canopy grow quickly and may close the gap in 10 – 20 years, leading to clusters of fir within mature spruce forests, as was found at the field sites. Such fir clusters would not appear at a simulated site, which reflects basal area averages over 200 plots.

The longer a spruce-fir forest retains a closed canopy, the greater the amount of fir in the understory because of its shade tolerance relative to spruce. Black fir can reach 30 m height and has a maximum life span of 200 years. As this generation dies out, Yezo spruce saplings grow quickly. Like Black fir, spruce can survive under the forest canopy and can regenerate without a canopy gap (Ishikawa *et al.*, 1999; Krestov, 2003). Over centuries, the forest becomes increasingly spruce-dominated (Nakamura and Krestov, 2005) relative to Black fir, which the model indicates (Figure 3.25).

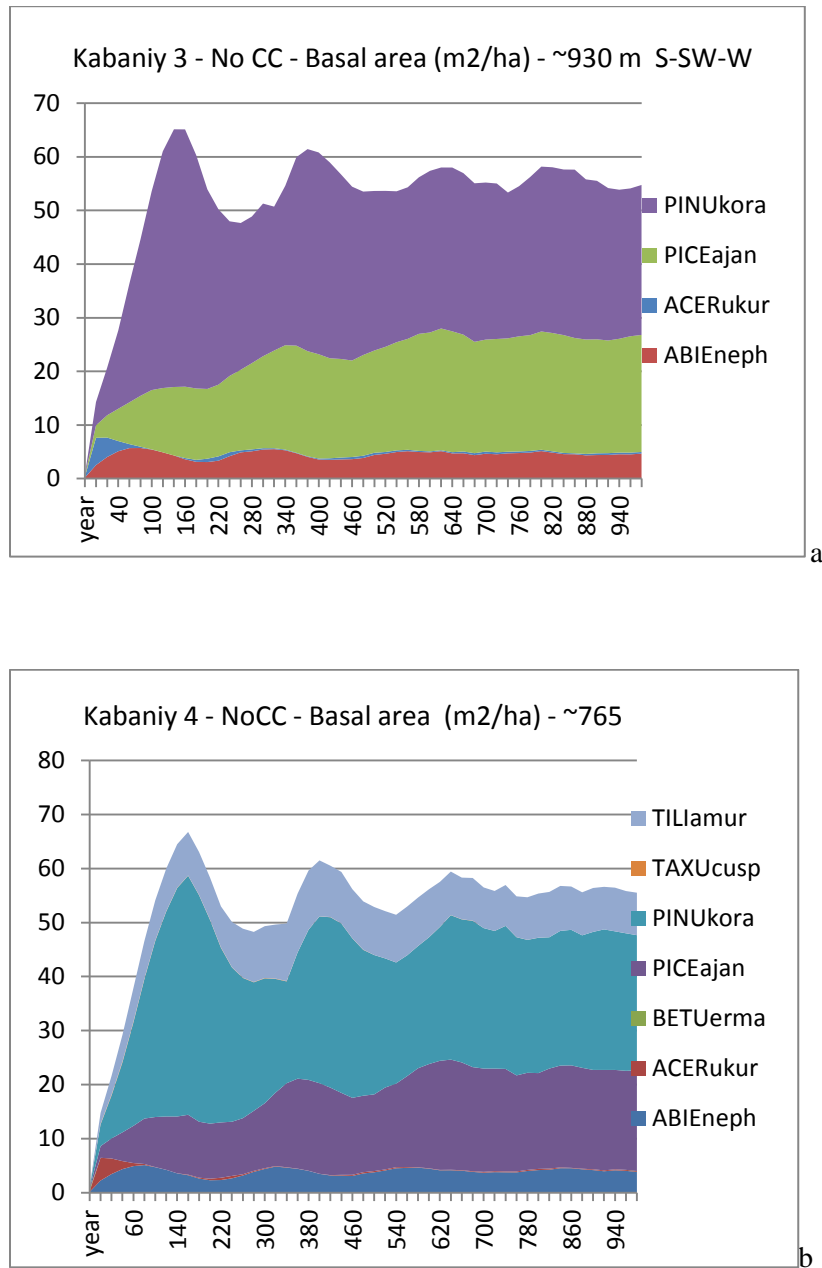


Fig 3.25 a & b Forest succession over time in current climate (no adjustment for altitude) at high elevation forests.

At Kabaniy 4 (~765 m asl, NW aspect), simulated total basal area with no adjustment for altitude (49.6 m²/ha) was very close to observed (48.3 m²/ha) (Fig. 3.14). Slightly more Korean pine and

less Black fir and Yezo spruce appeared at the site relative to Kabaniy 3, which had a S-SW-W aspect (Figure 3.6 e&f). Modeled results produced more Korean pine and Amur linden than appeared at the site, which might be associated with the lack of elevation adjustment, since more Korean pine might be expected at lower elevations (Krestov, 2003; Nakamura and Krestov, 2005).

3.5.2.3 Maysa – Fire Disturbance Site

Maysa (~200 m asl, level – E aspect) was a level and slightly eastward facing site in SABZ that experienced a severe fire about 80 years prior to the field research. The Maysa site originally was a mature mixed deciduous/Korean pine/conifer forests, and FAREAST indicates that Korean pine will eventually dominate under current climate conditions. Young pines are growing under mature pines along a distinct boundary of the severe wildfire (Fig. 3.26).

The regenerating forest is dominated by Manchurian birch (*Betula mandshurica*) and Korean pine. The model was run for 80 years, at which point the birch genus, including Manchurian birch and Black birch (*B. dahurica*), totaled 10.14 m²/ha or about ½ of observed birch by genus (21.77 m²/ha) and Korean pine matched observed (4.9 m²/ha). Observed Mongolian oak basal area at the site was 3.1 m²/ha. In FAREAST, oak basal area also was minimal and never surpassed 2 m²/ha, possibly because Korean pine and ruderal species such as birch grow quickly and create too much shade for oak to flourish.



Fig. 3.26 Korean pine growing at the edge of the Maysa burn site.

FAREAST suggests that after 300 years, Korean pine, Yezo spruce and Black fir will mature and form a canopy at Maysa, with smaller amounts of Amur linden and Laciniata elm (Figure 3.27). Although a very small amount of Yezo spruce was found at the site ($0.06 \text{ m}^2/\text{ha}$), the species is considered to be a late successional species (Zyryanova *et al.*, 2005) and can regenerate under a canopy (Ishikawa *et al.*, 1999; Krestov, 2003). Seeds are produced after 30 – 40 years in the interior of a stand and after 15 – 20 years near the exterior of the stand (Zyryanova *et al.*, 2005).

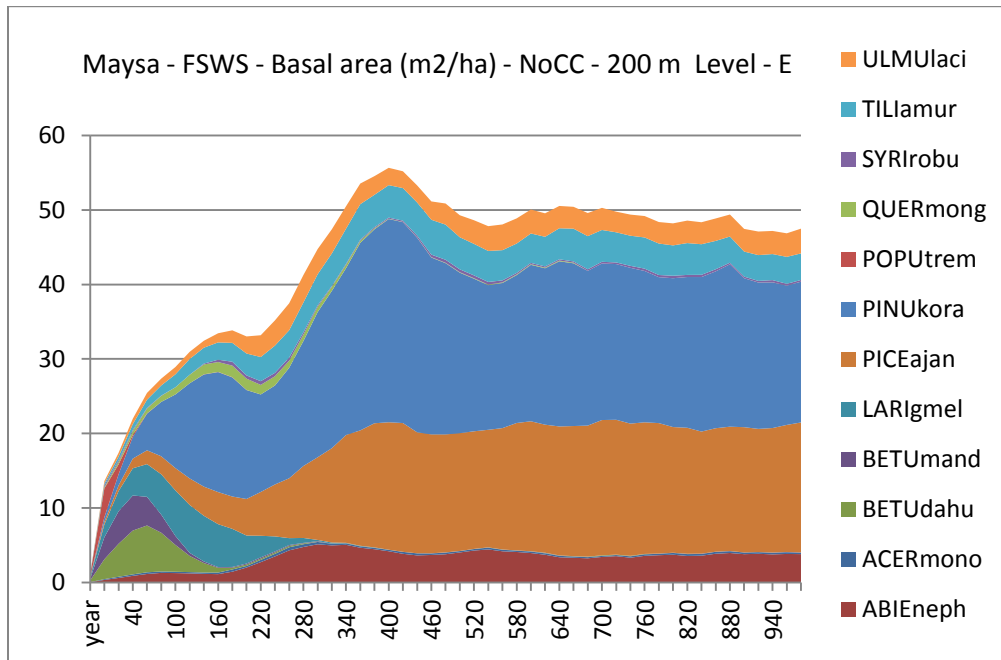


Fig. 3.27 FAREAST indicates that the regenerating forest at Maysa will eventually be dominated by Korean pine and form a canopy with spruce and fir under current climate conditions.

Dahurian larch (*Larix dahurica*), typical of the Eurasian boreal forest, was found in smaller quantities at Maysa than the simulation suggested. Larch generally occurs at disturbed sites in middle and northern Sikhote-Alin rather than in primary forests (Krestov, 2003).

3.5.2.4 Coastal oak forests – Blagodatnoye

Two field sites, Blagodatnoye 1 and 2, were located at low elevations in Sikhote-Alin Biosphere Reserve near the Sea of Japan. The Blagodatnoye coastal forests are typical of one of two types of oak forests in Eastern Asia identified by Krestov, Song *et al.* (2006), and are characterized by a precipitation peak in summer and sufficient soil moisture year-round. In addition to Sikhote –

Alin, these types of forests occur in Korea and in a mountainous area of China “east of the Lesser Hingan” (Krestov *et al.*, 2006).



Fig. 3.28 a. M. Gromyko and S. Bondazchuk measuring dbh at Blagodatnoye 1 b. S. Bondazchuk measuring dbh in the coastal oak forest at the Blagodatnoye 2 field site.

The forest at Blagodatnoye 1, 52 – 110 m asl, S-SE aspect, was dominated by Mongolian oak and Dahurian birch. Early human settlements in this area led to disturbance such as clearing or burning of the original forest, which likely consisted of Korean pine and broadleaf deciduous species (Cushman and Wallin, 2000; Vrishch, 2002; Nakamura and Krestov, 2005; Kobayashi *et al.*, 2007; Miquelle *et al.*, 2010b). When fire occurs regularly, as may have occurred in this area, a mixed pine and oak forest will become an oak-dominated forest, because oak is better able to withstand fire. Mongolian oak has “well-protected” herb buds and “a very high sprouting

capability,” characteristics that make it fire tolerant (Rosenberg *et al.*, 1998; Zyryanova *et al.*, 2005; Krestov *et al.*, 2006).

Oak also reproduces more quickly than Korean pine, and therefore can form a closed canopy that does not allow enough light to penetrate for other species to flourish unless new major disturbance occurs (Nakamura and Krestov, 2005; Zyryanova *et al.*, 2005). The maximum height of these post-disturbance oak canopies is 25 meters, well below the canopy height of a mixed forest that includes Korean pine, which can grow to 33 meters (Nakamura and Krestov, 2005; Yan and Shugart, 2005). Acorns in coastal oak forests provide important nutrition for deer and other animals that serve as prey for Amur tigers, which are found in these forests (Heptner and Sludskii, 1988; Liu and Zhu, 1991; Nakamura and Krestov, 2005).

When FAREAST is run with all species at the site, simulated Mongolian oak basal area is less than one-third of observed basal area, whereas in the observed forest, it comprises 94%. In the simulation, oak gradually declines as Painted maple (*Acer mono*) takes over (Figure 3.30). Painted maple reproduces in shade, so basal area can expand under a canopy (Koike, 1988; Ishikawa *et al.*, 1999). Maple also produces shade, which may be a factor in preventing sunlight-dependent oak from expanding. Black birch is in the process of declining under current climate conditions, opening up opportunities for Painted maple to flourish. However, wildfire occurrence may reduce Painted maple expansion and benefit Mongolian oak, as maple is more sensitive to fire (Botkin, 1992).

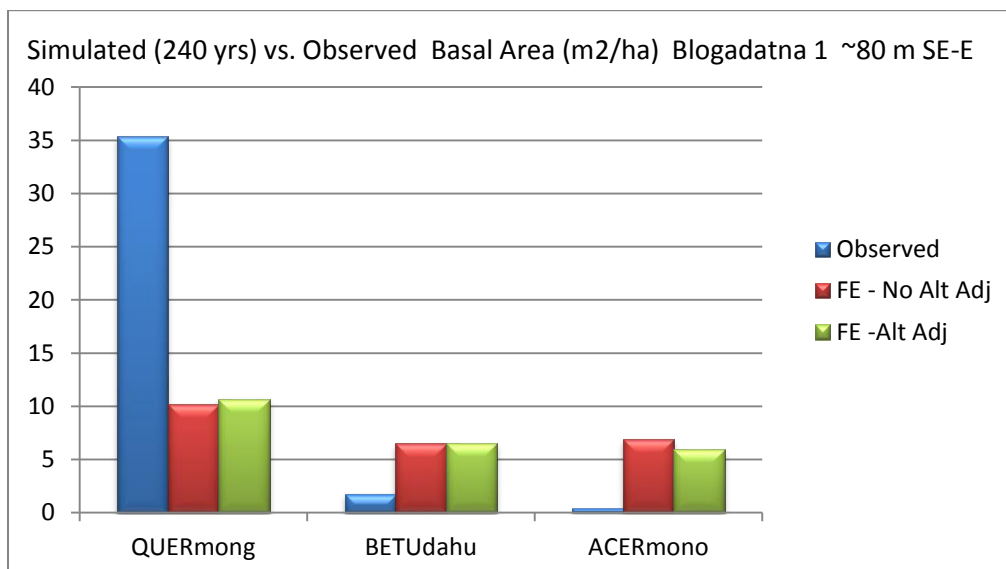


Fig. 3.29 Simulated basal area corresponds most closely with observed at 240 years. The exact age of secondary oak forests at Blagodatnoye is unknown.

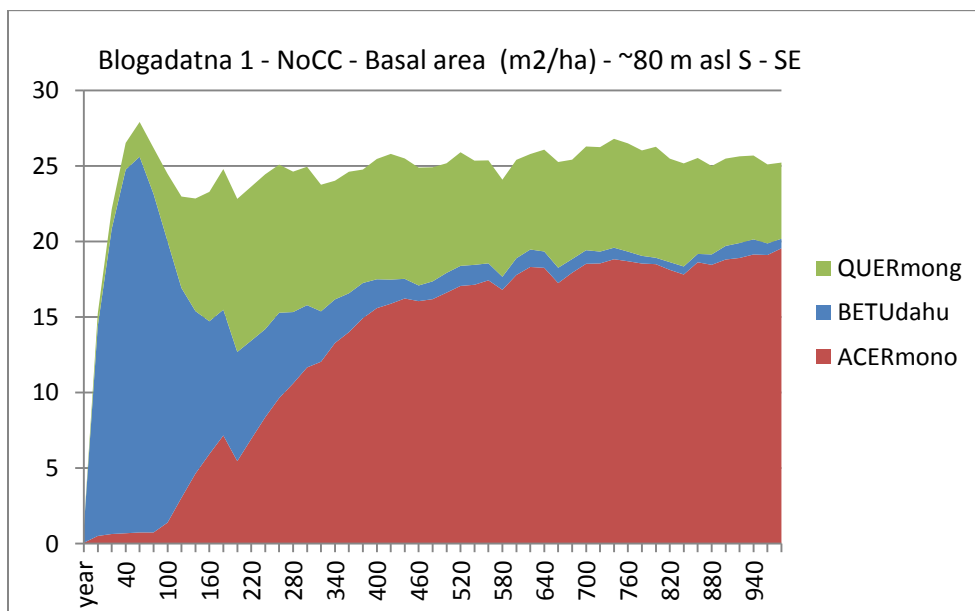


Figure 3.30 Under current climate conditions at Blagodatnoye 1, Painted maple (*Acer mono*) gradually expands as Black birch (*B. Dahurica*) declines.

At Blagodatnoye 2, when FAREAST is run with only the species at the site, with no altitude adjustment and no climate change, the output is a Korean pine forest, with negligible amounts of Mongolian oak. When Korean pine is removed from the simulation (Figure 3.32), as occurred long ago in this area, the model re-creates an oak forest similar to the one found at the site, with basal area of about 22 m²/ha for Mongolian oak after 460 years of simulation (Figure 3.33). This is consistent with literature reporting that a Mongolian oak/Black birch forest replaces a mixed deciduous/Korean pine forest after a severe disturbance (Krestov 2003; Nakamura and Krestov 2005). When the simulated forest with no Korean pine has reached full stability after 1,000 years (Yan and Shugart 2005), FAREAST produces results that resemble the observed oak forest at Blagodatnoye 2 in terms of species proportions, although total oak basal area is 48% percent higher (33.59 m²/ha vs. 22.65 m²/ha observed)(Figure 3.32).

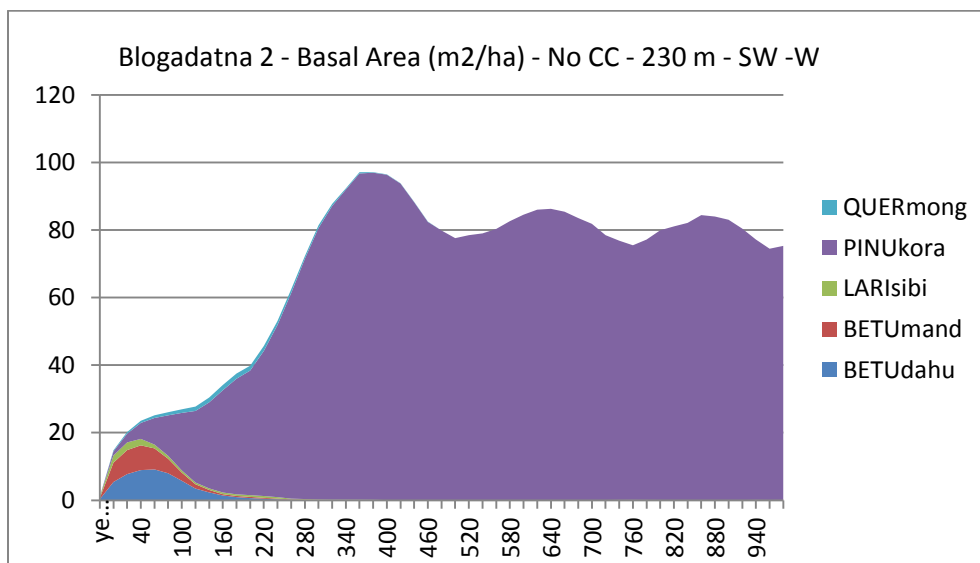


Figure 3.31 If Korean pine is not removed, FAREAST indicates that climate conditions will allow it to dominate a mature forest ecosystem.

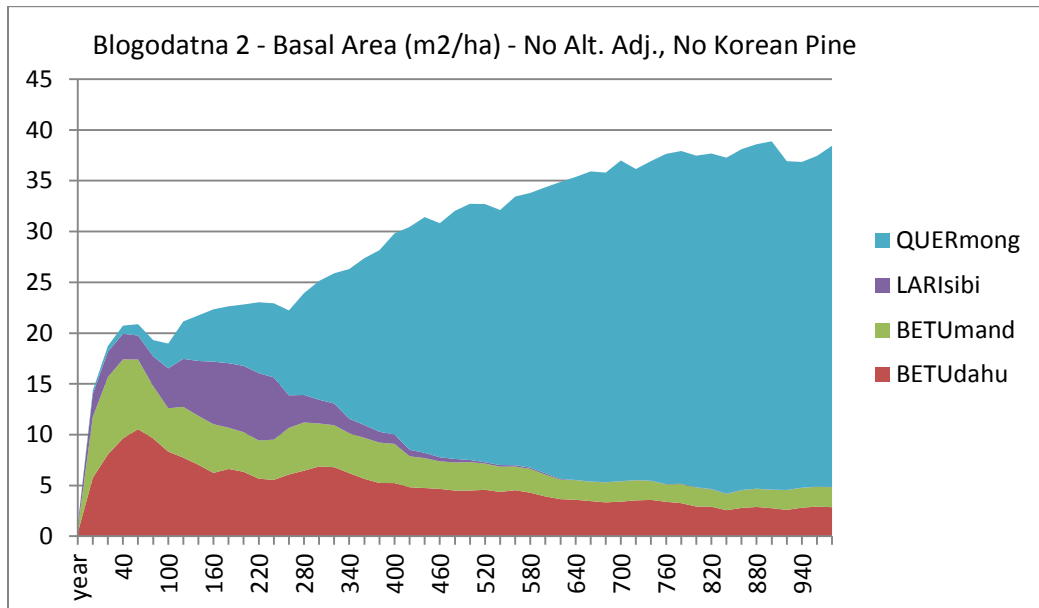


Figure 3.32 FAREAST simulation of Blagodatnoye 2, with Korean pine removed.

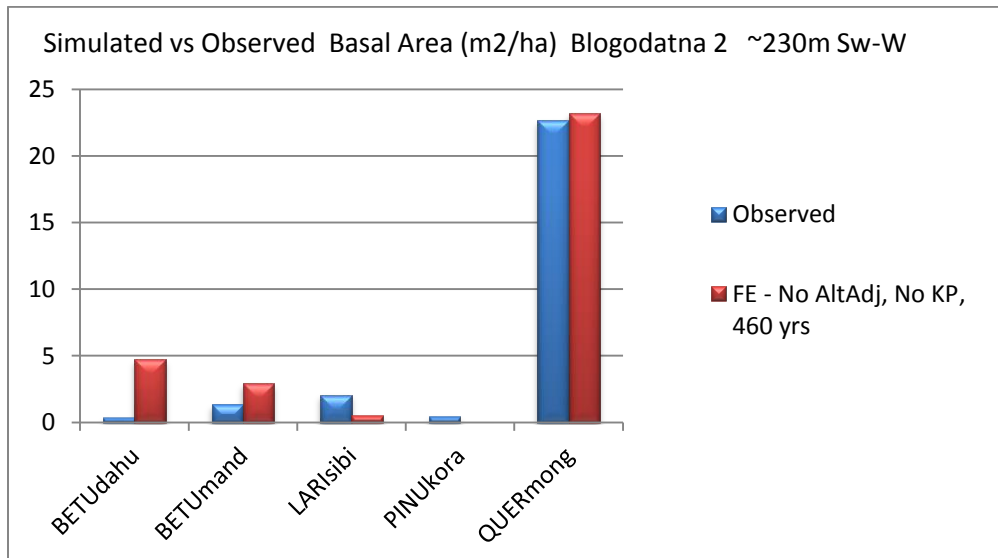


Fig. 3.33 Simulated vs. observed basal area of a mature forest with Korean pine removed.

3.5.3 Northernmost sites (*Polovinka 1 and 2*)

At the northernmost sites, Polovinka 1 and 2 in Bolshekhokhtsirskiy Reserve, the observed species mix and basal area were very similar for both the NW aspect of Polovinka 1 (310 m) and the S-SE-E aspect of Polovinka 2 (315 m), and FAREAST produced similar results by aspect. Polovinka 1 and 2 are about 4.6 degrees (4.6×10^4 km) of latitude further north than Ussurisky 1 and 2. The model's latitude adjustment at the northernmost sites, Polovinka 1 and 2 in Bolshekhokhtsirskiy Reserve, means that the angle of solar insolation at both sites is slightly smaller than at lower latitudes.

Total basal area simulated by FAREAST was higher than field results. Greater basal area for Korean pine and Amur linden, the dominant species at both locations, accounted for much of the discrepancy (Figures 3.15 and 3.17). FAREAST results indicate that basal area of both oak and pine are declining, but pine will expand and remain stable in the future under current climate conditions (Figure 3.34a&b). Mongolian oak basal area peaks during years 120 – 160 at 35 – 38 m²/ha, and then declines permanently.

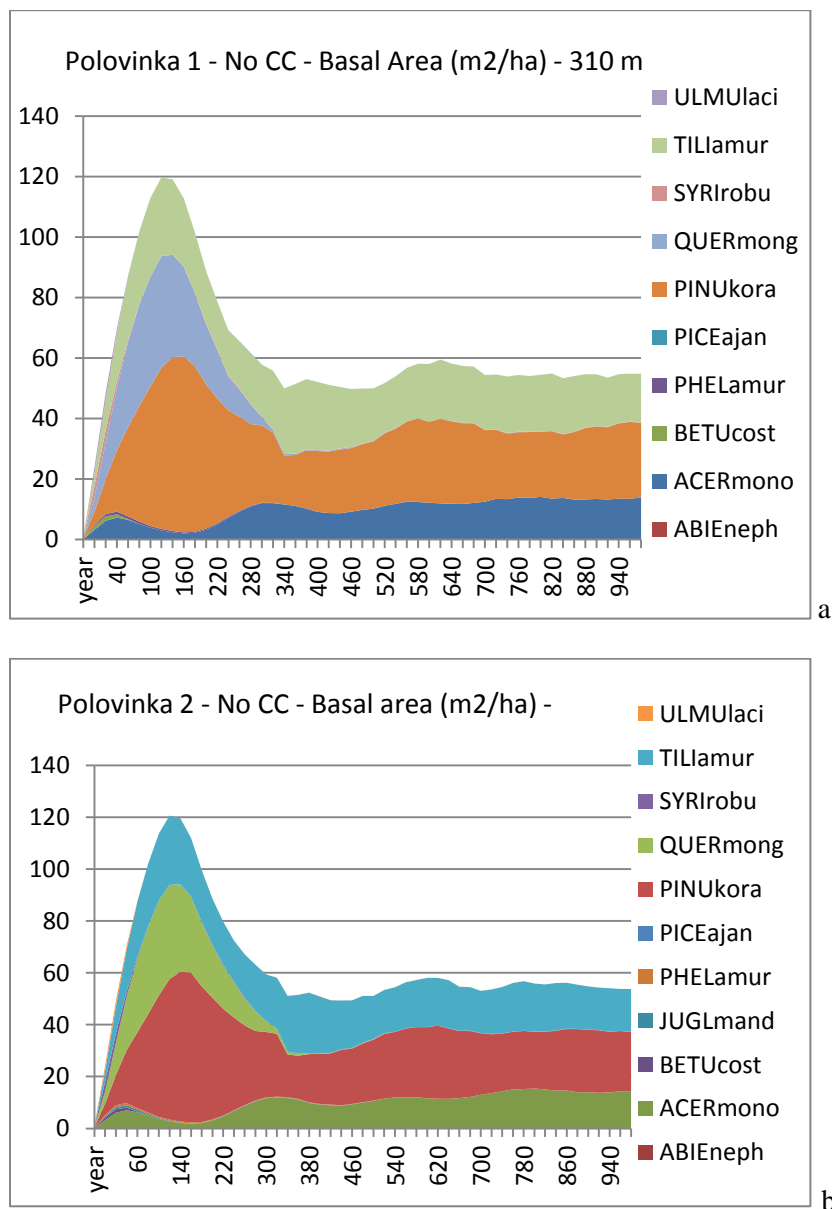


Figure 3.34 a & b. Mongolian oak will die out and Korean pine will maintain stable basal area at Polovinka 1 and 2 under current climate conditions.

The Bolshekhekhtsirskiy *Zapovednik* was founded in 1963 (www.wild-russia.org). Although logging is prohibited in strictly protected reserves such as Bolshekhekhtsirskiy, it is located near the large metropolitan area of Khabarovsk, so limited or illegal logging may have occurred to

meet population needs in the past. A study based on forest inventory data found that commercially valuable species may have been preferentially harvested in productive, old growth forests (Krankina *et al.*, 2005).

Forests with Korean pine also have experienced wildfires, especially in areas close to human settlements (Rosenberg, 2000; Loboda and Csiszar, 2007). The presence of simulated Chinese birch at both sites in slightly larger quantities than observed reinforces the idea that wildfire or other disturbance may have occurred at the time the trees were established. Mature Chinese birch in the canopy is consistent with a possible wildfire event, as Chinese birch cannot withstand fire, but can grow well on burn sites (Yaborov, 2000; Zyryanova *et al.*, 2005). Chinese birch, like most birch species, does not tolerate shade and saplings will not thrive under a closed canopy, but can grow when the canopy is removed (Ishikawa *et al.*, 1999).

The sapling population at Polovinka 1 was dominated by Manchurian fir, Yezo spruce, Korean pine, maple species, and Amur tree lilac. For Polovinka 2, Manchurian fir, Yezo spruce, and Maple species prevailed. Korean pine saplings were present, but sparse. This suggests that, in the future, although the soil type and climate conditions are favorable for Korean pine at Polovinka, the forest at Polovinka 2 will be dominated by fir, spruce and maple rather than Korean pine, as the model suggests (Figure 3.34b).

3.5.4 *Summary of modeled versus site results*

Following is a table comparing simulated and observed results at the years with the best match in terms of basal area by species.

Table 3.2 Summary of simulated vs. observed at year of best match

<i>Site</i>	<i>Current forest type (Observed)</i>	<i>Current forest type (Simulated)</i>	<i>Dominant species (Observed)</i>	<i>Dominant species (Simulated)</i>	<i>Dominant species in 200 years with no climate change (Sim)</i>
Ussurisky 1 – 240 years	Mixed	Mixed	Korean pine	Korean pine	Korean pine
Ussurisky 2 – 280 years	Mixed	Mixed	Korean pine	Korean pine	Korean pine
Kab 1 – 300 yrs	Mixed	Mixed	Korean pine	Korean pine	Korean pine
Kab 2 – 340 yrs	Mixed	Mixed	Korean pine	Korean pine	Korean pine
Kab 3 – 340 yrs	Dark conif	Dark conifer	Yezo spruce	Korean pine ₁	Korean pine ₁
Kab 4 – 340 yrs	Dark conif	Dark conifer + Amur linden	Yezo spruce	Korean pine ₁	Korean pine ₁
Maysa – 80 yrs	Mixed	Mixed	Manchurian birch (Dom. Genus = birch)	Black birch (Dom. Genus = birch)	Korean pine
Blagodatnoye 1 – 240 years	Mongolian oak	Mixed oak/birch/ maple	Mongolian oak	Mongolian Oak	Painted maple (starting yr 300)
Blagodatnoye 2 – 160 years	Mongolian oak	Korean pine – minimal KP at site	Mongolian oak	Korean pine	N/A
Blagodatnoye 2 – 460 years, No KP	Mongolian oak	Mongolian oak	Mongolian oak	Mongolian oak	Mongolian oak
Polovinka 1 – 320 years	Mixed	Mixed	Korean pine	Korean pine	Korean pine
Polovinka 2 – 300 years	Mixed	Mixed	Chinese birch/Korean pine	Korean pine	Korean pine

1 More Korean pine than observed may be a result of not adjusting for elevation.

3.5.5 *Possible causes of differences in simulated vs. observed*

FAREAST simulates a largely undisturbed forest, except for tree mortality and the creation of gaps in the canopy. The composition of a forest stand can vary widely, depending on natural factors, such as climate, soil type and moisture, as well as disturbances such as fire, harsh weather and insect outbreaks (Bonan and Shugart, 1989; Shugart, Leemans and Bonan, 1992). For example, studies in Quebec, Canada, found that biomass can range from 10 to 29 tC/ ha in spruce-lichen woodlands and from 78 to 164 tC/ha when better soils are available (Moore and Verspoor, 1973; Shugart *et al.*, 1992). This variation contributes to the mosaic pattern of mature forests (Shugart *et al.*, 1992)

Although every effort was made to select sites with vegetation typical of the ecosystem, disturbance history of any specific patch is unknown. Indeed, a certain degree of disturbance is typical, though unpredictable, in all ecosystems. The model may not always be able to reproduce the extant forest at a particular time because of factors such as variability within a small space comparable to a forest canopy gap, microclimates, topographical and aspect variations, species interactions, varying stages of succession (the mosaic effect) and processes including randomness in the model itself (Yan and Shugart, 2005; Shugart *et al.*, 2010).

3.5.6 *Future studies*

The humid, moderate climate of coastal Central Sikhote-Alin affects the adiabatic rate. As a result, adjusting altitude in the model produced results that did not match observed forest

composition as well as it did at other sites. Future studies might include manipulation of the adiabatic lapse rate to simulate the coastal climate of Central-eastern Sikhote-Alin.

More adjustments of the model to achieve the larger quantities of Black fir relative to Yezo spruce in dark conifer forests would be valuable, since this spruce-fir ecosystem is widespread across the southeastern RFE.

Changes in this sensitive and biologically diverse ecosystem could cause modifications in the range of vegetation, which would affect the wildlife species that depend on particular species (Liu and Zhu, 1991; Kobayashi *et al.*, 2007). The effect of predicted climate change on forests in this area is covered in Chapter 4.

3.6 CONCLUSION

Previous studies have shown that the gap model FAREAST can accurately simulate forest composition at the landscape scale, based on comparisons with forest inventory and remotely sensed data. This study examined the consistency of simulated forest composition and structure with observations at the gap scale at sites that varied in climate, latitude, elevation, aspect and disturbance history.

While eight of the field sites represent a largely undisturbed forest, except for tree mortality and the creation of gaps in the canopy, the approximately 300-year-old forests actually are in a dynamic period, which is reflected in model results.

Model output most closely matched field observations at the southernmost sites in Ussurisky Reserve near Vladivostok, which were the nearest to Changbai Mountain, China, where the model was verified. Model parameters may need to be adjusted for greater consistency with observed at a detailed scale for humid coastal climates and as distance increases from the site from which data were used to create the model, although the discrepancy at northern sites may be associated with anthropogenic disturbance.

At the six sites where Korean pine was the dominant observed species, FAREAST also showed Korean pine to have the greatest basal area. The simulation suggests that Korean pine will maintain current basal area indefinitely under current climate conditions at sites where it plays a dominant role, which is consistent with scientific literature. Because the simulation shows that Mongolian oak peaks after about 140 years at all mixed pine/conifer/broadleaf forest sites where oak is present, and then starts to die out, unless fire or logging creates big clearings, Korean pine is especially important for wildlife.

Modeling is a useful tool to predict forest composition at a detailed scale under current climate conditions at inaccessible locations. Ground truthing would increase the confidence with which model results could be used.

3.7 REFERENCES

Bonan GB, Shugart HH (1989) Environmental factors and ecological processes in boreal forests. *Annual Review of Ecology and Systematics*, **20**, 1-28.

Botkin DB, Janak JF, Wallis FR (1972) Some ecological consequences of a computer model of forest growth. *Journal of Ecology*, **60**, 849-873.

Cheng X, Yan X (2009) Effects of climate change on typical forests in northeastern China. *Frontiers of Forestry in China*, **4**, 409-415.

Cushman SA, Wallin DO (2000) Rates and patterns of landscape change in the Central Sikhote-Alin Mountains, Russian Far East. *Landscape Ecology*, **15**, 643-659.

Davis R, Holmgren P (2000) Forestry Dept. Food and Agriculture Organization of the United Nations. FRA 2000 Forest Cover Mapping and Monitoring with NOAA-AVHRR & Other Coarse Spatial Resolution Sensors. Forest Resources Programme, Working paper 29. Rome.

Dinerstein E, Loucks C, Heydlauff A (2006) *Setting Priorities for the Conservation and Recovery of Wild Tigers: 2005-2015. A User's Guide*. WWF, WCS, Smithsonian, and NFWF-STF, Washington, DC – New York.

Gromyko MN (2006) Climate Change and catastrophic disturbances of forest ecosystems in the Sikhote-Alin State Nature Reserve. In: WWF Moscow Climate Change Impact on Ecosystems of the Amur River Basin. WWF Russia/Moscow/Vladivostok. In Russian with abstracts in English.

Gomez-Pompa A, Vazquez-Yanes C (1981) Successional Studies of a Rain Forest in Mexico. In: *Forest Succession Concepts and Application* (eds West DC, Shugart HH, Botkin DB) Springer-Verlag, New York.

Hargreaves GH, Allen RE (2003) History and evaluation of Hargreaves' evapotranspiration equation. *Journal of Irrigation and Drainage Engineering*, **129**, 53 – 63.

Heptner VG, Nasimovich AA, Bannikov AG (1992) *Mammals of the Soviet Union, Vol 1, Artiodactyla and Perissodactyla*. Smithsonian Institution Libraries and National Science Foundation, Washington, DC.

Heptner VG, Sludskii AA (1992) *Mammals of the Soviet Union, Vol 2, Part 2 Carnivora*. Smithsonian Institution Libraries and National Science Foundation, Washington, DC.

Horn HS (1974) The Ecology of Secondary Succession. *Annual Review of Ecology and Systematics*, **5**, 25 – 37.

Horn HH (2002) Some Causes of Variety in Patterns of Secondary Succession. In: *Forest Succession, Concepts and Application* (eds West DC, Shugart HH, Botkin DB) Springer-Verlag, New York.

Horn HS, Cody ML, Diamond JM (1975) *Markovian properties of forest succession*. pp 196-211.

Ishikawa Y, Krestov PV, Namikawa K (1999) Disturbance history and tree establishment in old-growth *Pinus koraiensis*-hardwood forests in the Russian Far East. *Journal of Vegetation Science*, **10**, 439-448.

Ivanov GI (1964) *The soils of Primorskiy Kray*. Vladivostok (IIASA maps) (In Russian).

Katsuta M, Morij T, Yokoyama T (1998) Seed of woody plants in Japan. pp. 42-43. Japan Forest Tree Breeding Association, Tokyo (in Japanese).

Kobayashi M, Nemilostiv YP, Zyryanova OA *et al.* (2007) Regeneration after Forest Fires in mixed Conifer Broad-leaved Forests of the Amur Region in Far Eastern Russia: the Relationship between Species Specific Traits Against Fire and Recent Fire Regimes. *Eurasian Journal of Forestry Research*, **10**, 51-8.

Koike T (1991) Photosynthetic characteristics of deciduous broad-leaved tree species. *Technical Report* (Hokkaido: FFPRI) **23**, 1-8.

Kolesnikov BP (1956) Korean pine forests of the [Russian] Far East. [Kedroviye lesa Dalnego Vostoka.] 1956. Trudy DVF AN SSSR, Ser. Botl, Izdatelstvo AN SSSR, Moscow 2 (in Russian).

Koop H (1987) Vegetative reproduction of trees in some European natural forests. *Vegetatio*, **72**, 103-10.

Kostak M, Krestov PV, Okitsu S (2003) Basic Geomorphological and Geological Characteristics of Northeast Asia. In: *Forest Vegetation of Northeast Asia* (eds Kolbek J, Srutek M, Box EO) Kluwer Academic Publishers, Norwell, MA.

- Krankina ON, Houghton RA, Harmon ME *et al.* (2005) Effects of climate, disturbance and species on forest biomass across Russia. *Canadian Journal of Forest Research*, **35**, 2281 – 93.
- Krestov PV (2003) Forest Vegetation of Easternmost Russia (Russian Far East). In: *Forest Vegetation of Northeast Asia* (eds Kolbek T, Strutek M, Box EO), pp. 93 – 180. Kluwer Academic Publishers, Norwell, MA.
- Krestov PV, Song J-S, Nakamura Y *et al.* (2006) A phytosociological survey of the deciduous temperate forests of mainland Northeast Asia. *Phytocoenologica*, **36**, 77-150.
- Lauenroth WK, Urban DL, Coffin DP *et al.* (1993) Modeling vegetation structure-ecosystem process interactions across sites and ecosystems. *Ecological Modelling*, **67**, 49-80.
- Leemans R, Prentice IC (1989) *FORSKA, a general forest succession model*. Institute of Ecological Botany, Uppsala, Sweden.
- Li J, Zhu N (1991) Structure and process of Korean pine population in the natural forests. *Forest Ecology and Management*, **43**, 125–135.
- Lillifors HW (1967) On the Kolmogorov-Smirnov Test for normality with mean and variance unknown. *Journal of the American Statistical Association*, **62**, 399-402.
- Loboda TV (2009) Modeling fire danger in data-poor regions: a case study from the Russian Far

East. *International Journal of Wildland Fire*, **18**, 19-35.

Miquelle DG, Goodrich JM, Kerley LL *et al.* (2010a) Science-based Conservation of Amur Tigers in the Russian Far East and Northeast China. In: *Tigers of the World* (eds Tilson R, Nyhus PJ), pp. 403 - 423. Elsevier, Burlington, MA.

Miquelle DG, Goodrich JM, Smirnov EN *et al.* (2010b) Amur tiger: a case study of living on the edge. In: *Biology and Conservation of Wild Felids* (eds MacDonald DW, Loveridge AJ), pp. 325-339. Oxford University Press, Oxford.

Miquelle DG, Merrill TM, Dunishenko YM *et al.* (1999) A habitat protection plan for the Amur tiger: developing political and ecological criteria for a viable land-use plan. In: *Riding the Tiger* (eds Seidensticker J, Christie S, Jackson P), pp. 273-295. Cambridge University Press, Cambridge, UK.

Moore TR, Verspoor E (1973) Aboveground biomass of black spruce stands in subarctic Quebec. *Canadian Journal of Forest Research*, **3**, 596-598.

Monsi M, Saeki T (1953) Über den Lichtfaktor in den Pflanzengesellschaften und seine Bedeutung für die Stoffproduktion. *Japanese Journal of Botany*, **14**, 22-52.

Nakamura Y, Krestov P (2005) Coniferous forests of the temperate zone of Asia. In: *Ecosystems of the World 6: Coniferous Forests* (ed Andersson F), pp. 163-220. Elsevier, New York.

Newell J (2004) *The Russian Far East: A Reference Guide for Conservation and Development*.

Daniel & Daniel, McKinleyville, CA.

Post WM, Pastor J. (1996) Linkages – an individual-based forest ecosystem model. *Climatic Change*, **34**, 253-61.

Prentice IC, Leemans R (1990) Pattern and Process and the Dynamics of Forest Structure: A Simulation Approach. *Journal of Ecology*, **78**, 340–355.

Qian H, Song J-S, Krestov P *et al.* (2003) Large-scale phytogeographical patterns in East Asia in relation to latitudinal and climatic gradients. *Journal of Biogeography*, **30**, 129-141.

Rosenberg VA, Bocharnikov VN, Krasnopeev SM (1998) Biological Diversity in the Sikhote-Alin Forests and Measures of its Conservation. In: *Integrated Tools for Natural Resources Inventories in the 21st Century*, Gen. Tech. Rep. NC-212 (eds Hansen M, Burk T), pp. 326-33.

U.S. Dept. of Agriculture, Forest Service, North Central Forest Experiment Station, St. Paul, MN.

Shugart HH (1984) (reprint 2003) *A Theory of Forest Dynamics: The Ecological Implications of Forest Succession Models*. Caldwell: The Blackburn Press.

Shugart HH, Leemans R, Bonan G (1992) *A Systems Analysis of the Global Boreal Forest*. Cambridge University Press, New York.

Shugart HH, Saatchi S, Hall FG (2010) Importance of structure and its measurement in

quantifying function of forest ecosystems. *Journal of Geophysical Research*, **115**, G00E13.

Shugart HH (1998) *Terrestrial Ecosystems in Changing Environments*. Cambridge University Press, Cambridge.

Shuman JK, Shugart HH (2009) Evaluating the sensitivity of Eurasian forest biomass to climate change using a dynamic vegetation model. *Environmental Research Letters*, **4**, 045024, 1-7.

Stolbovi V, McCallum I (2002) CD-ROM land resources of Russia. International Institute for Applied Systems Analysis and the Russian Academy of Science (IIASA), Laxenburg, Austria.

Vrishch AE, Skirina IF, Bulah EM *et al.* (2002) *Green Book of Sikhote-Alin*. WWF, Phoenix Fund, USAID, Vladivostok, Russia.

Watt AS (1947) Pattern and process in the plant community. *Journal of Ecology* **35**, 1-22.

Yan X, Shugart HH (2005) FAREAST: a forest gap model to simulate dynamics and patterns of eastern Eurasian forests. *Journal of Biogeography* **32**, 1641-1658.

Zhang N, Shugart HH, Yan X (2009) Simulating the effects of climate changes on Eastern Eurasian forests. *Climatic Change*, **95**, 341-361.

Zyryanova OA, Yaborov VT, Abaimov AP *et al.* (2005) Problems in the Maintenance and Sustainable Use of Forest Resources in Priamurye in the Russian Far East. *Eurasian Journal of Forestry Research*, **8**, 53-64.

Websites

Chundawat RS, Habib B, Karanth U *et al.* (2010) *Panthera tigris*. In: IUCN 2010. *IUCN Red List of Threatened Species*. Version 2010.4 <www.iucnredlist.org> 02/03/2011.

Russian Nature Press. Current Zapovedniks of the Russian Federation.
<<http://www.rusnatpress.org.uk/rnp-zaps3.htm>> 03/15/13.

Wild Russia. Center for Russian Nature Conservation.<http://www.wild-russia.org/bioregion13/13_USSURISKY/13.ussur.htm> 03/15/13.

Jackson P, Nowell K (2008) *Panthera pardus ssp. orientalis*. In: IUCN 2012. *IUCN Redlist of Threatened Species*. Version 2012.2 <www.iucnredlist.org> 01/30/2013.

Miquelle, D. G. Darman, Y. and Seryodkin, I. (2011) *Panthera tigris ssp altaica*. In: IUCN 2012. *IUCN Red List of Threatened Species*. Version 2012.2 <www.iucnredlist.org> 01/30/2013.

United Nations Educational, Scientific and Cultural Organization (UNESCO) World Heritage Convention. World Heritage List <<http://whc.unesco.org/en/list/766>> 02/28/13.

3.8 APPENDIX

English translation of Latin species names

<i>Latin name</i>	<i>English</i>
<i>Abies holophylla</i>	Holo or Manchurian fir
<i>Abies nephrolepis</i>	Black or Hinggan fir
<i>Acer mono</i>	Painted maple
<i>Betula costata</i>	Chinese or yellow birch
<i>Betula dahurica</i>	Black birch
<i>Betula mandshurica</i>	Manchurian birch
<i>Betula ermanii</i>	Alpine or Erman's birch
<i>Carpinus cordata</i>	Hornbeam
<i>Larix gmelinii</i> , <i>Larix dahurica</i>	Dahurian or Xing'an larch
<i>Fraxinus mandshurica</i>	Manchurian Northeast ash
<i>Juglans mandshurica</i>	Manchurian walnut
<i>Phellodendron amurense</i>	Amur cork tree
<i>Picea ajanensis</i>	Yezo or Ayan spruce
<i>Pinus koraiensis</i>	Korean pine
<i>Quercus mongolica</i>	Mongolian oak
<i>Syringa robusta</i>	Tree lilac
<i>Tilia amurensis</i>	Amur linden
<i>Ulmus laciniata</i>	Laciniata elm

*CHAPTER 4. USING REMOTE SENSING AND MODELING TO PREDICT
THE EFFECT OF CLIMATE CHANGE ON AMUR TIGER HABITAT IN
THE RUSSIAN FAR EAST*

ABSTRACT

Numerous studies have shown that future changes in temperature and precipitation may affect trophic webs at scales ranging from microscopic to comprehensive. The impact of climate change on keystone species resulting from modification of the ecosystem on which their prey depend has been less researched. The endangered wild Amur (or Siberian) tiger (*Panthera tigris altaica*) is an umbrella and keystone species in the southeastern Russian Far East (RFE), an unusual and biologically diverse region. After increasing in number following near extinction in the 1940s, the wild Amur tiger population again may be declining. Habitat loss and insufficient prey are two of the three principle threats to the Amur tiger's survival in the wild; the third major threat is illegal hunting, or poaching.

This project examines the future of Amur tigers in a changing climate in the context of availability of food for its primary ungulate prey species. My hypothesis is that climate change will change forest composition, which, in turn, will impact tigers by modifying the range of tree species on which its ungulate prey depend for food and shelter. Resource Selection Function

analysis has shown that tracks of Amur tigers and their ungulate prey occur most frequently in forests containing Korean pine (*Pinus koraiensis*) and Mongolian oak (*Quercus mongolica*). Nuts and seeds from Korean pine and Mongolian oak provide important energy and nutrition for deer and wild boar, the preferred prey of Amur tigers.

I used the forest succession model FAREAST to assess the effect of warmer atmospheric temperature on future forest composition and structure. FAREAST simulates the tree growth cycle that starts when a large tree falls, creating a gap in the forest canopy, which allows sunlight to reach the forest floor and triggers regeneration and maturation. Temperature was modified to reflect the A1F1 and B1 climate change scenarios for this century utilized by the Intergovernmental Panel on Climate Change (2007).

The simulation indicates that Korean pine will decline at southernmost research sites with local climate warming less than 2.0 °C. Climate warming is projected to occur more quickly in East Asia than elsewhere, so a 2.0 °C increase in southeastern Russian Far East would reflect a lower global average increase. With 3.5 °C warming, implemented over 100 years, the simulation suggests that Korean pine and Mongolian oak would disappear from the southernmost field sites at Ussurisky Reserve. With 6.0 °C warming, Korean pine dies out across most of Amur tiger range, and forests at many locations disappear. Korean pine will withstand greater climate change in the humid coastal conditions of Sikhote-Alin Biosphere Reserve than in Ussurisky Reserve in southern Primorski Krai or the more northern Bolshekhkhtsirskiy Reserve near Khabarovsk.

Modeling suggests that Mongolian oak in primary forests in the study area will not re-regenerate, but the species may persist even with climate warming of 6.0 °C in coastal oak forests.

At 1,000 random points, or simulation sites, across the study area, climate warming of 3.5 °C caused 95% of sites representing dark conifer forests to convert to mixed deciduous broadleaf/Korean pine/conifer. Forests at all points that indicated southern mixed forests changed to broadleaf with 3.5 °C temperature increase. With 6 °C of warming, all mixed forests and dark conifer forests convert to deciduous broadleaf, and forests disappear at about 10% of sites.

4.1 INTRODUCTION

Although threats to the persistence of the wild Amur, or Siberian, tiger (*Panthera tigris altaica*) are well-documented (Miquelle *et al.*, 1999a; Kerley *et al.*, 2002; Goodrich *et al.*, 2008, Miquelle *et al.*, 2010a&b), the impact of potential climate change on the Amur tiger and the ecosystem on which it depends is less understood. This project utilizes a gap-based forest succession model to explore the effects of predicted climate change scenarios on forest structure and composition in Amur tiger range in the Russian Far East, the consequences of any vegetation changes for tiger prey, and implications for the tiger itself.

Endangered Amur tigers exist in the wild only in this vast landscape near the Sea of Japan. A few individuals related to the Russian tiger population have been reported across the Russian border in northeastern China (Miquelle *et al.*, 1999; Miquelle *et al.*, 2010a & b; Hebblewhite *et al.*,

2011). The Amur tiger subspecies has been shown by DNA analysis to have descended from the extinct Caspian tiger, which historically ranged from eastern Turkey to the eastern Russian coast up to about latitude 60 °N (Driscoll *et al.*, 2009). In the 1940s, Amur tiger population was estimated at only 20 – 30 individuals (Kaplanov, 1948; Miquelle *et al.*, 2010a), which led to a ban on tiger hunting and the taking of cubs for zoos. Tiger populations expanded in the RFE until the late 1980s, when poaching surged after the Soviet Union collapsed. Conservation efforts starting in the early 1990s supported growth in the tiger population to an estimated 431-502 adults and sub-adults in the 2005 census (Miquelle *et al.*, 2007; Miquelle *et al.*, 2010a&b). Since 2004, however, a generally downward trend has been measured in the number of tigers as well as its prey (Miquelle *et al.*, 2009; Stephens *et al.*, 2006) and fewer than 400 adults and sub-adults were estimated in 2010 (Miquelle *et al.*, 2010b).

Amur or Siberian tiger habitat in Russia is located in the province (or *krai*) of Primorski (also called Primorye) and southern Khabarovski krai (Figure 4.1). Total unbroken forest in this area is 192,000 km², of which about two-thirds (128,000 km²) is considered to be potential tiger habitat (Miquelle *et al.*, 1999; Miquelle *et al.*, 2010b).

Two Global Priority Class 1 Tiger Conservation Landscapes (TCL) (Dinerstein *et al.*, 2006; Sanderson *et al.*, 2006) have been delineated in the Russian Far East. Global Priority Class 1 TCLs are areas that offer the greatest promise for wild tiger survival and are characterized by: 1. landscape large enough to support at least 100 tigers, 2. evidence of breeding, 3. lower than 50% of the range of threat for all tiger territories, and 4. achievement of “conservation effectiveness” in the 25th percentile or above (Sanderson *et al.*, 2006). One TCL is located throughout much of

Primorski Krai in the Sikhote-Alin mountain range and foothills, where nine field sites were located, and the other is in the East Manchurian Mountains in southwestern Primorski Krai (Miquelle *et al.*, 2010b), the location of two field sites. The two landscapes are divided by a corridor of development that includes highways, railroad tracks, urban and agricultural areas.



Fig. 4.1 Amur tiger range in southeastern Russian Far East. Source: Wildlife Conservation Society.

The presence and persistence of tigers, as well as their home range size, depend largely on the availability of sufficient prey (Karanth and Stith, 1999; Miquelle *et al.*, 1999b; Sunquist *et al.*, 1999; Karanth *et al.*, 2004; Miquelle *et al.*, 2010b). The population dynamics of tigers and their

ungulate prey, their habitat preferences, and chances for recovery are linked to vegetation type (Miquelle *et al.*, 2010a&b), which is shaped by climate, soil characteristics, forest disturbance and successional dynamics (Lauenroth *et al.*, 1993; Chapin *et al.*, 2002; Shugart, 1998; Shugart and Woodward, 2011). Resource Selection Function (RSF) analyses and other studies (Carroll and Miquelle, 2006; Hebblewhite, 2011) have linked tigers and their prey with particular tree species. Forests containing Korean pine (*Pinus koraiensis*) and Mongolian oak (*Quercus mongolica*), along with riverine forests, are most frequently used by tigers and their prey, based on the association of tree species with winter census ungulate and tiger track occurrence (Miquelle *et al.*, 1999; Carroll and Miquelle, 2006; Miquelle *et al.*, 2010a; Hebblewhite *et al.*, 2011).

Acorns from Mongolian oak trees and nuts from the pine cones of the Korean pine (Figure 4.2) form the base of a large trophic web that includes, in addition to the tiger and its prey, squirrels, voles, birds, mink, black bear, and the Amur leopard (Heptner and Sludskii, 1992; Nakamura and Krestov, 2005; Zyryanova *et al.*, 2005). Energy and protein-providing seeds and nuts are especially important during harsh winters in this area (Heptner and Sludskii, 1992), where the average January temperature is -19.5 °C (-3.1 °F) in the south near Vladivostok (Ishikawa *et al.*, 1999; Krestov *et al.*, 2006) and -22.3 °C in the north, at Khabarovsk (Nakamura and Krestov, 2005).



Fig. 4.2 The seed, or pine nut, from the Korean pine cone provides sustenance for a large trophic network. (Pictured: Alexander Omelko, PhD, Institute of Biology and Soil Science, Far Eastern Branch of the Russian Academy of Sciences).

In addition to vegetation type, protection from poaching, distance from roads and settlements, and quality of habitat, such as lack of fragmentation and degradation, are important factors in tiger persistence (Kerley *et al.*, 2002; Goodrich *et al.*, 2008; Seidensticker *et al.*, 2010; Miquelle *et al.*, 2010 a&b).

In the southeastern RFE, Pacific Ocean monsoonal and continental Asian climates intersect, as do Siberian boreal forest and Manchurian temperate forests. This leads to unusual assemblages of forest vegetation and many rare and endemic tree species (Krestov, 2003; Nakamura and Krestov, 2005). The United Nations Educational, Scientific and Cultural Organization (UNESCO) has designated mixed temperate deciduous broadleaf/Korean pine/conifer forests in Central Sikhote-Alin, in the heart of this area, as a World Heritage Site in recognition of its unique forests and

wildlife. The Sikhote-Alin Biosphere *Zapovednik* (SABZ), or Reserve, where seven of the eleven field sites were located, is an International Union for Conservation of Nature (IUCN) Category 1 protected area (Miquelle *et al.*, 2010b).

Climate models predict that average global surface temperatures will increase 1.8 – 4.0° C (3.2 – 7.2 °F) during the 21st century (from 1980 – 1999 to 2070 - 2099) (IPCC2007a), with larger gains across land areas. The Intergovernmental Panel on Climate Change (IPCC 2007) forecasts average annual temperature increases greater than 6.0° for Eastern Asia, including coastal areas of the southeastern Russian Far East (IPCC, 2007a). Global mean surface temperatures rose 0.76 °C from 1850 – 1899 to 2001 – 2005, and the rate of increase per decade during the 1956 - 2006 period (0.13 °C) was twice that of the previous 100 years (IPCC, 2007b). The number of extreme warm days and warm nights also has risen worldwide since 1950 (Stocker, 2011).

Climate change effects already have been observed for a variety of species, such as the male broad-tailed humming bird in Colorado (McKinney *et al.*, 2012), the polar bear (Hunter *et al.*, 2010), possibly the wolverine (Peacock *et al.*, 2011), and a host of amphibians and insects (Parmesan, 2006, 2007). My hypothesis is that climate change will change forest composition, which in turn, will impact ungulates, particularly deer and wild pigs, which depend on particular forest vegetation for food and shelter, and tigers, which rely on these types of wildlife for energy and nutrition.

Predicting forest composition and structure at a detailed scale across large and inaccessible landscapes can be difficult. The FAREAST model is an individual-based “gap” model, meaning that it simulates growth of individual trees within an area representing the gap created in the forest canopy when a large tree falls, allowing sunlight to reach the forest floor and stimulate vegetation growth (Watt, 1947; Shugart, 1984; Shugart *et al.*, 1998; Shugart *et al.*, 2010). It was developed and verified on the northern slope of Changbai Mountain in eastern Jilin Province in northeastern China. It has been validated against forest inventory data at numerous sites in Russia and northeastern China (Yan and Shugart, 2005; Shuman and Shugart, 2009). The model has been used to study Russian boreal forest structure and forest response to climate change based on forest inventory data (Shuman and Shugart, 2009; Zhang *et al.*, 2009; Cheng and Yan, 2009). For this study, the model was run using climate, soil and tree species parameters from eleven field locations in strictly protected reserves (*zapovedniks*). (See Chapter 3 for more details).

Temperature inputs were adjusted to reflect predicted best-case and worst-case climate change scenarios for the region (IPCC, 2007). Results in terms of basal area by tree species were analyzed in the context of tree types associated with ungulate prey presence, determined using Resource Selection Function (RSF) analysis. The effects of warmer temperatures on forest composition also were simulated at 1,000 random points across Amur tiger habitat.

4.2 BACKGROUND

The tiger has been cherished for centuries as a symbol of power, grace, beauty, wildness and raw intelligence (Jackson, 1999). The World Conservation Union (IUCN) recognizes six tiger subspecies (Luo, 2004; Jackson, 2010; Chundawat *et al.*, 2012), all of which are endangered or

critically endangered. Between 3,800 – 5,180 adult tigers were estimated to exist in the wild in 2008 (Seidensticker *et al.*, 2010), but about 3,000 adult tigers may remain today (Chundawat *et al.*, 2012), down from an estimated 100,000 in a broad distribution across Asia around 1900 (Kitchener, 1999; Damania *et al.*, 2008; Wikramanayake, 2011). Fewer than 2,500 breeding adults exist globally today (Chundawat *et al.*, 2012), and tiger range has dropped by about 93% since 1900 (Sanderson *et al.*, 2006; Walston *et al.*, 2010), including a decline of 41% from 1994 to 2004 (Dinerstein, 2007; Seidensticker *et al.*, 2010).

Besides the Amur, other living tiger subspecies and their locations (Luo *et al.*, 2004; Chundawat *et al.*, 2012) are:

1. Bengal (*Panthera tigris tigris*) – India, Nepal, Bhutan, Bangladesh
2. Sumatran (*P.t. sumatrae*) - Sumatra Island, off the western coast of Indonesia
3. Northern Indochinese (*P.t. corbetti*) - Indochina north of the Malayan peninsula, including Thailand, Myanmar, Cambodia, Vietnam, Lao PDR, and southwestern China
4. Malayan (*P. t. jacksoni*) – Malaysian peninsula
5. So. China (*P. t. amoyensis*) – formerly southern China, but possibly extinct in the wild. Has not been observed in the wild since the 1970s

The Amur tiger sub-species inhabits the most northernmost latitudes of all the tiger subspecies, existing in temperate rather than tropical ecosystems and withstanding far colder winters than

occur in Tiger Conservation Landscapes to the south. Consistent with Bergmann's Rule (Blackburn *et al.*, 1999), the Amur tiger is considered to be the largest *panthera tigris* subspecies, especially the males, although Bengal tigers as large as Amur tiger average size have been identified in Nepal and northern India (Kitchener, 1999).

4.2.1 Amur tigers (*Panthera tigris altaica*) in the RFE

The Amur tiger is an umbrella species (Meffe *et al.*, 1997) that represents the apex of a complex food web. It is also a keystone species, since it has a much larger impact than its low numbers would suggest (Paine, 1995; Meffe *et al.*, 1997). Changes in the ecosystem occupied by the Amur tiger may affect other species in this area, some of which are rare, endemic or endangered, such as the critically endangered Amur leopard (*Panthera pardus orientalis*), of which an estimated 25 – 35 individuals remain in the wild (Hebblewhite *et al.*, 2011).

Tiger range in the RFE is large compared with other wild tiger locations in part because of the scarcity of prey (Karanth *et al.*, 2004; Goodrich *et al.*, 2010; Miquelle *et al.*, 2010 a&b). Male tiger range may exceed 1000 km² and overlap ranges of 1 - 4 females (Miquelle *et al.*, 1999b; Goodrich *et al.*, 2010; Miquelle *et al.*, 2010a). Female Amur tiger home range is estimated to be about 200 – 440 km². An exclusive 400 km² is needed for successful reproduction (Goodrich *et al.*, 2010; Miquelle *et al.*, 2010a&b). Several studies have found that prey biomass determines carnivore density at both the landscape and site scale, if poaching and other disturbance aren't factors (Carbone and Gittleman, 2002; Karanth *et al.*, 2004; Karanth *et al.*, 2006; Seidensticker

2010 a&b; Miquelle *et al.*, 2010a&b). Ungulates are at very low densities in the Sikhote-Alin area, which includes most of Amur tiger range. Tiger density in the Terai Arc, for example, on the northern India/Nepal/Bhutan border, where prey is abundant, may be more than 15 per 100 km², compared with about 0.5/100 km² in the RFE (Damania *et al.*, 2008; Seidensticker *et al.*, 2010; Miquelle *et al.*, 2010b). In the Terai Arc, prey abundance may be as high as 2800 kg/km², compared with a carrying capacity of less than 600 kg/km² (Miquelle *et al.*, 2010b) for the RFE (Seidensticker *et al.*, 2010). Low prey density in the RFE is mainly a result of legal and illegal hunting, harsh winters, disease and other factors (Heptner and Sludskii, 1992; Seidensticker *et al.*, 2010; Miquelle *et al.*, 2010b).

4.2.2 *Tiger nutritive requirements*

Tigers are “obligate carnivores,” meaning that their nutritional needs are best met by proteins from animal tissue (Seidensticker *et al.*, 1999; Seidensticker *et al.*, 2010). The persistence of tigers in an area where poaching occurs, such as the RFE, depends on the reproductive success of tigers, which is associated with adequate prey (Karanth and Stith, 1999; Seidensticker *et al.*, 2010). A male Amur tiger requires about 4.8 kg of meat per day, which translates to about 3,400 kg of live ungulate prey per year (Sunkist and Sunkist, 2002). A tigress needs about 3,000 kg of ungulate prey per year, or 1825 – 2190 kg/year kg of meat (Sunkist *et al.*, 1999; Sunkist & Sunkist, 2002). Amur tiger consumption of prey biomass per day recently was estimated at 8.8 – 9.0 kg/day, 95% confidence level by Miller *et al.* (2013). During pregnancy, nutritional and caloric requirements are elevated and are about 50% greater for lactating females, a period that extends from the time cubs are born until they are able to kill prey independently, about 19 months (Sunkist *et al.*, 1999; Seidensticker *et al.*, 2010).

Although tigers have been known to eat small mammals, bears, fish, seals, moose and other animals (Heptner and Sludskii, 1992; Miquelle *et al.*, 2010b; Seidensticker *et al.*, 2010), killing the largest prey possible is the most advantageous because it provides maximum energy and nutrition for the energy expended (Pyke *et al.*, 1977; Hayward and Kerley, 2005; Miquelle *et al.*, 2010b). Targeting large prey is especially beneficial in low prey density areas such as the RFE because search time is greater and encounter rates are lower than in high prey density areas (Karanth and Stith, 1999; Sunquist and Sunquist, 2001).

Red deer (*Cervus elaphus*), known as the elk or wapiti in North America (Heptner *et al.*, 1992), and wild boar (*Sus scrofa*) are the most common Amur tiger prey in Central Sikhote-Alin, based on kill and scat data. An analysis of scat data in the Sikhote-Alin Biosphere Reserve in the Central Sikhote-Alin area from 1962 to 2003 found the vast majority of tiger kills to be ungulates (94% of 720 kills), of which 54% were red deer, 28 % were wild boar, 6% Siberian roe deer (*Capreolus pygargus*), 3 % sika deer, and 1 % musk deer (Miquelle *et al.*, 2010a). Brown bears (*Ursus arctos*) comprised less than 3% (Miquelle *et al.*, 2010b) of kills.

Analysis of historical kill data using Jacob's index showed that wild boar is the most preferred prey, followed by red deer (Miquelle *et al.*, 2010a). Kaplanov (1948 in Heptner and Sludskii, 1992) found that wild boar was the most frequent Amur tiger prey based on carcasses and percentage of stomach contents. The body mass of an adult female red deer is about twice that of a sika deer (149 kg vs. 74 kg, respectively) (Dalnikin 1999 as cited in Miquelle *et al.*, 2010b) or a wild boar (86 kg)(Bromley and Kucherenko as cited in Miquelle *et al.*, 2010b). Wild boar may be easier to catch than red deer because it likely is slower and its head-down foraging position

may make it less aware of its surroundings (Miquelle *et al.*, 2010b).

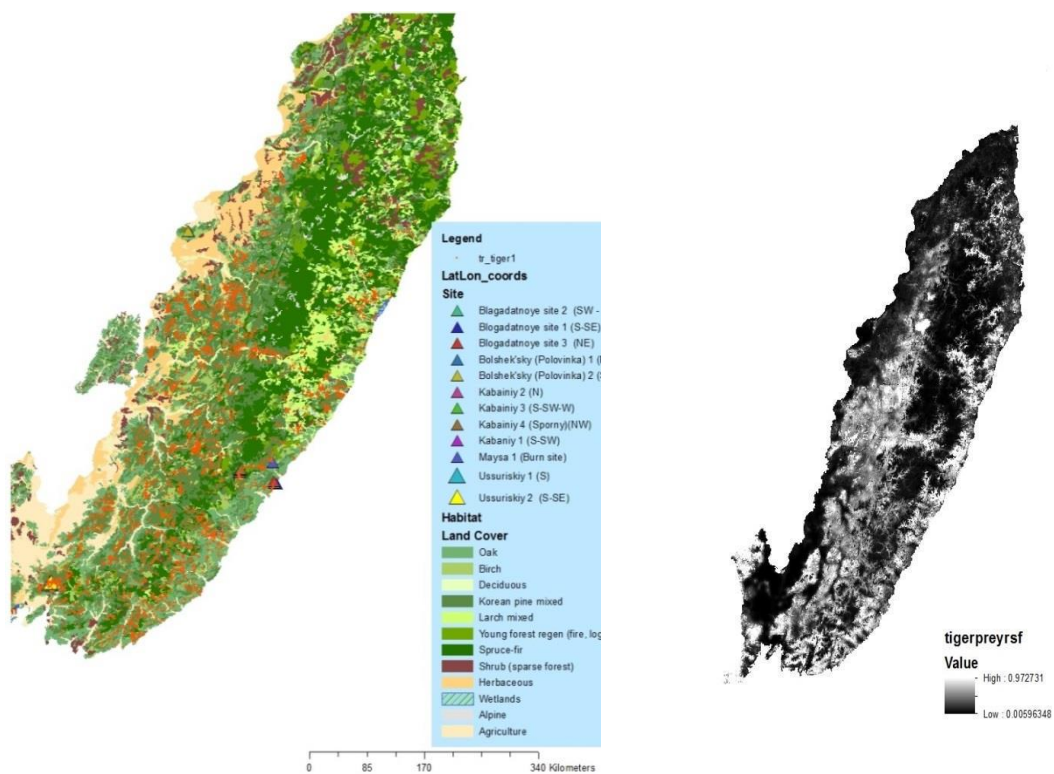
Wild boars in Far Eastern Russia have declined in size during the past sixty years. Traditionally, they were the largest of *sus scrofa* in Russia, and old boars weighing 300 – 320 kg have been reported (Abramov, 1954, as cited in Heptner *et al.*, 1992). By the early 1990s, the largest boars weighed around 200 kg. The decline in size is attributed to hunting of the largest individuals (Heptner *et al.*, 1992). Wild boar are vulnerable to zootic diseases and consecutive years of very snowy winters (snow >70 cm by November) can cause population decline. Prey shortages associated with deep snow lead to more tiger deaths from starvation during severe winters (Heptner and Sludskii, 1992).

In southern parts of the research area, such as Ussurisky Reserve, red deer occur less frequently and sika deer more frequently than in Central Sikhote-Alin (Miquelle *et al.*, 1999b; Miquelle *et al.*, 2010b). Roe deer and wild boar form part of the tiger diet. RSF and spatial models showed that these species preferentially used oak forests. Wild boar and sika deer also selected for Korean pine (Hebblewhite *et al.*, 2011)

4.2.3 Resource Selection Function Analysis (RSF)

Resource Selection Probability Function (RSPF) analyses (Carroll and Miquelle, 2006; Mitchell and Hebblewhite, 2012; Hebblewhite *et al.*, 2012) have been used to determine statistically the types of forest vegetation most utilized by tiger prey and quantified the vegetation-ungulate relationship. The RSF analysis ranked habitat quality on a scale of one to ten using a used/unused

approach, where “used” referred to where tracks in the snow were observed. Sample units numbered 1,041 and averaged 172 km² in size. Tracks of ungulate prey, including red deer, wild boar, sika deer, roe deer (*Capreolus capreolus*), musk deer (*Moschus spp.*) and moose (*Alces alces*) were counted. Used and unused locations were compared using logistic regression (Mitchell and Hebblewhite, 2010). Covariates included spatial variables, such as elevation from MODIS satellite data and digital elevation models (DEMs), land cover variables, distance to roads and *zapovedniks*, and prey presence (Mitchell and Hebblewhite, 2010) (Figure 4.3).



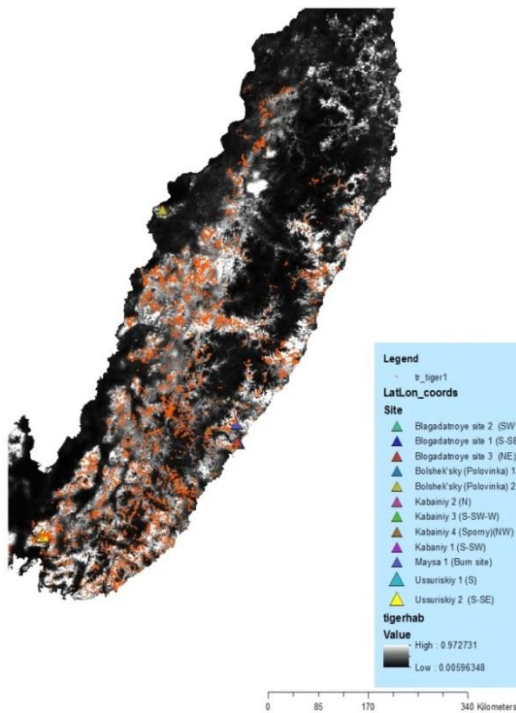


Figure 4.3 Resource selection function analysis (RSF) has shown that tigers and tiger prey preferentially use forests that contain Korean pine and Mongolian oak, as well as riverine forests that often include these species. ArcGIS layers by M. Hebblewhite.

The RSF had a two-tiered approach. The first level of analysis addressed the importance of environmental variables, such as elevation, land cover (including forest vegetation), net primary productivity and snow cover. The second analysis level included ungulate prey track density as well as the environmental variables. The latter RSF had greater explanatory power than the first, based on k-folds Spearman Rank Correlation (Mitchell and Hebblewhite, 2012) and shows that, in evaluating potential tiger habitat, it is essential to consider actual prey occurrence, rather than conditions suitable for prey persistence alone.

Data based on winter snow track surveys during the winter of 2004-05 found the occurrence of red deer to be associated with Mongolian oak (*Quercus mongolica*) and Korean pine (*Pinus koraiensis*). Red deer avoided dark conifer (spruce-fir) and larch forests (Stephens *et al.*, 2006) (Table 4.1).

As mentioned previously, smaller ungulate species, such as sika deer, roe deer and musk deer are considered less optimal prey for tigers because they provide less energy and nutrients for the effort expended to capture them (Hayward and Kerley, 2005; Miquelle *et al.*, 2010b). Sika deer tracks were found in riverine forests and areas with a large proportion of oak, and appeared to avoid other forest types. Roe deer selected for riverine forests, and avoided Korean pine and other pine forests, as well as dark conifer and larch forests. Musk deer, which accounted for less than 1% of kills (Miquelle *et al.*, 2010b), selected for higher elevation and northern larch forests, spruce/fir, and used mixed deciduous/Korean pine forests in proportion to its availability (Stephens *et al.*, 2006).

Wild boar selected only oak and Korean pine forests (Stephens *et al.*, 2006; Hebblewhite *et al.*, 2012). This is consistent with Heptner *et al.* (1992), who reported that wild pigs in Sikhote-Alin are found in coastal oak forest, mixed forests containing Korean pine and Mongolian oak, and “swampy mixed taiga.” Moose are at the southern border of their range in Central Sikhote-Alin and occur very rarely (Miquelle *et al.*, 2010b). Moose selected for spruce-fir forests and larch forests, and used mixed deciduous/Korean pine in proportion to its availability.

Table 4.1 Summary of relationships between forest type and prey presence, based on track encounter rate. Forest types with “+” = tracks encountered most frequently, “-“ = habitats avoided. Blank space means the forest type is used in accordance with its availability (Stephens *et al.*, 2006; Hebblewhite *et al.*, 2012)

Prey Species – Vegetation Relationship						
<i>Vegetation type</i>	<i>Red deer</i>	<i>Wild boar</i>	<i>Sika deer</i>	<i>Roe deer</i>	<i>Musk deer</i>	<i>Moose</i>
Riverine (oak-birch, Korean pine-Deciduous, spruce-fir)	+	+	+	+		–
Mongolian oak	+	+	+	+		-
Birch/aspen			–			
Pine-deciduous	+	+	–	–		
Korean pine	+	+	–	–		–
Larch	–	–	–	–	+	+
Fir	–	–	–	–	+	+

Miquelle *et al.* (2006) reported that tigers, as opposed to just prey, used four (out of twelve) forest zones preferably: Korean pine, Mongolian oak, birch, and riverine. Only Korean pine and oak forests were “preferred” across Amur tiger range. Tigers avoided dark conifer forests, meadows and “Young disturbed forests” (Miquelle *et al.*, 2006). Mature riverine forests typically are composed of deciduous broadleaf or mixed broadleaf\Korean pine (Nakamura and Krestov,

2005). Research has shown that deer range close to fresh water sources (Dinerstein, 1987; Seidensticker *et al.*, 2010).

4.2.4 *Diet of ungulate prey*

The diet of ungulate prey consists of herbaceous browse, grasses, roots, acorns, pine nuts and other organic material (Heptner *et al.*, 1992; Miquelle *et al.*, 1999b; Miquelle *et al.*, 2010 a & b). Deer eat most parts of trees, such as leaves, shoots, bark, branches, and buds, and lichen. Conifer needles are consumed only when nothing else is available, but can cause digestive problems and may be fatal for young animals. Deer eat acorns, which become inaccessible when snow depth exceeds 25 – 30 cm (Heptner *et al.*, 1992). Red deer, sika deer and roe deer also eat grasses when shoots are tender, typically from May to late autumn (Heptner *et al.*, 1992).

Pine nuts from the Korean pine and acorns from Mongolian oak are important for nutrition and energy, especially since underground plant parts become inaccessible when the ground freezes. In abundant mast years, deer and wild boar eat nuts and seeds from September until the ground thaws in spring, when roots and aboveground green plant parts become available. A study by P.A. Stephens *et al.* (2006) found oak mast to be an important factor for red deer, roe deer and wild boar. An alternative mast index showed that pine nuts are important for wild boar in years of low acorn mast.

Korean pine cones are relatively large, and may measure 20 cm in length (Figure 4.2). They occur at the canopy layer of the tree (Hutchins *et al.*, 1996) and may fall off the tree naturally or

squirrels may cut them off. Caching of pine nuts by birds and squirrels is an important mechanism for the reproduction of Korean pines. Birds remove pine nuts while cones are still on the tree, but squirrels and chipmunks chew the scales off the cones on the ground so that the pine nuts may be accessed (Hayashida, 1989; Hutchins *et al.*, 1996). Squirrels cache the nuts by carrying them in their mouths and burying them, but can only carry two to five seeds at a time, so the pine cones are left unattended and the seeds may be eaten by other species, such as wild pigs and deer (Miyaki, 1987; Hayashida, 1989; Hutchins *et al.*, 1996). In poor mast years, wild pigs survive on mountain cranberries, winter horsetail, and sometimes conifer needles and branch tips. Other components of wild pig diet are insects, worms, rodents, amphibians, fish, and, when other parts of plants are unavailable, bark and twigs (Heptner *et al.*, 1992).

4.2.5 *Forest vegetation in Amur tiger range*

John Vaillant coined the term “boreal jungle” in his 2010 non-fiction book *The Tiger* to describe the mix of tropical, temperate and boreal species in the southern RFE. The unusually rich and unique mix of vegetation and wildlife in this area stems from: 1. Paleogeological history and lack of glaciation during the Pleistocene Ice Age (18,000 – 20,000 ybp) (Nakamura and Krestov, 2005) 2. Varied topography, conducive to microclimates offering refugia for cold intolerant species (Nakamura and Krestov, 2005; Krestov *et al.*, 2006) 3. Intersection of the Pacific monsoonal climate with the Asian continental climate, divided by the Sikhote-Alin Mountains, which extend most of the length of Primorski Krai (Nakamura and Krestov, 2005) 4. Location along an unbroken latitudinal vegetation gradient that extends from the tropics to the Arctic (Qian *et al.*, 2003b) that allows mixing of biomes such as temperate and boreal vegetation (Krestov, 2003), and 5. Natural and anthropogenic disturbance (Nakamura and Krestov, 2005).

The principle types of forest in this area are temperate mixed deciduous broadleaf/Korean pine/conifer, and spruce-fir (dark conifer) (Krestov, 2003) (Fig. 4.3a). The composition and structure of mixed deciduous broadleaf/Korean pine/conifer forests vary according to latitude, elevation, and site history (Krestov, 2003; Qian *et al.*, 2003b; Nakamura and Krestov, 2005). In the south, very diverse mixed forests include species with a northern latitudinal limit of 44° N, such as endangered Manchurian fir (*Abies holophylla*), Heart leaf hornbeam (*Carpinus cordata*) and Mongolian oak (Qian *et al.* 2003 p. 77; Nakamura and Krestov 2005). In these lower latitudes, mixed deciduous broadleaf/Korean pine forest occurs up to 800 – 900m (Qian *et al.*, 2003; Nakamura and Krestov, 2005). Farther north, in the cool, humid ocean climate of the eastern slope of the Sikhote-Alin Mountains, mixed forests contain relatively more Korean pine and Mongolian oak (Ishikawa *et al.*, 1999). Broadleaf/Korean pine forests occur up to 400-500 m (Qian *et al.*, 2003).

Yezo or Ayan spruce (*Picea ajanensis*) and Black or Hinggan fir (*Abies nephrolepis*) mix in with deciduous broadleaf/Korean pine at about 600 – 800 m asl, and Korean pine co-occurs with spruce and fir up to about 900 m (Krestov, 2003; Nakamura and Krestov, 2005). Above about 900m, dark conifer forests consist primarily of Black Fir and Yezo spruce (Qian *et al.*, 2003). Dark conifer forests extend all the way to the sea level in northern latitudes, rather than transitioning to mixed broadleaf/pine or pure deciduous broadleaf forests at lower elevations (Nakamura and Krestov, 2005). Dark conifer forests extend northward to latitude 55° – 57° N, where they give way to Dahurian larch (*Larix dahurica/ gmelinii*) deciduous conifer forests

(Nakamura and Krestov 2005). In coastal areas in Central Sikhote-Alin, coastal oak forests have grown on the site of past fire disturbances (Krestov *et al.*, 2006; Nakamura & Krestov, 2005).

4.2.6 *Climate in Amur tiger range*

Climate strongly influences vegetation in this area (Krestov, 2003; Qian *et al.*, 2003; Nakamura and Krestov, 2005). The Sikhote-Alin mountains, which extend about 1200 miles from north to south almost parallel to the coastline, divide the region into a dry, continental climate to the west and a humid, ocean monsoonal climate to the east (Qian *et al.*, 2003a). West of the Sikhote-Alin Mountains, mean temperature during the coldest month (January) temperature is -22 to -26 °C, compared with a mean of -17 to -21 °C on the eastern slope near the coast (Nakamura and Krestov, 2005). Mean summer temperature on the continental side of the mountains is 18.5 to 20 °C, with a peak in July of about 25 °C (Qian *et al.* 2003), and mean summer temperatures of 15 to 17.5 °C on the coastal side (Ishikawa *et al.*, 1999; Nakamura and Krestov, 2005), with peak temperature in August.

Annual precipitation in the central Sikhote-Alin area is 650-820 mm (Ishikawa *et al.*, 1999; Miquelle *et al.*, 2010b). More than 75% of rainfall occurs April through November (Miquelle *et al.*, 2010b). Average snow depth in February is 13.7 ± 3.5 cm in coastal Sikhote-Alin and 22.6 ± 2.9 cm inland (Miquelle *et al.*, 2010b). Heavy snowfalls can occur in March (Miquelle *et al.*, 2010b). On the continental side of the mountains, annual precipitation is about 300 mm lower than coastal areas (Qian *et al.*, 2003a).

The mean annual temperature difference between the northernmost and southernmost parts of the study area is about 3.0 °C (-0.4 °C vs. 2.6 °C, respectively) (Qian *et al.*, 2003a). At Suputinka, near the Ussurisky Reserve, mean annual temperature is 2.6 °C. August mean temperature at Suputinka is 20.3 °C and the January mean is -19.5 °C. Mean annual rainfall is 719 mm (Ishikawa *et al.*, 1999; Qian *et al.*, 2003a). The climate of Sikhote-Alin Reserve (SABZ) is moister, cooler in summer and warmer in winter than at Ussurisky. At Khabarovsk, near the Bolshekhokhtsirskiy Reserve, mean annual minimum temperature is -2.5 °C and mean annual maximum is 6.7 °C (Yan and Shugart 2005). The mean temperature during the coldest month is -22.3 °C and mean temperature during the warmest month is 21.2 °C (Krestov, 2003). Average annual rainfall in Khabarovsk is 665 mm (Yan and Shugart, 2005)

Predicting the effects of climate change in this region is especially challenging because of the varied topography, the orographic effect of the Sikhote-Alin Mountains, and the subarctic climate, with humid conditions and weather systems associated with the Pacific Ocean to the east and south. Utilizing a “best” case (lowest fossil fuel emissions) (B1) and “worst” case (highest fossil fuel emissions) (A1F1) scenario produces a range of potential climate change impacts. A faster rate of warming is expected at higher latitudes, including the range of the Amur tiger, because of diminished albedo associated with the loss of snow cover (Chapin *et al.*, 2005) and changes in vegetation (Bonan *et al.*, 1992; Chapin *et al.*, 2005; Sturm *et al.*, 2001). Increased decomposition of frozen tundra and plant matter is expected to add carbon dioxide (CO₂) to the atmosphere, which also would accelerate warming globally, particularly at northern latitudes (Keyser *et al.*, 2000). The global mean average temperature change for the 2090s is predicted to be about 1.9 °C under the B1 scenario and about 4.0 °C for the A1F1 scenario (IPCC, 2007a).

4.2.7 FAREAST Model - Overview

The FAREAST computer model simulates forest succession in the forest canopy gap that occurs when a large tree falls. The plot size is 1/20th hectare (500 m²), and the model processes 200 plots to produce average site level results. FAREAST simulates old growth forests, such as those found at eight of the eleven field sites, which were in strictly protected scientific reserves (*zapovedniks*). Basal area field data from the sites, which represented different climates and latitudes in tiger range, were compared with model results (See Chapter 3). Climate inputs were then adjusted to reflect different predicted climate change scenarios to simulate the potential impact on forest vegetation.

The model also was run with atmospheric temperatures adjusted for climate change at 1,000 points selected at random by computer across tiger range to examine climate change impacts at a regional scale.

4.3 MATERIALS AND METHODS

Key elements of the research included a field campaign in the Russian Far East in September and October of 2007, computer modeling, and comparison of model output at 1,000 randomly selected points across tiger range with forest covers developed from remote sensing and Russian vegetation maps by T. V. Loboda at the University of Maryland, Department of Geography.

4.3.1 *Field research*

Eleven field sites were selected at random in southern, central and northern sections of tiger habitat. All were located in strictly protected scientific reserves (*zapovedniks*), and eight of the eleven sites represented typical undisturbed forest vegetation.

Seven of the eleven sites were located in the 401, 428 hectare Sikhote-Alin Biosphere *Zapovednik* (SABZ) in central Primorski Krai (~136° E, 45° N). At each site, ten 30-m diameter circular transects were delineated at random. The diameter at breast height (DBH, 1.37 m) of each tree with DBH greater than 8.0 cm was measured and recorded for the purpose of determining basal area by species. Saplings (< 8.0 cm DBH) at the site also were identified by species and counted.

Field methods are described in more detail in Chapter 3.

4.3.2 *FAREAST model*

The FAREAST model was used to predict changes in forest composition associated with climate change at eleven field locations that represent typical tiger habitat forest composition. The model also was run at 1000 random points across tiger habitat. FAREAST consists of four sub-models:

ENVIRON, GROWTH, REGENERATION, and MORTALITY. The sub-models GROWTH and ENVIRON are particularly relevant to this study. The GROWTH sub-model is described in Chapter 3 and in Yan and Shugart 2005. The sub-model ENVIRON calculates soil moisture, soil nutrients and climate conditions based on climate inputs. Climate inputs are monthly average maximum and minimum temperature and standard deviations from these averages, from which daily temperatures are calculated using a random approach. Average monthly precipitation and its standard deviation are used to calculate daily precipitation amounts. Soil moisture, soil carbon, and soil nitrogen are calculated on an annual time-step based on a carbon and nitrogen cycle model (Post and Paster, 1996).

FAREAST soil parameters include field capacity, A_o (top) and humus (active) soil layer nitrogen and carbon, and permanent wilting point. Parameters are updated continuously based on species characteristics and interactions among individual trees on a plot. For example, deciduous trees such as oak need more nitrogen and contribute nitrogen to the soil through litter fall, thus providing resources to benefit the next generation of its species (Zyryanova *et al.*, 2005)

The temperature tolerance of a species, calculated in the GROWTH sub-model, is based on growing degree day requirements and the observed maximum and minimum growing degree days at the limits of the species' range (Botkin *et al.*, 1972; Yan and Shugart, 2005).

$$f_T(DEGD) = \frac{4(DEGD_{\max} - DEGD)(DEGD - DEGD_{\min})}{(DEGD_{\max} - DEGD_{\min})^2}$$

Equation 4.1

In FAREAST, atmospheric temperature affects potential evapotranspiration (PET) and soil water availability. Soil water availability is calculated using the Hargreaves evaporation equation (Hargreaves & Allen, 2003; Yan & Shugart, 2005), which uses maximum and minimum temperatures to estimate drought conditions. The impact of drought on a particular species (f_D) depends on the number of drought days, the impact on soil moisture, and the species' tolerance of drought (D_0). Drought impact is calculated using the equation:

$$f_D(DROUT) = \begin{cases} \sqrt{(D_0 - DROUT)/D_0} & DROUT < D_0 \\ 0 & DROUT \geq D_0 \end{cases} \quad \text{Equation 4.2}$$

As temperature warms, increased evapotranspiration reduces soil moisture (Zhang *et al.*, 2009). Soil moisture also is calculated as a function of precipitation. Increased soil moisture associated with greater rainfall may be mitigated by greater evapotranspiration associated with warmer temperatures (Zhang *et al.*, 2009).

Tree death in FAREAST is calculated in the MORTALITY sub-model. The probability of a tree's mortality is $p_n = 1 - \exp(-death/Age \text{ max})$, where *death* is a species-category dependent parameter (Yan and Shugart 2005). Probability of death increases for slower growing trees, a result of factors such as temperature, shading, drought, lack of nutrients and inter-species competition (Yan and Shugart 2005). For detailed information about the FAREAST model and its sub-models, see Yan and Shugart 2005 and Sherman *et al.*, 2012.

4.3.2.1 Temperature inputs and scenarios used

World Meteorological Organization (WMO) data were used as climate inputs for temperature and precipitation. For the field sites, data from the closest weather station were used. For random points, weather station data were used based on proximity, topography and reliability of data (see Chap. 3 for details). Best case and worst case climate change scenarios were used to develop temperature inputs to the FAREAST model.

For Eastern Asia, defined as 20 – 50° N latitude and 100 – 150° E longitude, the projected change in surface air temperature for the period 2070 to 2099 compared with the baseline period of 1961 – 1990 under scenario B1, which represents the lowest future greenhouse gas emissions and the best case scenario, is 3.88 °C for December-January-February (DJF), 3.69 °C for March-April-May (MAM), 3.00 °C for June-July-August (JJA), and 3.04 °C for September-October-November (SON). For the A1F1 scenario, which represents the temperature trajectory in the case with the highest greenhouse gas emissions, the projected increase in surface air temperature for this region is 6.95 °C (DJF), 6.41 °C (MAM), 5.48 °C (JJA), and 5.51 °C (SON) (IPCC 2007a, Table 10.5, p. 480).

The IPCC predicts that precipitation in East Asia would increase an average of 9.25% annually under the B1 scenario and 15.25% annually under the A1F1 scenario. The increase is greatest in winter and breaks down as follows (IPCC 2007a, Table 10.5, p. 480):

Table 4.2 Predicted precipitation increases (%) by season for East Asia

	B1 (%)	A1F1 (%)
DJF	15	21
MAM	10	15
JJA	8	14
SON	4	11

4.3.2.1 FAREAST simulation

For the field site simulations, species found at each field site were used for the model's species input parameter because of the statistical weight associated with species presence. Having a seed source at a site greatly increases the likelihood of persistence of that species in that location (Horn 1974; Horn *et al.*, 1975; Horn, 2002) as compared with species that might tolerate local soil and climate conditions, but are not found in the area. Using only species at the site might also create a more realistic climate change scenario than using all species possible for the conditions, as the latter might produce conversion to new species faster than might occur in nature (Zhang *et al.*, 2009).

Elevation was not adjusted for the simulation because the adiabatic rate incorporated in the model is not consistent with the adiabatic rate associated with the humid conditions at eight field sites in Central Sikhote-Alin, which caused results that would be typical of a higher elevation. Kabaniy 3

and 4 are at higher altitudes than Kabaniy 1 and 2, but for the simulation differ from Kabaniy 1 and 2 only in terms of slope and the species found at the site.

Forest categories of broadleaf deciduous, dark conifer, or Korean pine were defined when 60% or more of basal area at the site consisted of one of these forest types. When these types were represented, but none achieved 60% of basal area, a “mixed” category was assigned. The sites were:

	Latitude	Longitude	Elevation	Aspect
Ussurisky Reserve				
Ussurisky 1	43.654 N	132.35 E	230 – 270 m	S
Ussurisky 2	43.654 N	132.379 E	290 – 325 m	S-SE
Sikhote-Alin Biosphere Reserve				
Kabaniy 1	45.111 N	135.865 E	500 – 600 m	S-SW
Kabaniy 2	45.114 N	135.87 E	585 – 620 m	N
Kabaniy 3	45.139 N	135.884 E	920 – 940 m	S-SW-W
Kabaniy 4	45.152 N	135.9 E	750 – 780 m	NW
Blagodatnoye 1	44.96 N	136.563E	52 – 110 m	S-SE
Blagodatnoye 2	44.972 N	136.526 E	210 – 240 m	SW-W

Maysa 1	45.23 N	136.511 E	200 m	level
---------	---------	-----------	-------	-------

Bolshekhkhtsirskiy Reserve

Polovinka 1	48.24 N	134.906 E	300 – 315 m	NW
-------------	---------	-----------	-------------	----

Polovinka 2	48.24 N	134.9 E	290 – 335 m	SE-E
-------------	---------	---------	-------------	------

4.3.2.3 *Random points*

One thousand points were selected at random by computer across tiger range (Figure 4.4). Forty-three tree species were used as input. Climate data was used from the nearest WMO weather station or the station most appropriate for the geographic region. Soil parameters were selected based on the assumption that old growth mixed deciduous/Korean pine/conifer forests occur on brown soils (brownzems), with moderate moisture and relatively good drainage (Krestov, 2003; Nakamura and Krestov, 2005). The FAREAST model was run at each point using the University of Virginia cluster system, a Linux-based large memory system managed by the UVA Alliance for Computational Science and Engineering.

For each point, forest covers developed from FAREAST results were assigned. When 65% of basal area consisted of spruce, fir or Korean pine, Dark Conifer was designated. If deciduous broadleaf species comprised 65% of basal area, the site was considered to be Broadleaf forest. When FAREAST output included Korean pine, conifer and broad leaf at a point, but neither

conifer nor broadleaf species accounted for 65% of basal area, a mixed forest label was applied.

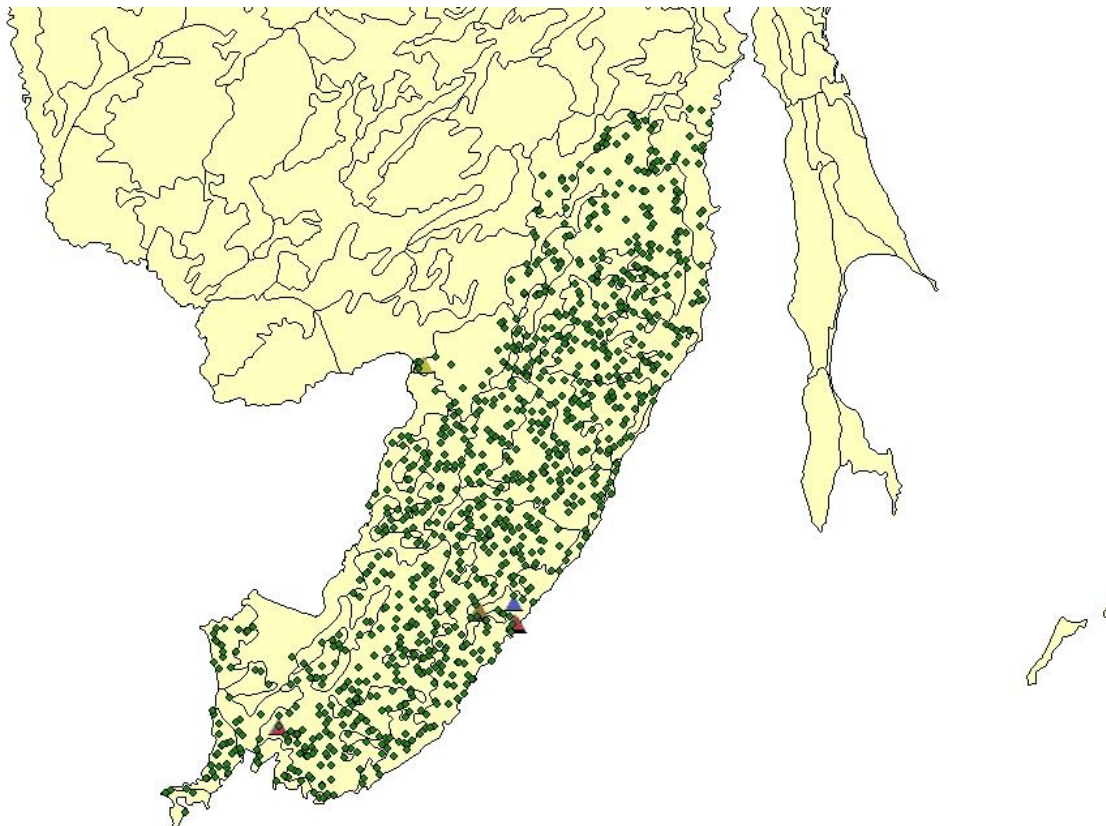


Figure 4.4 FAREAST was run with 3.5 °C and 6.0 °C climate change at 1,000 points randomly selected in forested areas across tiger habitat. Colored triangles represent field sites.

4.3.2.4 *Adjusting FAREAST for climate change*

The FAREAST model processed data to simulate 1000 years. After the initial 300 years, the approximate age of forests in the nature reserves, atmospheric temperature was increased

incrementally at a fixed rate on an annual time-step over 100 years to achieve the designated new climate regime.

Temperatures first were increased by 3.5 °C to represent the growing season in the B1 (lowest fossil fuel emission) scenario. The year-round average surface air temperature increase for the B1 scenario is projected to be 3.4°, with the largest increases occurring December through May (IPCC 2007). Next, temperatures were increased by 6 °C to reflect the A1F1 (highest fossil fuel) scenario. Under the A1F1 scenario conditions, average surface temperature in East Asia is projected to increase by 6.09 °C. I also tested temperature increases at each field site to determine the level of climate warming that causes Korean pine to permanently decline.

4.4 RESULTS

Overall, the simulation indicates that warmer temperatures and drier soil conditions would cause transitions from biologically diverse ecosystems to biomes with a few tree species, monodiversity, or a complete forest collapse. Climate warming of 3.5 °C favors Korean pine at Kabaniy 3 and 4. Warming of 6 °C over 100 years causes the collapse of most forest tree species, with the exception of Painted maple and Manchurian walnut, and Mongolian oak at a slightly inland Blagodatnoye site.

With a 3.5° C increase incrementally applied over 100 years, Korean pine disappears at the northernmost and southernmost sites (Ussurisky 1&2, Polovinka 1&2), but continues at the non-coastal sites of Kabaniy 1 – 4 in Sikhote-Alin. Mongolian oak, which currently occurs in small quantities at some field sites, continues to decline at Ussurisky 1 and 2, Kabaniy 1, and Polovinka 1 and 2. At the coastal site of Blagodatnoye 1, Mongolian oak dies out with 3.5 °C climate change, but flourishes at Blagodatnoye 2, if Korean pine is removed from the simulation. Blagodatnoye 2 was 150 m higher and more inland than Blagodatnoye 1. At the burn site Maysa in SABZ, with 3.5 climate change starting at year 80, the estimated age of the regenerating forest, Korean pine would persist indefinitely, and the small number of oak trees would die out and not regenerate.

With 6 °C warming, basal area drops sharply or the forest disappears at the Ussurisky sites and the Kabaniy sites, except for Kabaniy 1, where Painted maple persists. Painted maple also remains at Maysa and the coastal oak forest of Blagodatnoye 1. At Blagodatnoye 2, with Korean pine removed to better simulate current conditions, Mongolian oak would persist.

4.4.1 Ussurisky Zapovednik (Reserve)

FAREAST results at Ussurisky 1 without climate change and with no adjustment for altitude had almost a 1:1 relationship with observed for years 240 – 260. Adjusting for altitude produced an even closer relationship for years 260 and 280 (See Chapter 3). If current climate conditions were to continue, Korean pine would persist indefinitely, along with Painted maple and Amur

linden (Figure 4.5). With 3.5 °C climate change starting at year 350, forests that include oak and pine give way to a forest of Painted maple (*Acer mono*) (Fig. 4.6a), with less than 1 m²/ha of several other species. With 6.0 °C climate change, total basal area drops dramatically and only Manchurian walnut (*Juglans mandshurica*) and Heart leaf hornbeam (*Carpinus cordata*) remain (Figure 4.6b).

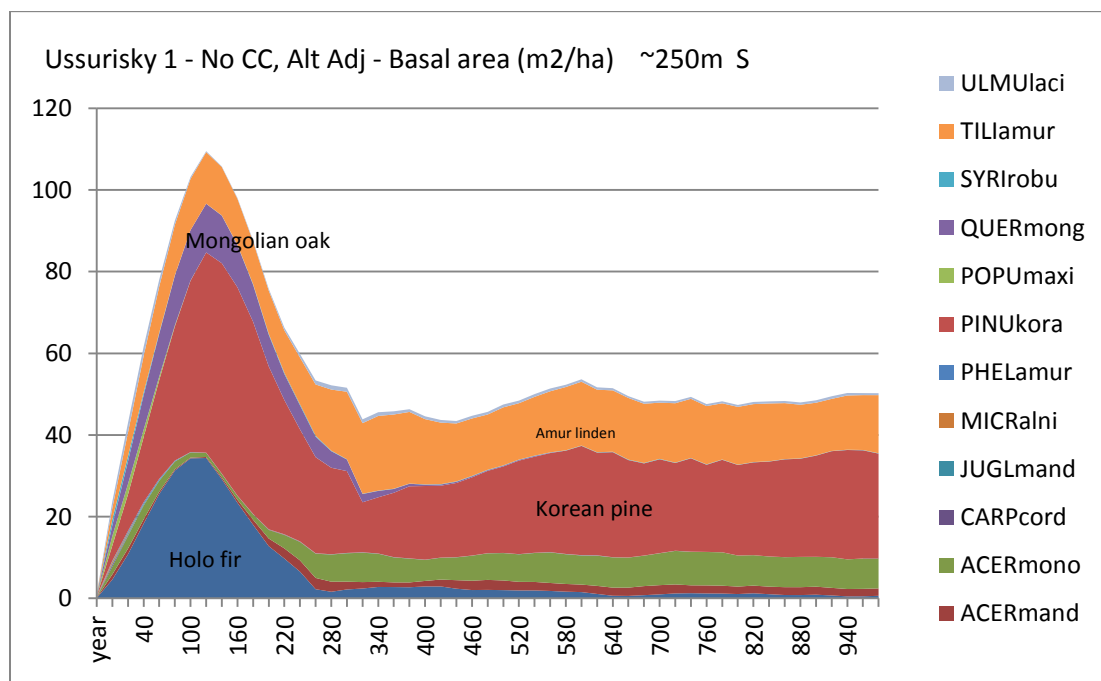


Figure 4.5 Under current climate conditions, Korean pine would continue indefinitely at Ussurisky 1. Mongolian oak dies out after about 400 years (about 140 years from present).

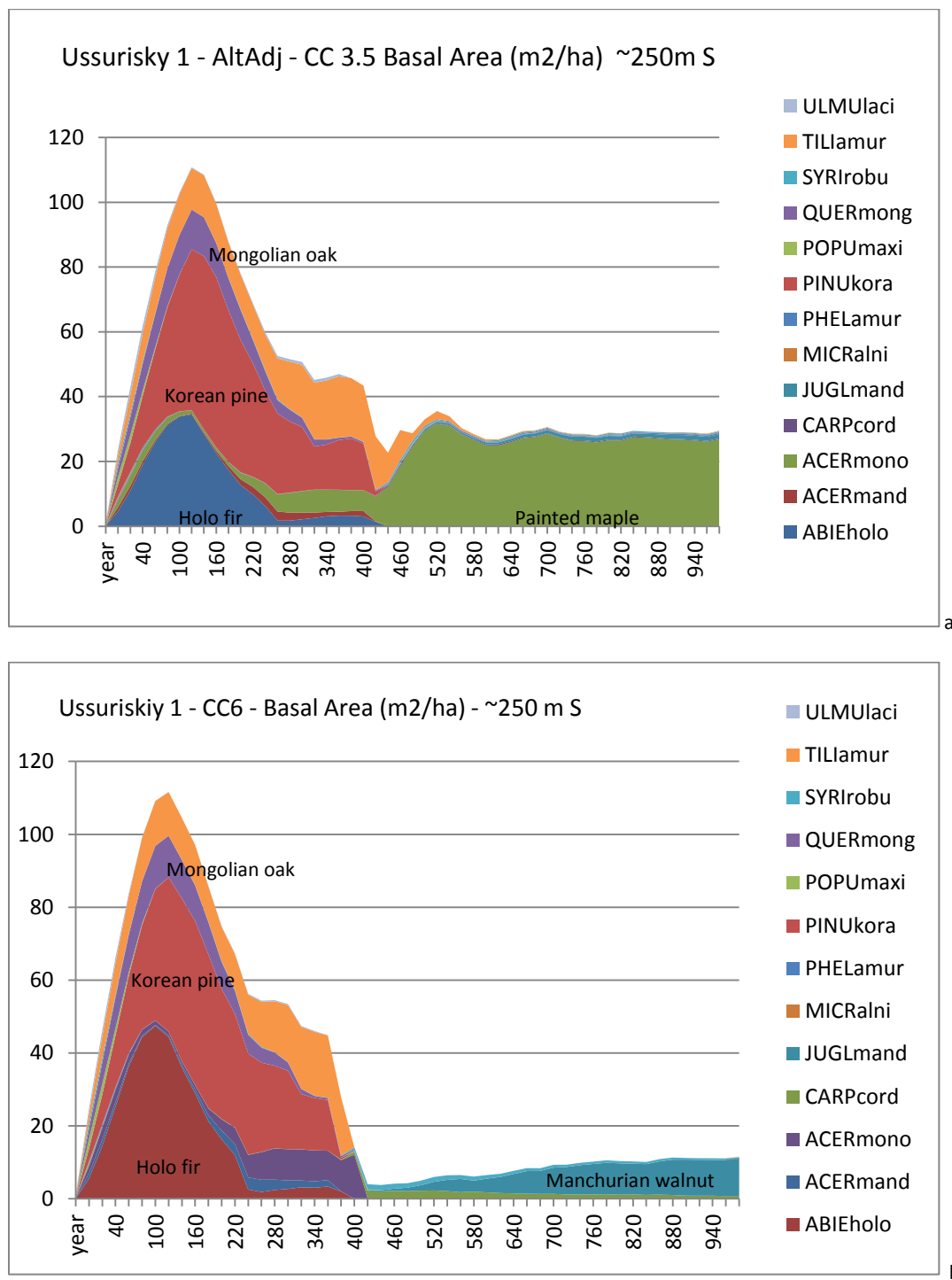
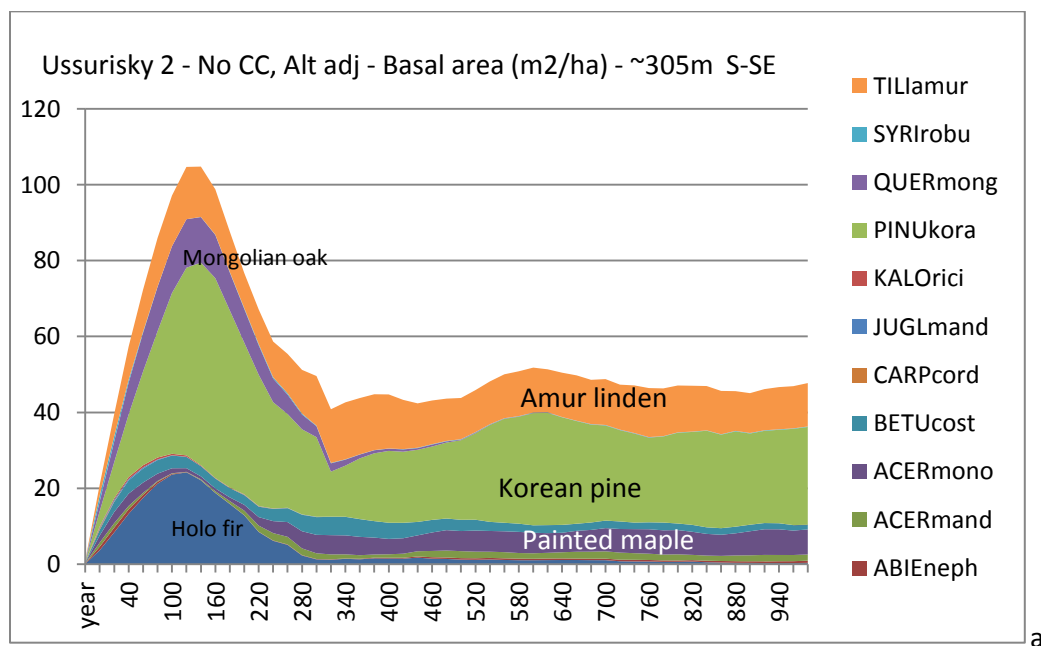


Figure 4.6 (a) With 3.5 °C climate change, mixed deciduous broadleaf/Korean pine/conifer forest gives way to monoculture dominated by Painted maple (*Acer mono*). (b) With 6.0 °C climate

change, total basal area at Ussurisky 1 drops dramatically and only Manchurian walnut and Hornbeam survive.

FAREAST simulation with no climate change for Ussurisky 2, 290 – 325 m, S-SE aspect, was slightly less consistent than Ussurisky 1 with field results. However, using the Kolmogorov-Smirnov statistical approach, the null hypothesis, which was that observed and modeled results were from the same distribution, could not be rejected ($p < 0.05$). With 3.5 °C climate change, the mixed forest converts to Painted maple and Amur linden. With 6.0 °C climate change, total basal area drops sharply and Manchurian walnut dominates (Figure 4.7).



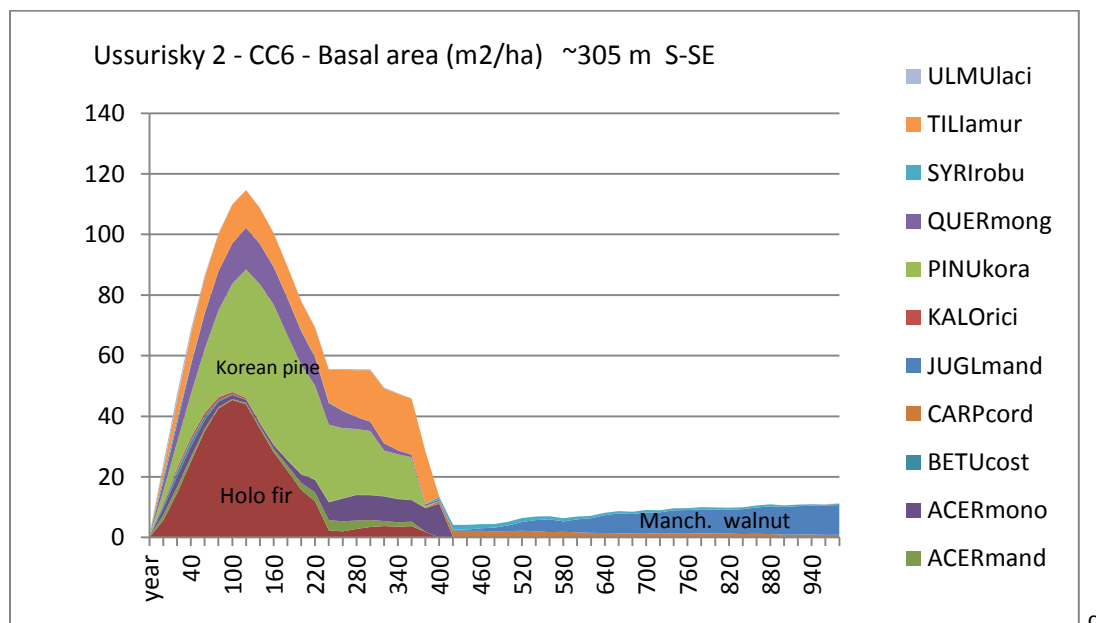
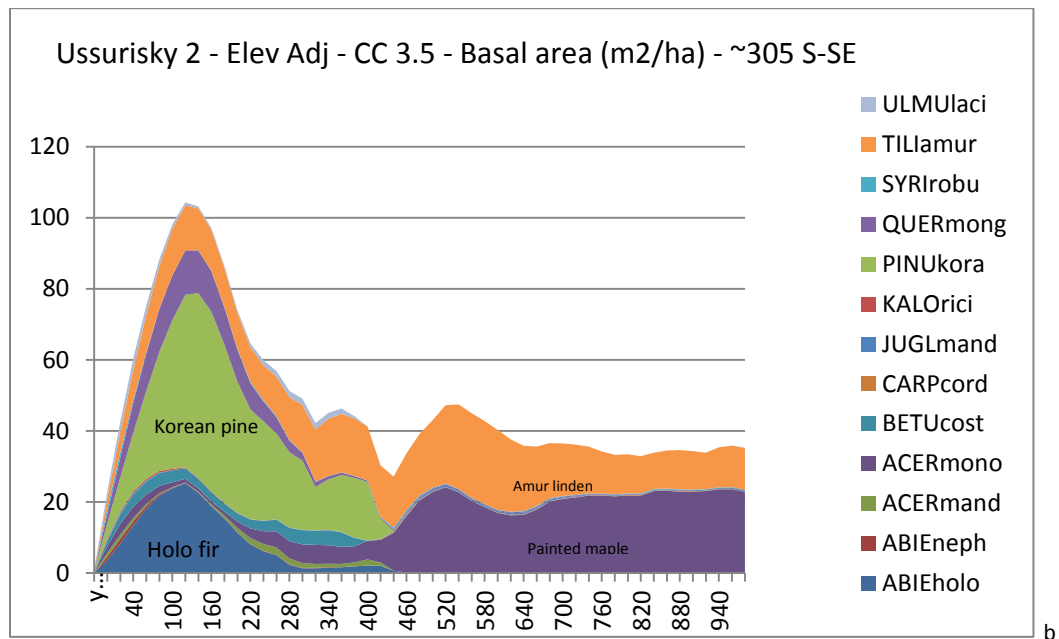
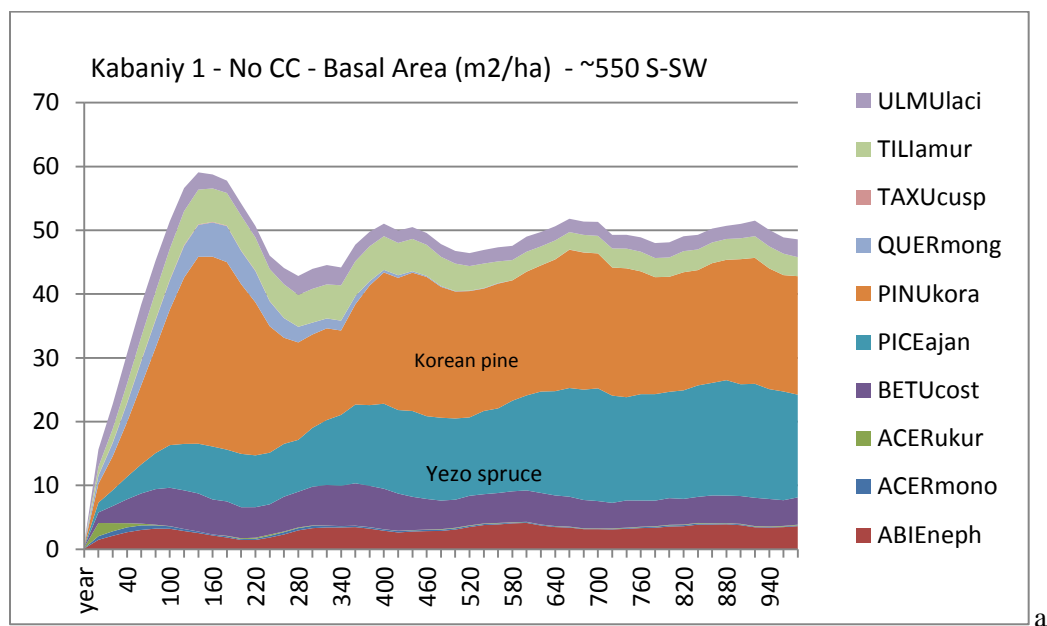


Figure 4.7 a – c Under current climate conditions (a), Korean pine continues indefinitely, but Mongolian oak dies out. (b) With 3.5 °C temperature increase, the mixed forest converts to Painted maple and Amur linden. (c) With 6 °C climate change, the mixed forest converts to a Manchurian walnut forest with very small amounts of hornbeam and lilac.

4.4.2 Kabaniy sites in Sikhote-Alin Biosphere Reserve (Zapovednik) (SABZ)

Kabaniy 1 was located in Sikhote-Alin Biosphere Reserve at ~550 m elevation on a S-SW slope of about 25 degrees. Kabaniy 2 was on a northern slope at a slightly higher (600m asl elevation). FAREAST model results at Kabaniy 1 and 2 indicate that, with 3.5° C climate warming, diverse mixed broadleaf/ Korean pine/conifer forests increase in total basal area, but convert to a mixed forest composed only of Korean pine, Amur linden, and Painted maple at Kabaniy 1 (Figure 4.8) and only Korean pine and Amur linden at Kabaniy 2 (Figure 4.9), because Painted maple wasn't present. Mongolian oak disappears after about 400 years without climate change, and persists at very low levels with 3.5 °C temperature increase. With 6.0 °C warming over 100 years, total basal area drops sharply and the mixed forest converts to Painted maple, if the species is present. If maple isn't present, like at Kabaniy 2, the forest disappears.



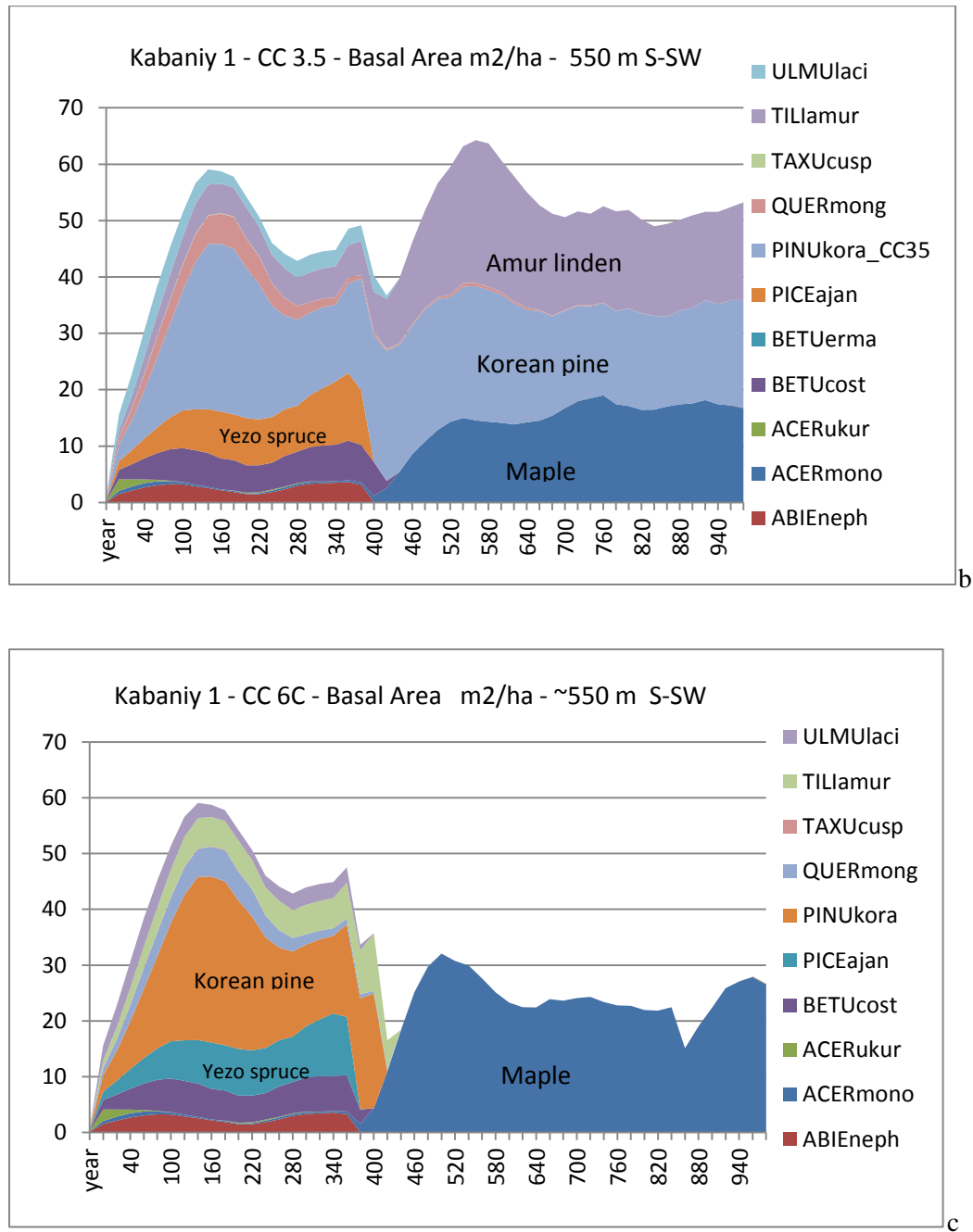
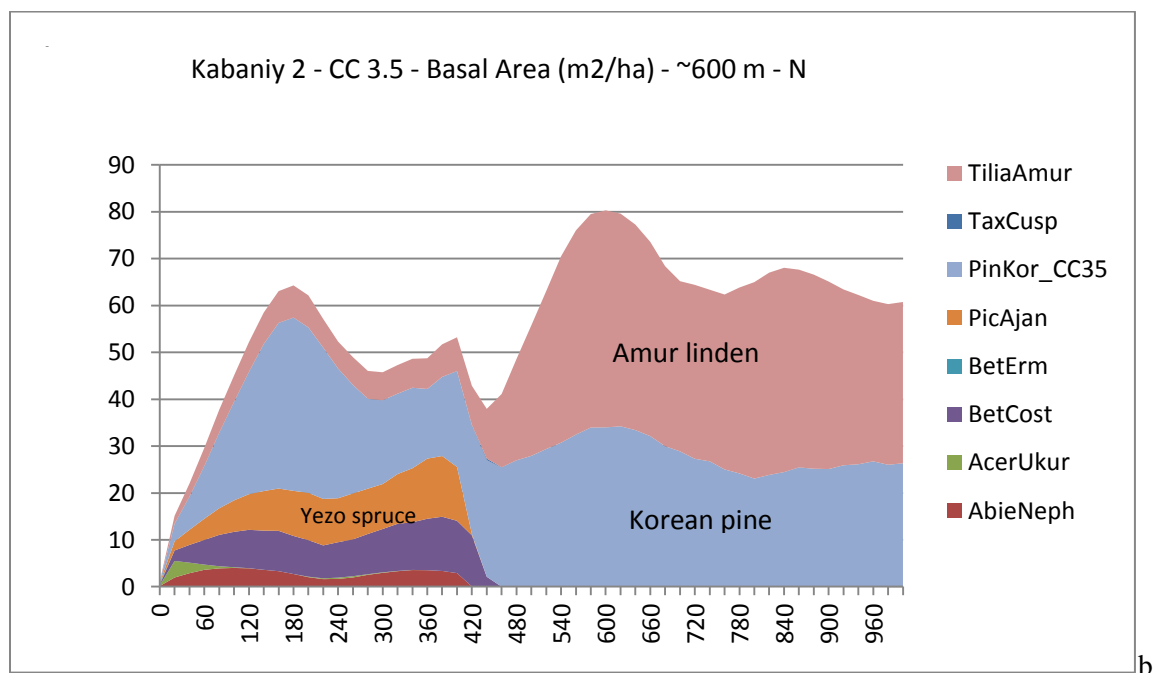
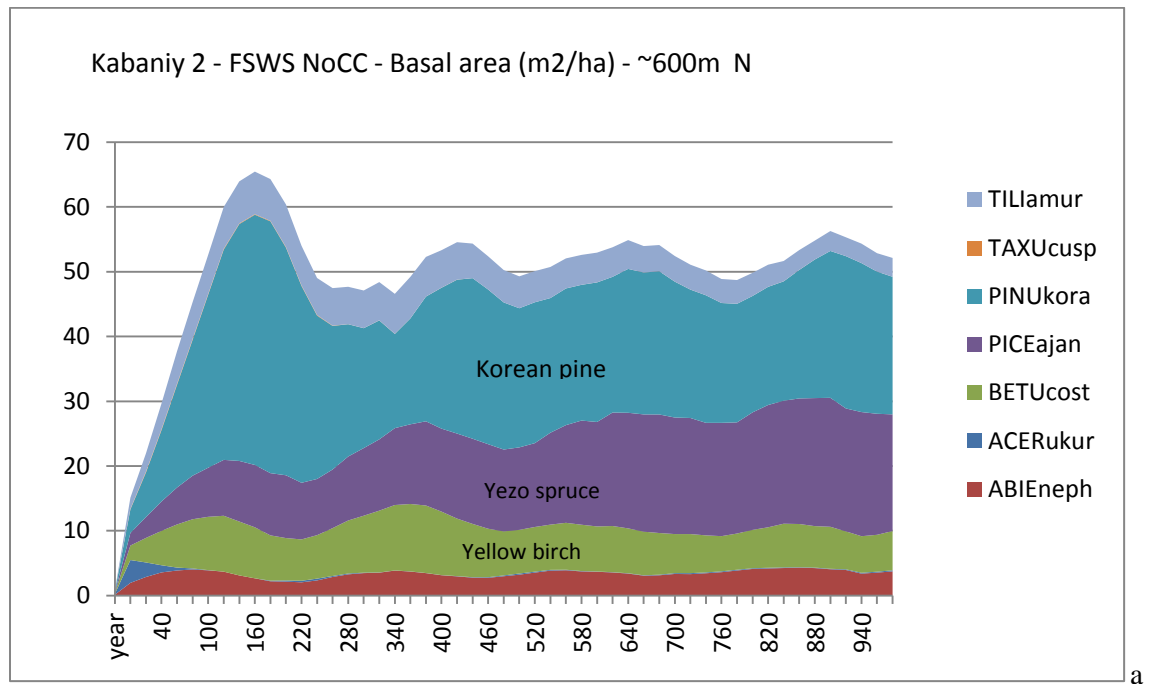


Figure 4.8 (a) Under current climate conditions, basal area of Korean pine and Yezo spruce would expand and stabilize at proportions larger than at present. (b) With 3.5 °C warming starting

at year 350, Korean pine persists, but the forest changes composition. (c) With 6° C climate warming over 100 years, only Painted maple (*acer mono*) survives.



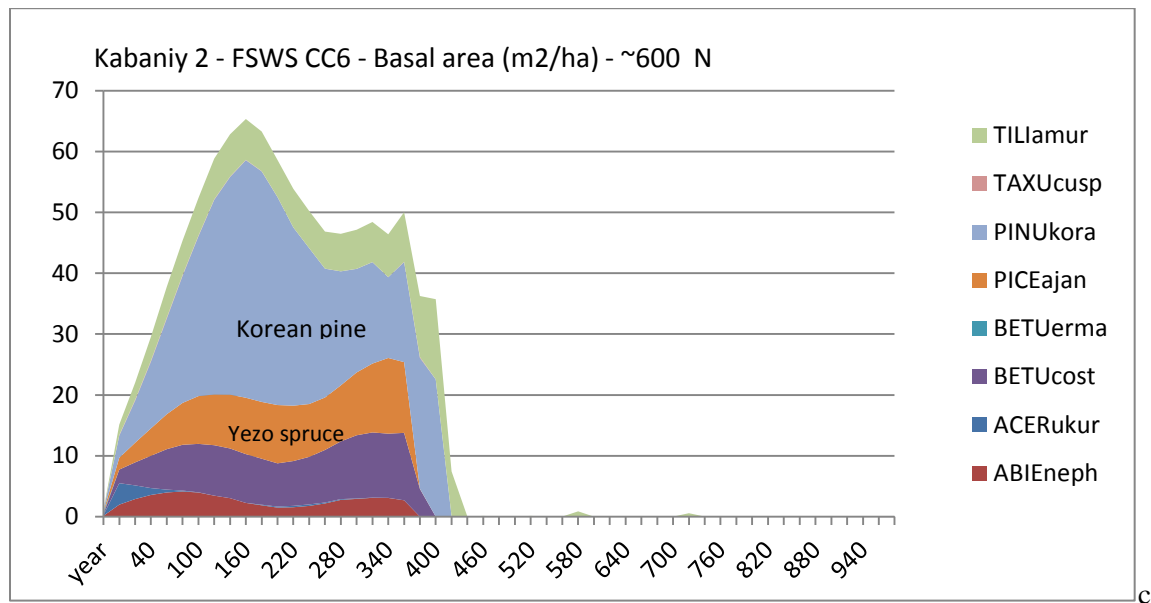
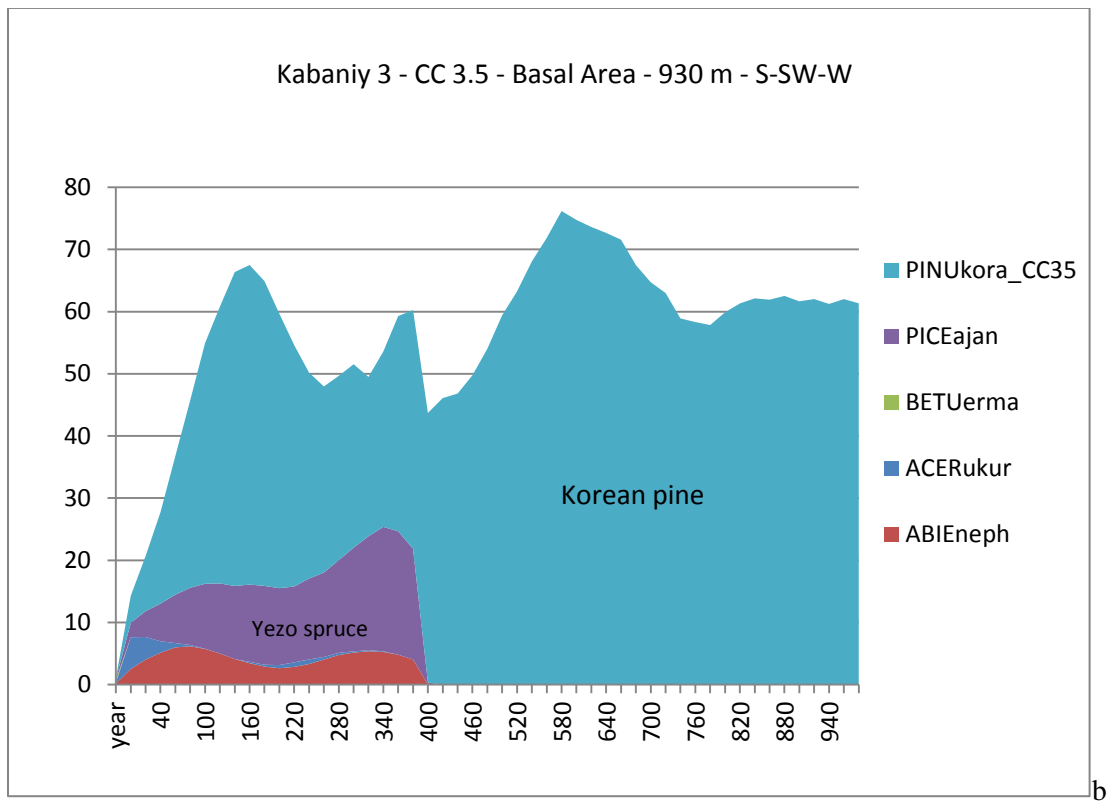
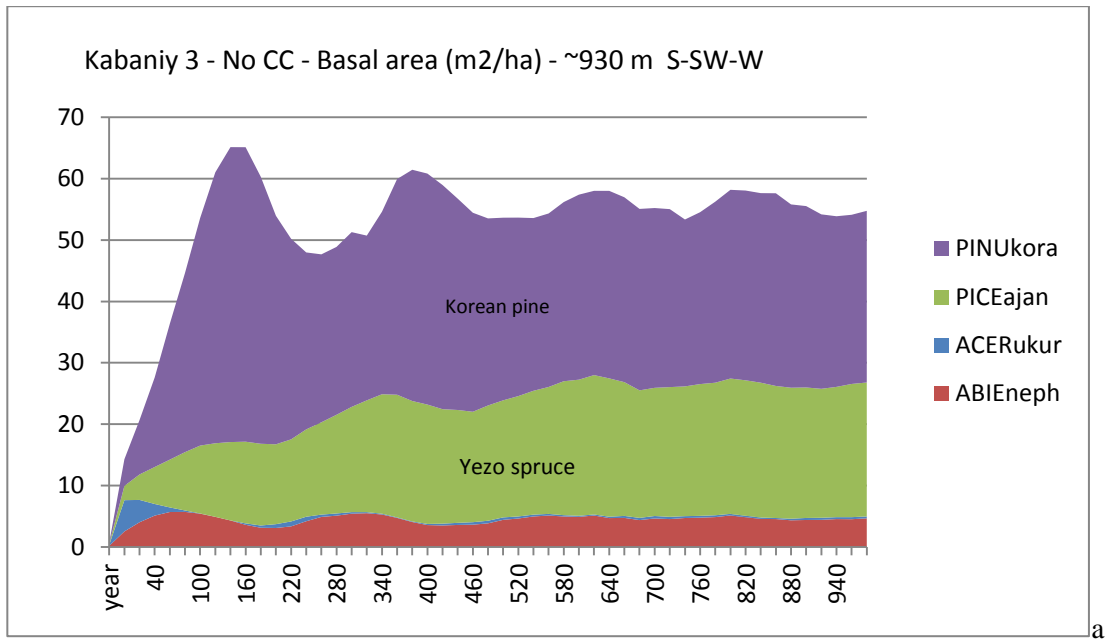


Figure 4.9 (a) Under current climate conditions at Kabaniy 2, Korean pine basal area would expand and be part of a mostly conifer forest indefinitely. (b) With 3.5 °C warming, Korean pine persists as a co-dominant species with Amur linden. (c) Painted maple isn't present, and the forest dies out with 6° C climate warming over 100 years.

At Kabaniy 3, with 3.5 °C climate change, with a S-SW-W aspect, climate change of 3.5 °C causes the mixed forest to change to a Korean pine forest. Current species disappear with an increase of 6.0 °C (Figure 4.10).



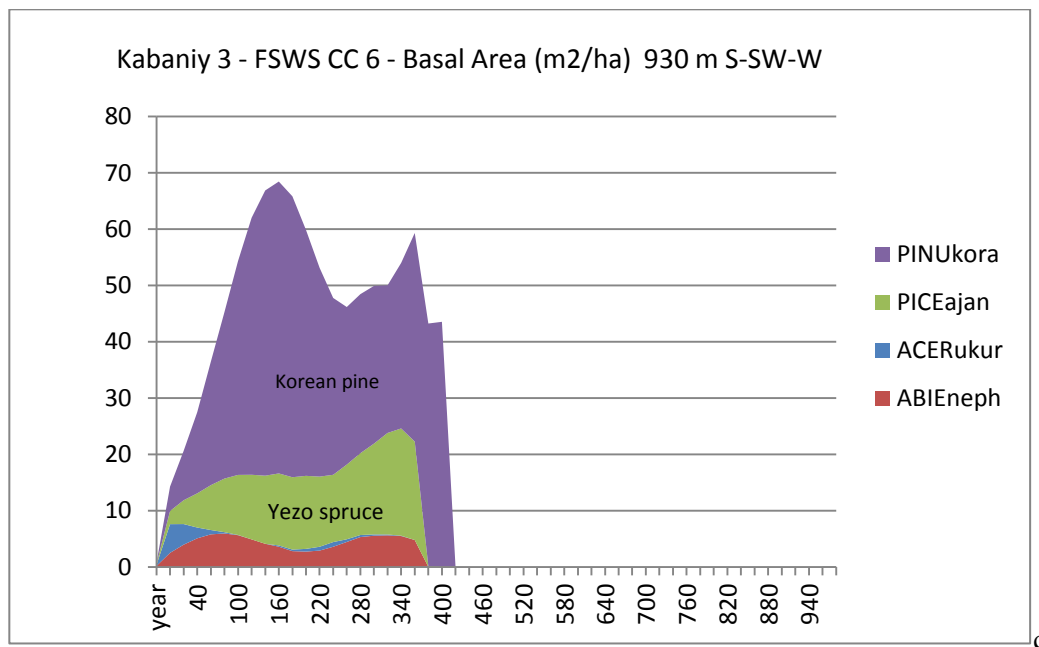
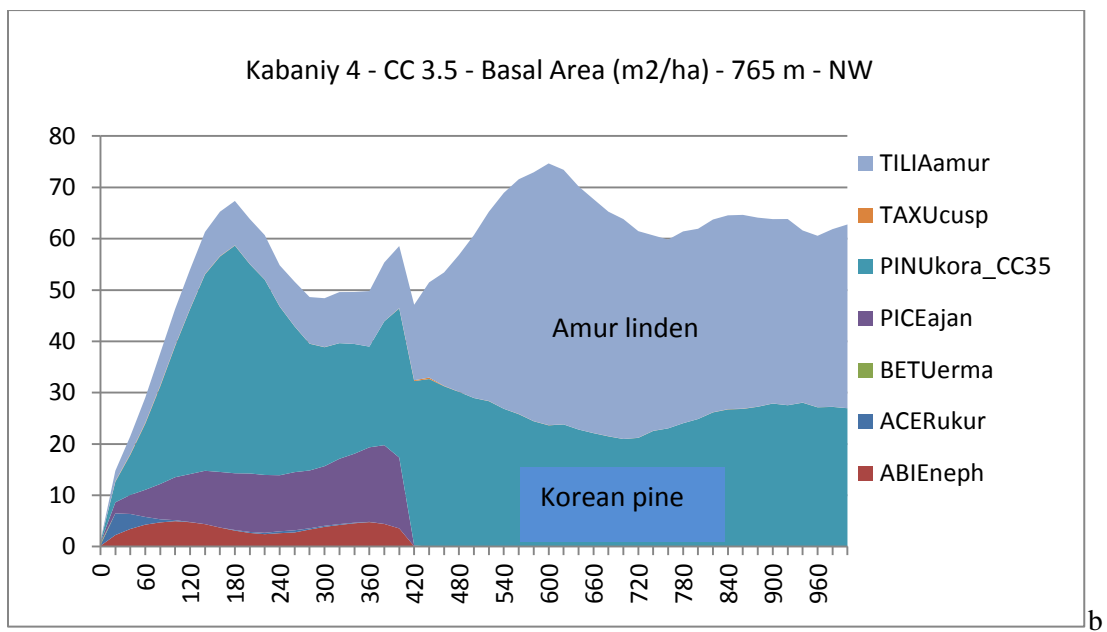
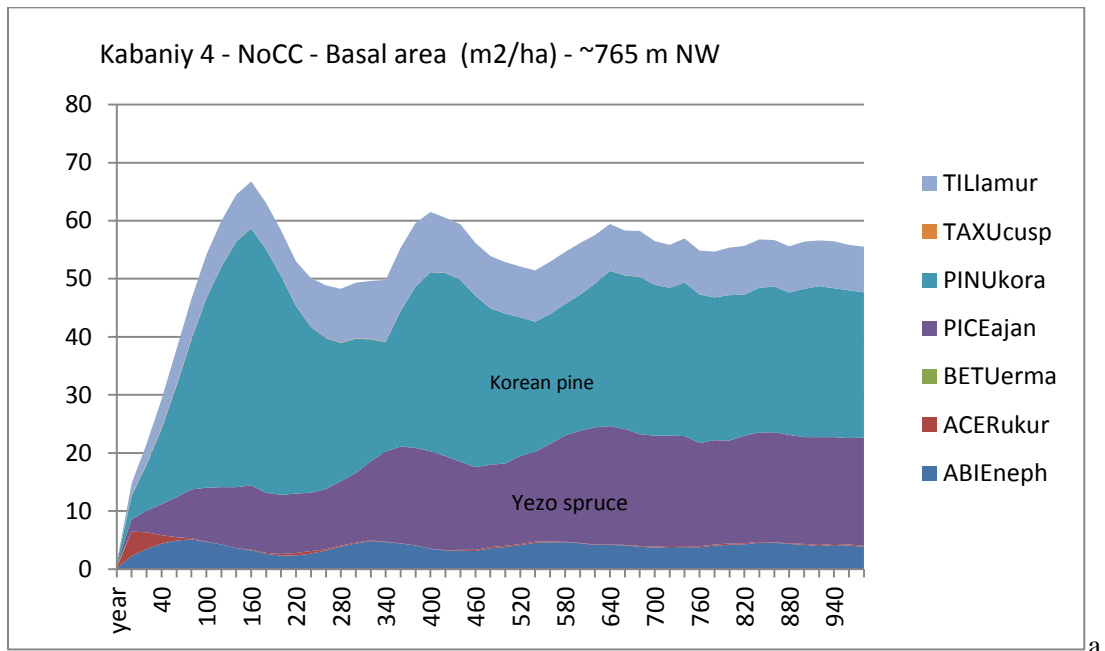


Figure 4.10 (a) Under current climate conditions, Korean pine, spruce and fir would continue indefinitely in approximately the same proportions as today. (b) With 3.5 °C warming, Korean pine would flourish and other conifer species would die out. (c) All species would perish with 6.0 °C warming.

At northwest-facing Kabaniy 4 (~765 m, northern aspect), FAREAST without climate change produced results similar to field results for Kabaniy 1 – domination by Korean pine, with smaller proportions of Yezo spruce, Amur linden and Black fir (Figure 4.11). With 3.5° climate change, Korean pine maintains considerable basal area and Amur linden gains basal area. With 6.0 °C climate change, all species die out by year 450, fifty years after temperature adjustment is completed.



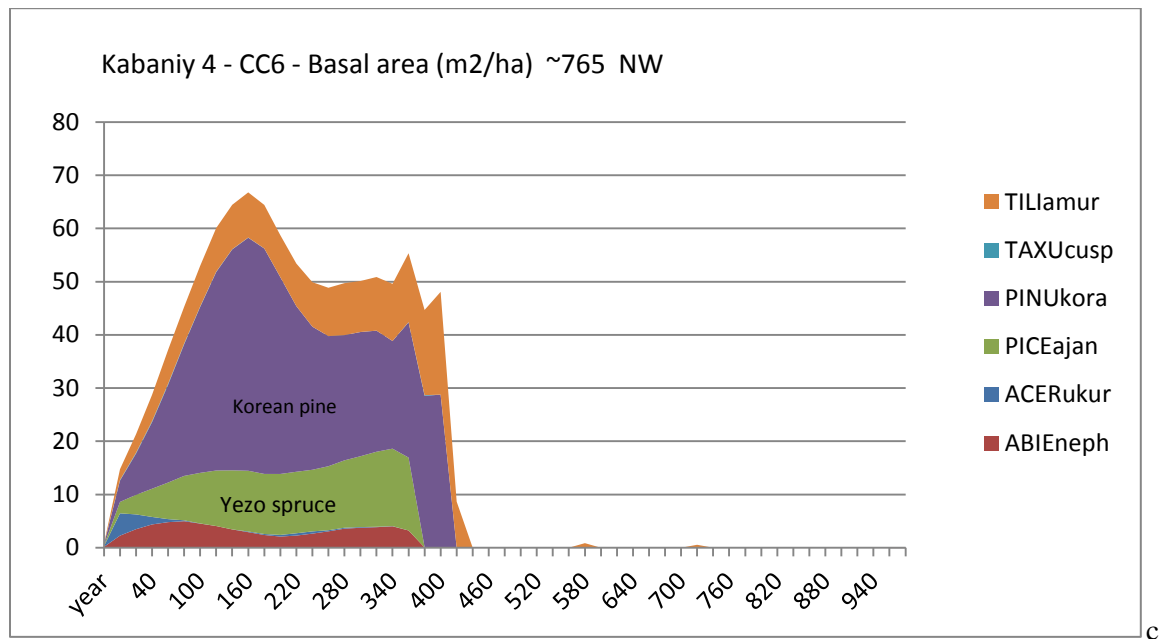
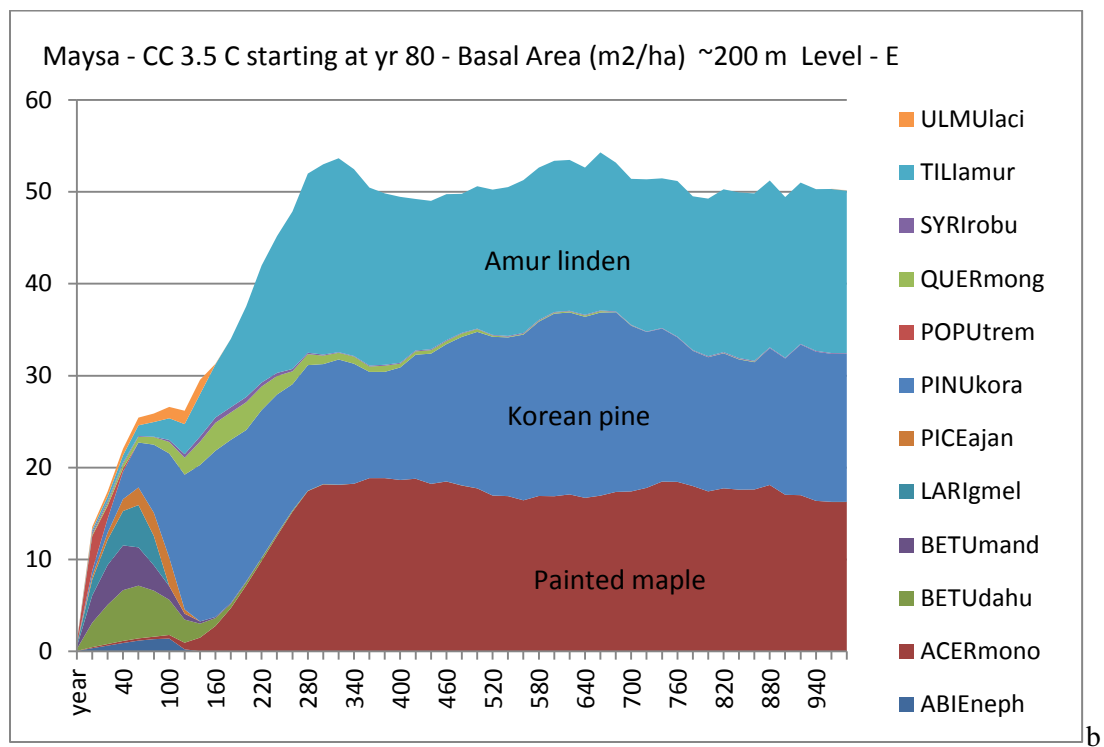
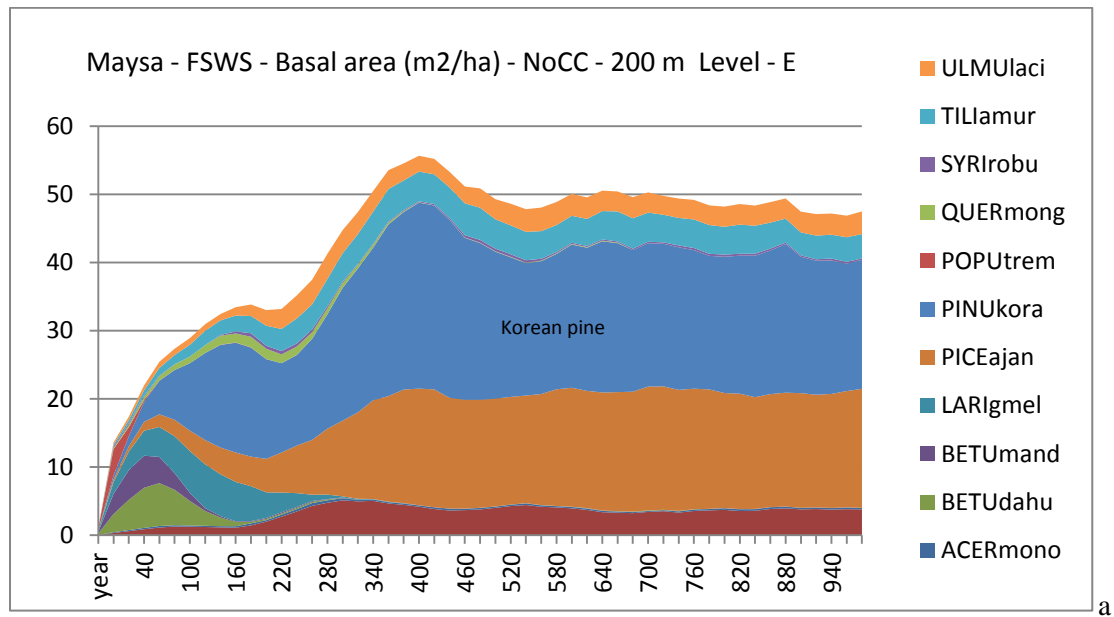


Figure 4.11 (a) & (b) Korean pine and Amur linden survive with 3.5 °C climate change. (c) With warming of 6.0 °C at the high elevation Central Sikhote-Alin sites, all species die out.

4.4.3 Wildfire site in SABZ - Maysa

Maysa is a level and slightly eastward facing site that experienced a severe fire about 80 years before field work was conducted. With current climate conditions, Korean pine and several other species would expand in basal area and continue indefinitely (Figure 4.12a). Mongolian oak would die out after about 400 years. With 3.5 °C of climate warming starting at 80 years to approximate the current age of the forest, the Korean pine, Amur linden, and Painted maple would flourish, while other species would disappear (Figure 4.12b). With climate change of 6 °C beginning at year 80, currently emerging species die out at Maysa except for Painted maple,

which dominates the new forest, along with small amounts of lilac tree (*Syringa robustus*) (Figure 4.12c).



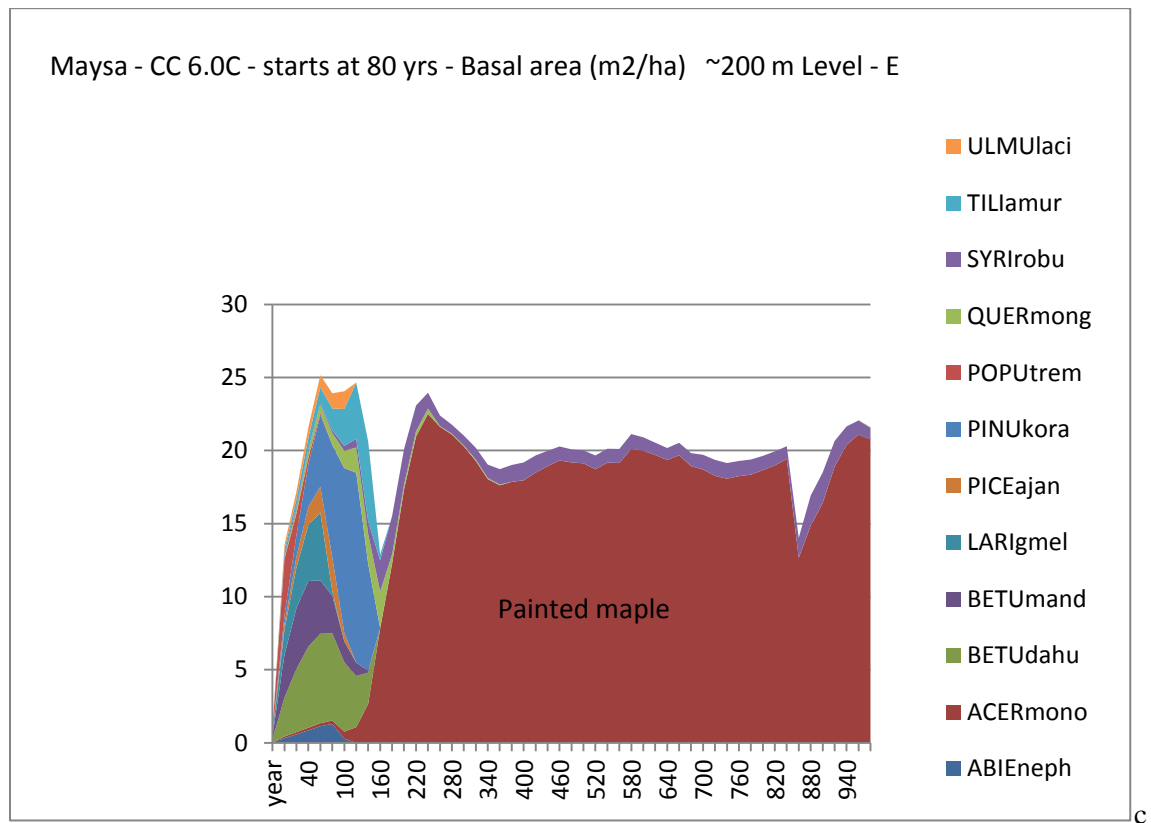
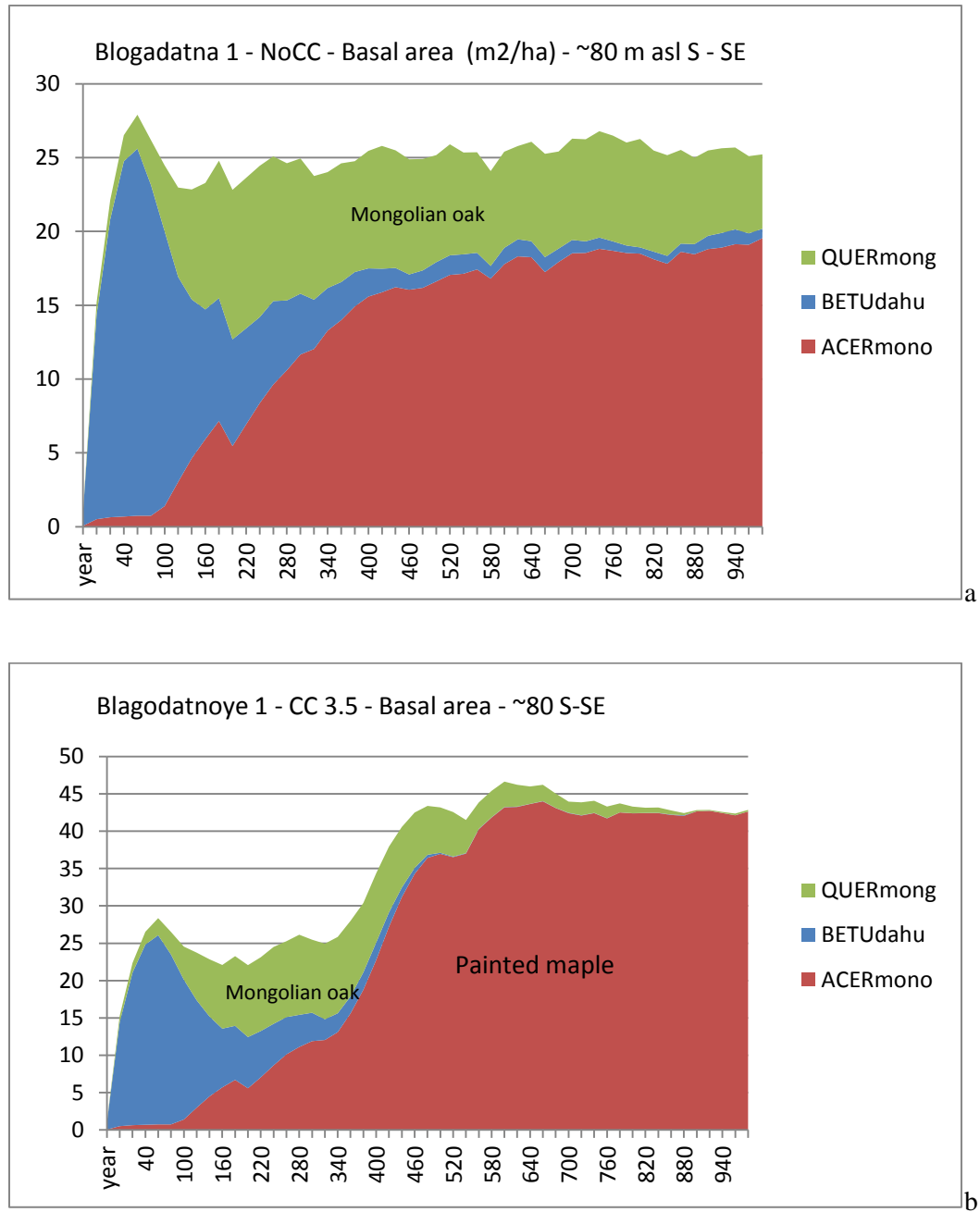


Fig. 4.12 a-c At Maysa in Sikhote-Alin Biosphere Reserve, a regenerating mixed broadleaf/pine/conifer forest converts to a pine/linden/maple forest with 3.5° C of climate warming. Warming of 6.0 °C changes the developing forest to a Painted maple forest with a small amount of lilac tree.

4.4.4 Oak forests in SABZ

FAREAST simulates old growth primary forests and was not able to recreate the secondary oak birch forest in the proportions of basal area that occurred at Blagodatnoye 1. Testing climate change of 3.5 °C on the field site species mix of Mongolian oak, Dahurian birch and Painted maple indicated that maple would gain ground at the expense of the other species, although oak

would continue in smaller quantities for centuries. With 6.0 °C warming, Painted maple takes over as soon as the increased temperature level is reached (Figure 4.13).



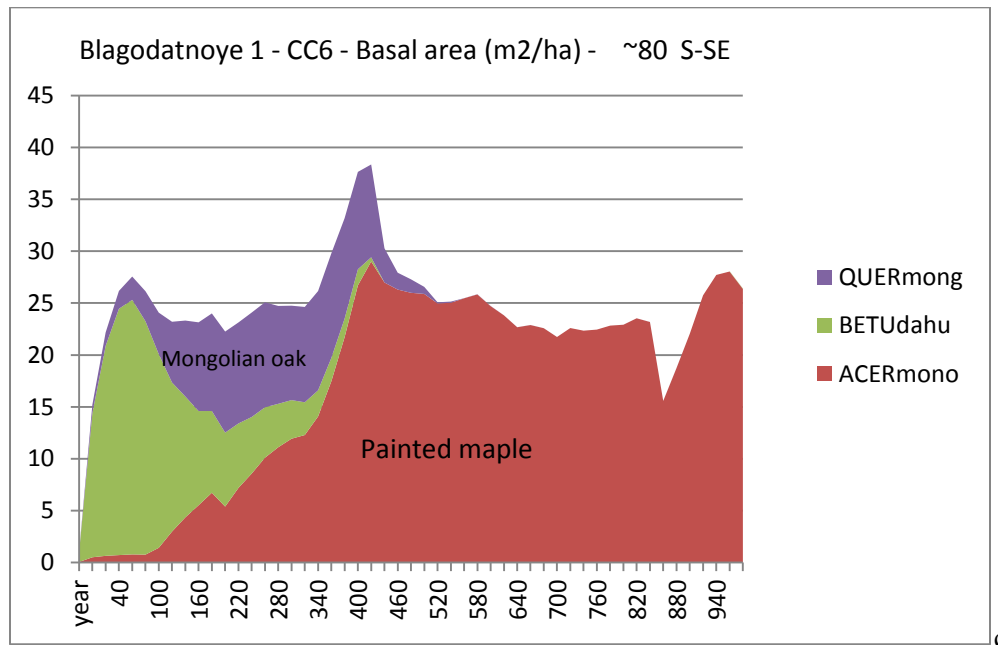
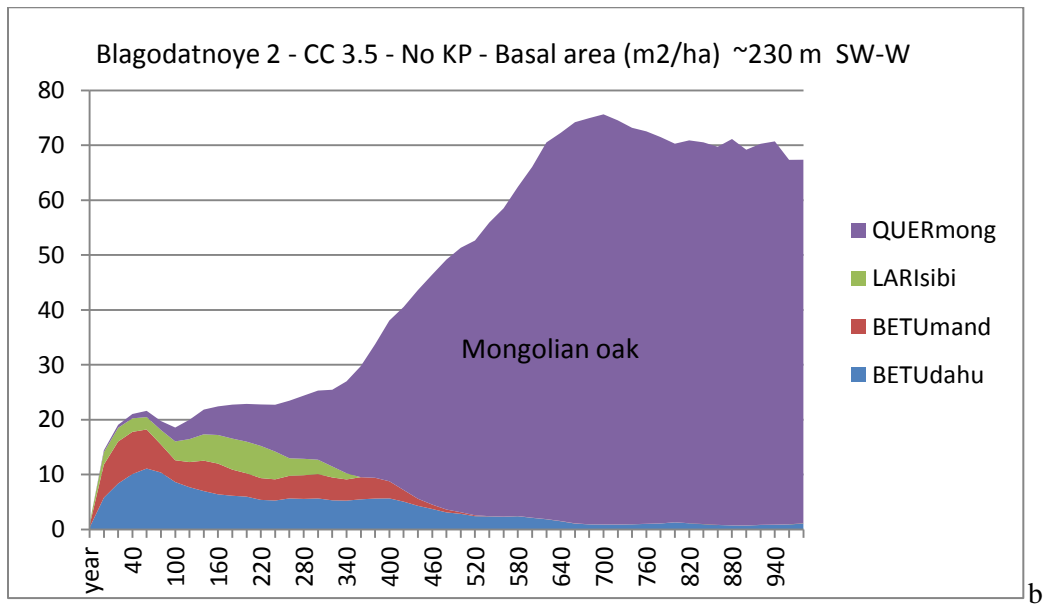
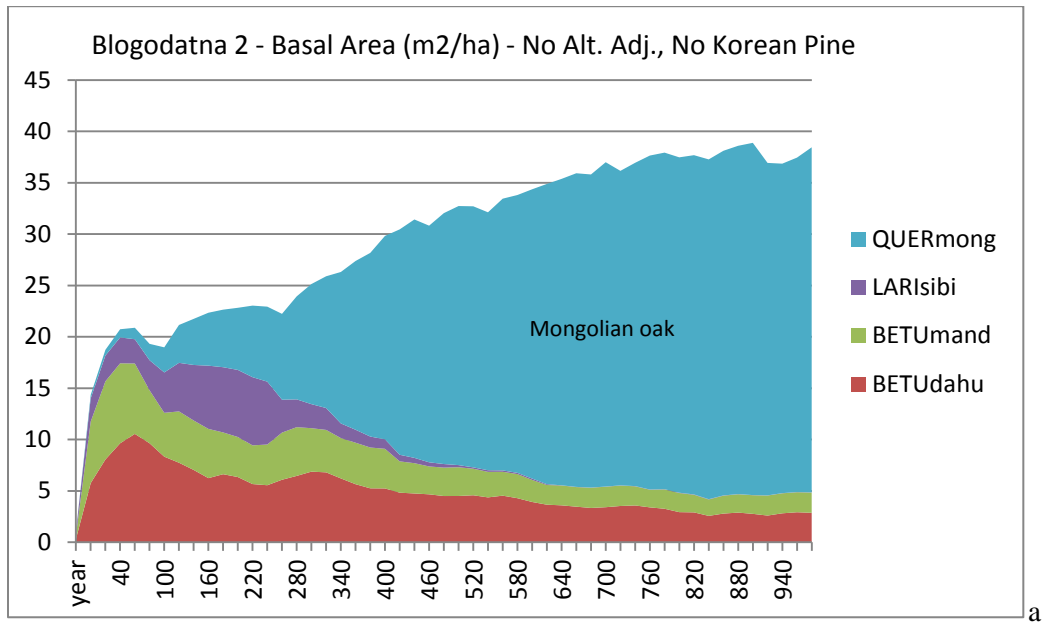


Figure 4.13 a - c In the secondary oak forest of Blagodatnoye 1, with climate change of 3.5 °C and 6.0 °C, Mongolian oak dies out and Painted maple takes over.

At Blagodatnoye 2, removing Korean pine, as occurred through fire or logging during the early years of settlement in the Blagodatnoye area, results in FAREAST output after 460 years of simulation that closely resembles observed forest in terms of basal area by species (23.2 m²/ha simulated vs. 22.65 m²/ha observed) (See Chapter 3). Applying 3.5 °C climate warming to this forest leads to great expansion in oak basal area (Figure 4.14b). With 6 °C climate warming over 100 years, model results suggest that oak will continue to dominate, but will undergo cyclical peaks and valleys as forests mature, die back and regenerate (Figure 4.14c).



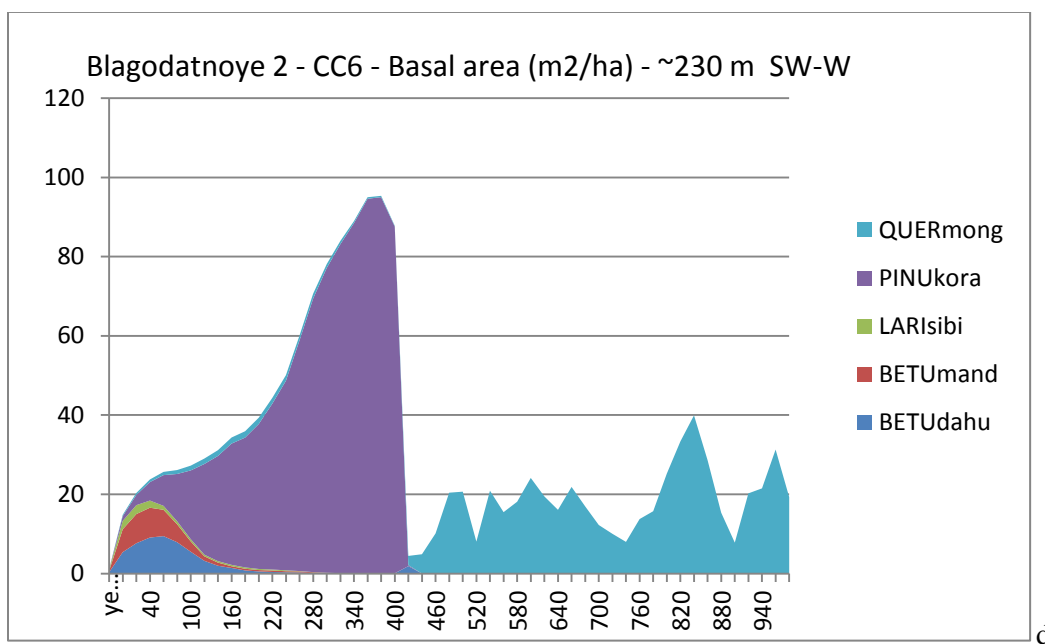
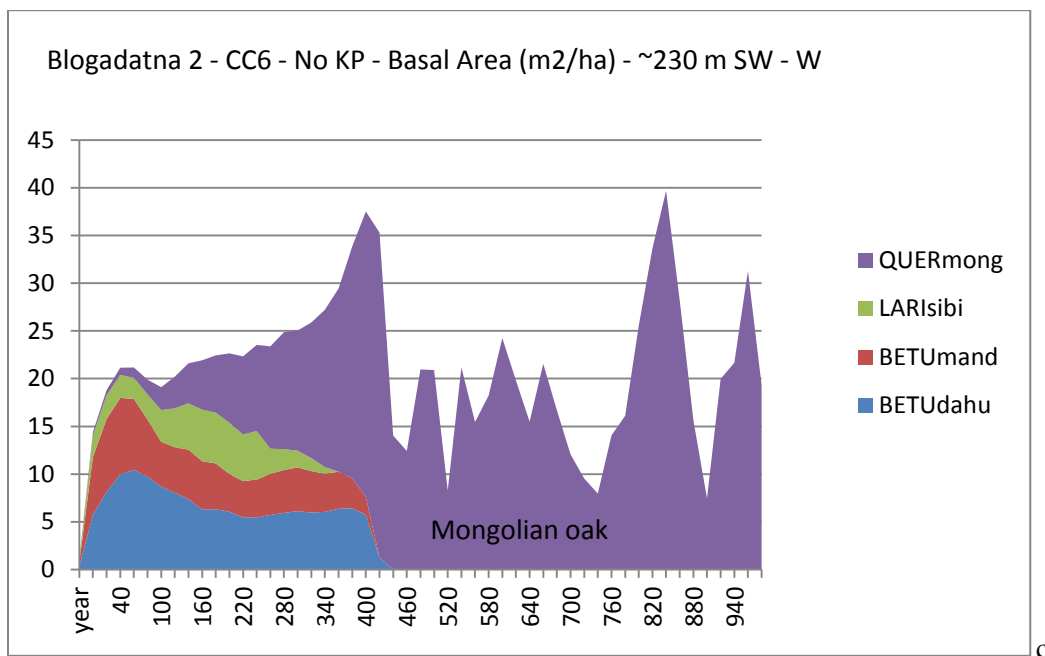
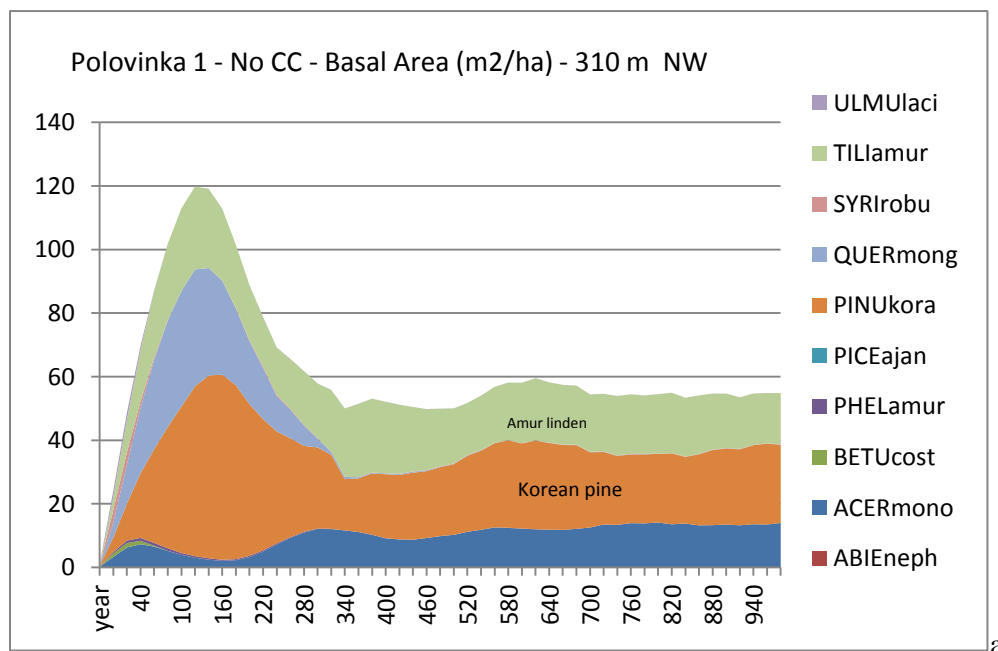


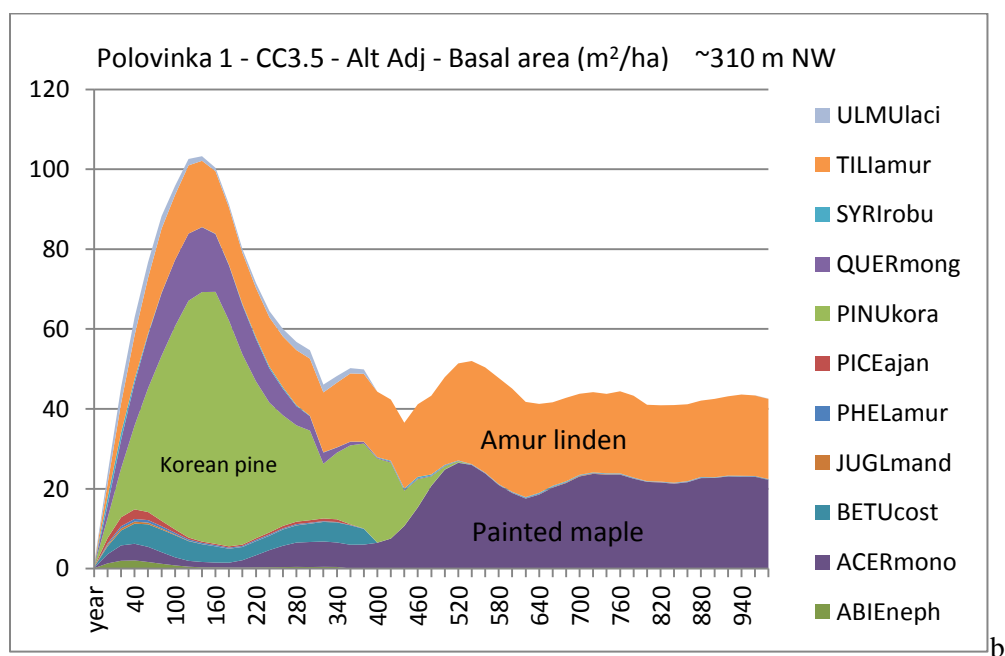
Figure 4.14 a-d With Korean pine removed, FAREAST indicates that Mongolian oak in coastal oak forests at Blagodatnoye 2 will persist. If Korean pine had not been removed (d), 6° climate

warming over 100 years would have caused the species to disappear, leaving only a cyclical regeneration pattern of Mongolian oak.

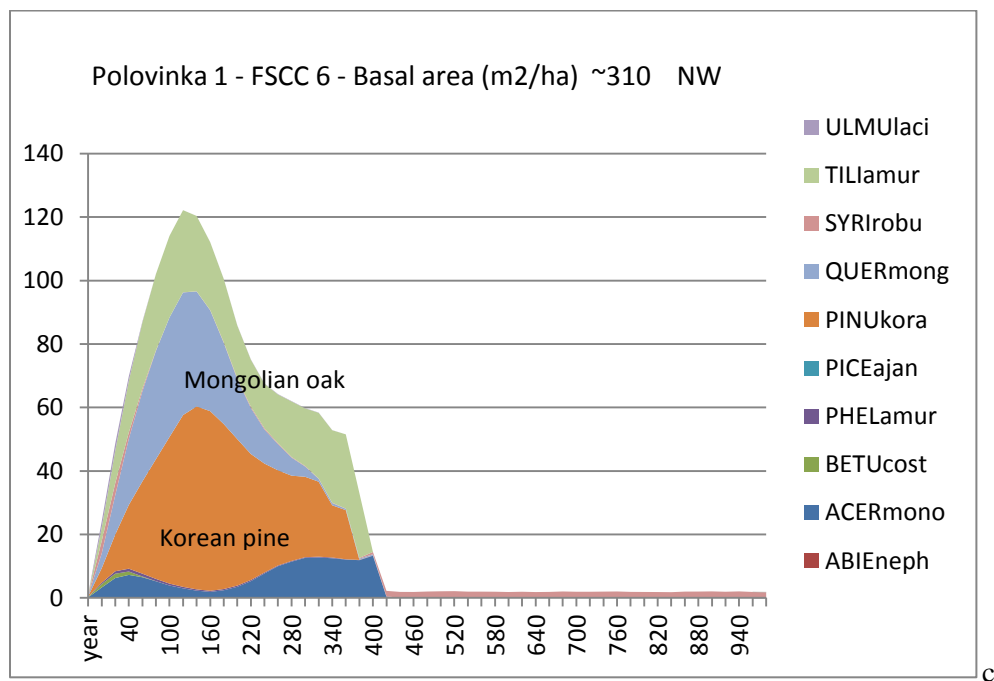
4.4.5 Polovinka sites in Bolshekhkhehtsirskiy Zapovednik (Reserve)

With climate change of 3.5 °C beginning at year 350, Korean pine disappears at both field sites in Bolshekhkhehtsirskiy Reserve near Khabarovsk. At northwest-facing Polovinka 1, Painted maple and Amur linden take over (Figure 4.15b), while at S-SE facing Polovinka 2, Painted maple completely dominates the forest (Figure 4.16b), with few other species, each comprising less than 1 m²/ha. With 6 °C temperature increase, the forest disappears at Polovinka 1 (Figure 4.15c) and, at Polovinka 2, basal area drops precipitously, with only small amounts of Manchurian walnut and Lilac tree remaining (Figure 4.16c).



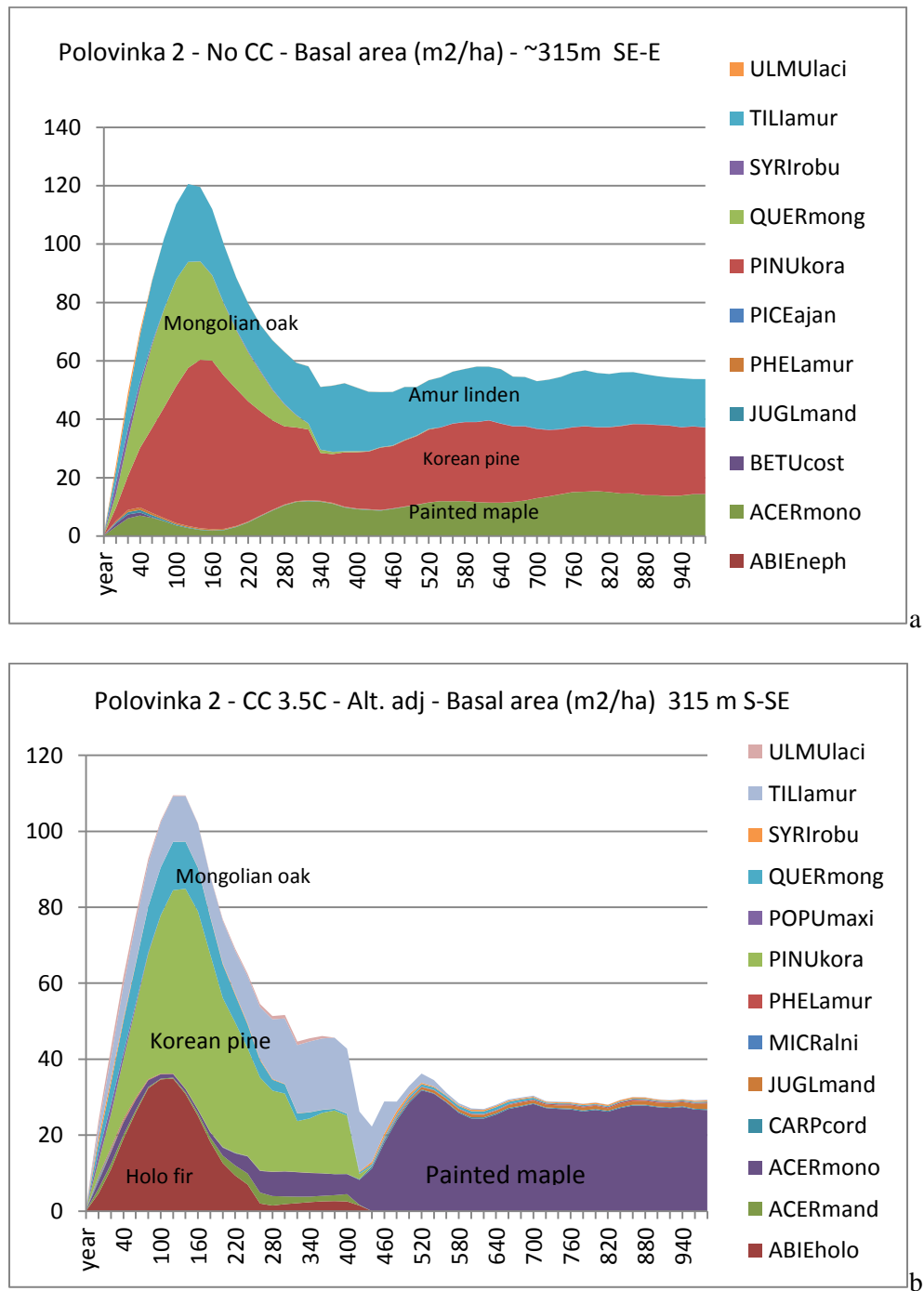


b



c

Figure 4.15 (a) Korean pine would persist under current climate conditions, but would die out with 3.5 °C climate change (b). With 6.0 °C climate change, all tree species die out (c).



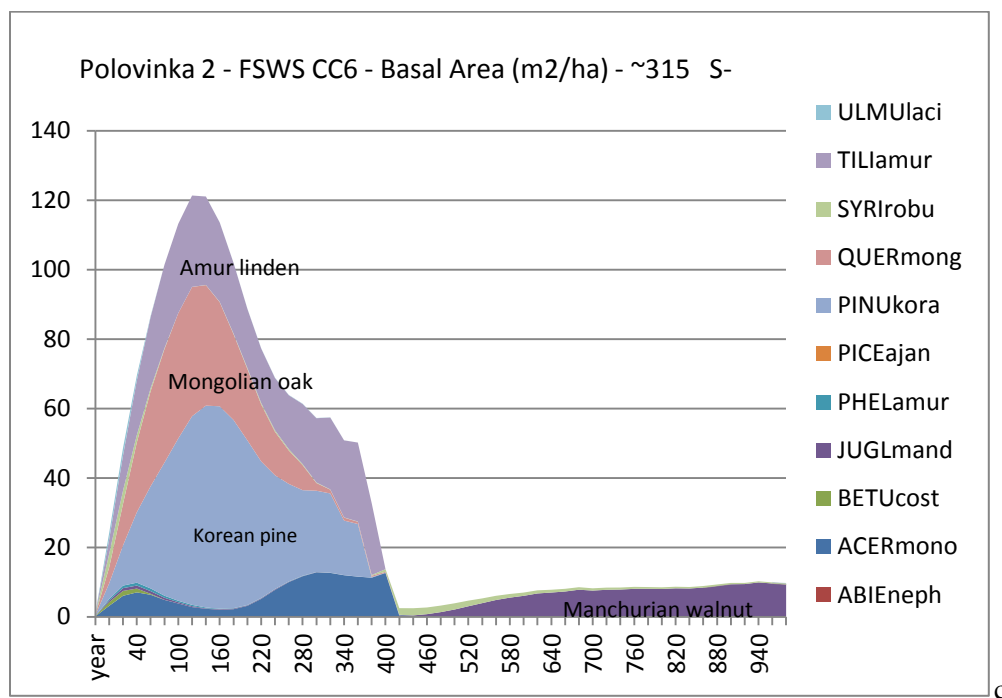


Fig. 4.16 a-c (b) At Polovinka 2, Korean pine dies out with 3.5 °C climate change. (c) With 6 °C warming, basal area drops sharply and only Manchurian walnut remains.

On the following page is a summary of current and projected (150 years from present) forest type and dominant species under current climate conditions and with 3.5 °C and 6.0 °C climate change (Table 4.3).

Table 4.3 Summary of site results

<i>Site and estimated forest age</i>	<i>Current forest type (observed)</i>	<i>Projected dominant spp in 150 years with no climate change</i>	<i>Projected forest in 150 years with +3.5 °C</i>	<i>Projected forest in 150 years with +6.0 °C</i>
Ussurisky 1 – 260 – 280 years	Mixed	Korean pine	Painted maple	Manchurian walnut (sparse)
Ussurisky 2 – 260 – 280 years	Mixed	Korean pine	Amur linden/ Painted maple	Manchurian walnut (sparse)
Kabaniy 1- 300 years	Mixed	Korean pine	Korean pine/ Amur linden/ Painted maple	Painted maple
Kabaniy 2 – 300 years	Mixed	Korean pine	Korean pine/Amur linden	Forest disappears
Kabaniy 3 – 300 years	Dark conifer + Korean pine	Korean pine	Korean pine	Forest disappears
Kabaniy 4 – 300 yrs	Dark conifer + Korean pine	Korean pine	Amur linden/ Painted maple	Forest disappears
Maysa- 80 yrs	Mixed	Korean pine/ Yezo spruce	Korean pine/ Amur linden/ Painted maple	Painted maple
Blagodatnoye 1- 240 years	Mongolian oak/ Dahurian birch/ Painted maple	Painted maple	Painted maple	Painted maple
Blagodatnoye 2 – 160 years	Mongolian oak	Korean pine	Korean pine	Korean pine
Blogadatnoye2 – no K. pine – 460 years	Mongolian oak	M. oak	Mongolian oak	Mongolian oak
Polovinka 1 – 280 years	Mixed	Korean pine/ Amur linden/ Painted maple	Painted maple/ Painted maple	Forest disappears
Polovinka 2 – 280 years	Mixed	Painted maple	Painted maple	Manchurian walnut (very sparse)

4.4.6 Results at 1,000 random points

For the 1,000 random points, with no climate change, 67% (211 of 313 points) of broadleaf deciduous broadleaf forests mature into mixed broadleaf/Korean pine/conifer by year 460 (160 years from present) and beyond (Figure 4.17). Most of this change occurs on the west side of the Sikhote-Alin Mountains. Current dark conifer and mixed forests continue indefinitely.

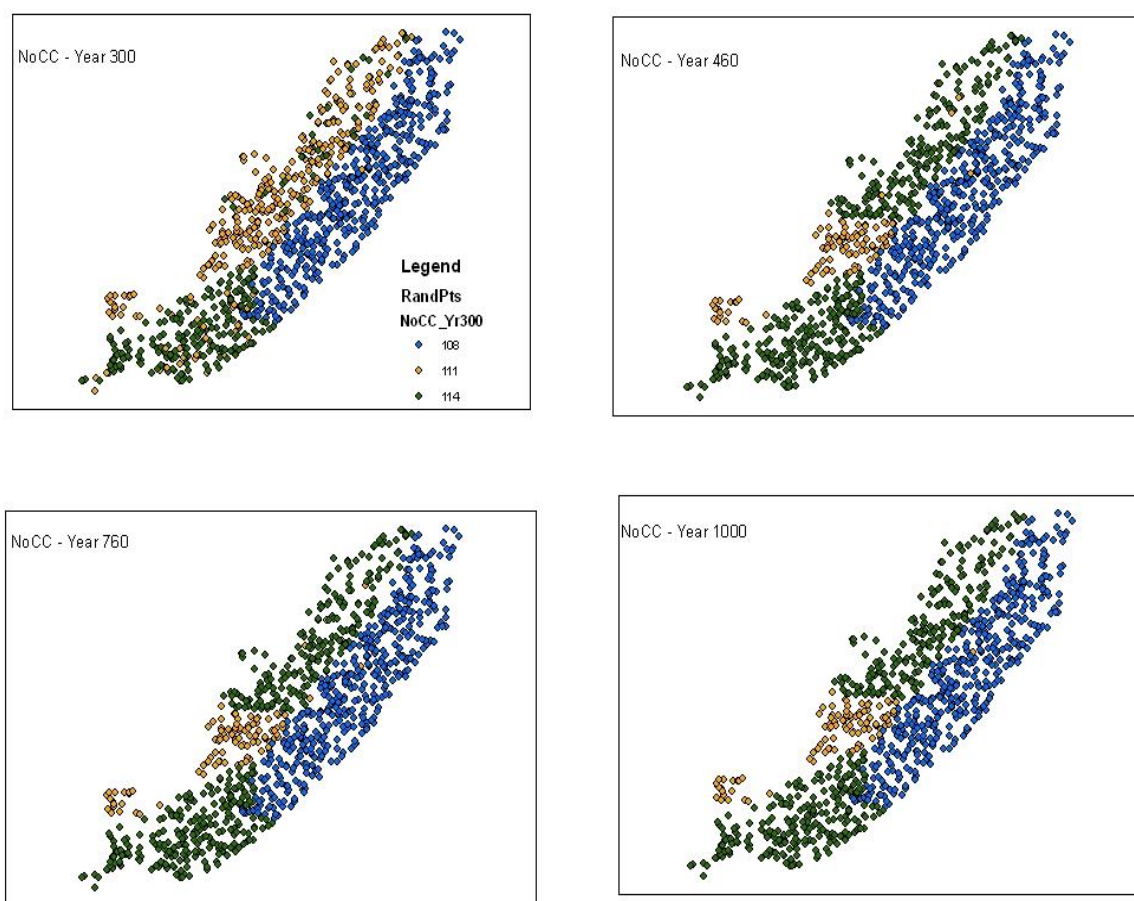


Fig. 4.17 Simulated forest covers based on current climate conditions at 1,000 computer-selected points. Category 108 – Dark conifer (Yezo spruce/Black fir/Korean pine; 114 – Mixed broadleaf deciduous/Korean pine/conifer; 111 – Broadleaf deciduous).

With 3.5 °C increase over 100 years, starting with year 300 to correspond the approximate age of current old growth forest, 95% of sites representing northern dark conifer forests (395 of 415 points) change to mixed forests (Figure 4.18). This is consistent with results at high elevation dark conifer sites Kabaniy 3 and 4.

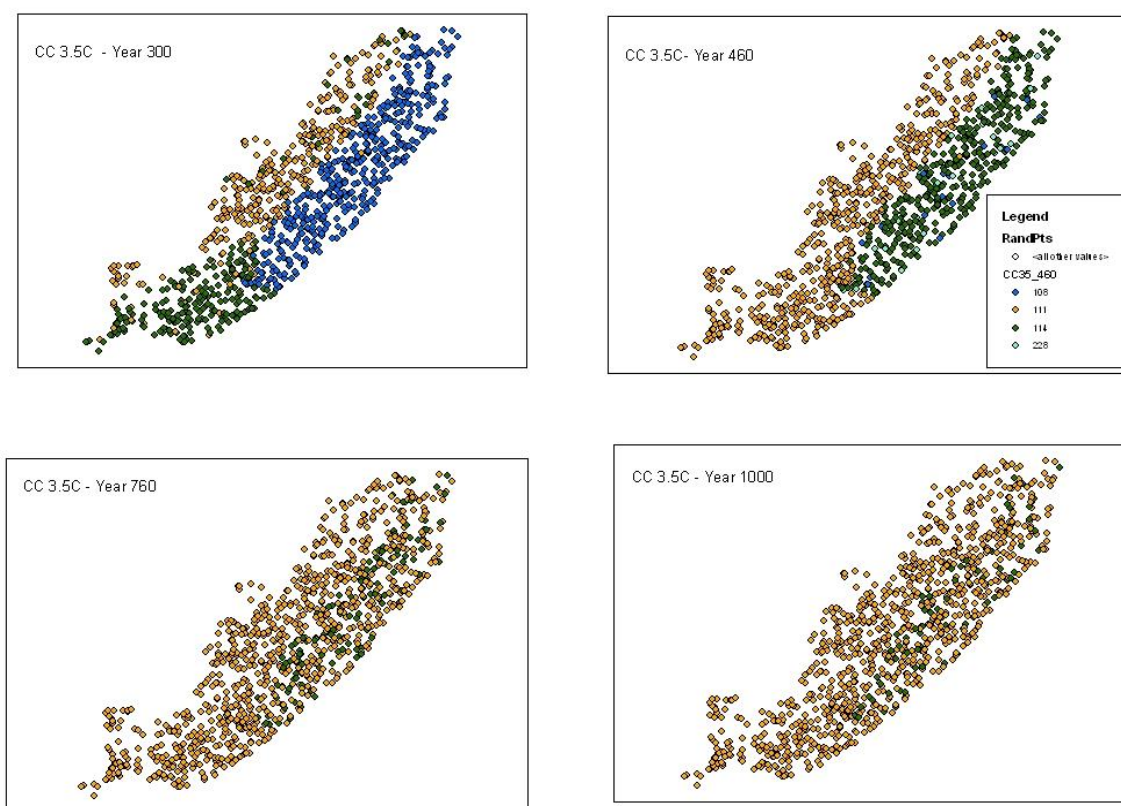


Fig. 4.18 Simulated forest covers based on climate warming of 3.5 °C. Category 108 – Dark conifer (Yezo spruce/Black fir/Korean pine; 114 – Mixed broadleaf deciduous/Korean pine/conifer; 111 – Broadleaf deciduous). Dark conifer and mixed forests gradually convert to mostly deciduous broadleaf forests, with some mixed forests remaining along the eastern slope of the Sikhote-Alin Mountains.

All points with southern mixed forests (244 points) convert to broadleaf within fifty years after reaching the higher temperatures, which is consistent with forest changes associated with 3.5 °C climate warming at the southernmost sites, Ussurisky 1 and 2. After 250 years of the new climate regime, the simulation suggests that most of Primorski Krai would be covered with broadleaf forest, with pockets of mixed forest, especially on the eastern slope of the Sikhote-Alin Mountains (Figure 4.18).

With 6.0 °C, all the forest types changed to broadleaf. Forest disappeared at 22 locations within 60 years of reaching the higher temperature regime (Figure 4.19), and at 99 locations 300 years later and beyond. These results are generally consistent with simulations for the field sites; the field site simulations suggested that forests would disappear in more locations than did the 1000 point simulation.

Because the random points were not adjusted for altitude, forest cover changes at higher elevations may not be as large as model output suggested. Temperatures at lower elevations would be warmer than would be expected at elevations where spruce and fir are found, which might cause these conifer species to die out more quickly.

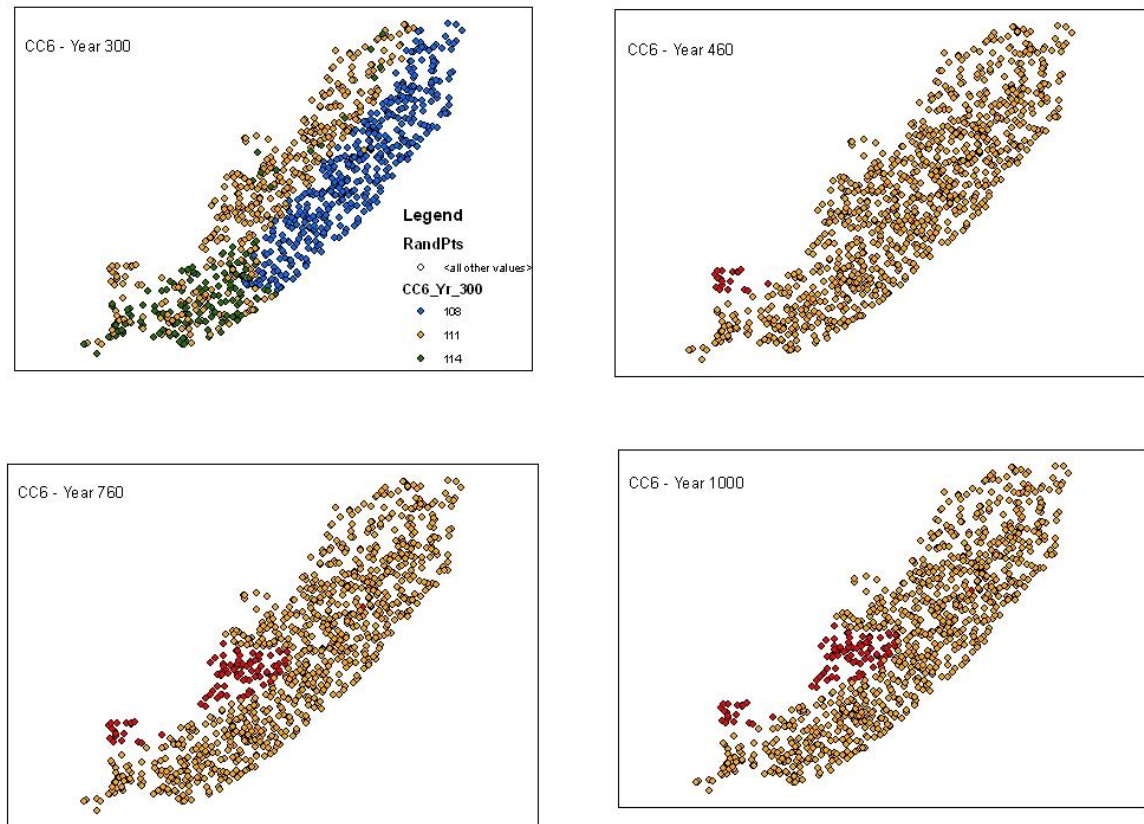


Figure 4.19 Simulated forest covers based on climate warming of 6.0 °C. Category 108 – Dark conifer (Yezo spruce/Black fir/Korean pine; 114 – Mixed broadleaf deciduous/Korean pine/conifer; 111 – Broadleaf deciduous). Red dots indicate no forest (0 basal area). Dark conifer and mixed forests convert to broadleaf deciduous, and forests disappear in some inland areas with continental climates (cold winters, warm summers).

4.5 DISCUSSION

Climate change has the potential to exacerbate habitat loss and reduce already insufficient prey, two of the three greatest threats to the survival of the wild tiger in Asia. The third of the largest threats is illegal hunting, or poaching (Miquelle *et al.*, 2010a). If adequate protection against poaching exists, prey density is the most important determining factor for the presence of tigers (Karanth & Stith, 1999; Karanth *et al.*, 2004; Karanth *et al.*, 2006; Goodrich *et al.*, 2008; Karanth *et al.*, 2010; Miquelle *et al.*, 2010 a&b; Karanth *et al.*, 2011).

Forests provide food, shelter and cover while stalking prey. Resource selection function (RSF) analyses (Carroll and Miquelle, 2006; Mitchell and Hebblewhite, 2012) and other studies (Miquelle *et al.*, 1999b) have shown that the presence of ungulate prey statistically corresponds with forests containing Korean pine and Mongolian oak.

Simulations using the gap model FAREAST suggest that profound changes in forest composition and structure will occur if atmospheric temperature rises to levels predicted in IPCC 2007.

Climate warming may benefit Korean pine up to the point where higher temperatures and drier soil conditions are too extreme for survival or regeneration. Assessing different climate change scenarios using the model helps to pinpoint this critical temperature.

4.5.1 Southernmost sites - Ussurisky Reserve

In the Ussurisky region, many tree species are moderately drought tolerant because they are adapted to a climate with little snow melt, which creates a soil moisture deficit early in the annual growing season (Krestov *et al.*, 2003, Nakamura and Krestov, 2005). FAREAST shows that Korean pine is negatively affected by smaller climate change in this region than at more northern latitudes. At the two southernmost sites, with 3.5 °C warming starting at year 350, Korean pine dies out and gives way to Amur linden and Painted maple at Ussurisky 1 and changes to predominantly Painted maple at Ussurisky 2 (Figures 4.6a and 4.7b). If warming starts from current temperatures, pine would die out by about 2093. With a steeper warming trajectory of 6.0 °C of climate change implemented over 100 years, Korean pine would disappear after less than 40 years, so tree species that support tiger prey populations would be gone by 2053 (Figures 4.6b and 4.7b). Temperature increases are implemented over 100 years, so the rate of increase is sharper in the A1F1 6 °C scenario (0.06 °C/yr) than in the B1 3.5 °C scenario (0.035 °C/yr).

Among the impacts of higher temperatures are drier soils, slower litter decomposition, and potentially fewer soil nutrients (Lauenroth *et al.*, 1993; Nakamura *et al.*, 2009). Korean pine is adaptable to varied conditions and grows equally well on moist and fertile soil on a north-facing 6 – 15° slope as on drier and less fertile south-facing 16 – 25° slopes (Li and Zhu, 1991; Krestov, 2003). This gives them advantages over other species in a warmer and drier climate. The most favorable conditions are on slopes from sea level up to 800 – 900 m in soils that are mesic, well-drained and rich in nutrients (Krestov, 2003).

Modeling suggests that Korean pine persists for different lengths of time at different latitudes under a 3.5 °C climate change scenario. To determine the maximum climate change Korean pine could withstand, I tested different temperature scenarios at each field site. Although all species were used as input in order to incorporate realistic competitive interactions, only results for Korean pine are shown to facilitate comparative analysis.

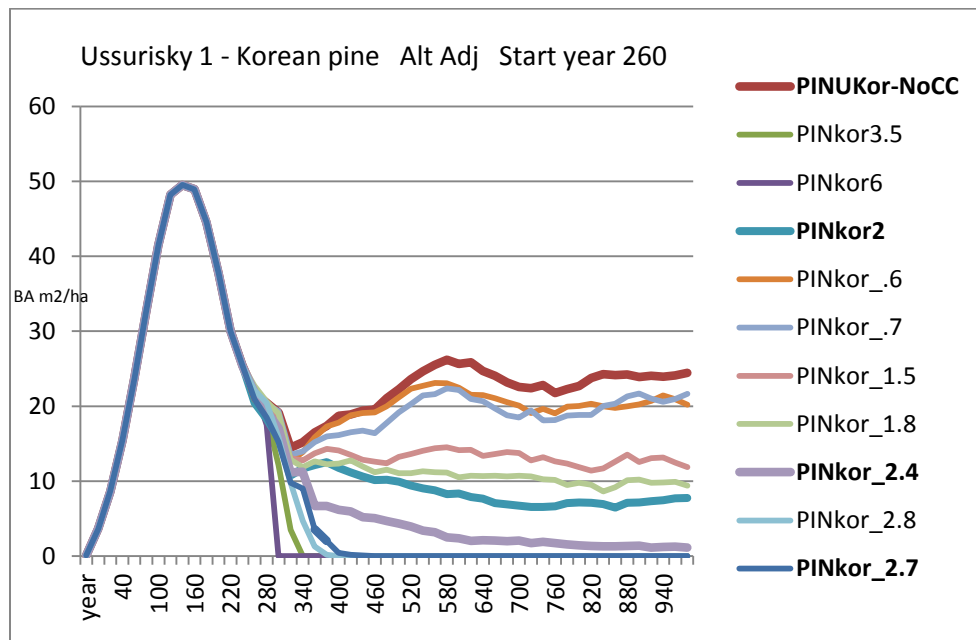


Figure 4.20 Korean pine basal area declines with climate change. With temperature increase of 2.4 °C and greater, Korean pine dies out.

At the first of the two southernmost sites, Ussurisky 1, Korean pine basal area increases indefinitely relative to that of other species under current climate conditions. With climate change of 0.6 and 0.7 °C, Korean pine survives at only slightly less basal area than at current

temperatures (Figure 4.20). With warming of 1.5 °C, Korean pine gradually declines. With climate warming of 2.7 °C or greater, Korean pine disappears quickly.

FAREAST results indicate that a temperature increase of just 2.0 °C at the Ussurisky sites reduces Korean pine dramatically (Figures 4.20 - 4.23). The “Copenhagen Accord,” agreed to by the G8 countries and signed by 167 countries following a 2009 international climate conference in Copenhagen, referenced a limit of 2 °C (about 3.6° F) increase in global temperature above pre-industrial levels as a target that would balance attainability with the need to avoid catastrophic impacts on the Earth’s ecosystems (UNEP, 2012). In the 2010 Cancun Agreements, the 2 °C target was formally recognized, but the United Nations Environment Programme (UNEP) Emissions Gap Report 2012 reports that the gaps between greenhouse gas emissions reductions needed to meet the target and actual worldwide emissions is widening, increasing the likelihood that the target won’t be met (UNEP 2012). Climate in East Asia and at northern latitudes is occurring more rapidly than elsewhere; an average global temperature increase of 2 °C would reflect even warmer temperatures in the study area. Global mean annual temperatures are predicted to increase by about 1.9 °C by the 2090s under the B1 scenario and by about 4.0 °C by the 2090s under the A1F1 scenario (IPCC, 2007a).

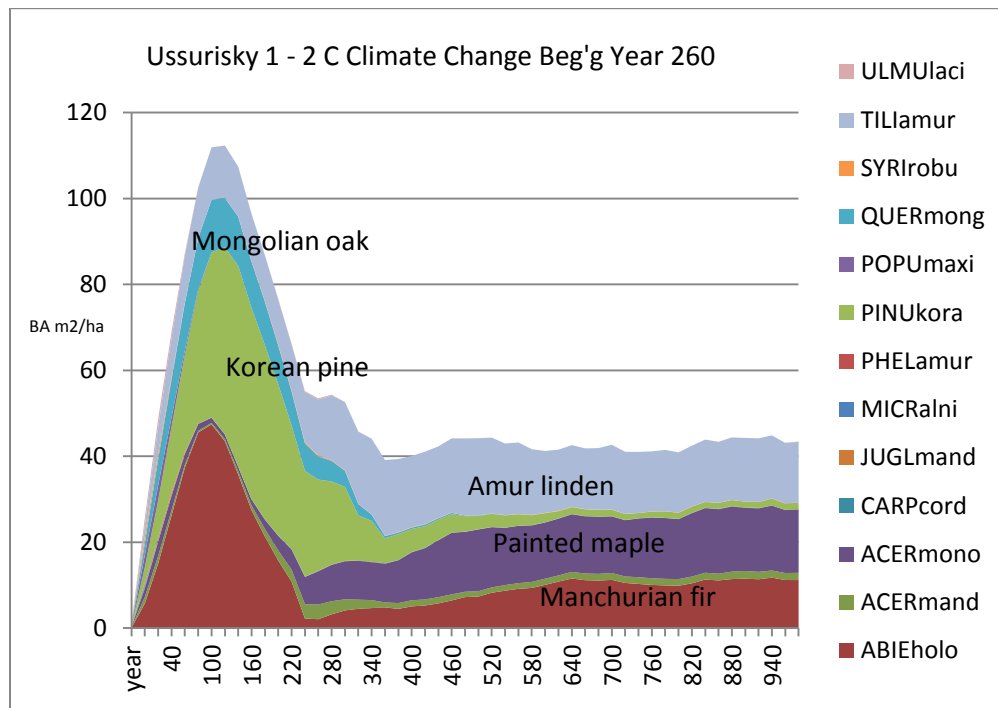


Figure 4.21 Climate change of 2 °C implemented over 100 years beginning at today's estimated age (260 years) would cause a rapid and steep drop in Korean pine basal area.

Results at Ussurisky 2 are the same as at Ussurisky 1, except that Korean pine persists until climate change of 2.8 °C is reached. Ussurisky 2 had a slightly steeper slope (10° vs. 5° at Ussurisky 1), which favors drought-tolerant species like Korean pine, since in the model water runs off steeper slopes faster.

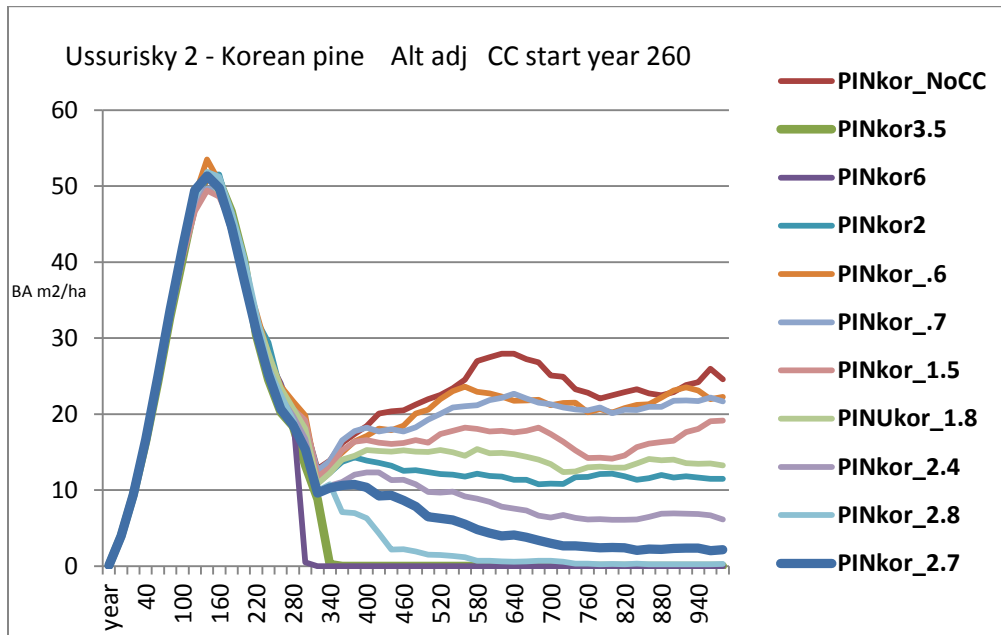


Figure 4.22 At Ussurisky 2, Korean pine persists, but with about half of normal basal area with an increase of 2 °C. With 2.7 °C increase, Korean pine declines permanently.

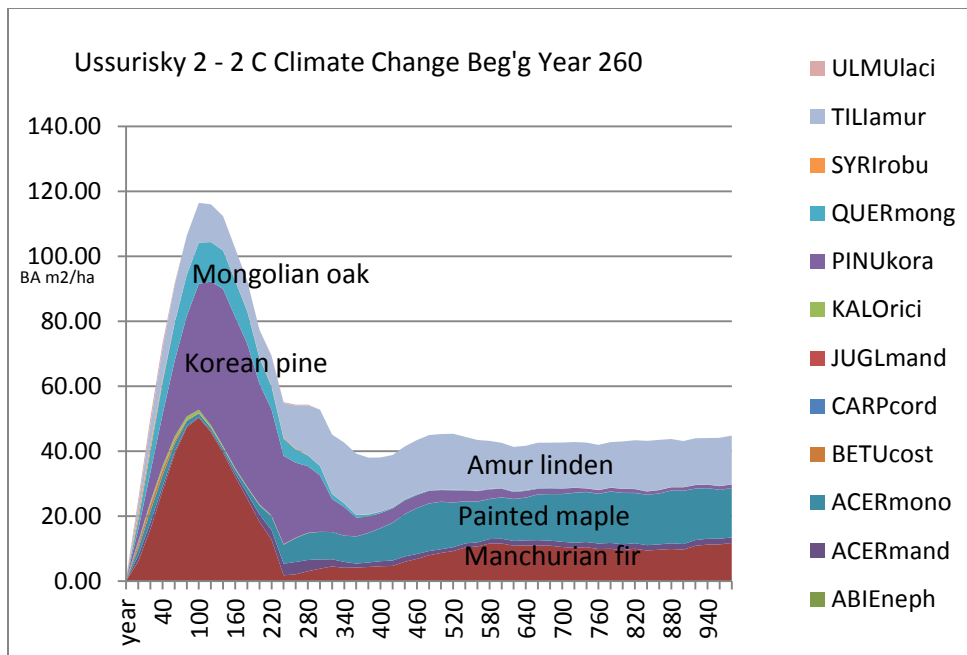


Figure 4.23 With climate change of 2 °C, Korean pine almost disappears at Ussurisky 2, and a broadleaf deciduous forest remains.

4.5.2 Coastal climate - Sikhote-Alin Biosphere Reserve

Further north, forests in the Sikhote-Alin Mountain area have been traced to the Tertiary Period (65 – 1.8 ybp) , when warm temperatures allowed tropical and temperate tree species to flourish (Qian *et al.*, 2003b; Nakamura and Krestov, 2005). During the late Pleistocene (~126,000 ybp - ~11,700 ybp), many tree species were eliminated by extremely cold temperatures in East Asia, followed by a very dry climate (Qian *et al.*, 2003b; Nakamura and Krestov, 2005). Species that required warmer and moister conditions, such as Yezo spruce and Manchurian fir, survived only in Sikhote-Alin, in Changbai in northeastern China, and on Hokkaido in Japan (Grichuk, 1984; Krestov, 2003). On the eastern slope of the Sikhote-Alin Mountains, cold winter temperatures are moderated by the subarctic climate, and spring snowmelt provides essential soil moisture for these species early in the growing season (Krestov *et al.*, 2003; Nakamura and Krestov, 2005).

In Sikhote-Alin Biosphere *Zapovednik* (SABZ) in Central Sikhote-Alin, Mongolian oak and Painted maple occurred on the southern slope of Kabaniy 1, but not the northern slope of Kabaniy 2. At Kabaniy 1, with no climate change, FAREAST indicates that Mongolian oak basal area drops from a peak of 5.64 m²/ha around year 200 to less than 2 m²/ha by year 320, and to less than 1 m²/ha by year 400. This is consistent with field results, where Mongolian oak basal area was only 0.7 m²/ha in the approximately 300 year old forests. Mongolian oak disappeared from Kabaniy 1 forests at about year 450 (~150 years from present) with no climate change (See Chapter 3), with similar trajectories in 3.5 °C and 6.0 °C warming scenarios.

Field data showed that Korean pine basal area was 23.4 m²/ha on a south-facing slope (Kabaniy 1) and 16.7 m²/ha on a northern aspect (Kabaniy 2), illustrating how the species is able to persist in a variety of soil and atmospheric conditions. With 3.5 °C climate change, the mixed deciduous broadleaf/Korean pine/conifer forest at Kabaniy 1 becomes dominated by Korean pine, Painted maple, and Amur linden, whereas only Korean pine and Amur linden dominate on the north-facing Kabaniy 1 slope, where Painted maple wasn't present.

Testing to find the temperature that causes Korean pine to die out at Kabaniy 1 and 2 showed that Korean pine initially benefits with climate warming (Figure 4.24). With 3.5 °C climate change starting at year 350, Korean pine at Kabaniy 1 begins a 400-year decline, and then appears to begin to recover. A sharp decline occurs with 3.8 °C warming and long-term decline occurs with temperature increases greater than 4.1 °C. At Kabaniy 2, with 4.0 °C temperature increase, Korean pine seems to recover at very low levels, but it dies out quickly with a 4.2 °C increase.

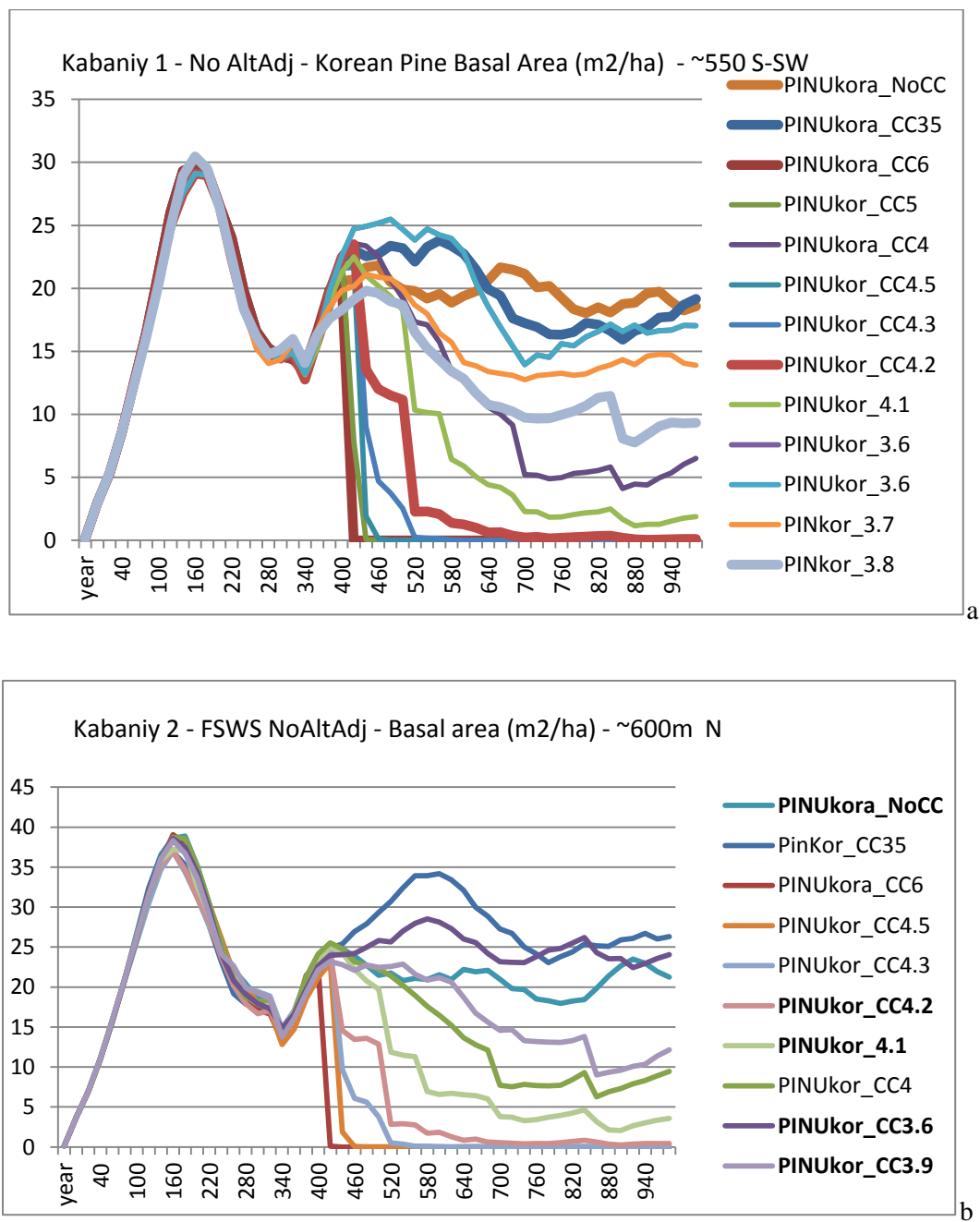


Figure 4.24 a&b. At Kabaniy 1 and 2, Korean pine undergoes a steep decline with warming of 3.9 °C or more.

With 6 °C change, Korean pine dies out shortly after the new temperature regime becomes established. At Kabaniy 1, Painted maple, which can regenerate under the forest canopy in low light conditions (Koike, 1988; Ishikawa *et al.*, 1999), flourishes when competitors disappear due to warmer and drier conditions and is the only species remaining in the 6.0 °C increase scenario (Figure 4.8). On the north-facing site, where there was no maple, all existing tree species died out in the 6.0 °C climate change scenario (Figure 4.9).

Species found at Kabaniy 3 and 4 were typical of high elevation forest vegetation in this area and consisted mostly of Yezo spruce and Black fir (Krestov, 2003; Nakamura and Krestov, 2005). With 3.5°C warming, FAREAST indicated that basal area of Korean pine would increase as spruce and fir, which are sensitive to drought and high temperatures (Manko *et al.*, 1998; Krestov, 2003), disappear (Figures 4.10 and 4.11). Kabaniy 3 was located at about 930 m asl on an S-SW-W slope that extended from a southern to a western aspect. Korean pine was at a slightly higher elevation than expected, based on scientific literature, because Korean pine typically is found in pure or mixed broadleaf/pine/conifer forests at altitudes up to 800-900 m in the central Sikhote-Alin area (Krestov, 2003; Nakamura and Krestov, 2005). The presence of Amur linden at Kabaniy 4 may help to prevent the cyclical peaks and troughs in Korean pine basal area that the model suggests would occur at Kabaniy 3 (Figure 4.25) by allowing Korean pine to mature continuously under the mixed species canopy rather than following the 200-year generational pattern associated with Korean pine (Liu and Zhu, 1991; Ishikawa *et al.*, 1999; Qian *et al.*, 2003a).

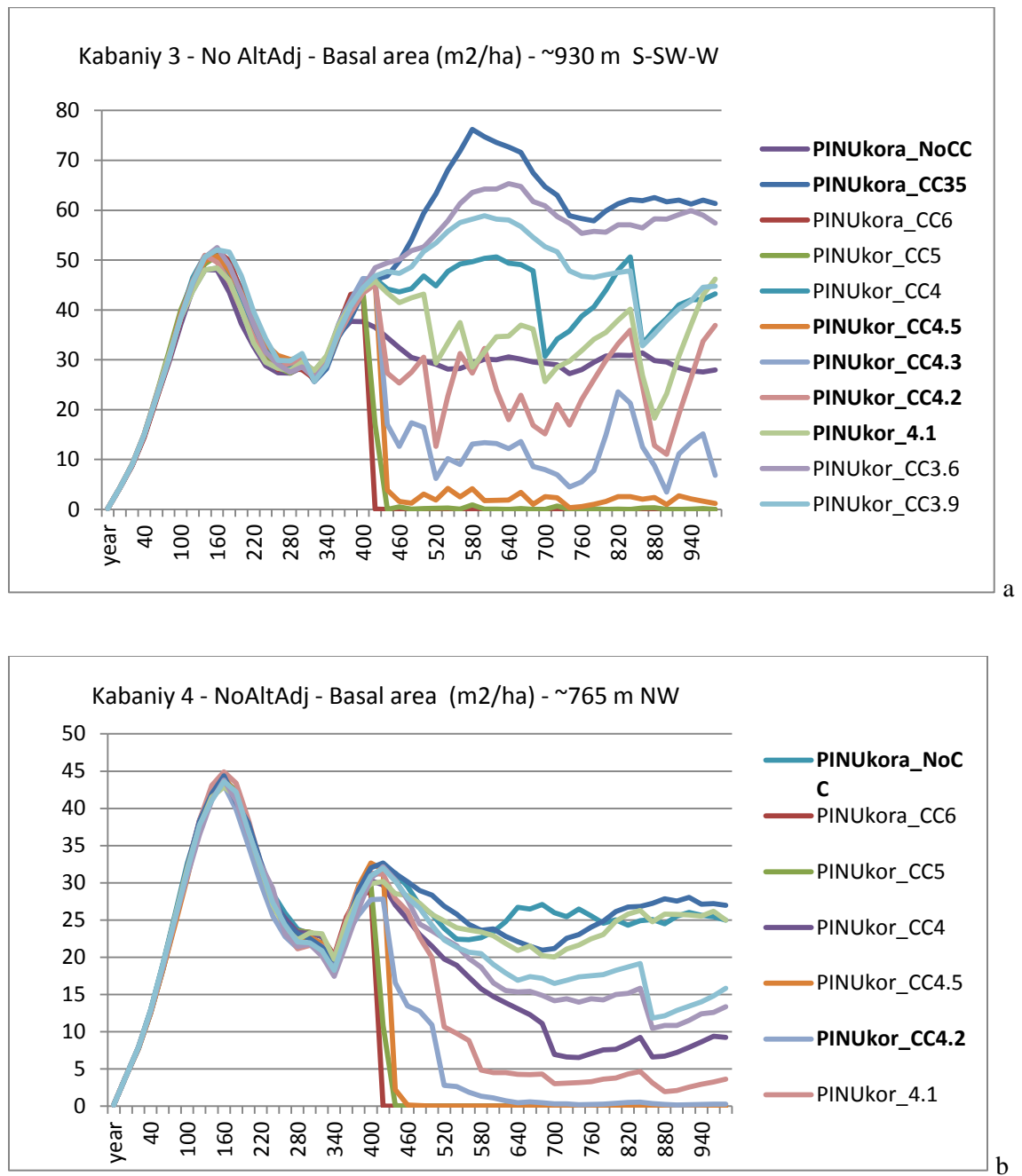


Figure 4.25 a&b At Kabaniy 4, Korean pine basal area drops steeply with 4.2 °C climate change, compared with 4.3 °C for Kabaniy 3.

With 6 °C climate change, the forest disappears at both sites. Since the model was not adjusted for elevation at the Sikhote-Alin sites, species changes in the two climate scenarios might occur more slowly in reality because temperatures are likely to be higher at lower elevations than would actually occur at the sites.

Korean pine is a canopy species that can grow up to 35 – 40 m tall, 120 cm diameter, and 500 years maximum age (Ishikawa *et al.*, 1999; Nakamura and Krestov, 2005; Yan & Shugart 2005; Zyryanova *et al.*, 2005). It is like a Role 2 species, since it can regenerate under the canopy and is long-lived, but also resembles a Role 1 species, which needs gaps to grow and creates gaps when it dies, but has a relatively short life span (Shugart, 1984; Shugart, 1998; Ishikawa *et al.*, 1999; Nakamura and Krestov, 2005). Studies in a plantation setting have shown that Korean pine has evolved to have a strategy that facilitates the growth of large, canopy dominating trees. As a generation of trees grows, the tallest individual emerges and the rate of increase in biomass of other seedlings and saplings declines. The dominant tree has greater access to sunlight, soil moisture and soil nutrients (Ishikawa *et al.*, 1999) than other individuals. Saplings typically grow in clusters of 18 m² and 144 m² and are suppressed as they grow under the forest canopy and later as part of a subordinate canopy layer. The suppressed generation remains stunted until a canopy gap opens, allowing sunlight to stimulate growth. A small scale disturbance such as gap creation from large tree mortality and wind or snow damage allows Korean pine to mature (Ishikawa *et al.*, 1999). Regeneration occurs in clusters every 35-40 years, and maturity occurs at around 120 years (Nakamura and Krestov 2005). Mature Korean pine generations typically are separated by 200 years or more (Li and Zhu, 1991).

The ability of Korean pine to grow in gaps and areas of disturbance and their adaptability to a wide range of conditions suggests that the species would move higher up the slope as disturbance, such as diebacks, snow, wind or fire, creates opportunities for regeneration. Waves of dieback of spruce-fir forests have occurred since 1972 in Central Sikhote-Alin and further south (Krestov, 2003). Although a definitive cause of the dieback has not been identified, Krestov (2003) hypothesizes that drought during the growing season may be an important factor, as drought can lead to water stress, an overabundance of soil minerals and susceptibility to fungus and insects (Manko *et al.*, 1998). Black fir between 100 and 160 years old experienced the highest mortality rate, and patches of dead canopy trees have merged and expanded over time. Like Yezo spruce, Black fir is sensitive to drought (Yan and Shugart, 2005) and it is also sensitive to hot temperatures (Nakamura and Krestov, 2005), which might be factors. Black fir as well as Yezo spruce were able to re-generate following the diebacks, but, since the time between precipitation events is predicted to increase with climate change (IPCC, 2007), additional dieback of spruce-fir forests might be anticipated, creating an opportunity for Korean pine range to expand its upper elevational boundary.

This is consistent with the findings of Wang *et al.* (2013), who modeled Korean pine radial growth – climate relationships based on tree ring width chronologies at three mountain elevations at Changbai Mountain, northeastern China, and found that Korean pine radial growth diminished in warmer and drier climate conditions at the lowest elevation (740 m asl), lower elevations, but increased at higher elevations (940 m asl and 1258 m asl). Because of the more southerly latitude, Korean pine occurs at higher elevations at Changbai Mountain than in Primorski Krai, where the species rarely occurs above 900 m (Krestov, 2003; Nakamura and Krestov, 2005).

Mongolian oak forests at Blagodatnoye 1 and 2 sites are typical of secondary ecosystems that grow on disturbed sites that previously supported Korean pine and mixed conifer/pine/broadleaf forests (Cushman and Wallin, 2000; Krestov *et al.*, 2006). These forests are dominated by oak trees that reach a maximum of 25 m in height and 80 cm diameter (Zyryanova *et al.*, 2005) and flourish in the humid, ocean monsoonal climate near the Sea of Japan. Summer precipitation is higher than winter precipitation and, because of winter snowfall, springtime soil moisture deficits typical of more southern locations rarely occur (Krestov *et al.*, 2006).

At Blagodatnoye 1, FAREAST suggests that Painted maple gradually will take over from Black birch (*Betula dahurica*) and Mongolian oak after climate change of 3.5 °C and almost immediately with 6.0 °C change (Figure 4.13). Controlled fire might help oak persist as maple starts to expand.

In the coastal oak forest of Blagodatnoye 2, pine was either logged or burned by early settlers. Because the pine canopy was gone, oak could flourish (Miquelle *et al.*, 2010b; Kobayashi *et al.*, 2007; Nakamura and Krestov, 2005; Vrishch, 2002; Cushman & Wallin, 2000). If Korean pine is removed from the FAREAST input species in the simulation, the mature forest after 460 years closely resembles field observations (Figure 4.14a). When climate change of 3.5 °C is applied to this forest, Mongolian oak basal area expands continuously to more than 30 m²/ha, compared with an average of 22.65 m²/ha presently at the field site, suggesting that moderately warmer temperatures would provide more food for ungulates (Figure 4.14b). With 6.0 °C increase, Mongolian oak prevails, but undergoes cycles of sharp peaks and deep troughs (Figure 4.14c).

4.5.3 *Northernmost sites - Bolshekhkhtsirskiy Reserve*

At the northernmost sites, Polovinka 1 and 2, in Bolshekhkhtsirskiy Reserve in southern Khabarovsk Krai, a continental climate prevails, with colder winters and warmer summers than at southerly sub-maritime locations. FAREAST suggests that more Korean pine should exist than observed in these forests, given the climate and soil conditions. Logging in the past for commercially valuable species may have reduced Korean pine as well as Amur linden (See Chapter 3).

With climate change of 3.5 °C, Korean pine disappears at both sites. At northwest-facing Polovinka 1, Painted maple and Amur linden take over, while at S-SE facing Polovinka 2, Painted maple completely dominates the forest (Figures 4.15 and 4.16).

The temperature at which Korean pine would permanently decline after an initial increase in basal area is 2.1 °C for Polovinka 1 and Polovinka 2 (Figure 4.26 a&b)

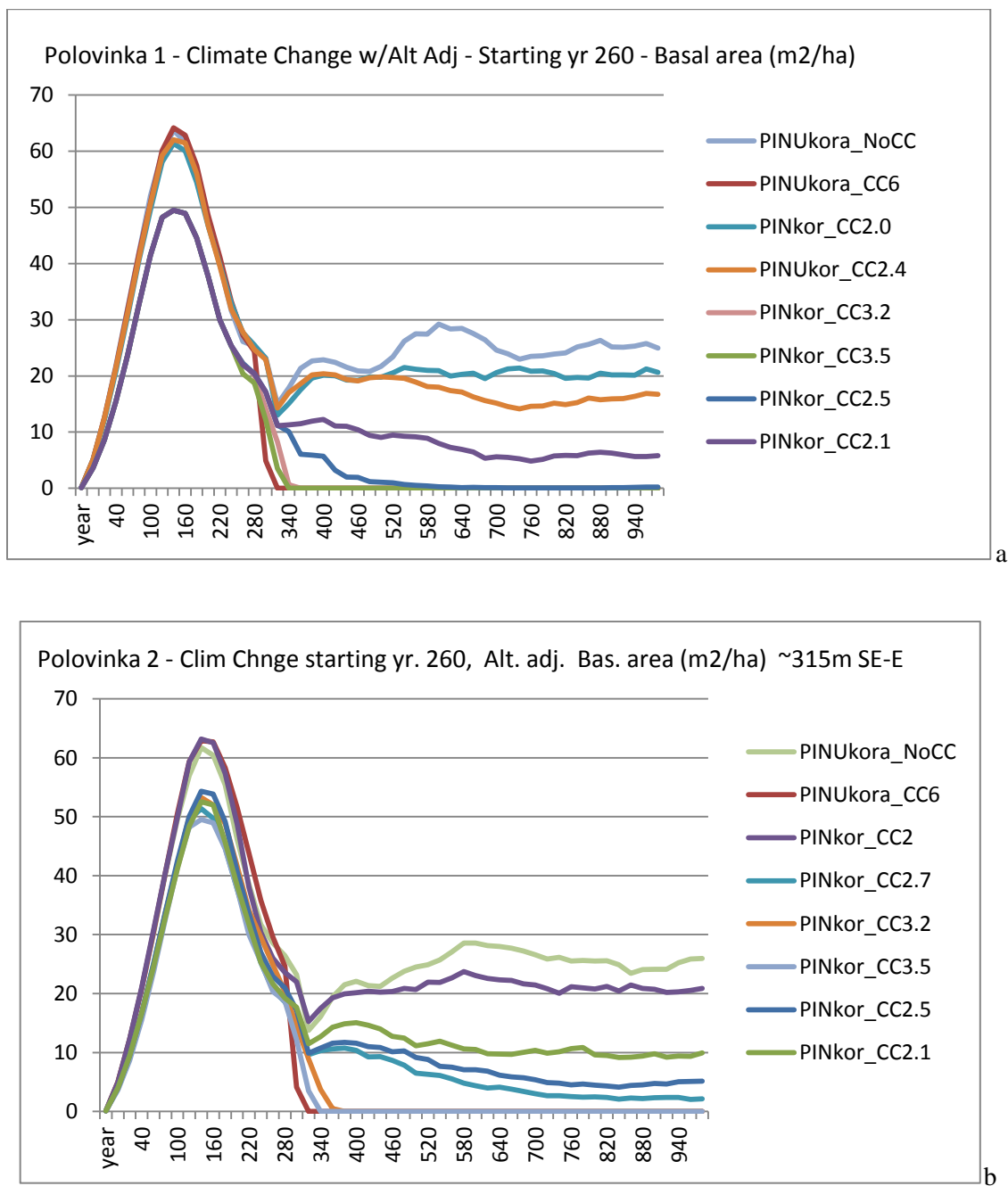


Figure 4.26 FAREAST indicates that Korean pine basal area would decline permanently with climate warming of 2.1 °C at Polovinka 1&2.

With 3.2 °C temperature increase, the forest disappears at Polovinka 1 and, at Polovinka 2, and basal area drops precipitously, with only small amounts of Manchurian walnut and Lilac tree remaining (Figure 4.15 and 4.16).

4.5.4 *Mongolian oak*

While it might be expected that oak would thrive in a warmer and drier climate, FAREAST results suggest that, with or without climate change, Mongolian oak reaches a peak and begins to decline after 120 - 140 years at the Ussurisky and Polovinka sites. Mongolian oak peaks around year 200 at the Kabaniy 1 site in Sikhote-Alin, then declines, and expands continuously in the coastal Sikhote-Alin sites of Blagodatnoye, where oak competes only with Dahurian birch and Painted maple. The most likely reason for Mongolian oak's decline is that a continuous canopy would prevent the sunlight needed for oak regeneration from reaching the forest floor. Oak needs sunlight to regenerate and is unlikely to re-grow under an established canopy unless disturbance occurs.

Oak declines as Painted maple takes over with 3.5 °C warming at Ussurisky 1, Blagodatnoye 1, and Polovinka 1 and 2, and with 6 °C warming at Kabaniy 1, Maysa, and Blagodatnoye 1.

Painted maple has a high rate of photosynthesis even in low light, which allows it to reproduce continuously, even under a canopy (Koike, 1988; Ishikawa *et al.*, 1999). However, maple is more sensitive to fire than oak (Botkin, 1982), which may prevent it from taking over at drier southern locations where fire occurs more frequently. Managed wildfires would allow sunlight to penetrate

the canopy, which might provide opportunities for Mongolian oak to prevail, where a seed source exists.

If Korean pine is removed in the simulation at Blagodatnoye 2, oak basal area in the mature forest (460 years) resembles current observed level. This is the only site where oak persists long-term, with or without climate warming.

4.5.5 Analysis at 1,000 random points

At 1,000 randomly selected points, simulated land cover changes associated with climate change suggest that dark conifer forests would convert to mixed forests with 3.5 °C climate change throughout most of southeastern RFE (Figure 4.18), and mixed forests would change to broadleaf deciduous forests. Dark conifer and mixed forests would persist along the eastern slope of the Sikhote-Alin Mountains, where precipitation is greater and summers are cooler than in more inland locations. With a sharper climate change gradient of 6.0 °C over 100 years, dark conifer and mixed forests convert to deciduous broadleaf forests across the study area (Figure 4.19) or disappear.

These findings were consistent with projected forest trajectories at a more detailed scale, based on modeled results for species and conditions at the eleven field sites, except that basal area dropped more precipitously at the field sites with 6.0 °C warming. Since FAREAST results represent an

old growth forest, these results might be most pertinent for undisturbed or protected areas, or any location where mature conifer and mixed forests occur.

4.5.6 *Impact of forest vegetation changes on tiger prey*

“Where there is nut pine, there is wild boar; where there is wild boar, tiger will also be found”
(Baikov, 1925 in Heptner and Sludskii, 1992).

The decline of Korean pine at Ussurisky sites with as little as 2.0 °C warming (Figures 4.21 – 4.23) and its rapid disappearance with a temperature increase of 2.4 °C or more would reduce food supplies for deer and wild boars. With Mongolian oak basal area having peaked and not projected to increase with or without climate change (Figures 4.5 - 4.7), the presence of Korean pine is especially important.

Overall basal area increases and Korean pine persists in the mixed forest at south-facing Kabaniy 1 with 3.5°C climate change. Above this temperature level, Korean pine begins to decline and a sharp drop-off occurs with climate change of 3.8 °C and more. At the high elevation sites, Kabaniy 3 and 4, if the upper altitudinal boundary of Korean pine moves higher as the species grows in newly-formed gaps, RSF and track survey results suggest that ungulates and tigers would move higher in this mountainous Central Sikhote-Alin area as well. Amur tigers currently are not found in high elevations or on steep slopes, and avoid dark conifer forests (Miquelle *et al.*, 1999b; Miquelle *et al.*, 2010a), so expansion of Korean pine at slightly higher elevations might also increase the range of tiger prey and tigers.

Ungulates, especially deer, are found in greater numbers in coastal oak forests than in inland oak-birch forests, which contain a greater diversity of tree species (Stephens *et al.*, 2006). In addition to the availability of nutritious oak mast, temperatures in coastal areas are more moderate than further inland and snowfall is less frequent and deep. Seaweed and algae also provide salt and other minerals (Heptner *et al.*, 1992)

In coastal oak forests such as Blagodatnoye, the number of red deer is declining and the sika deer population is increasing (Stephans *et al.*, 2006; Miquelle *et al.*, 2010b). Sika deer historically have occurred in warmer climates and their range is limited by deep snow, but they are moving north, possibly a sign of climate change (Stephens *et al.*, 2006; Miquelle *et al.*, 2010b). Ungulate studies in 1980 found no Sika deer in the oak-birch zone of SABZ but their number has increased rapidly (Stephens *et al.*, 2006). Herds of sika deer tend to stay in one place and deplete vegetation and damage soils (Heptner *et al.*, 1992). The trend of competitive exclusion in which sika deer populations are expanding as red deer decline is disadvantageous for tigers because sika deer are very small and do not represent optimal prey, since they do not provide as much nutrition for the energy expended for capture as do red deer and wild pig. Continued displacement of red deer would be a negative trend for tigers.

Model results indicate that the forest at Blagodatnoye 1 would no longer provide adequate nutrition and energy for tigers with climate change of 3.5 °C because Painted maple will expand at the expense of Mongolian oak. Maple will increase from having about equal basal area at year 340 (12.05 m²/ha maple vs. 10.12 m²/ha oak) to three times as much (27.22 m²/ha maple vs. 8.8 m²/ha oak) when the transition to 3.5 °C climate change is complete 100 years later (Figure

4.13b). Mongolian oak eventually would decline to very low levels in the warmer climate. Replacement of Mongolian oak by Painted maple occurs much more rapidly in the 6.0 °C warming scenario (Figure 4.13c). At Blagodatnoye 2, where Painted maple doesn't occur, Mongolian oak would survive even 6.0 °C climate change, although cyclical fluctuations in basal area at the higher temperatures would cause oak mast shortages (Figure 4.14c). Mongolian oak might also be able to persist at more northerly locations, since it is one of several tree species that currently have a northern limit of 44° N (Krestov, 2003; Zyryanova *et al.*, 2005). At cooler temperatures north of about 40° N, where current mean average temperature is less than 10 °C (50 °F), Korean pine and Mongolian oak are spread widely across a latitudinal band (Qian *et al.*, 2003), and form a seed source to expand if conditions permit. Mast supply in northern oak stands may be less reliable on a year to year basis than in milder climates further south because production of oak mast is sensitive to spring temperatures and a hard spring freeze can dramatically reduce the availability of acorns (Johnson, 1994).

If both Korean pine and Mongolian oak disappear or tree density drops dramatically at southern and low elevation locations, the RSF and the ecology of deer and wild pigs suggests that the territory of these ungulates would move northward and upward in elevation, to follow the ranges of these critical seed and nut trees. Already, track census data have indicated that red deer, the principle prey of Amur tigers are moving from the coastal oak-birch zone toward fir-spruce forests, which are associated with higher elevations and colder climates to the north (Stephens *et al.*, 2006; Miquelle *et al.*, 2010a). A comparison of 1995 and 2005 winter track survey data found a northward expansion of Amur tiger range (Miquelle *et al.*, 2010a). Tigers tracks were observed north of the Amur River for the first time since the 1930s (Miquelle *et al.*, 2010a) in the 2005 census.

Miquelle *et al.* (2010b) has reconstructed the northern limit of red deer and wild boar range (based on Bromley and Kucherenko, 1983) and found that no high density areas of wild pigs and very few high density locations of red deer extend beyond the northern edge of the mixed Korean pine-deciduous forest, which is slightly north of the Amur river near latitude 51 °N. Miquelle suggests that these mixed forests might be considered a proxy for northernmost border of red deer and wild boar.

Mixed deciduous broadleaf/Korean pine forests currently can survive as far north as 44° N latitude (Nakamura and Krestov 2005). Genetic and pollen studies indicate that Korean pine range was much larger during warmer climates in the past than it is today. Pollen studies from Pleistocene peat samples show evidence of the species (Neishtadt 1957; Potenko and Velikov, 1998), and it appeared in mountain vegetation in the RFE in the still warm but cooling climate of the early-mid Holocene period (~9,800 ybp) (Potenko and Velikov, 1998). During the Holocene climate optimum (6880 ± 270 ybp), when mean July temperatures in Eastern Siberia were estimated to be up to 1.5 °C warmer than today (Potenko and Velikov, 1998; Nazarova *et al.*, 2013), the northern boundary of deciduous broadleaf/Korean pine/conifer forests was farther north, at latitude 54.56° N and close to the westernmost coast the Sea of Okhotsk (Potenko and Velikov, 1998). This is close to the current northern boundary of spruce-fir dark conifer forests (55 – 57° N latitude in subarctic climate locations) (Nakamura and Krestov, 2005), north of which they give way to larch (*Larix dahurica*). During the cooling climate of the late Holocene (2500 ybp – present), Korean pine has been replaced by spruce, fir and larch species in the southern parts of its range (Potenko and Velikov, 1998).

North of the Amur River, spruce-fir forests reach all the way to sea level, but small stands of broadleaved forests that include Mongolian oak occur on south-facing slopes near the Amur River (Qian *et al.* 2003; Kolbek *et al.*, 2003), suggesting that future climate and soil conditions might allow Mongolian oak as well as Korean pine to thrive here if restoration efforts were undertaken and climate conditions are favorable.

Although Korean pine has a moderate tolerance for frost (Nakamura and Krestov, 2005), occasional extreme cold spells and shorter growing seasons at northern latitudes might reduce Korean pine regeneration and large-scale establishment. Former northern mixed forests with Korean pine have been greatly reduced by human activity as early as 500 to 800 AD, as well as fires and clear cutting, and replaced by Paper birch (*Betula platyphylla*) and larch (*Larix dahurica*) forests (Nakamura and Krestov, 2005), tree species not associated with tiger prey range.

In addition to forest type and shortage of prey, however, deep snow and extremely low winter temperatures would challenge expansion of tiger distribution in this area (Miquelle *et al.*, 2010b). Also, if tree species' range shift fails to occur rapidly enough, some ungulates might not survive, especially through the long cold winter, when acorns and pine nuts provide important food and energy.

4.5.7 *Potential range shift and wildlife corridors*

A landscape scale approach to tiger conservation is essential in the RFE (Sanderson, 2006, Carroll and Miquelle, 2006; Dinerstein *et al.*, 2007; Dinerstein, 2011; Miquelle *et al.*, 2010a&b; Seidensticker 2010; Seidensticker *et al.*, 2010) because only 10% of potential Amur tiger habitat is in protected areas (Miquelle *et al.*, 2010a). Even though the landscape is vast, much of the territory is unsuitable for tigers because it fails to meet the requirements of adequate prey, access to water, sufficient cover for shelter and hunting, and protection from poaching (Dinerstein, 1987; Miquelle *et al.*, 1999b; Miquelle *et al.*, 2010a; Seidensticker *et al.*, 2010). Well-managed corridors will increase the distribution of tigers and help their population withstand increasing anthropogenic and environmental pressure in the future (Carroll and Miquelle, 2006).

The small fraction of tiger range in reserves is in part a result of the large range of individual tigers, which low prey density makes necessary (Karanth *et al.*, 2004; Miquelle *et al.*, 2005; Miquelle *et al.*, 2010b; Seidensticker *et al.*, 2010b). Reserves serve as “core source areas” (Miquelle *et al.*, 2010b; Walston *et al.*, 2010), and play an important role in population expansion because tiger reproduction rates are higher and tiger densities are twice as large in reserves compared with outside reserve boundaries (Miquelle 1999; Miquelle *et al.*, 2010 a&b).

In addition to core areas, such as strictly protected reserves, tigers and other wildlife need a buffer zone around the protected areas, and landscape for dispersal (Sanderson *et al.*, 2006; Dinerstein *et al.*, 2007; Ranganathan *et al.*, 2008; Walston *et al.*, 2010; Miquelle *et al.*, 2010a&b;

Wikramanayake *et al.*, 2004 and 2011). Corridors allow species dispersal, gene flow, movement between highly distant protected habitat areas and a buffer against resource extraction activities, such as logging and agriculture (Miquelle *et al.*, 1999a; Carroll and Miquelle, 2006; Miquelle *et al.*, 2010b). As climate becomes warmer and drier, the boundaries of reserves and corridors may need to change to continue these functions.

International and Russian non-governmental organizations (NGOs) and Russian government officials have worked together to identify and, in several cases, formally protect corridors between protected areas in the RFE. A comprehensive network of existing protected areas and linking corridors for Russia and China was proposed in 1995 by the Wildlife Conservation Society (WCS), Worldwide Fund for Nature (WWF), and government. The proposed network represented about 70,000 km² of contiguous landscape in Primorski Krai, Khabarovski Krai and northeastern China, and included the home ranges of approximately 70 tigresses (Miquelle *et al.*, 2010a). In developing the network, it was recognized that maintaining the forest in unprotected forest land is critical (Miquelle *et al.*, 2010a). A refined version of the section of the plan for Khabarovski Krai was adopted and implemented in 2006, with the exception of one recommended national park. The plan was not adopted in Primorski Krai, although two proposed national parks were approved (Miquelle *et al.*, 2010a).

It is important to consider climate change as a factor in planning for corridors and future reserve boundaries (Stephens *et al.*, 2006), as tigers as well as prey species may shift range because of temperature and snow tolerance as well as changes in Korean pine and Mongolian oak.

Ecological restoration of pines and oaks would increase the abundance of acorns and pine nuts and speed up the rate that basal area of these species increases with climate warming. Restoration efforts would need to consider the time required for oaks and pines to produce acorns and pine cones.

With as little as 2.0 °C of climate warming, tigers in Ussurisky might need to change range, should prey disappear. Korean pine vegetation belts can't move upward in elevation in the Ussurisky area as climate warms because the hills are low in elevation. Ussurisky is located near a highly populated area and an industrial corridor, which limits options for dispersal. Current conservation efforts focus on Changbai Mountain in China and building corridors from current tiger range in Southeastern RFE to Changbai, which may become even more important in changed climate conditions. Tigers and their prey once ranged throughout China (Seidensticker, 2010) but, in the late 1990s, only four to six tigers were reported in Jilin Province and five to seven in Heilongjiang (Miquelle *et al.*, 2010a). These most likely are related to the Russian Amur tiger population and are dispersing individuals, not reproducing pairs (Miquelle *et al.*, 2010a). Forested areas suitable for tigers have been identified in the East Manchurian Mountains between Changbai Mountain and Ussurisky in eastern Jilin Province and southeastern Heilongjiang provinces (Miquelle *et al.*, 2010a; Xiaofeng *et al.*, 2011). Linkage of these areas creates a wildlife corridor from Russia into Changbai reserve area (Figure 4.27).

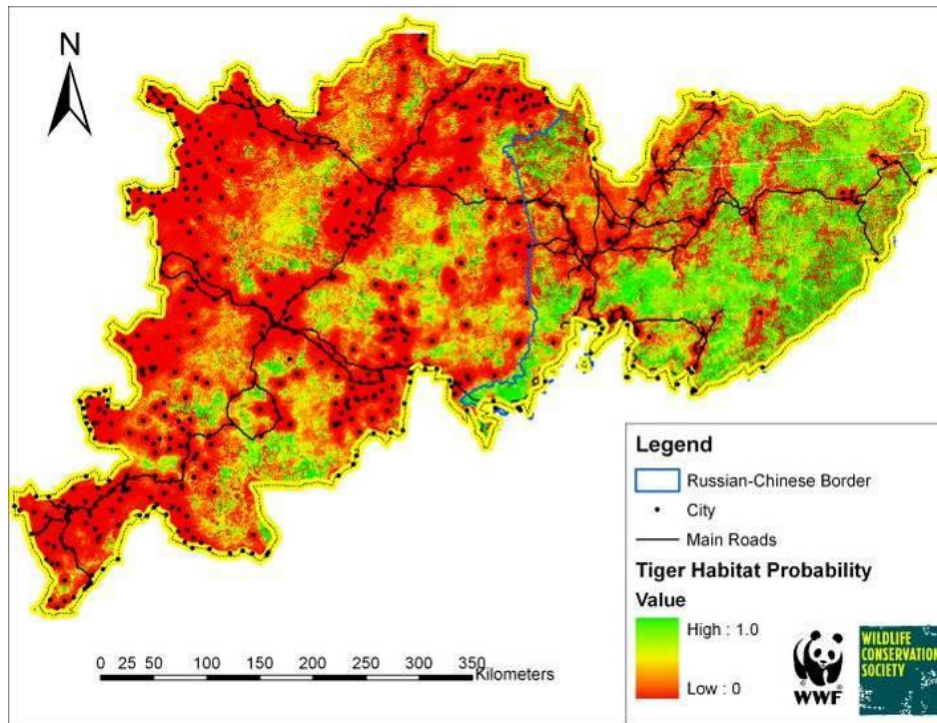


Figure 4.27 Potential tiger habitat in Northeastern China, including Changbai Mountain, and the Ussurisky area in Russia based on Resource Selection Function Analysis (Hebblewhite *et al.*, 2012).

Forests in the Changbai area of northeastern China are associated with humid conditions and moist soils from snow melt in the spring and early summer, similar to conditions in the Central Sikhote-Alin coastal area, and contain many of the same species, such as Korean pine, Yezo spruce and fir species (Krestov *et al.*, 2006). Korean pine occurs in mixed forests up to 1100 – 1200 m in Changbai Shan, above which are Yezo spruce – Black fir forests up to 2000 m (Qian *et al.*, 2003a; Nakamura and Krestov, 2005). South of the Changbai Mountain area, Korean pine and Amur linden forests give way to ecosystems shaped by a warmer climate and dominated by maple species and Mongolian oak (Krestov *et al.*, 2006). The Wildlife Conservation Society,

World Wide Fund for Nature (WWF), and the Chinese government, developed a plan based on resource selection function analyses, environmental niche factor analysis, and expert opinion (Xiaofeng *et al.*, 2011; Hebblewhite *et al.*, 2012) to identify optimal tiger habitat in northeastern China (Hebblewhite *et al.*, 2012). The plan identified nine areas, designated Tiger Conservation Areas (TCAs), that meet statistically-derived criteria for tiger habitat: Korean pine and deciduous forests, distance from human activity, lack of deep snow, lack of high elevations and steep slopes and lack of dark conifer forests (Hebblewhite *et al.*, 2012).

Many challenges exist to the restoration of habitat priority areas and corridors, including large human populations, development, and highways. The Hunchun Tiger and Leopard Reserve was established along the Russia-China border in 2002, and initiatives are underway to restore tigers and prey, such as the removal of snares (Miquelle *et al.*, 2010a).

In the Democratic People's Republic of Korean (North Korea), landscapes with appropriate forest vegetation exist that could support tigers, leopards and their prey. Surveys that meet international standards are needed to determine the number of tigers and the potential for building long-term sustainable habitat using a system of reserves and wildlife corridors (Miquelle *et al.*, 2010a).

In Central Sikhote-Alin, spruce and fir die out at higher latitudes, Korean pine and Mongolian oak may expand range. Most of the landscape surrounding the reserve is state forestry land, where commercial logging and hunting are permitted, and public access is generally unrestricted (Goodrich *et al.*, 2008; Miquelle *et al.*, 2010b). Current threats to tigers include being hit by

vehicles on roads, illegal hunting because of greater public access, and retaliation when tigers kill humans, livestock, or pets (Goodrich *et al.*, 2008). The proposed multi-use corridor system would allow tigers and their prey to reach more upland and isolated areas.

Another area identified as an ecological corridor that would facilitate dispersal of Amur tigers is the Strel'nikov Range along the border of Primorski Krai and Khabarovsk Krai. The range connects tiger range in the Sikhote-Alin mountains to the Eastern Wandashan Mountains in northeastern China, an area considered to be good potential tiger habitat (Miquelle *et al.*, 2010a), where red deer is abundant, but human activity is widespread and potentially disruptive (Jiang *et al.*, 2007).

Population viability analysis has indicated that illegal hunting and lack of prey are greater threats to the persistence of Amur tigers than habitat fragmentation in both Russia and China (Tian *et al.*, 2011). If poaching were strictly prohibited and habitat quality, including sufficient prey, were maintained or improved, Amur tiger populations would be persist for the next 100 years.

Consideration of projected climate change during this period that reduces food supply for ungulate prey increases the importance of maintaining connectivity with suitable habitat that can withstand a new climate regime.

4.5.8 *Other Climate Considerations*

The Intergovernmental Panel on Climate Change (IPCC, 2007a) predicts that more heat waves and intense precipitation episodes separated by longer dry periods will occur in the future in Eastern Asia. Tropical cyclones that over the Pacific and sometimes make landfall in Primorski Krai may increase in frequency and intensity, which is attributed to warmer sea surface temperatures and the capacity of warmer atmosphere to hold more moisture (IPCC, 2007b). It is projected that a one-in-twenty year heavy precipitation event will become a one-in-five to a one-in-fifteen event by 2090 – 2100 (IPCC, 2007b). Heat waves and longer dry periods between precipitation events could be important even in drought-tolerant areas such as southern Primorye by amplifying the impact of warmer conditions on soil moisture.

It is likely that wind speeds in tropical cyclones will increase (IPCC, 2007a), which would contribute to more downed tree limbs and fallen trees. During the period 1765 – 1995, wind damage was the most likely cause of canopy gap formation in Sikhote-Alin Reserves, since there is no evidence of severe fires (Ishikawa *et al.*, 1999). Storms that topple trees or bring down large branches will benefit Korean pine, since forest canopy gaps are needed for Korean pine to regenerate (Ishikawa *et al.*, 1999; Zyryanova *et al.*, 2005; Nakamura and Krestov, 2005). Mongolian oak also will benefit from newly opened gaps in the canopy.

Mean summer and winter precipitation is projected to increase in East Asia (IPCC, 2007a).

Warmer winter temperatures and more atmospheric moisture may lead to larger snow storms,

which would contribute to more canopy gaps from fallen trees and branches. Snowy winters also increase mortality for tigers and prey (Heptner *et al.*, 1992; Heptner and Sludskii, 1992; Miquelle *et al.*, 2010b), with especially negative effects on roe deer, red deer, and wild boar (Stephens *et al.*, 2006). Small deer and pigs have difficulty getting through deep snow, and at snow depths greater than 25 – 30 cm, deer are unable to dig up acorns (Heptner *et al.*, 1992). Deep snow may reduce travel of wild pigs from the usual range of 6 – 8 km daily to just a few hundred meters, which makes finding adequate nutrition more difficult. A frozen crust on snow can cause fatal cuts to the legs of tigers and their prey (Heptner & Sludskii, 1992).

The global rate of sea level rise (SLR) from 1992 – 2012 was $3.1 \text{ mm} \pm 0.4 \text{ mm/yr}$, compared with a rate of 1.7 to 2.4 mm/year for the entire 20th century (Arendt *et al.*, 2002; Rignot *et al.*, 2003; IPCC 2007a), which suggests that the rate of sea level rise is accelerating. The current rate of sea level rise (SLR) in Asia is 1 – 3 mm/year (IPCC 2007a). Along the East Asia coast, predicted sea level rise varies from 1.5 to 4.4 mm/year (Mimura and Yokoki, 2004; IPCC 2007a). Sea level rise and increased coastal flooding potentially would affect areas where tigers and ungulates currently range, such as the Blagodatnoye area of Sikhote-Alin Biosphere *Zapovednik* (SABZ). Flooding already occurs in August in the coastal town of Terney (Newell, 2004), which is adjacent to SABZ (Figure 4.28). Stronger winds associated with higher sea surface temperatures and low pressures from tropical storms could cause higher storm surges, resulting in greater coastal flooding. Declining sea ice near coastal shores and rising sea levels also will contribute to more coastal erosion (IPCC, 2007a). Flooding and sea level rise might force communities and agricultural areas inland toward SABZ unless bulwarks, dikes, and seawalls are

built. High coastal ridges along the coast currently support forests where wildlife potentially could persist and that provide transit areas to more inland areas.



Figure 4.28 a. Tiger tracks in Blagodatnoye near Terney b. Low elevation coastal town of Terney

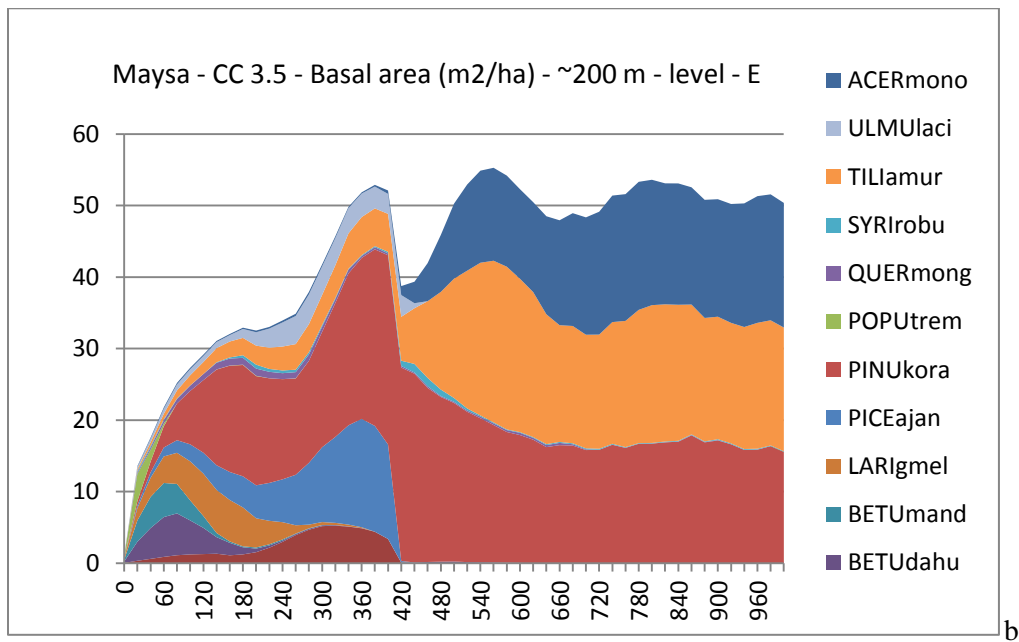
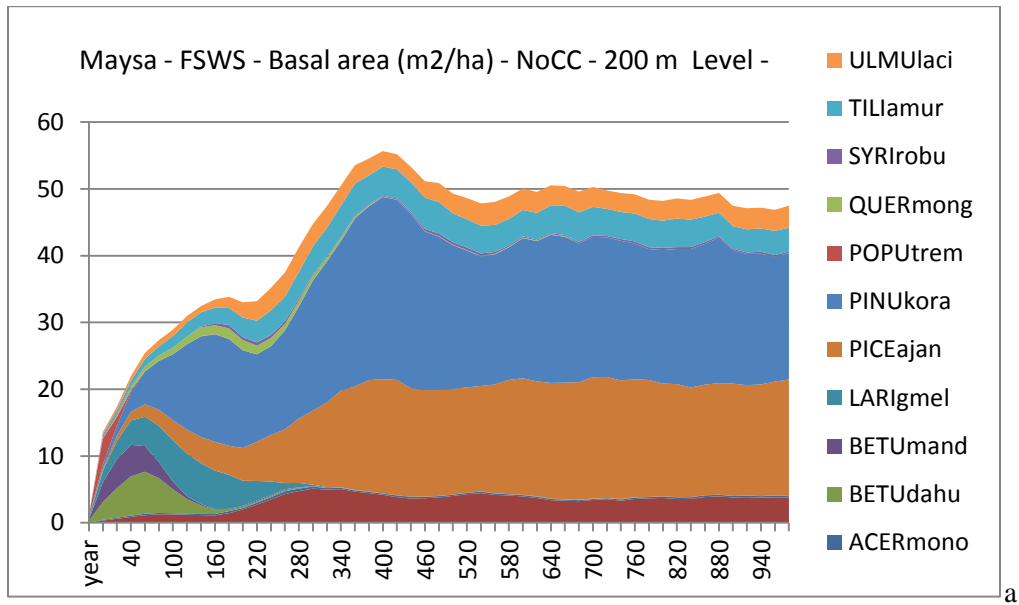
4.5.9 *Effects of fire and other disturbances*

Wildfires are an important force shaping forest composition and structure in the southeastern Russian Far East (Loboda and Csiszar, 2007; Loboda, 2009; Loboda *et al.*, 2012; Sherman *et al.*, 2012; Korovin, 2012). Clear-cutting and wildfires close to settlements have greatly reduced mixed broadleaf/Korean pine/conifer forests in Central Sikhote-Alin during the 1900s (Krestov, 2003; Nakamura and Krestov, 2005). The number of wildfires has increased recently because of greater human activity such as campfires associated with logging (Rosenberg *et al.*, 1998; Makoto 2007). Wildfires occur mostly in spring and fall and often are associated with agricultural activity (Loboda and Csiszar, 2007). In summer, lightening can cause large wildfires, especially during drought years (Loboda and Csiszar, 2007). Wildfires are expected to increase even more with

climate change, as warm and dry conditions contribute to fire probability (Soja *et al.*, 2006; Loboda and Csiszar 2007).

Forests in the study area re-grow slowly after disturbance such as logging or wildfire (Krestov, 2003; Loboda *et al.*, 2012). Logged or fire-damaged areas may remain as grassland or shrub-dominated for 10 – 30 years after the disturbance (Krestov 2003; Nakamura and Krestov, 2005; Loboda *et al.*, 2012). In a deciduous broadleaf/Korean pine forest, the post-fire succession process can take centuries, and the original forest may never recur if a stable, “self-regenerating” ecosystem dominated by Mongolian oak or larch (*L. dahurica*) gets established (Rosenberg *et al.*, 1998; Nakamura and Krestov, 2005; Krestov *et al.*, 2006). Complete regeneration of dark conifer forests takes 100 – 180 years under optimal conditions (Nakamura and Krestov, 2005).

At the wildfire burn site, Maysa, the regenerating forest was dominated by Manchurian birch (*Betula mandshurica*) (21.15 m²/ha) and included Korean pine (4.9 m²/ha), Amur linden (4.06 m²/ha), Mongolian oak (3.08 m²/ha), and Xing'an larch (*Larix gmelinii*) (1.8 m²/ha). In FAREAST, oak basal area never surpassed 2 m²/ha, possibly because Korean pine and other ruderal species grow quickly and create too much shade for oak to flourish. FAREAST indicates that Korean pine will eventually co-dominate with Yezo spruce under current climate conditions (Figure 4.12a). With 3.5 °C climate warming, Korean pine would continue at approximately the same basal area as with warming, but Yezo spruce would disappear and be replaced by Amur linden and Painted maple (Figure 4.12b). With 6 °C temperature increase, Korean pine disappears and the forest converts to Painted maple (Figure 4.12c).



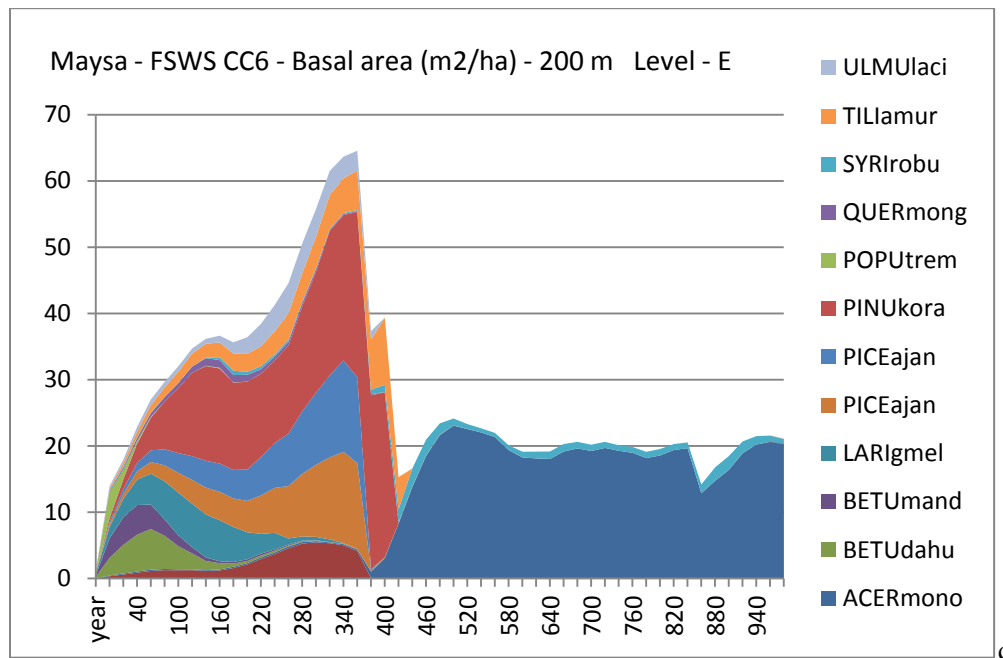


Figure 4.28 (a) Forest composition under current climate conditions (b) Korean pine persists in a 3.5 °C temperature increase scenario (c) With 6.0 °C increase, Painted maple (*Acer mono*) dominates the forest.

More fires would create and help to maintain more gaps and open areas (Anderson, 1982; Nakamura and Krestov, 2007; Makoto *et al.*, 2007), which would favor growth of full light tolerant species such as oak and pine. Southern Primorye tree species generally have greater fire tolerance than species in more humid climates to the north and typically are resistant to spring ground fires, but seedlings of conifers such as Korean pine may perish with intense or repeated fires (Krestov *et al.*, 2006). A mixed pine/broadleaf forest exposed to repeated fires will give way to a fire-tolerant oak-birch forest (Nakamura and Krestov, 2005). Mongolian oak sprouts often were observed in forests of White birch (*Betula platyphylla*), the most commonly occurring broadleaf species in the RFE (Zyryanova *et al.*, 2005; Makota *et al.*, 2007) and Xing'an larch (*Larix gmelinii*), the most common species overall (Zyryanova *et al.*, 2005; Makota *et al.*, 2007),

and could be expected to eventually dominate in these forests in a moderate fire regime. An oak-birch forest could support deer and wild pigs and withstand an ongoing moderate fire regime (Zyryanova *et al.*, 2005). Mongolian oak has good sprouting ability and produces abundant mast (Makoto *et al.*, 2007). Oak also grows well in xeric soil and on burned sites (Zyryanova *et al.*, 2005; Makoto *et al.*, 2007). If fires are too frequent or too intense, forests may convert to shrubs or meadowland (Nakamura and Krestov, 2005).



Figure 4.29 Site of severe wildfire in high-elevation dark conifer forest. Only birch is re-generating at this stage.

Dark conifer forests are vulnerable to fire and drought associated with a warmer and drier climate (Figure 4.29). Spruce has thin bark and shallow roots, and lower branches can be damaged by fire. “Flammable epiphytic lichen” can lead to crown fires (Krestov 2003; Zyryanova *et al.*, 2005). After a severe fire, dark conifer forests typically form spruce stands (Krestov, 2003), but factors such as availability of seed sources, climate, and soil conditions may favor or inhibit competitors, which reinforces the hypothesis that Korean pine could migrate upwards in elevation and northward into areas now dominated by dark conifer forests. Oak is less likely to replace fir and

spruce because it more typically is found at elevations and latitudes with warmer temperatures (Yan and Shugart, 2005) and freezing spring temperatures can prevent oak mast as well as kill saplings (Johnson, 1994).

Adding to the effect of more fires, FAREAST suggests that climate change of 6.0 °C will cause forests to disappear, possibly giving way to meadows and savannah. Open and mixed forest areas, as well as regenerating forests, potentially provide good browse for deer, but both deer and wild boar require more mature forests for shelter, food, and protection in winter (Heptner *et al.*, 1992).

In conclusion, if more fires and fires of greater intensity occur in a warmer climate, in addition to loss of trees from heat and drought, many years may be needed for red deer and wild pig habitat to become reestablished. Given the lack of prey and tree cover, tigers might avoid the area until the forest re-grows.

4.5.10 Political, social and economic considerations

The catalysts for modification of tiger habitat for this study are climate change and the natural process of forest succession. Political, socioeconomic, technological and cultural drivers also are important for the future of the tiger in its natural habitat (Burgi *et al.*, 2004; Miquelle *et al.*, 2010a&b; Seidensticker *et al.*, 2010). It is estimated that 83% of Amur tiger mortality is human-caused, mostly by illegal hunting, or poaching (Goodrich *et al.*, 2008; Miquelle *et al.*, 2010b). When prey is limited, as it is in the RFE, tiger populations are particularly vulnerable to collapse from poaching (Damania *et al.*, 2008). Protection of breeding females is especially critical for

population persistence and expansion. Tiger populations will decline if female tiger mortality exceeds 15%, even if prey is sufficient (Chapron *et al.*, 2008). If poaching of tigers is controlled and sufficient prey exists, tiger populations may expand quickly in high quality habitat areas (Sunquist and Sunquist, 1999; Seidensticker *et al.*, 2010).

4.5.11 Possible future studies

New studies might include adjusting the FAREAST model to mimic more precisely the expected pattern of intense precipitation events separated by longer dry periods, disproportionately warmer winter minimum temperatures, and warmer nighttime temperatures. The implications of higher peak temperatures and stronger precipitation events on particular species also need to be explored. Modification of the model to allow analyst manipulation of precipitation events would permit a finer-grained exploration of climate change impacts. The model also might be expanded to consider inter-gap effects, such as cross-pollination by wind, water runoff, and bird and other animal transport of seeds.

Refining the wildfire component of FAREAST could contribute valuable insights regarding the future of these forests. The impact of wildfire could be significant because it would reduce the amount of Painted maple that FAREAST predicts would eventually dominate at the Ussurisky sites, coastal forests that include the species, and the Polovinka sites.

4.6 CONCLUSION

Modeling of forest succession under climate regimes predicted for the southeastern RFE suggests that changes in temperature projected for this century are likely to modify the quality and location of potential habitat for Amur tiger prey and, consequently, for the Amur tiger itself. RSF analyses have statistically linked tiger and prey presence with forests containing Korean pine and Mongolian oak, which are key nut- and seed-producing species. The decline or disappearance of acorns and pine nuts would eliminate important nutrient and energy sources for deer and wild pigs, the main food sources for Amur tigers and many other species.

Korean pine and Mongolian oak basal area may range from slightly increased under the B1 lowest carbon emission scenario, to dramatically changed, with the loss of Korean pine and Mongolian oak, in all sections of Amur tiger range under the A1F1 fossil-fuel-intensive scenario. Fir and spruce, species that are most sensitive to heat and dry soil conditions associated with drought, died out most quickly, but the simulations showed at the southernmost research sites, even a 2 °C change caused drought and heat-resistant Korean pine to decline permanently. Because atmospheric temperature is increasing more rapidly in East Asia than in other parts of the globe, a 2 °C increase in this area would occur at a lower mean temperature increase globally.

Consistent soil conditions and the current presence of Korean pine and Mongolian oak at higher elevations and historically at more northern latitudes suggest that these species might adjust their range as climate becomes warmer and drier. Whether they could do so in the time frame and quantity needed to support an adequate population prey species is hard to predict. Also,

occasional extreme cold events, especially in spring, and deep snow may reduce tree mast and regeneration, as well as reduce recruitment for both tigers and their prey. Protection of these tree species from logging along with restoration projects would help to maintain and expand forests that could support ungulates and tigers.

Protection of riverine areas also is important, especially those with Mongolian oak and Korean pine, since tigers have been shown to preferentially use these areas (Carroll and Miquelle, 2006; Miquelle *et al.*, 2010a).

Tiger presence is associated with adequate prey; therefore, climate change alone, even without other important stressors, such as poaching and habitat loss, could cause a reduction in the number of wild Amur tigers in this area. Successful efforts to increase prey levels by maintaining and increasing the food supply for deer, pigs and small mammals would help to meet human needs as well as enable tiger populations to better withstand poaching pressure. Flexibility to change reserve boundaries as needed to include potential new areas of pine and oak growth and to incorporate such areas into wildlife corridors should be part of current and future initiatives to identify and address all the factors that may promote or inhibit the persistence of these iconic and ecologically important animals.

4.7 REFERENCES

Anderson RC (1982) An evolutionary model summarizing the roles of fire, climate, and grazing animals in the origin and maintenance of grasslands: an end paper. In: *Grasses and Grasslands: Systematics and Ecology* (eds Estes JR, Tyrl RJ, Brunken JN), pp. 297-308. U. of Oklahoma Press, Norman, OK.

Arendt A, Echelmeyer K, Harrison C *et al.* (2002) Rapid wastage of Alaska glaciers and their contribution to rising sea level. *Science*, **297**, 382 – 386.

Blackburn T, Gaston AJ, Loder N (1999) Geographic gradients in body size: a clarification of Bergmann's rule. *Diversity and Distributions*. **5**, 165-174.

Bonan GB, Pollard D, Thompson SL (1992) Effects of boreal forest vegetation on global climate. *Nature*, **359**, 716 – 718.

Botkin D (1992) A Natural Myth. *Nature Conservancy*, May/June, 38.

Botkin DB, Janak JF, Wallis FR (1972) Some ecological consequences of a computer model of

forest growth. *Journal of Ecology*, **60**, 849-873.

Bromley GF, Kucherenko SP (1983) *Ungulates of the Southern Part of the USSR*. Nauka, Moscow.

Burgi M, Hersperger AM, Schneeberger N (2004) Driving forces of landscape change – current and new directions. *Landscape Ecology*, **19**, 857-868.

Carbone C, Gittleman JL (2002) A common rule for the scaling of carnivore density. *Science*, **295**, 2273-2276.

Carroll C, Miquelle DG (2006) Spatial viability analysis of Amur tiger *Panthera tigris altaica* in the Russian Far East: the role of protected areas and landscape matrix in population persistence. *Journal of Applied Ecology*, **43**, 1056-1068.

Chapin III, FS, Matson PA, Mooney, HA (2002) *Principles of Terrestrial System Ecology*. Springer, New York.

Chapin III FS, Sturm M, Serreze MC *et al.* (2005) Role of Land-Surface Changes in Arctic Summer Warming. *Science*, **310**, 657 – 660.

Chapron G, Miquelle DG, Lambert A *et al.* (2008) The impact on tigers of poaching versus prey depletion. *Journal of Applied Ecology*, **45**, 1667 – 1674.

Cushman SA, Wallin DO (2000) Rates and patterns of landscape change in the Central Sikhote-Alin Mountains, Russian Far East. *Landscape Ecology*, **15**, 643-659.

Dalnikin AA (1999) *Mammals of Russia and adjacent regions: Deer (Cervidae)*. GEOS, Moscow.

Damania RJ, Seidensticker J, Whitten A *et al.* (2008) *A Future for Wild Tigers*. The World Bank and Smithsonian National Zoological Park, Washington, D.C.

Dinerstein E (1987) Deer, plant phenology, and succession in the lowland forest of Nepal. In: *Biology and Management of the Cervidae* (ed Wemmer CW), pp. 272 – 288. Smithsonian Institution Press, Washington, D.C.

Dinerstein E, Loucks C, Heydlauff A *et al.* (2006) *Setting Priorities for the Conservation of Wild Tigers: 2005 – 2015. A User's Guide.* WWF, WCS, Smithsonian, NFWF-STF, Washington, D.C., New York.

Dinerstein E, Loucks C, Wikramanayake E *et al.* (2007) The fate of wild tigers. *Bioscience*, **57**, 508-514.

Fan DD, Li CX (2006) Complexities of Chinese coast in response to climate change. *Advances in Climate Change Research*. Suppl. 1-0054-05, 1673-1719.

Goodrich J, Kerley L, Smirnov E *et al.* (2008) Survival rates and causes of mortality of Amur tigers on and near the Sikhote-Alin Biosphere Zapovednik. *Journal of Zoology*, 1-7.

Goodrich J, Miquelle D, Smirnov E *et al.* (2010) Spatial Structure of Amur (Siberian) tigers (*Panthera tigris altaica*) on Sikhote-Alin Biosphere Zapovednik, Russia. *Journal of Mammology*, **91**, 737-748.

Goodrich J, Seryodkin I, Miquelle DG *et al.* (2011) Conflicts between Amur (Siberian) tigers and humans in the Russian Far East. *Biological Conservation*, **144**, 584-592.

Grichuk, VP (1984) Late Pleistocene vegetation history. *Late Quaternary environments of Soviet Union*. pp. 155-178. Minnesota Press, Minneapolis.

Gromyko, MN (2006) Climate Change and catastrophic disturbances of forest ecosystems in the Sikhote-Alin State Nature Reserve. In: *Climate Change Impact on Ecosystems of the Amur River Basin*. WWF Russia, Moscow/Vladivostok (In Russian with abstracts in English).

Hargreaves GH, Allen RG (2003) History and evaluation of Hargreaves' evapotranspiration equation. *Journal of Irrigation and Drainage Engineering*, **129**, 429-450.

Hayashida, M (1989) Seed Dispersal by Red Squirrels and Subsequent Establishment of Korean Pine. *Forest Ecology and Management*, **28**, 115 – 129.

Hayward MW, Kerley GIH (2005) Prey preferences of the lion (*Panthera leo*). *Journal of Zoology*, **267**, 309-322.

Hebblewhite M, Miquelle DG, Murzin AA *et al.* (2011) Predicting potential habitat and population size for reintroduction of the Far Eastern leopards in the Russian Far East. *Biological Conservation*, **144**, 2403 - 2413.

Hebblewhite MF, Zimmerman F, Li Z *et al.* (2012) Is there a future for Amur tigers in a restored tiger conservation landscape in Northeast China? *Animal Conservation*, 1469-1795.

Heptner VG, Nasimovich AA, Bannikov AG (1992) *Mammals of the Soviet Union Vol I Artiodactyla and Perissodactyla*. Smithsonian Institution Libraries and National Science Foundation, Washington, D.C.

Heptner VG, Sludskii AA (1992) *Mammals of the Soviet Union Vol II Part 2 Carnivora (Hyaenas and Cats)* pp. 95 – 355. Smithsonian Institution Libraries and National Science Foundation, Washington, D.C.

Horn HS (1974) The Ecology of Secondary Succession. *Annual Review of Ecology and Systematics*, **5**, 25–37.

Horn HS (2002) Some Causes of Variety in Patterns of Secondary Succession. In: *Forest Succession Concepts and Application* (eds West DC, Shugart HH, Botkin DB) Springer-Verlag, New York.

Horn HS, Cody ML, Diamond JM (1975) *Markovian properties of forest succession*. pp. 196-211.

Hunter CM, Caswell H, Runge MC *et al.* (2010) Climate change threatens polar bear populations: a stochastic demographic analysis. *Ecology*, **91**, 2883-2897.

Hutchins HE, Hutchins SA, Liu B (1996) The Role of Birds and Mammals in Korean Pine (*Pinus koraiensis*) Regeneration Dynamics. *Oecologia*, **107**, 120-130.

International Institute for Applied Systems Analysis (IIASA) (2002) *Land Resources of Russia*, CD-ROM.

IPCC (2007a) *Climate Change 2007. Impacts, Adaptation and Vulnerability. Contribution of Working Group II to the Fourth Assessment Report of the Intergovernmental Panel on Climate Change* (eds Parry M, Canziani O, Palutikof J, van der Linden P, Hanson C), pp. 479, 484.

Cambridge University Press, Cambridge, UK.

IPCC (2007b) *Climate Change 2007: The Physical Science Basis. Working Group I Contribution to the Fourth Assessment Report of the Intergovernmental Panel on Climate Change* (eds Solomon S, Qin D, Manning M) Cambridge University Press, Cambridge.

Ishikawa Y, Krestov P, Namikawa K (1999) Disturbance history and tree establishment in old-growth *Pinus koraiensis*-hardwood forests in the Russian Far East. *Journal of Vegetation Science*, **10**, 439-448.

Jackson P (2010) Fifty years in the Tiger World: An Introduction. In: *Tigers of the World 2nd Edition* (eds Tilson R, Nyhus P), pp. 1-15. Elsevier Inc., London.

Jackson P (1999) The tiger in human consciousness and its significance in crafting solutions for tiger conservation. In: *Riding the Tiger* (eds Seidensticker J, Christie S, Jackson P), pp. 50-54. Cambridge University Press, Cambridge.

Jiang G, Zhang M, Ma J (2007) Effects of human disturbance on movement, foraging and bed selection in red deer *Cervus elaphus xanthopygus* from the Wandashan Mountains, northeastern China. *Acta Theriologica*, **52**, 435–446.

Kaplanov LG (1948) Tiger, red deer, and moose. Moskoski obschestva ispytateley prirody. Novaya seria. *Otdel Zool.*, **14**, 18-49 (in Russian).

Karanth KO, Gopalaswamy AM, Kumar NS, *et al.* (2011) Monitoring carnivore populations at the landscape scale: occupancy modeling of tigers from sign surveys. *Journal of Applied Ecology* **48**, 1048-1056.

Karanth KK, Nichols JD, Karanth KU *et al.* (2010) The Shrinking Ark: patterns of mammal extinctions in India. *Proceedings of the Royal Society-B*, **227**, 1971-1979.

Karanth KU, Nichols JD, Kumar NS *et al.* (2006) Assessing tiger population dynamics using photographic capture-recapture sampling. *Ecology*, **87**, 2925-2937.

Karanth, KU, Nichols JD, Kumar NS *et al.* (2004) Tigers and their prey: predicting carnivore densities from prey abundance. *Proceedings of the National Academy of Sciences, USA*, **101**, 4854-4858.

Karanth, KU, Stith BM (1999) Prey depletion as a critical determinant of tiger population viability. In: *Riding the Tiger: Tiger Conservation in Human Dominated Landscapes* (eds Seidensticker, Christie S, and Jackson P), pp. 100-113, Cambridge University Press, Cambridge, UK.

Katsuta M, Morij T, Yokoyama T (1998) Seed of woody plants in Japan. Japan Forest Tree Breeding Association, Tokyo, Japan (in Japanese).

Kerley LL, Goodrich JM, Miquelle DG *et al.* (2002) Effects of roads and human disturbance on Amur tigers. *Conservation Biology*, **16**, 97-108.

Kitchener A (1999) Tiger distribution, phenotypic variation and conservation issues. In: *Riding the Tiger* (eds Seidensticker J, Christie S, Jackson P), pp. 19 – 49. Cambridge University Press, Cambridge.

Koike T (1988) Leaf structure and photosynthetic performance as related to the forest succession of deciduous broad-leaved trees. *Plant Species Biology*, **3**, 77-87.

Kolbek T, Strutek M, Box EO (2003) *Forest Vegetation of Northeast Asia*. Kluwer, New York.

Krestov PV (2003) Forest Vegetation of Easternmost Russia (Russian Far East). In: *Forest Vegetation of Northeast Asia* (eds Kolbek T, Strutek M, Box EO), pp. 93-180. Kluwer, New York.

Krestov PV, Song J-S, Nakamura Y, Verkholat VP (2006) A phytosociological survey of the deciduous temperate forests of mainland Northeast Asia. *Phytocoenologica*, **36**, 77-150.

Lauenroth WK, Urban DL, Coffin DP *et al.* (1993) Modeling vegetation structure-ecosystem process interactions across sites and ecosystems. *Ecological Modeling*, **67**, 49-80.

Li H.-L (1952) Floristic relationships between eastern Asia and eastern North America. *Transactions of the American Philosophical Society (New Series)*, **42**, 371-429.

Li J and Zhu N (1991) Structure and process of Korean pine population in the natural forests.

Forest Ecology and Management, **43**, 125 – 135.

Loboda TV (2009) Modeling fire danger in data-poor regions: a case study from the Russian Far

East. *International Journal of Wildland Fire*, **18**, 19-35.

Loboda, TV, Csiszar IA (2007) Assessing the risk of ignition in the Russian Far East within a modeling framework. *Ecological Applications*, **17**, 791-805.

Loboda, TV, Zhang Z, O’Neal K *et al.* (2012) Reconstructing disturbance history using satellite-based assessment of the distribution of land cover in the Russian Far East. *Remote Sensing of the Environment*, **118**, 241-248.

Luo SJ, Kim JH, Johnson WE *et al.* (2004) Phylogeography and genetic ancestry of tigers (*Panthera tigris*). *PLoS Biology*, **22**, 2275-2293.

Makoto K, Nemilsov YP, Zyryanova OA *et al.* (2007) Regeneration after Forest Fires in mixed Conifer Broad-leaved Forests of the Amur Region in Far Eastern Russia: the Relationship between Species Specific Traits against Fire and Recent Fire Regimes. *Eurasian Journal of Forest Research*, **10**, 51-58.

Matyushkin EN (2006) Carnivora: the Amur tiger. In *Flora and Fauna of the Sikhote-Alin Nature Reserve* (eds A. Astafiev and M. Gromyko), pp. 335-341. Primpoligraphcombinat Ltd.,

Vladivostok

McKinney AM, CaraDonna PJ, Inouye, DW *et al.* (2012) Asynchronous changes in phenology of migrating Broad-tailed Hummingbirds and their early-season nectar resources. *Ecology*, **93**, 1987 – 1993.

Meffe GK, Carroll CR (1997) Genetics: Conservation of Diversity within Species. In: *Principles of Conservation Biology 2nd Edition* (eds Meffe G, Carroll C, Sunderland MA) Sinauer Associates, Inc., Sunderland, MA.

Miles J, French DD, Xu ZB & Chen LZ (1985) Transition matrix models of succession in a stand of mixed Broadleaved/*Pinus koraiensis* forest in Changbaishan, Kirin Province, Northeast China. *Journal of Environmental Management*, **20**, 357-375.

Miller CS, Hebblewhite M, Petrunenko YK *et al.* (2013) Estimating tiger (*Panthera tigris altaica*) kill rates and potential consumption rates using global positioning system collars. *Journal of Mammology*, *in press*.

Miquelle DG, Dunishenko Y, Aramilev V *et al.* (2009) A Monitoring Program for the Amur Tiger Twelve-Year Report: 1998 – 2009. Wildlife Conservation Society, New York.

Miquelle DG, Smirnov EN, Quigley HB *et al.* (1996) Food habits of Amur tigers in Sikhote-Alin Zapovednik and the Russian Far East, and implications for conservation. *Journal of Wildlife Research*, **1**, 138-147.

Miquelle DG, Pikunov DG, Dunishenko VV *et al.* (2006) *A survey of Amur (Siberian) tigers in the Russian Far East, 2004-2005.*

Miquelle DG, Goodrich JM, Kerley L *et al.* (2010a). Science-based Conservation of Amur Tigers in the Russian Far East and Northeast China. In: *Tigers of the World 2nd Edition* (eds Tilson R, Nyhus P), pp. 403 – 423. Elsevier Inc., London.

Miquelle DG, Goodrich JM, Smirnov EN *et al.* (2010b) Amur tiger: a case study of living on the edge. In: *Biology and Conservation of Wild Felids* (eds MacDonald DW, Loveridge AJ), pp. 325-339. Oxford Press, Oxford.

Miquelle DG, Nikolaev I, Goodrich J *et al.* (2004) Searching for the co-existence recipe: a case study of conflicts between people and tigers in the Russian Far East. In: *People and Wildlife: conflict or co-existence?* (eds Woodroffe R, Thirgood SJ, Rabinowitz A) Cambridge University Press, Cambridge.

Miquelle DG, Merrill TW, Dunishenko YM *et al.* (1999a) A habitat protection plan for the Amur tiger: developing political and ecological criteria for a viable land-use plan. In: *Riding the Tiger* (eds Seidensticker J, Christie S, Jackson P), pp. 273-295. Cambridge University Press, Cambridge.

Miquelle DG, Pikunov DG, Dunishenko YM, *et al.* (2007) 2005 Amur tiger census. *Cat News*, **46**, 11-14.

Miquelle DG, Seryodkin I, Kostyria A (2009) *Amur Tigers and Far Eastern Leopards in Russia: Research, Training and Capacity Building in the Russian Far East: Interim Report to 21st Century Tiger from the Wildlife Conservation Society*. Wildlife Conservation Society, New York.

Miquelle DG, Smirnov EN, Merrill TW *et al.* (1999b) Hierarchical spatial analysis of Amur tiger relationships to habitat and prey. In: *Riding the Tiger* (eds Seidensticker J, Christie S, Jackson P), pp. 71-99. Cambridge University Press, Cambridge.

Miquelle DG, Smirnov E, Salkina G *et al.* (2005) The importance of protected areas in Amur tiger conservation: a comparison of tiger and prey abundance in protected areas versus unprotected areas. In: *Results of Protection and Research of the Sikhote-Alin Natural Landscape* (eds Potikha I, Miquelle D, Gromyko M, *et al.*) Papers presented at the International Science and Management Conference devoted to the 70th Anniversary of the Sikhote-Alin State Reserve, Terney, Primorski Region, September 20 – 23, 2005. Primpoligraphkombinat, Vladivostok.

Mitchell M, Hebblewhite M. (2012) Carnivore habitat ecology: integrating theory and application. In: *Carnivore Ecology and Conservation: A Handbook of Techniques* (eds Boitani L, Powell R), pp. 218-255. Oxford University Press, New York.

Miyaki M (1987) Seed dispersal of Korean pine (*Pinus koraiensis*) by red squirrels (*Sciurus vulgaris*) *Ecological Research*, **2**, 147 – 157.

- Nakamura Y, Krestov PV (2005) Coniferous forests of the temperate zone of Asia. In: *Ecosystems of the World 6: Coniferous Forests* (ed Andersson F), pp. 163-220. Elsevier, New York.
- Nakamura Y, Krestov PV, Omelko AM (2009) Bioclimate and zonal vegetation in Northeast Asia: first approximation to an integrated study. *Phytocoenologia*, **37**, 443-470.
- Nazarova L, Lupfert H, Subetto D *et al.* (2013) Holocene climate conditions in central Yakutia (Eastern Siberia) inferred from sediment composition and fossil chironomids of Lake Temje. *Quaternary International*, **290**, 264–274.
- Neishstadt M (1957) *History of forests and paleogeography of the USSR. Holocene*. Academy of Sciences, Moscow.
- Newell J (2004) *The Russian Far East: A Reference Guide for Conservation and Development*. Daniel & Daniel, McKinleyville, CA.
- Paine RT (1995) A Conversation on Refining the Concept of Keystone Species. *Conservation Biology*, **9**, 962-964.
- Parmesan C (2006) Ecological and Evolutionary Responses to Recent Climate Change. *Annual Review of Ecology, Evolution, and Systematics*, **37**, 637-639.
- Parmesan C (2007) Influence of species, latitude and methodologies on estimates of phenological

response to global warming. *Global Change Biology*, **13**, 1860–1872.

Post WM, Pastor J (1996) Linkages – an individual-based forest ecosystem model. *Climatic Change*, **34**, 253–261.

Potenko VV, Velikov AV (1998) Genetic diversity and Differentiation of Natural Populations of *Pinus koraiensis* (Sieb. et Zucc.) in Russia. *Silvae Genetica*, **47**, 4.

Prentice IC, Leemans R (1990) Pattern and Process and the Dynamics of Forest Structure: A Simulation Approach. *Journal of Ecology*, **78**, 340 – 355.

Prynn, D (2004) *Amur Tiger*, Russian Nature Press, Edinburgh.

Pyke GH, Pulliam HR, Charnov EL (1977) Optimal foraging: a selective review of theory and tests. *Quarterly Review of Biology*, **52**, 137–154.

Qian H, Krestov P, Pei-Yun F *et al.* (2003a) Phytography of Northeast Asia. In: *Forest Vegetation of Northeast Asia* (eds Kolbek J, Strutek M, Box SO), pp. 51–91. Kluwer, New York.

Qian H, Song J-S, Krestov P *et al.* (2003b) Large-scale phytogeographical patterns in East Asia in relation to latitudinal and climatic gradients. *Journal of Biogeography*, **30**, 129–141.

Ranganathan, J, Chan K, Karanth K *et al.* (2008) Where can tigers persist in the future? A landscape-scale, density-based population model for the Indian subcontinent. *Biological*

Conservation, **141**, 67-77.

Rignot E, Rivera A, Casassa G (2003) Contribution of the Patagonia ice fields of South America to sea level rise. *Science*, **302**, 434-437.

Rosenberg VA, Bocharnikov VN, Krasnopeev SM (1998) Biological Diversity in the Sikhote-Alin Forests and Measures of its Conservation. In: *Integrated Tools for Natural Resources Inventories in the 21st Century, Gen. Tech. Rep. NC-212* (eds Hansen M, Burk T), pp. 326-333. U.S. Dept. of Agriculture, Forest Service, North Central Forest Experiment Station, St. Paul, MN.

Sanderson E, Forrest J, Loucks C *et al.* (2006) *Setting Priorities for the Conservation and Recovery of Wild Tigers: 2005-2015. The Technical Assessment*. WCS, WWF, Smithsonian and NFWF-STF, New York-Washington, DC.

Seidensticker, J (2010) Saving wild tigers: a case study in biodiversity loss and challenges to be met for recovery beyond 2010. *Integrative Zoology*, **5**, 285-299.

Seidensticker, J, Dinerstein E, Goyal S *et al.* (2010a) Tiger range collapse and recovery at the base of the Himalayas. In: *Biology and Conservation of Wild Felids* (eds MacDonald D, Loveridge A), pp. 305 – 323. Oxford University Press, New York.

Seidensticker J, Christie S, Jackson P (1999) *Riding the Tiger: Tiger conservation in human-dominated landscapes*. Cambridge University Press, Cambridge.

Seidensticker J, Graticke B, Shrestha M (2010b) How Many Wild Tigers Are There? An Estimate for 2008. In: *Tigers of the World* (eds Tilson R, Nyhus P), pp. 295-300. Elsevier, New York.

Sherman NJ, Loboda TV, Sun G, Shugart HH (2012) Remote Sensing and Modeling for Assessment of Complex Amur (Siberian) Tiger and Amur (Far Eastern) Leopard Habitats in the Russian Far East. In: *Remote Sensing of Protected Lands* (ed Y. Q. Wang), pp. 379-407. CRC Press, New York.

Shugart HH (1984) (reprint 2003) *A Theory of Forest Dynamics: The Ecological Implications of Forest Succession Models*. pp. 121-122. The Blackburn Press, Caldwell, NJ.

Shugart HH (1998) *Terrestrial Ecosystems in Changing Environments*. pp. 249–252. Cambridge University Press, Cambridge.

Shugart HH, Saatchi S, Hall FG (2010) Importance of structure and its measurement in quantifying function of forest ecosystems. *Journal of Geophysical Research*, **115**, 1–16.

Shugart HH, Woodward FI (2011) *Global Change and the Terrestrial Biosphere*. Wiley-Blackwell, Hoboken, NJ.

Shuman JK, Shugart HH (2009) Evaluating the sensitivity of Eurasian forest biomass to climate change using a dynamic vegetation model. *Environmental Research Letters*, **4**, 045024.

Smirnov EV, Miquelle DG (1999) Population dynamics of the Amur tiger in Sikhote-Alin Zapovednik, Russia. In: *Riding the Tiger: Tiger conservation in human-dominated landscapes* (eds Seidensticker J, Christie S, Jackson P), pp. 61-70. Cambridge University Press, Cambridge.

Soja AJ, Tchebakova NM, French NJF *et al.* (2006) Climate-induced boreal forest change: Predictions versus current observations. *Global and Planetary Change*, **56**, 274-296.

Stephens PA, Zaumyslova O, Hayward G *et al.* (2005) Ungulate abundance in Sikhote-Alin Zapovednik: trends and causal factors. In: *Tigers of the Sikhote-Alin Nature Reserve: Ecology and Conservation* (eds D. Miquelle, E. Smirnov, J. Goodrich), pp. 113-124. Vladivostok <in Russian>.

Stephens PA, Zaumyslova OY, Hayward GD, Miquelle DG (2006) Analysis of the long-term dynamics of ungulates in Sikhote-Alin Zapovednik, Russian Far East. Report to Sikhote-Alin Zapovednik and USDA Forest Service. Wildlife Conservation Society, New York.

Stocker T (2011) Presentation by Co-Chair of Working Group on November 30, 2011, at the UNFCCC Seventeenth Conference of the Parties in Durban, South Africa.

Sturm M, McFadden JP, Liston GE *et al.* (2001) Snow-Shrub Interactions in Arctic Tundra: a Hypothesis with Climate Implications. *Journal of Climate*, **14**, 336-344.

Sunquist M, Karanth K, Sunquist F (1999) Ecology, behavior and resilience of the tiger and its conservation needs. In: *Riding the Tiger* (eds Seidensticker J, Christie S, Jackson P), pp. 5-18. Cambridge University Press, Cambridge.

Sunquist ME, Sunquist F (2001) Changing landscapes: consequences for carnivores. In: *Carnivore Conservation* (eds Gittleman JL, Funk SM, MacDonald DW *et al.*), pp.13, 399 – 418. Cambridge University Press, Cambridge.

Sunquist F, Sunquist M (2002) *Wild Cats of the World*, pp. 343-372, University of Chicago Press, Chicago.

UNEP 2012. *The Emissions Gap Report 2012*. United Nations Environment Programme (UNEP), Nairobi.

Vaillant, J. (2010) *The Tiger*, Alfred A. Knopf, New York.

Walston J, Robinson JG, Bennett EL *et al.* (2010) Bringing the Tiger Back from the Brink – The Six Percent Solution. *PLoS Biology*, **8**, 1-4.

Wikramanayake E, Dinerstein E, Seidensticker J *et al.* (2011) A landscape-based conservation strategy to double the wild tiger population. *Conservation Letters*, 1-9.

Wikramanayake E, McKnight M, Dinerstein E (2004) Designing a Conservation Landscape for Tigers in Human-Dominated Environments. *Conservation Biology*, **19**, 839-844.

Xiaofeng L, Yi Q, Diqiang L *et al.* (2011) Habitat evaluation of wild Amur tiger (*Panthera tigris altaica*) and conservation priority setting in north-eastern China. *Journal of Environmental Management*, **92**, 31 – 42.

Yan X, Shugart HH (2005) FAREAST: a forest gap model to simulate dynamics and patterns of eastern Eurasian forests. *Journal of Biogeography*, **32**, 1641-1658.

Zhang N, Shugart HH, Yan X (2009) Simulating the effects of climate changes on Eastern Eurasian forests. *Climatic Change*, **95**, 341-361.

Zyryanova OA, Yaborov VT, Abaimov AP *et al.* (2005) Problems in the Maintenance and Sustainable Use of Forest Resources in Priamurye in the Russian Far East. *Eurasian Journal of Forestry Research*, **8**, 53-64.

WEBSITES

Chundawat RS, Habib B, Karanth U *et al.* (2011) *Panthera tigris*. In: IUCN 2012. IUCN Red List of Threatened Species. Version 2012.2 <www.iucnredlist.org> 06/19/13.

Johnson PS (1994) How to manage oak forests for acorn production. USDA Technical Brief. North Central Forest Experiment Station <<http://www.ncrs.fs.fed.us/pubs/tb/tb1/techbrf1>> 06/24/13.

Korovin, G (2012) Forest fires. Land Resources of Russia, IIASA <http://www.iiasa.ac.at/Research/FPR/russia_cd/forestry_des.htm> 06/08/12.

Lynam AJ, Nowell K (2011) *Panthera tigris ssp. corbetti*. In: IUCN 2012. IUCN Red List of Threatened Species. Version 2012.2 <www.iucnredlist.org> 06/19/13.

Miquelle DG, Darman Y, Seryodkin I (2011) *Panthera tigris ssp altaica*. In: IUCN 2012. *IUCN Red List of Threatened Species*. Version 2012.2 <www.iucnredlist.org> 01/30/13.

United Nations Educational, Scientific and Cultural Organization (UNESCO) World Heritage Convention. World Heritage List <<http://whc.unesco.org/en/list/766>> 02/04/11.

4.8 APPENDIX 1

English translation of Latin species names

<i>Latin name</i>	<i>English</i>
<i>Abies holophylla</i>	Holo or Manchurian fir
<i>Abies nephrolepis</i>	Black or Hinggan fir
<i>Acer mono</i>	Painted maple
<i>Betula costata</i>	Chinese or yellow birch
<i>Betula dahurica</i>	Black birch
<i>Betula ermani</i>	Alpine or Erman's birch
<i>Betula mandshurica</i>	Manchurian birch
<i>Carpinus cordata</i>	Hornbeam
<i>Larix gmelinii</i> , <i>Larix dahurica</i>	Dahurian or Xing'an larch
<i>Fraxinus mandshurica</i>	Manchurian Northeast ash
<i>Juglans mandshurica</i>	Manchurian walnut
<i>Phellodendron amurense</i>	Amur cork tree
<i>Picea ajanensis</i>	Yezo or Ayan spruce
<i>Pinus koraiensis</i>	Korean pine
<i>Quercus mongolica</i>	Mongolian oak
<i>Syringa robusta</i>	Tree lilac
<i>Tilia amurensis</i>	Amur linden
<i>Ulmus laciniata</i>	Laciniata elm

CHAPTER 5. CONCLUSION

This research has three principal components: 1. Comparison of results from the forest gap model FAREAST output with remotely sensed land covers and metrics in the biologically diverse temperate forests of the southeastern Russian Far East in order to confirm the correspondence of the two approaches and to reinforce their utility in determining land covers and forest characteristics in large-scale, inaccessible landscapes, 2. Comparison of simulated results with field data at eleven sites in the Russian Far East to validate the model at a detailed scale, and 3. Exploration of the effects of climate change predicted by the model in the area of study, and the implications for the Amur, or Siberian, tiger, which exists in the wild only in this region.

Comparing FAREAST results with land covers developed from a synthesis of MODIS and Russian vegetation and land cover maps demonstrated that disturbance, such as wildfire or logging, may have occurred when modeling produces a forest at a later stage of succession than remote sensing. Ground-truthing is necessary to verify disturbance as well as to confirm the cause. A comparison of the relationship between canopy height and biomass derived from FAREAST with the same relationship developed from the GLAS LiDAR instrument showed continuity between the two approaches. FAREAST results generally showed taller canopy height and greater biomass, which might be expected, since the model simulates old growth, primary forests, whereas LiDAR assesses current conditions.

Tree basal area data from field research corresponded most closely to FAREAST results on a species basis at the southernmost sites, which were closest to Changbai Mountain in northeastern China, data from which were used to develop and verify the model. The dominant species was correctly identified at five of eight old-growth forest sites, and Kolmogorov-Smirnov statistical testing showed that, in many cases, modeled and observed species data originated in the same distribution. The model indicates that Mongolian oak basal area has already peaked and is in decline at all sites except the secondary oak forests of Blagodatnoye, where Mongolian oak basal area expands. Under current climate conditions, Korean pine would be the dominant species indefinitely in old growth forests.

When FAREAST was adjusted to reflect predicted warmer temperatures, forest composition changed. Korean pine, one of the most important tree species for Amur tiger prey, fared differently according to latitude. At the southernmost sites, a temperature increase as small as 2.0 °C caused the decline and eventual disappearance of Korean pine. At mid-elevation sites in the Sikhote-Alin Mountains in the subarctic climate near the Sea of Japan, climate warming of 3.5 °C benefits Korean pine, but the species declines in basal area rapidly with a 3.8 °C temperature increase on a southern aspect and a 4.0 °C increase on a north-facing slope. Further north, in a continental climate in southern Khabarovsk Krai, FAREAST indicates that Korean pine basal area would decline permanently with climate warming of 2.1 °C and total forest basal area would drop steeply with a 3.2 °C temperature increase.

These results suggest that the range of Amur tigers may need to change because of modification in the range of Korean pine, which has been statistically associated with the presence of tigers and their ungulate prey. Conservation organizations, citizens and local, regional and national governments have been working together to identify corridors between habitat areas. In planning for the future, climate change effects associated with latitude, elevation, and continental versus maritime climates need to be incorporated into planning processes.

Amur tigers are resilient and able to adapt to new territories that meet the requirements of adequate prey, shelter, access to water and protection from poaching. Addressing the habitat and nutrition requirements of ungulates as part of an effort to maintain and expand the tiger population is important for the survival of this charismatic and irreplaceable subspecies. Modeling indicates that Korean pine and Mongolian oak need to be protected or restored, where necessary, to ensure an adequate food supply for tiger prey in a climate predicted to become warmer and drier.